

UNIVERSIDADE FEDERAL DO RIO GRANDE - FURG  
INSTITUTO DE CIÊNCIAS BIOLÓGICAS - ICB  
PROGRAMA DE PÓS-GRADUAÇÃO EM CIÊNCIAS FISIOLÓGICAS

AValiação DO POTENCIAL TERAPêUTICO DE TIAZOLIDINONAS PARA O  
TRATAMENTO DE GLIOMAS.

*Elita Ferreira da Silveira*

Tese defendida no âmbito do Programa de Pós-Graduação  
em Ciências Fisiológicas como parte dos requisitos para a  
obtenção do título de DOUTOR em Ciências Fisiológicas

Orientadora: Prof<sup>a</sup>. Dra. Ana Paula Horn  
Co-orientadora: Prof<sup>a</sup>. Dra. Elizandra Braganhol

Rio Grande

2017

**Banca Examinadora:**

Prof<sup>a</sup> Dra. Ana Paula Horn (Presidente)

Prof<sup>a</sup> Dra. Gilma Trindade

Prof<sup>a</sup> Dra. Karina Paese

Prof<sup>a</sup> Dra. Mariana Appel Hort

Prof<sup>a</sup> Dra. Marta Marques de Souza

## **Dedico**

Aquele que nunca me diz não, meu Pai  
Aquele que sempre me diz sim, minha Mãe  
Meu motivo de chegar até aqui, minha filha.

Amo vocês!

## **Agradecimentos**

O importante na vida não é somente construir algo, mas ter com quem compartilhar nossos feitos, pois esses, raramente se constituem mérito exclusivo. Por isso, dedico essa conquista a todos aqueles que comigo se empenharam na concretização desse trabalho. Em especial:

Aos meus pais, Erion e Luísa, agradeço por me mostrarem todos os dias o quanto sou amada e por juntos até hoje cuidarem para que nada nunca me falte, oportunizando assim, que eu trilhasse esse longo caminho de formação profissional. Ainda gostaria de agradecer por priorizarem e apoiarem todas as minhas escolhas.

A minha filha Amanda, que tem vivenciado comigo a necessidade de se priorizar o estudo, e que muitas vezes precisa aceitar minha ausência. Que essa conquista te sirva de exemplo de esforço e dedicação, e te motive a sempre acreditar que com dedicação tudo é possível.

Um agradecimento especial à amiga, Juliana, pelas horas incansáveis dedicadas a realização deste trabalho, pela paciência, persistência e competência nos experimentos que realizamos juntas. Ainda agradeço por dar sequência aos meus experimentos quando era impossível estar na FURG e na UFPEL ao mesmo tempo. Pelos cancelamentos de férias e finais de semana dedicados a este trabalho, pelo companheirismo nos momentos de angústia e pela paciência durante esses anos de convivência. Pela parceria nos congressos, e por sempre mesmo atolada de trabalho dizer sim para mais uma parceria inventada por mim. Por dividir comigo a responsabilidade de cuidar de um laboratório sem termos noção de por onde começar. Por ser a minha eterna IC, com todo respeito a profissional que te tornastes. E por fim e acima de tudo, pela tua amizade, teu incentivo e palavras de conforto que foram essenciais para a conclusão desta etapa. Saiba que tua amizade sempre foi e sempre vai ser muito além do profissional, teu carinho, palavra sincera, teu “calma que tudo vai dar certo” não foi para o Lattes, tá guardado no meu coração.

A amiga Maiara, pessoa cheia de vida e energia positiva, que trouxe luz para minha vida pessoal e profissional. Amiga querida que sempre teve uma palavra de conforto nas horas de angústias, e sempre um sorriso largo na mesa do bar. És um exemplo de pessoa do bem, de um positivismo, fé, e claro de autoestima, inabaláveis. Tu me ensinaste que não é por acaso que pessoas entram e saem das nossas vidas, que passamos por momentos difíceis, mas a recompensa sempre chega. Que cumplicidade e

amizade existem sim. Que o amor está acima de tudo. E que tudo acontece por uma razão maior. Saibas que tu foste o melhor presente que a FURG me deu e que te ter na minha vida faz meus dias mais felizes. Teu incentivo e palavras de conforto foram essenciais para a conclusão deste ciclo. E tua amizade é maior que tudo isso.

A amiga Ana por me ajudar a enxergar a vida por outro ângulo, me apresentando sempre o lado bom da vida, o otimismo, a energia positiva. Também por quando necessário, me apontar os erros e assim contribuir para que eu me renove a cada dia, sempre em busca do melhor. Por ter sido o incentivo que eu precisava para estudar para o concurso ao qual sem tua ajuda eu não teria sido aprovada. Graças a ti, logo estarei iniciando minha vida profissional. Por saber que mesmo longe, tenho tua amizade, sempre que precisar.

À amiga Mayara pelo exemplo de profissionalismo, pela parceria nos meus experimentos e pelas contribuições neste trabalho. Ainda agradeço por me permitir conviver contigo, pessoa íntegra, sempre disposta a ajudar o próximo sem esperar nada em troca. Pessoas assim estão escassas no mundo, me sinto privilegiada de ter construído uma amizade contigo, de dividir o espaço de trabalho contigo, e de saber que posso contar contigo. Obrigada ainda pelas correções forçadas, pelo café diário e por sempre ter uma palavra de apoio.

A amiga Fernanda, por mesmo afastada do laboratório se disponibilizar em contribuir nos meus experimentos in vivo. Pela parceria desde o mestrado. Pela amizade e cumplicidade no ambiente de trabalho e fora dele. Por me escutar, entender e ter sempre uma palavra de conforto. Por tornar esse final de doutorado mais alegre e cheio de vida, pelo teu retorno ao laboratório.

À Nathy Pedra, Nati Bona e Priscila por assumirem o cultivo com todo profissionalismo e dedicação possível. Por darem sequência aos meus experimentos enquanto eu me dedicava a parte escrita do meu trabalho. Por aceitarem minhas ideias e parcerias com apoio. Pela convivência diária. Pela amizade. E pela grande parceria nessa incessante persistência de manter o laboratório de cultivo funcionando.

A equipe Neurocan, pela convivência diária, pelas risadas, pelas parcerias, por tornarem esse ambiente rico em conhecimento e alegria. Em especial, a todos aqueles já citados aqui e as colegas Luiza, Simone, Bruna e Jessié.

As minhas amigas Raquel e Mariana, pela amizade, por me lembrarem de que a cada dia podemos recomeçar e por me estenderem a mão sempre que precisei de vocês.

Agradeço também as famílias de vocês, por sempre me acolher e comemorar minhas conquistas.

A Daniela Gôuvea pela síntese das moléculas que compõem parte deste trabalho e, além disso, por não se importar com a primeira autoria cedida para mim. No ambiente da pesquisa, é difícil presenciar atitudes como a que tu tiveste. Fico imensamente feliz em ter o prazer de estabelecer parceria com uma profissional como tu. A vida certamente retribui atitudes assim.

A Alice Kunzler e Daniel Schuch, pela síntese das moléculas que compõem parte deste trabalho. Principalmente ao Daniel, que sempre esteve disposto a sintetizar quantidades altas para que eu pudesse realizar meus experimentos in vivo.

Aos colegas Juliano e Silvana, casal sempre disposto a contribuir com o próximo. Obrigada pela parceria nas disciplinas.

A minha orientadora, Prof<sup>ª</sup>. Dr<sup>a</sup> Ana Paula Horn, por me receber na FURG, mesmo eu propondo desenvolver minha pesquisa na UFPEL, por confiar e me permitir desenvolver um trabalho com ideias próprias, pelo apoio em momentos de dúvidas e pelos ensinamentos nesses 4 anos de orientação.

Um agradecimento sincero à minha co-orientadora, Prof<sup>ª</sup>. Dr<sup>a</sup> Elizandra Braganhol! Por ainda no meu mestrado ter me acolhido e ensinado com paciência e carinho. Pela confiança depositada em mim na sua ausência. Pelas palavras de incentivo durante todo esse período. Por muitas vezes precisar abdicar da sua vida pessoal para se dedicar ao meu trabalho. Sou grata por ter tua amizade e saber que posso contar contigo.

Um agradecimento especial ao Professor Wilson Cunico, não só pela parceria na síntese das moléculas que compõem este trabalho, mas por dar oportunidade e incentivar minhas ideias. Por sempre me receber com carinho e atenção aos meus questionamentos. Pelas diversas correções que iam além da química, realizadas nos meus trabalhos. Por, na ausência da Eliz, ter se tornado meu orientador na UFPEL dando a mesma importância ao meu trabalho, que para teus orientados. Pela pessoa e profissional que és sempre disposto a contribuir de alguma forma para o melhor. Agradeço pela atenção, que sem obrigação, tu dedicaste a mim e ao meu trabalho.

Às Prof<sup>as</sup>. Rosélia Spanevello e Francieli Stefanello, por me receberem no Neurocan e por estarem sempre atentas e dispostas a ajudar as pessoas que estão a sua volta. Por serem o suporte e apoio financeiro, que eu e o “cultivo celular” precisamos na ausência da Eliz.

À Prof<sup>a</sup> Dr<sup>a</sup> Leticia Cruz e a Luana, pela parceria na preparação das formulações de Tiazolidinonas em nanocápsulas utilizadas neste trabalho. Em especial a Luana pelo apoio em todas as ideias de experimentos e por auxiliar nas dúvidas durante a construção de parte deste trabalho.

À professora Fátima Beira da UFPEL, por permitir que eu me responsabilizasse pelo laboratório de cultivo celular na ausência da professora Elizandra Braganhol.

A Anelize, veterinária responsável pelo biotério central da UFPEL, por sempre se fazer presente para tirar cada dúvida, por auxiliar nos experimentos sempre que solicitada e ainda pela compreensão nos momentos burocráticos.

A técnicas, Carol, Mirian e Sabrina, do laboratório de Histologia da FURG, pelos ensinamentos e pela ajuda no preparo das lâminas que foram essenciais para análise dos resultados deste trabalho. Ainda agradeço a Sabrina pela amizade construída ao longo destes anos, por ser uma pessoa admirável que tem sempre uma palavra de conforto e otimismo.

Aos professores do Programa de Pós-Graduação em ciências Fisiológicas da FURG, pelos ensinamentos. A UFPEL pela estrutura onde eu tive a oportunidade de realizar meu projeto de doutorado e a CAPES, pelo apoio financeiro.

A todos os amigos, colegas, pessoas que durante esses 4 anos, contribuíram de alguma forma para a realização deste doutorado, sendo com empréstimo ou auxílio em algum equipamento, com materiais, com algum ensinamento, ou mesmo com uma palavra de apoio ou uma genteliza. Meu muito obrigado! As conquistas não fazem sentido sem amizades e amores ao nosso redor.

## Lista de Abreviaturas

AINEs- anti-inflamatório não esteróides

AKT/PKB - proteína quinase B

BCL-2- célula-B de linfoma 2

BCL-XL- Linfoma de células B - extra grande

BER- reparo por excisão de base

BH3- domínio de homologia Bcl-2

BHE – Barreira Hematoencefálica

BVZ- bevacizumab

CAT- catalase

CDK1 - ciclina dependente de cinase 1

COX – enzima ciclooxygenase

EGF- fator de crescimento epidermal

EGFR - receptor de fator de crescimento epidermal

ERK 1/2- quinases reguladas por sinal extracelular

GBM - Glioblastoma Multiforme

GFAP- proteína glial fibrilar ácida

GPO- glutationala peroxidase

IDH- Isocitrato desidrogenase

INCA- Instituto Nacional do Câncer

IL\_ - interleucina

MCP-1 – proteína quimiotática de monócitos

MIF- fator inibitório de migração de macrófagos

MGMT- O6-metilguanina-DNA-metiltransferase

MMR- reparo aleatório



NO- óxido nítrico

OH- hidroxila

OCh<sub>3</sub>- metóxi

OMS- Organização Mundial de Saúde

p53- gene supressor tumoral

PCL- policaprolactona

PDGFR- receptor de crescimento derivado de plaquetas

PGI<sub>2</sub> – prostaglandina I<sub>2</sub>

PGE – prostaglandina E

PI- iodeto de propídeo

PI3K - fosfatidilinositol 3-quinase

PIP<sub>2</sub>-fosfatidilinositol-4,5-bifosfato

PIP<sub>3</sub>-fosfatidilinositol-3,4,5-trifosfato

PTEN - homólogo fosfatase e tensina deletado do cromossomo 10

ROS- espécies reativas de oxigênio

SNC- Sistema Nervoso Central

SOD- superóxido dismutase

STAT-3- proteína pertencente a família das STATs

TBARS- substâncias reativas ao ácido tiobarbitúrico

TMZ- Temozolomida

TNF- $\alpha$  - fator de necrose tumoral- alfa

TNF- $\beta$  - fator de necrose tumoral- beta

VEGF-a-fator de crescimento vascular endotelial A

## Sumário

Lista de abreviaturas.....	9
Lista de Figuras.....	11
Lista de Tabelas.....	12
Resumo.....	13
Abstract.....	15
<b>1 Introdução.....</b>	<b>17</b>
1.1 Cânceres e os tumores do Sistema Nervoso Central (SNC) .....	17
1.2 Gliomas: origem e classificação.....	18
1.3 Terapia para gliomas.....	22
1.4 Genes e vias moleculares envolvidas na patogênese dos gliomas.....	24
1.5 O processo inflamatório e os gliomas.....	25
1.6 Tiazolidinonas.....	28
1.7 Nanocápsulas como estratégia para entrega de fármacos.....	30
<b>2 Objetivos .....</b>	<b>34</b>
2.1 Objetivo Geral.....	34
2.2 Objetivos específicos.....	34
<b>3 Artigo/ Manuscritos Científicos.....</b>	<b>36</b>
3.1 Artigo I/ Capítulo 1.....	37
3.2 Manuscrito I/ Capítulo 2.....	59
3.3 Manuscrito II/ Capítulo 3.....	93
<b>4 Discussão geral.....</b>	<b>124</b>
<b>5 Conclusões e perspectivas.....</b>	<b>132</b>
<b>6 Bibliografia Geral.....</b>	<b>135</b>
<b>7 Anexos.....</b>	<b>146</b>

## Lista de Figuras

<b>Figura 1</b> Teoria atual sobre a origem dos gliomas.....	19
<b>Figura 2</b> Nova classificação dos gliomas.....	21
<b>Figura 3</b> Principais vias de sinalizações envolvidas na patogênese dos gliomas.....	25
<b>Figura 4</b> Modelo de como as células tumorais “educam” as células imunes a desempenhar função de estímulo a progressão do tumor.....	27
<b>Figura 5</b> Estrutura geral de tiazolidinonas.....	28
<b>Figura 6</b> Vias envolvidas no mecanismo de ação de Tiazolidinonas.....	29
<b>Figura 7</b> Nanopartículas. Ilustração representativa de nanoesferas e nanocápsulas.....	31
<b>Figura 8</b> Resumo comparativo entre as classes derivadas de tiazolidinonas.....	133
<b>Figura 9</b> Resumo dos resultados obtidos nesta tese de Doutorado.....	134

## **Lista de Tabelas**

**Tabela 1** Pesquisas recentes envolvendo uso de nanotecnologia para o tratamento.....32  
de gliomas.

## Resumo

Entre os tipos de gliomas, o glioblastoma multiforme (GBM) é considerado o mais maligno e a pior forma de tumor cerebral primário. Esse tumor está normalmente associado à presença de um microambiente inflamatório, que contribui para a quimio/radorresistência, resultando em um prognóstico desfavorável para os pacientes. Compostos heterocíclicos, como os tiazolidinonas, se destacam porque possuem uma ampla gama de importantes propriedades farmacológicas, incluindo atividades anti-inflamatória e antitumoral. Assim, a proposta geral deste trabalho foi avaliar o potencial terapêutico de tiazolidinonas sintéticas para o tratamento de glioma. Primeiramente, investigamos o efeito antiglioma *in vitro* de um painel de dezesseis moléculas da classe 2-aril-3-((piperidin-1-il)etil)tiazolidin-4-onas, onde treze moléculas mostraram efeito na redução da viabilidade celular, com resultados promissores para os compostos **4d**, **4l**, **4m** e **4p**, que promoveram uma redução de viabilidade entre 50% e 85%, numa faixa de concentrações entre 12,5 e 100µM. Os mesmos induziram morte celular principalmente por mecanismos de necrose e apoptose tardia e, no geral, não foram citotóxicos para astrócitos primários. Nossos resultados também mostram que o tratamento com doses sub-terapêuticas de **4d**, **4l** e **4p** reduziram o crescimento e as características malignas do glioma *in vivo*, sem indução de mortalidade ou dano periférico para os animais. Sabendo que nanocápsulas de polímeros biodegradáveis tornam-se uma alternativa ao tratamento do câncer, nanoencapsulamos a molécula que apresentou melhor resultado *in vivo* e investigamos a atividade antitumoral *in vitro* e a toxicidade *in vivo* das nanocápsulas poliméricas (**4L-N**). O tratamento com **4L-N** diminuiu seletivamente a viabilidade e proliferação de células de glioma C6, sendo ainda mais eficiente do que a molécula livre. Além disso, **4L-N** não promoveu toxicidade para astrócitos primários. Demonstramos ainda que o tratamento com dose sub-terapêutica de **4L-N** não alterou o peso ou causou mortalidade e não causou toxicidade ou danos periféricos aos ratos. Finalmente, **4L**, bem como **4L-N**, não alteraram parâmetros de dano oxidativo no fígado e cérebro de ratos. Esses dados mostram que o nanoencapsulamento de **4L** potencializou seu efeito antiglioma, e não causou toxicidade *in vivo*. Sabemos que modificações estruturais na molécula acarretam em mudanças nas propriedades físico-químicas, sendo possível até mesmo um aumento do seu potencial terapêutico. Assim, uma nova série de derivados de tiazolidinonas foi sintetizada nesse trabalho, 2-aril-3-(3-morfolinopropil)tiazolidin-4-onas, e suas atividades anti-inflamatórias e antiglioma

foram avaliadas. Por meio de um modelo de edema de orelha induzido por óleo de cróton em camundongos, nove dos desesseis compostos testados apresentaram valores de inibição da inflamação entre 50 e 71%. As células de glioma foram expostas a estas nove tiazolidinonas e as viabilidades celulares foram medidas pelo ensaio MTT, quatro moléculas **4a**, **4d**, **4f** e **4h** foram capazes de reduzir a viabilidade das células C6 em 50% a 100  $\mu\text{M}$ , chegando à 80% quando testadas na maior concentração, 500 $\mu\text{M}$ . Salientamos também, que apenas uma molécula foi tóxica para astrócitos primários, e somente na maior concentração testada. Considerando a malignidade, a dificuldade de tratamento frente à quimiorresistência e o consequente prognóstico dos pacientes, os resultados que obtivemos nesse trabalho são de grande importância. Tomados em conjunto, esses dados sugerem o potencial terapêutico de compostos contendo o heterociclo tiazolidinona para o futuro tratamento de glioma.

**Palavras-chave: tiazolidinonas, glioma, inflamação, toxicidade, nanocapsula**

## Abstract

Among glioma types, glioblastoma multiforme (GBM) is considered the most malignant and worst form of primary brain tumor. This tumor is usually associated with the presence of an inflammatory microenvironment, which contributes to chemo / radioresistance, resulting in an unfavorable prognosis for the patients. Heterocyclic compounds, such as thiazolidinones, stand out because they have a wide range of important pharmacological properties, including anti-inflammatory and antitumor activities. Thus, the general proposal of this work was to evaluate the therapeutic potential of synthetic thiazolidinones for the treatment of glioma. First, we investigated the in vitro antiglioma effect of a panel of sixteen molecules of class 2-aryl-3 - ((piperidin-1-yl) ethyl) thiazolidin-4-ones, where thirteen molecules showed effect in reducing cell viability, with promising results for compounds **4d**, **4l**, **4m** and **4p**, which promoted a viability reduction between 50% and 85%, in a concentration range between 12.5 and 100 $\mu$ M. They induced cell death mainly by mechanisms of late apoptosis and necrosis and, in general, were not cytotoxic to primary astrocytes. Our results also show that treatment with sub-therapeutic doses of **4d**, **4l** and **4p** reduced the growth and malignant characteristics of the glioma in vivo without inducing mortality or peripheral damage to the animals. Knowing that nanocapsules of biodegradable polymers become an alternative to cancer treatment, we nanoencapsulated the molecule that showed the best in vivo results and investigated the in vitro antitumor activity and the in vivo toxicity of polymer nanocapsules (**4L-N**). Treatment with **4L-N** selectively decreased the viability and proliferation of C6 glioma cells, being even more efficient than the free molecule. In addition, **4L-N** did not promote toxicity to primary astrocytes. We further demonstrate that treatment with a sub-therapeutic dose of **4L-N** did not alter weight or cause mortality and did not cause peripheral toxicity or damage to rats. Finally, **4L**, as well as **4L-N**, did not alter parameters of oxidative damage in the liver and brain of rats. These data show that **4L** nanoencapsulation potentiated its antiglioma effect, and did not cause toxicity in vivo. We know that structural modifications in the molecule lead to changes in physico-chemical properties, and even an increase in its therapeutic potential is possible. Thus, a novel series of thiazolidinone derivatives was synthesized in this work, 2-aryl-3- (3-morpholinopropyl) thiazolidin-4-ones, and its anti-inflammatory and antiglioma activities were evaluated. By means of a mouse edema model induced by mouse oil, nine of the sixteen compounds tested showed inflammation inhibition values

between 50 and 71%. Glioma cells were exposed to these nine thiazolidinones and cell viabilities were measured by the MTT assay, four molecules **4a**, **4d**, **4f** and **4h** were able to reduce the viability of C6 cells by 50% to 100  $\mu\text{M}$ , reaching 80% when tested at the highest concentration, 500 $\mu\text{M}$ . We also noted that only one molecule was toxic to primary astrocytes, and only at the highest concentration tested. Considering the malignancy, the difficulty of treatment against chemoresistance and the consequent prognosis of the patients, the results that we obtained in this work are of great importance. Taken together, these data suggest the therapeutic potential of compounds containing the thiazolidinone heterocycle for the future treatment of glioma.

**Keywords:** thiazolidinones, glioma, inflammation, toxicity, nanocapsule.



## **1. Introdução**

### **1.1 Cânceres e os tumores do Sistema Nervoso Central (SNC)**

Câncer, neoplasia maligna ou tumor maligno são sinônimos, que classificam um grupo de doenças caracterizadas por um crescimento desordenado de células e capacidade de invasão a tecidos e órgãos, podendo espalhar-se para outras regiões do corpo, processo esse denominado de metástase (INCA, 2016). Esse grupo de doenças tornou-se um dos maiores problemas de saúde pública a atingir a população nos últimos anos, particularmente nos países em desenvolvimento, onde nas próximas décadas espera-se que o impacto na população seja de aproximadamente 80% dos mais de 20 milhões de novos casos que são estimados até o ano de 2025 (Stewart e Wild, 2014).

Dentre os cânceres existem os tumores do Sistema Nervoso Central (SNC), que se apresentam como uma massa de células anormais, com alta capacidade de crescimento e multiplicação, que ocorre de forma descontrolada no tecido nervoso, sendo que sua apresentação clínica varia conforme a sua localização (Preusser et al., 2006). Esses tumores são representados por um grupo de neoplasias benignas e malignas, que incluem meningiomas, meduloblastomas, schwannomas, craniofaringiomas, gangliogliomas e gliomas. Pacientes com suspeita de tumores no SNC normalmente apresentam sintomas como vômitos, cefaléias, fadigas, alterações cognitivas, desequilíbrio, transtorno de humor e distúrbio da marcha. Podem também apresentar um déficit neurológico agudo que se assemelha a um acidente vascular encefálico, porém esses sintomas aparecem com uma frequência menor (Chabner e Longo, 2015). O diagnóstico é realizado através de exames de neuroimagem, como tomografia computadorizada ou ressonância magnética, que detectam imagem contrastada do crânio. Tecnologias como a espectroscopia por ressonância magnética e a tomografia por emissão de pósitrons, são úteis em situações específicas como a orientação cirúrgica ou para fazer a diferenciação entre tumor recorrente e necrose relacionada com o tratamento (Chabner e Longo, 2015). Quando há suspeita de metástases para o SNC, ainda existem avaliações laboratoriais que são realizadas através de punção lombar, para que seja feita a análise do líquido cérebro espinhal (Chabner e Longo, 2015). Geralmente, a localização desses tumores são regiões de difícil acesso, complicando ou até mesmo, impossibilitando o procedimento cirúrgico de ressecção. Existe um alto risco de comprometimento das funções do cérebro e da integridade do SNC, que são vitais para a vida humana demonstrando a necessidade de novas e mais eficazes

estratégias de diagnóstico, prognóstico e tratamento dessas neoplasias (Gupta, 2012). Dessa forma, esses tumores se tornam um grande desafio para pacientes, médicos e pesquisadores.

Nesse trabalho focaremos nos gliomas, que ocorrem em todas as faixas etárias, no entanto, são mais predominantes em adultos com mais de 45 anos (Altieri et al., 2014). Esses tumores representam cerca de 70% de todas as neoplasias do SNC (Yin et al., 2007), sendo o tipo mais comum de tumor primário e considerados de maior incidência e letalidade na população (Jovcevska et al., 2013; Meir et al., 2010).

## **1.2 Gliomas: origem e classificação**

O termo glioma foi inicialmente utilizado para definir os tumores originários de células da glia (Talibi et al., 2014). Sabe-se que compartilham semelhanças morfológicas e de expressão gênica relacionadas às células gliais, tais como astrócitos, oligodendrócitos e seus precursores (Holland, 2001; Ramakrishna et al., 2015 e Suvà, 2014). A teoria mais aceita sobre a origem dos gliomas (representada na Figura 1) sugere que eles se originam de células progenitoras neurais, que sofrem transformação oncogênica durante seu desenvolvimento, tornando-se células iniciadoras de tumor (Piccirillo et al., 2009, Huse and Holland, 2010). Sendo as células tronco neurais precursoras de neurônios, astrócitos e oligodendrócitos, essa teoria explica de forma mais convincente a geração de tumores cerebrais compostos por mais de um tipo celular como, por exemplo, o oligoastrocitoma. Dessa forma, os gliomas são constituídos por populações de células tumorais diferenciadas e de uma minoria de células tumorigênicas indiferenciadas multipotentes, que varia em torno de 1-30%. Embora ambas contenham mutações oncogênicas que poderão contribuir para a tumorigênese, somente as células-tronco tumorais têm capacidade de se autorrenovar, sendo possivelmente as responsáveis pela sustentação e propagação do tumor (Sanai et al., 2005).

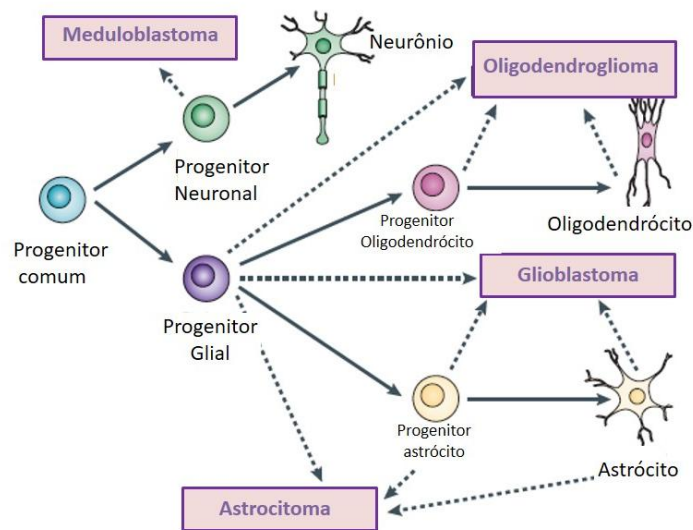


**Figura 1-** Teoria atual sobre a origem dos gliomas (adaptada de Huse e Holland, 2010).

A OMS, em 2007, classificou os gliomas em três diferentes parâmetros: sua localização tumoral, seu grau de malignidade e o tipo celular envolvido (Brat, Fuller e Scheithauer, 2007; Louis et al., 2007; Nakazato, 2008). Essa classificação permite determinar o tipo de terapia a ser utilizada no tratamento dos pacientes, determinando particularmente o uso de radioterapia adjuvante e os protocolos específicos de quimioterapia (Louis et al., 2007).

A classificação em relação à localização do glioma é feita com base no local onde ele se origina e se desenvolve, considerando a membrana que separa o cérebro (tentorium = “teto” cerebelar) do cerebelo. Desta forma, eles podem ser classificados como supra-tentoriais, acima do tentorium ou infra-tentoriais, que se desenvolvem abaixo do tentorium (Kaloshi et al., 2009). Já a classificação em relação ao grau de malignidade, utiliza quatro graus para descrever os gliomas, baseados na malignidade celular, nas características invasivas e na capacidade de desenvolver necrose (Chintala et al., 1999). Os gliomas considerados de grau I (astrocitoma pilocítico) são passíveis de cura por remoção cirúrgica sem necessidade de tratamento quimioterápico, pois apresentam baixa capacidade proliferativa. Os gliomas considerados de grau II - astrocitoma difuso, oligodendroglioma (grau II), oligoastrocitoma (grau II) e ependimoma (grau II), geralmente são infiltrativos, mas com crescimento lento, podendo reincidir após remoção cirúrgica ou progredir para gliomas mais malignos (Bromberg e Van den Bent, 2009). Estes gliomas de baixo grau não são benignos, mas

apresentam um melhor prognóstico e uma sobrevida média muito superior à dos pacientes diagnosticados com gliomas malignos de alto grau (gliomas de grau III e IV) (Bromberg e Van den Bent, 2009). Os gliomas de grau III - astrocitoma anaplásico (grau III), oligodendroglioma anaplásico (grau III) e ependimoma anaplásico (grau III), são caracterizados por apresentarem evidências histológicas de malignidade, como atipia nuclear e elevada atividade mitótica, podendo progredir rapidamente a glioblastoma multiforme. Finalmente, os tumores de grau IV, como os gliosarcomas (grau IV), glioblastomas de células gigantes (grau IV) e o glioblastoma multiforme (GBM) (Louis et al, 2007; Rousseau et al, 2008; Cruceiro et al, 2013), são os mais comuns e apresentam características de extrema malignidade, sendo quase sempre infiltrativos. Comumente apresentam características multifocais (Dai e Holland, 2001), caracterizadas pela formação de vários tumores espalhados pelo tecido sadio, o que explica sua grande capacidade de se infiltrar no parênquima cerebral que circunda o tumor, limitando a remoção cirúrgica (Stupp et al., 2007) e levando a uma rápida progressão e a elevados índices de recorrência (Stupp et al., 2006; Yin et al., 2007). Além disso, apresentam grande capacidade de necrose e são resistentes à quimioterapia (Fang et al., 2012). Os GBMs são considerados os mais letais de todos os gliomas, correspondendo a cerca de 70% dos gliomas de alto grau diagnosticados (Kanu et al., 2009; Vredenburg et al., 2009). Quanto maior o grau, pior o prognóstico (Ahmed et al., 2014 e Nanegrungsunk et al., 2015).

Quanto ao tipo celular, essa classificação é realizada com base em uma análise histológica, de acordo com a semelhança fenotípica das células tumorais com os diferentes tipos de células gliais, como astrócitos e oligodendrócitos. Além da comparação em relação a aparência morfológica, a presença de marcadores específicos como, por exemplo, a proteína glial fibrilar ácida (GFAP), marcadora de astrócitos, e o receptor do fator de crescimento derivado de plaquetas (PDGFR), receptor para oligodendrócitos, podem contribuir para essa classificação. Outra forma de diferenciar esses subtipos são as diferenças genéticas existentes entre eles (Da Fonseca *et al.*, 2008). Estudos mostram, por exemplo, que a perda dos cromossomos 1 p e 19 q em pacientes portadores de oligodendroglioma anaplásico aumenta a sensibilidade a diferentes quimioterápicos com consequências diretas na sobrevida (Cairncross *et al.*, 1998). Além disso, a presença das mutações em IDH em GBMs é considerada indicador de bom prognóstico, pois após cirurgia e tratamento com radioterapia esses pacientes possuem sobrevida média de 27,1 meses (Dang *et al.*, 2009). Nota-se então a

importância de uma distinção entre os tipos de gliomas, pois uma correta avaliação da biologia do tumor e seu grau clínico leva a um correto diagnóstico do paciente e a um melhor prognóstico.

Embora esta classificação da OMS ainda seja a base para a terapia dos pacientes nos dias atuais, em 2016 os tumores do SNC foram classificados novamente, desta vez com base em parâmetros moleculares, sendo possível assim a elaboração de diagnósticos de tumores do SNC estruturados na era molecular, baseando-se não apenas no seu padrão e comportamento de crescimento, mas também mais incisivamente nas suas características genéticas compartilhadas nos genes IDH1 e IDH2 (Louis et al., 2016)(Figura 2).

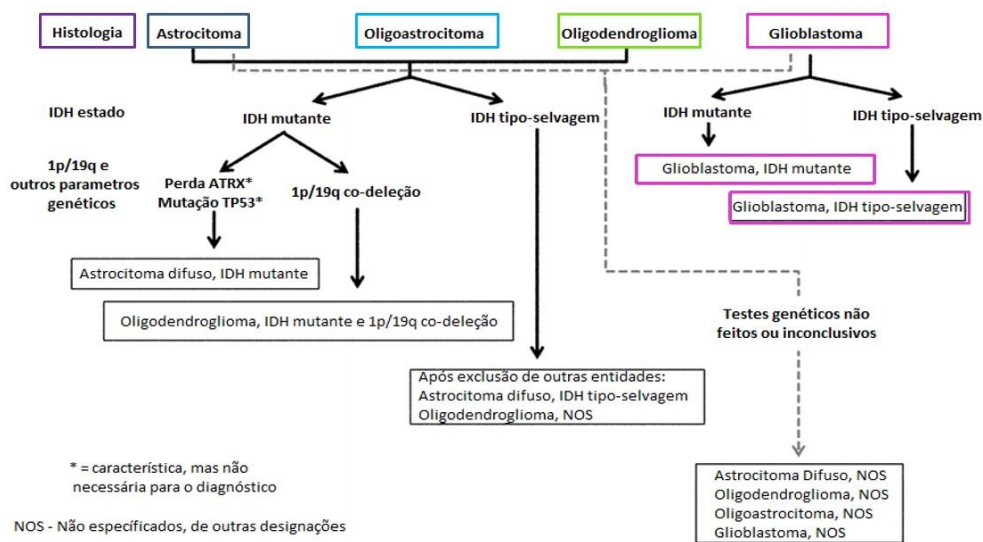


**Figura 2** – Nova classificação dos gliomas (adaptada de Louis et al., 2016).

O GBM, nosso alvo de estudo, é considerado o mais incidente e biologicamente mais agressivo dos gliomas (Furnari et al., 2007) e é dividido em dois subtipos, caracterizando o tumor como primário ou secundário (Maher et al., 2006). O GBM primário já se manifesta clinicamente como um tumor de grau IV, já o GBM secundário evolui a partir dos tumores de menores graus, podendo levar anos para atingir o maior grau (Maher et al., 2006). Esses tumores são considerados os mais agressivos e a forma mais comum de tumores cerebrais e, além de possuírem uma alta taxa de mortalidade, conferem ao paciente uma sobrevida de aproximadamente 12 meses após serem diagnosticados (Meir et al., 2010). São caracterizados por possuírem uma população de

células heterogêneas geneticamente instáveis, apresentando uma grande capacidade de infiltração e características multifocais, angiogênese e alta taxa de resistência à quimioterapia (Wen et al., 2008). Possuem também uma baixa capacidade de metástase (Armstrong et al., 2010). Porém, dentro de pouco tempo, no mesmo local da lesão primária principal ou muito próximo a ela, são observadas novas lesões (Sathornsumette e Rich, 2008), isso porque esses tumores possuem grande habilidade de infiltração pelo tecido cerebral (Meir et al., 2010), que é explicada pelo seu padrão de crescimento multifocal, caracterizado pela formação de vários tumores espalhados pelo tecido sadio. Apesar de avanços nos métodos cirúrgicos terem oportunizado uma maior segurança na cirurgia, permitindo assim a ressecção cirúrgica máxima possível (Asthagiri et al., 2007), essa característica de crescimento ainda limita a remoção cirúrgica total, levando a uma rápida progressão e tornando o GBM o tipo de glioma mais agressivo e com elevados índices de recorrência (Stupp et al., 2007; Yin et al., 2007).

### **1.3 Terapia para gliomas**

A ressecção cirúrgica, sempre que possível, faz parte do tratamento de primeira escolha para os gliomas malignos, associada à radioterapia, e, seguida ou não de quimioterapia (Grant et al., 2014).

Quando essa ressecção não é viável, realiza-se uma biópsia estereotáxica de série (Stupp et al., 2010), visto que a intervenção cirúrgica ainda é fundamental para o diagnóstico e prevenção dos sintomas do tumor. Na quimioterapia, o fármaco de primeira escolha atualmente é a temozolamida (TMZ) (Temodal<sup>®</sup>), um agente alquilante de DNA que é administrado concomitante ou após a radioterapia (Mrugala, 2013). A TMZ é administrada diariamente durante a radioterapia e durante 5 dias de 4 em 4 semanas durante seis ciclos, como um tratamento de manutenção após o fim da radiação (Stupp, 2010). No entanto, o tratamento apresenta eficácia limitada, uma vez que coincide com a resistência desenvolvida por estes tumores. Além disso, por se tratar de um agente alquilante de DNA, causa efeitos colaterais graves, tais como trombocitopenia, leucopenia, anemia, náuseas, vômitos e fadiga, entre outros (Altieri et al., 2014). Assim, a taxa de sobrevivência dos pacientes que apresentam esses tumores é inferior a 30% após um ano, 5% após três anos e somente 2,7% após cinco anos do diagnóstico (Johnson et al., 2012).

O mecanismo de ação da TMZ consiste na adição de um grupamento metil ao DNA nas posições N7 de guanina (70%), adenina N3 (9%) e resíduos de guanina O6 (6%). A eficácia da TMZ como um agente de dano ao DNA resulta principalmente da formação de O6-metilguanina, a qual parecia incorretamente com uma timina (e não como uma citosina). Esta mutação é repetidamente reparada pela via DNA de reparo aleatório (MMR), mas, eventualmente, esse processo falha e induz dano ao DNA seguido de parada do ciclo e apoptose, senescência ou autofagia (Mrugala, 2013). Os danos às células que são induzidos pela TMZ podem ser revertidos pela ação da maquinaria celular de reparo de DNA, não só da MMR, como também por outras vias como a O6-metilguanina-DNA-metiltransferase (MGMT) e a reparo por excisão de base (BER). Esse reparo, quando realizado de forma rápida e eficiente, impede a morte celular, permitindo que os genes associados ao reparo de DNA acarretem em resistência do GBM à quimioterapia.

Outra opção de tratamento é o bevacizumab (BVZ), um anticorpo monoclonal que é utilizado como tratamento adjuvante, que age reconhecendo e inativando o receptor do fator de crescimento endotelial vascular A (VEGF-A), reduzindo suas sinalizações subsequentes, envolvidas na angiogênese tumoral (Nanegrungsunk et al., 2015). Em complemento, também é utilizada a radioterapia em combinação com a quimioterapia, que tem como resultado um aumento na sobrevida mediana de 12,1 meses para 14,6 meses, quando comparada a radioterapia isolada (Stupp et al, 2005). A radioterapia é fundamental no tratamento, pela capacidade de irradiar os contornos irregulares dos tumores cerebrais, através de técnicas guiadas por imagem, permitindo assim que se minimizem as doses para as estruturas vizinhas (Van Meir et al., 2010).

Contudo, estes agentes ainda demonstram eficácia limitada, tanto pela ausência de especificidade terapêutica das drogas citotóxicas, como pela resistência intrínseca das células tumorais à radioterapia e à apoptose, fazendo com que as terapias pró-apoptóticas não sejam tão efetivas ou falhem em induzir a regressão tumoral (Van Meir et al., 2010). Sabe-se também que existe uma grande limitação da terapia farmacológica, devido às restrições impostas pela barreira hematoencefálica (BHE), de modo que

apenas fármacos com alta lipofilicidade conseguem atravessar a barreira sangue-cérebro (Jain, 2012; Da Silveira et al, 2013; Bernardi et al, 2013; Arshad et al, 2015).

#### **1.4 Genes e vias moleculares envolvidas na patogênese dos gliomas**

Alterações na expressão de muitos genes e anormalidades cromossômicas são usualmente encontradas em neoplasias e, na maioria dos casos, estão correlacionados com o grau clínico do tumor. O conhecimento dessas alterações é especialmente importante nos gliomas, sobretudo pela possibilidade de oferecer ao paciente um melhor prognóstico, ou utilizar essas vias de sinalização como potenciais alvos terapêuticos.

A PTEN (proteína fosfatase e homóloga a tensina) é considerada uma proteína derivada de um gene supressor de tumor importante, presente na porção cromossômica 10q22 – 25, sendo que mutações neste gene estão associadas a vários tipos de câncer (Mirantes et al., 2013). A PTEN age diretamente em fosfatidilinositol-3,4,5 trifosfato (PIP3), removendo o fosfato da posição três do anel inositol, dando origem ao fosfatidilinositol-4,5-bifosfato (PIP2) e assim, antagonizando diretamente a sinalização da via fosfatidilinositol-3-quinase (PI3K), que regula diversos processos celulares como crescimento, capacidade de proliferação, sobrevivência, apoptose, metabolismo e migração celular (Maehama & Dixon, 1999). Em gliomas, ocorre a perda da expressão da PTEN (Holland, 2001), o que influencia diretamente na ativação constitutiva das vias EGFR/PTEN/PI3K/AKT/mTOR, vias centrais responsáveis pela sobrevivência celular. Achados clínicos em gliomas de alto grau sugerem que alterações no gene PTEN estão associadas com um pior prognóstico e podem influenciar a resposta terapêutica (Tang et al., 2011).

Outro fator importante nas células tumorais é a proteína p53. Essa proteína é proveniente de um gene que é ativado em resposta a sinais de dano celular e tem como função a parada do ciclo celular na fase G1. Portanto, antes de ocorrer a duplicação do DNA (fase S), permite o reparo do DNA danificado. A p53 realiza também *check point* da fase S para G2, que depende da integridade do domínio C-terminal do gene e é capaz de indução de apoptose. No entanto, quando a p53 sofre mutações, as células com danos no DNA escapam do reparo destes danos e de sua destruição, podendo iniciar um clone maligno (Nakamura, 2004). Em gliomas, a p53 encontra-se normalmente mutada, acarretando em perda da sua função de supressão tumoral, contribuindo para a malignidade do tumor.



Entretanto, evidências sugerem que somente as alterações genéticas não garantem o desenvolvimento tumoral, mas a soma dos efeitos provocados por alterações das vias de controle de proliferação, sobrevivência, invasão, angiogênese e as interações entre as células tumorais, neurônios, glia, vasculatura e sistema imune, são fundamentais para a tumorigênese, contribuindo para a biologia desses tumores (Holland, 2001; Demuth e Berens, 2004). A Figura 3 resume as principais vias de sinalização que contribuem para a progressão dos gliomas.

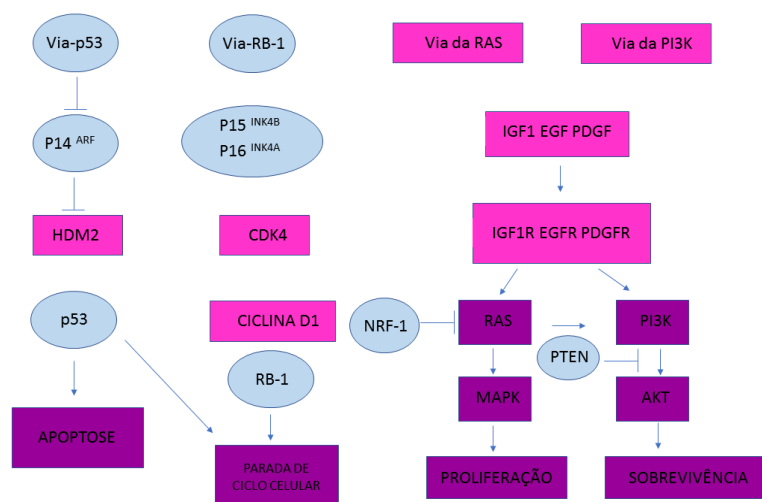


**Figura 3.** Principais vias de sinalizações envolvidas na patogênese dos gliomas. Elementos em azul estão frequentemente inativados por mutação, deleção ou metilação do promotor; elementos em rosa estão ativados através de superexpressão ou amplificação gênica; elementos em roxo são as vias que sofrem modulação dos elementos marcados em azul e em rosa, constituindo as efetoras diretas das ações pró-tumorais (adaptado de Rich e Bigner, 2004). (Via-p53- via de sinalização da proteína supressora tumoral p53, P14<sup>ARF</sup>- proteína supressora tumoral, HDM2- proto-oncoproteína, Via-RB-1- via de sinalização da proteína supressora tumoral retinoblastoma, P15<sup>INK4B</sup>- inibidor de ciclina dependente de quinase 4, CDK4- ciclina dependente de quinase 4, Via da RAS- via de sinalização relacionada a crescimento cancerígeno da proteína RAS, via-PI3K- via de sinalização fosfatidilinositol-3-quinase / serina-treonina quinase, IGF1- Fator de crescimento semelhante à insulina tipo 1, EGF- fator de crescimento epidermal, PDGF- fator de crescimento derivado de plaquetas, IGF1R- receptor de fator de crescimento semelhante à insulina tipo 1, EGFR- receptor de fator de crescimento epidermal, PDGFR- receptor de fator de crescimento derivado de plaquetas, MAPK- Proteína quinases ativadas por mitógenos, AKT- proteína quinase B.

### 1.5 O processo inflamatório e os gliomas

A inflamação é um processo fisiológico, que compreende a resposta biológica do organismo frente à infecção ou dano tecidual, que envolve uma ação em conjunto entre o sistema imunológico e o tecido em que a lesão ocorreu. No caso de uma evolução favorável, o processo inflamatório passa então para fase de reparação, havendo a eliminação do agente causal, a formação de tecido de granulação e a cicatrização

(Katzung, 2016). Entretanto, em algumas situações e doenças, essa resposta pode se tornar excessiva, sem qualquer benefício e com sérios efeitos adversos (Cotran et al., 2000) ou pode haver a cronificação do processo (Katzung, 2016). Estudos populacionais revelam que pacientes que desenvolvem um estado inflamatório crônico apresentam maior risco de desenvolver câncer (Karin et al., 2005) e que a inflamação é um componente crítico também para a progressão tumoral (Bernardi et al, 2013). Além disso, células mediadoras das respostas inflamatórias, como macrófagos, neutrófilos e linfócitos estão presentes na maioria dos tumores sólidos (Maniati et al., 2010) e estudos recentes têm mostrado o envolvimento dessas células imunológicas, principalmente microglia e macrófagos na malignidade do GBM, sendo componente indispensável nos processos de proliferação, migração, sobrevivência celular e angiogênese (Zhai et al., 2011; Azambuja et al, 2017).

Células microgлияis e macrófagos podem se infiltrar significativamente na massa tumoral e parecem favorecer o crescimento do tumor, e não a sua erradicação. Essas células, que em um primeiro momento seriam de defesa, tornam-se hiporresponsivas no microambiente tumoral (Hussain, 2006) e, assim, as células cancerosas conseguem desativar o sistema imunológico existente no local da origem do tumor (Blattman et al., 2004). Ainda, essas células são capazes de secretar certas substâncias que estimulam o crescimento neoplásico (Shurin et al., 2009). As células inflamatórias do tumor, agora infiltrado, são capazes de produzir uma variedade de citocinas que em altos níveis podem contribuir para a malignidade e a metástase de tumores, pois favorecem a invasão e a migração celulares (Yeung et al., 2012). Uma das formas é através da ativação das isoformas de p38/MAPK, que desencadeiam sinais que promovem crescimento, proliferação e diferenciação das células tumorais (Koul et al., 2013). O modelo proposto por Chen e colaboradores (2008) explica como este processo ocorre, em 3 diferentes etapas: (1) Processo de recrutamento: através da produção de citocinas (MCP-1 e IL-8), as células tumorais recrutam as células imunológicas para o microambiente tumoral; (2) Educação: via secreção de citocinas que regulam diferenciação celular (IL-6, TNF $\alpha$  e MIF), as células tumorais induzem as células imunológicas a desempenharem funções de suporte a progressão tumoral e (3) Resposta: as células imunológicas diferenciadas produzem citocinas, hormônios e fatores de crescimento que promovem o crescimento tumoral e o desenvolvimento de tolerância imunológica.

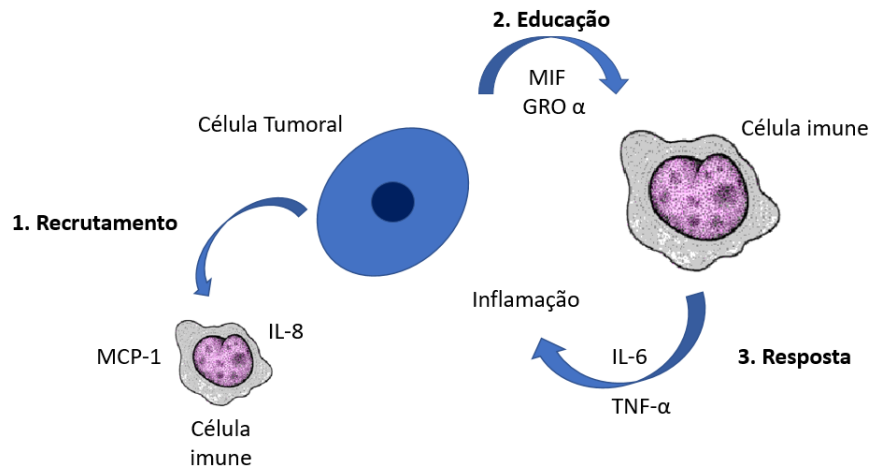


**Figura 4.** Modelo de como as células tumorais “educam” as células imunes a desempenhar função de estímulo a progressão do tumor. MCP-1 (proteína quimiotática de monócitos), IL-8 (Interleucina 8), MIF (Fator inibitório de migração de macrófagos) GRO- $\alpha$  (oncogene regulado por crescimento) IL-6 (Interleucina 6) TNF- $\alpha$  (Fator de crescimento tumoral  $\alpha$ ). (Adaptado de Chen et al, 2008)

Sabe-se também que as células tumorais podem apresentar características similares às células imunológicas, como por exemplo, receptores para migração, secreção de citocinas e expressão de ciclooxigenases (COX), particularmente a COX-2 (Lin e Karin, 2007). As COXs, também chamadas de prostaglandina H sintetases, são enzimas responsáveis pela formação de prostaglandinas (PGs), que estão envolvidas em diferentes processos patológicos, incluindo inflamação e câncer. A COX possui duas importantes isoformas: a COX-1 e a COX-2, e uma terceira isoforma recentemente descoberta, a COX-3, entretanto, essa enzima é uma proteína inativa e resultados demonstram que ela é um “splicing” alternativo da COX-1 (Cebola e Peinado, 2012).

A COX-2 é frequentemente uma enzima induzível e geralmente indetectável na maioria dos tecidos saudáveis, mas seu nível aumenta drasticamente em tecidos inflamados, sendo superexpressa em diversos tipos de cânceres, como em câncer de cólon, próstata e de mama (Higashi et al., 2000; Howe et al., 2001). Em gliomas, além da COX-2 estar superexpressa, a mesma encontra-se associada diretamente a tumores mais agressivos e com um pior prognóstico (Shono et al., 2001). A expressão de COX-2 e seus produtos PGE<sub>2</sub>, em combinação com a liberação de TGF- $\beta$  e a inibição de STAT-3, contribuem para o recrutamento e expansão de células reguladoras T e macrófagos associados a tumores, que modulam ainda mais o ambiente imunossupressivo de gliomas (Hussain, 2012). Neste contexto, estudos sugerem que moléculas com propriedades inibitórias da COX são potenciais agentes anticancerígenos

(Bernardi et al, 2013; Carrett-Dias et al, 2011; Dovizio et al, 2013). Além disso, uma correlação positiva entre a expressão de COX-2 e a menor sobrevida de pacientes com GBM foi relatada (Shono et al, 2011), sugerindo que os inibidores de COX também poderiam ser considerados no tratamento com GBM. Pesquisas *in vivo* já indicaram antiinflamatórios não esteroidais (AINEs), inibidores da COX, como a indometacina e o cetoprofeno, como potenciais agentes antigliomas (Bernardi et al, 2009; Silveira et al, 2013).

Assim, considerando que a presença de infiltrado inflamatório está diretamente correlacionada com o grau de malignidade do GBM, a utilização de moléculas com potencial atividade anti-inflamatória torna-se promissora para a prevenção e o tratamento de gliomas.

### 1.6 Tiazolidinonas

As tiazolidinonas pertencem a um importante grupo de substâncias heterocíclicas. Tais moléculas são heterociclos de 5 membros contendo um átomo de enxofre, um átomo de nitrogênio e uma carbonila (Cunico et al., 2008) (Figura 5). Essa classe de heterociclos possui amplo espectro de atividades biológicas já demonstradas na literatura, tais como antirretroviral (Chen et al., 2011), antifúngica (Verçoza et al, 2009; Kunzler et al, 2013), antimicrobiana (Patel et al., 2012a), antioxidante (Saudane et al., 2012), antibiótica (Feitosa et al, 2012) e recentemente, a atenção tem sido dedicada à construção de novos derivados com ação anti-inflamatória e antitumoral (Jain et al., 2012; Wang et al, 2012; Gouvêa et al; 2016; Da Silva et al, 2016). Essas duas últimas características as tornam uma opção terapêutica interessante para os gliomas, visto que, como vimos, um microambiente inflamatório pode favorecer a progressão tumoral (Leibovich-Rivkinj et al., 2014).

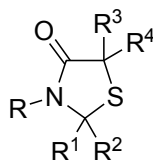


**Figura 5.** Estrutura geral de tiazolidinonas

Uma triagem antitumoral através de diferentes experimentos *in vitro* com várias 4-tiazolidinonas foi realizada pelo Instituto Nacional do Câncer e dois compostos revelaram atividade anticâncer frente à leucemia, melanoma, pulmão, cólon, ovário,

próstata, rins e mama (Havrylyuk, et al 2010). Esses resultados mostram o potencial dessas moléculas como agentes antineoplásicos, sendo os possíveis mecanismos de ação sumarizados na Figura 6.

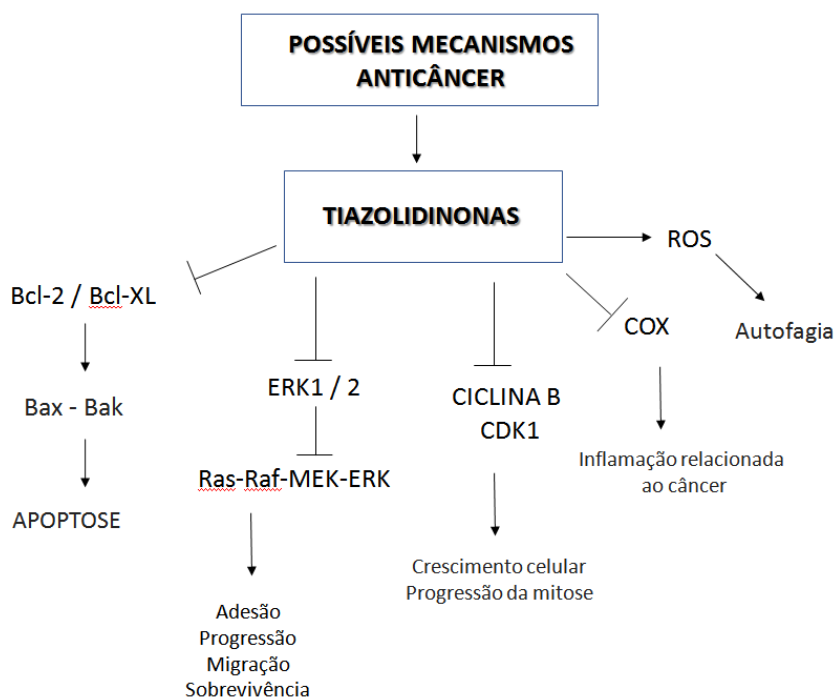


**Figura 6.** Ilustração representativa de vias envolvidas no mecanismo de ação de tiazolidinonas descritas na literatura. Fechas com barra indicam inibição causada pela ação da tiazolidinona, flechas indicam ativação.

Muitos quimioterápicos exercem a atividade anticancerígena ou desencadeando a morte celular apoptótica ou através de propriedades antiproliferativas (Zhang, et al, 2012). Dados da literatura sugerem o envolvimento de compostos derivados de tiazolidinonas induzindo apoptose (Wang et al, 2007; Onen-Bayram et al, 2012) ou agindo como inibidores de COX, controlando assim a inflamação relacionada ao câncer (Leibovich-Rivikin, 2014). O modo de ação desses compostos como indutores de apoptose é relacionado principalmente com a inibição da função Bcl-2/Bcl-XL. Degtrev e colaboradores (2001) relatavam que derivados de 4-tiazolidinonas inibem a heterodimerização Bcl-2/Bcl-xL mediada pelo domínio BH3 na função antiapoptótica, liberando membros pró-apoptóticos da família Bcl-2, os quais dão início à apoptose. No entanto, outras vias de ação anticâncer tem sido relatadas para esses compostos, como inibidores seletivos de regulação do sinal extracelular quinases-1 e 2 (ERK1/2) (Jung et al, 2013) e inibidores de CDK1 (Vassilev et al, 2006; Chandrappa et al, 2009) e CDK1 / ciclina B (Chen et al, 2007). Dados da literatura mostram ainda que derivados de

tiazolidinonas em alguns tipos de câncer como adrenocortical (Cerquett et al, 2011), células leucêmicas (Senkiv et al, 2016) e astrogliomas (Perez-Ortiz et al, 2007) estão ligados à indução de produção de espécies reativas de oxigênio (ROS), podendo esse processo estar relacionado a autofagia (Poillet-Perez et al, 2015). Esses mecanismos constituem possíveis formas de ação das tiazolidinonas como agentes antitumorais. É importante ressaltar que diferentes derivados de tiazolidinonas não apresentaram citotoxicidade para astrócitos primários, sendo seletivos para células tumorais (Silva et al, 2016; Souza et al, 2017). Estes dados apresentados reforçam o interesse e a importância em estudar novos compostos derivados de tiazolidinonas, a fim de verificar a ação farmacológica dos mesmos para o tratamento de gliomas.

### **1.7 Nanocápsulas como mecanismo de liberação de fármacos**

O desenvolvimento de formulações empregando nanotecnologia vêm crescendo no Brasil e no mundo nos últimos anos (Dimer et al, 2013). Nanopartículas poliméricas, nanoemulsões, dendrímeros, nanopartículas lipídicas e lipossomos são sistemas de tamanho submicrométrico e foco de diversas pesquisas de interesse farmacoterapêutico, uma vez que atuam como nanocarreadores. São poucos os fármacos que conseguem associar uma alta eficácia com baixos efeitos colaterais, o que tem estimulado o desenvolvimento de formulações que permitam a liberação controlada de fármacos em sítios específicos, visando à diminuição de efeitos tóxicos e/ou aumento do índice terapêutico. Os sistemas nanométricos apresentam diversas vantagens frente às formulações convencionais, tais como: tamanho reduzido, proteção frente à degradação química e enzimática, controle de liberação, maior facilidade de atravessar as barreiras biológicas e liberação sítio-específica (Guterres, Alves e Pohlmann, 2007; Marcato e Durán, 2008; Perez-Herrero et al, 2015).

Nesse contexto, as nanopartículas poliméricas tornam-se de grande interesse para a emergente área da nanomedicina, uma vez que modificam a tecnologia de entrega de medicamentos (Kulhari et al., 2014). As nanopartículas poliméricas são sistemas carreadores de fármacos constituídos por polímeros biodegradáveis, que apresentam tamanho entre 100-500 nm (Friedrich et al., 2016). Conforme sua composição e organização estrutural podem ser diferenciadas morfologicamente em nanocápsulas e nanoesferas (Mora-Huertas; Fessi; Elaissari, 2010). As nanoesferas são sistemas matriciais, onde o fármaco pode ficar retido ou adsorvido na matriz polimérica (Rawat

et al., 2006) e as nanocápsulas são estruturas vesiculares compostas por um núcleo oleoso, circundado por uma parede polimérica, onde o fármaco fica dissolvido ou disperso no núcleo e/ou adsorvido no material polimérico, Figura 7.

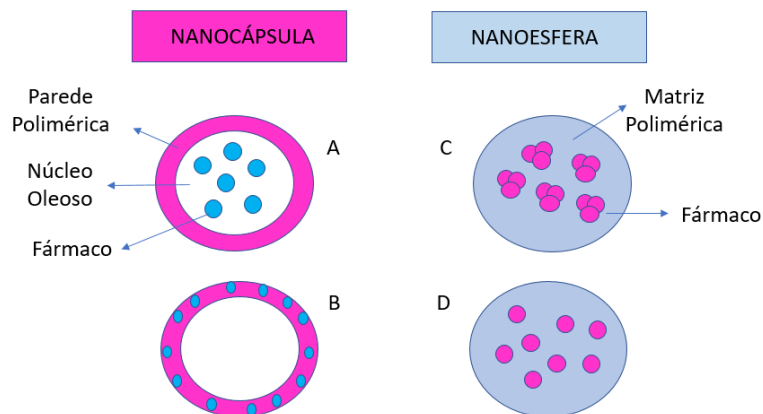


**Figura 7.** Nanopartículas. Ilustração representativa de nanocápsulas e nanoesferas. A- Fármaco dissolvido no núcleo oleoso das nanocápsulas; B- Fármaco adsorvido à parede polimérica das nanocápsulas; C- Fármaco retido na matriz polimérica das nanoesferas; D- Fármaco adsorvido ou disperso molecularmente na matriz polimérica das nanoesferas. (Adaptado de Dos Santos e Fialbo, 2008).

Nanocápsulas poliméricas possuem a capacidade de melhorar a eficácia e a segurança de fármacos, aumentando a sua solubilidade aquosa, protegendo-as da degradação, controlando a liberação do fármaco e melhorando a biodisponibilidade, possuindo seletividade para tecidos específicos (Bernardi et al., 2012; Dimer et al., 2014). Além disso, essa formulação tem a capacidade de reduzir efeitos colaterais e facilitar a penetração de fármacos através da BHE (Kulhari et al., 2014).

O mecanismo de ação para a passagem dessas estruturas pela BHE ainda não está estabelecido, mas alguns autores relatam que o cruzamento pode ocorrer por endocitose (Park, 2009). Portanto, a utilização de nanocápsulas pode ser uma alternativa promissora, por se tratar de uma formulação capaz de atravessar a BHE, chegando ao alvo da doença, e ainda um sistema que permite a liberação controlada do fármaco em locais específicos, visando uma diminuição dos efeitos tóxicos e um aumento do índice terapêutico. A baixa eficácia das terapias convencionais para o tratamento de GBM justifica a busca por alternativas promissoras para aumentar a resposta ao tratamento, bem como reduzir os efeitos adversos, aumentando assim o tempo de sobrevivência dos pacientes.

Sabe-se que as nanocápsulas tem sido muito estudadas para o tratamento do câncer (Bernardi et al, 2013; Arshad et al, 2015; Pérez-Herrero e Fernandez-Medarde, 2015) e nesse contexto, o desenvolvimento de sistemas nanoestruturados vem sendo empregado como uma tentativa de tratamento para o GMB. A tabela 1 sumariza alguns trabalhos recentes empregando nanosistemas para o tratamento de GMB.

**Tabela 1.** Pesquisas recentes envolvendo o uso de nanotecnologia para o tratamento de gliomas.

Nanosistemas	Fármaco	Modelo	Referência
Nanoemulsões (Óleo de romã)	Cetoprofeno	Células de glioma de rato (C6)	FERREIRA et al, 2015
Nanopartículas (PLGA)	Carboplatina	Células de GBM humano (UPAB e SNB19)	ARSHAD et al, 2015
Nanopartículas (PCL)	Carboplatina	Células de glioma humano U87-MG	KARANAM et al, 2015
Nanopartículas (PLGA)	Camptotecina	Modelo <i>in vivo</i> em camundongos	HOUSEOLDER , et al, 2015
Nanopartículas (Ácido hialurônico e quitosana)	Curcumina	Células de glioma de rato (C6)	YANG et al, 2015
Nanocápsulas (PCL)	Cetoprofeno	Modelo <i>in vivo</i> em ratos	DA SILVEIRA et al, 2013
Nanocápsulas (PCL)	Indometacina	Células de glioma de rato (C6) e humanos (U138-MG)	BERNARDI et al, 2013

Outra característica importante das nanopartículas é que elas podem ser revestidas com polímeros hidrofílicos e dessa forma adquirirem a propriedade de escapar da captura pelas células do sistema fagocitário mononuclear. Essa peculiaridade permite que as nanopartículas sejam direcionadas a tecidos altamente permeáveis, resultando num fenômeno de vetorização passiva conhecido como efeito de permeabilidade e retenção aumentada (efeito EPR; do inglês *enhanced permeability and retention effect*) (Granada et al, 2009). Esse efeito, além de tornar as partículas invisíveis ao sistema fagocitário monocítico, também favorece o direcionamento da formulação para o microambiente tumoral e promovem a sua captação (Pérez-Herrero e Fernández-Medarde, 2015).

Esses polímeros em geral apresentam uma cadeia flexível, capacidade de hidrofília, neutralidade elétrica e ausência de grupos funcionais, e com essas propriedades



conseguem evitar a interação com componentes biológicos (Mainairdes et al, 2007). São ainda capazes de fazer uma estabilização estérica, a qual repele as proteínas plasmáticas, e dessa forma consegue impedir a opsonização e a captação pelos macrófagos. Assim, permitem que as partículas tenham um tempo maior de circulação, fazendo com que uma maior concentração de fármaco alcance os tecidos tumorais (Mattheolabakis , Rigas e Constantinides, 2012).

Dentre os polímeros mais utilizados, a poli ( $\epsilon$ -caprolactona) se destaca por possuir biocompatibilidade, ser biodegradável e apresentar propriedades mecânicas, sendo um polímero semicristalino de liberação mais lenta quando comparado à polímeros amorfos (Bernardi et al, 2009; Zanotto-filho et al, 2013). Outra característica importante é a presença de polisorbato 80 (tween 80<sup>®</sup>) que é fundamental para vetorização cerebral (Bernardi et al, 2009; Zanotto-filho et al, 2013). Essas características contribuem para o transporte de fármacos através da BHE e somadas às funções das células endoteliais da BHE na vetorização cerebral através da adesão das nanopartículas com posterior, endocitose, transcitose, inibição da glicoproteína P e modulação das *tight junction*, contribuem para transporte de fármacos para a região cerebral (Frezza et al, 2010).

O uso de sistema nanotecnológico, como as nanocápsulas, vem demonstrando bons resultados em relação ao aumento da eficácia farmacológica no tratamento de gliomas, elas são capazes de favorecer a biodistribuição de compostos para o cérebro (Zanotto-filho et al, 2013). O conjunto de dados já referidos somados ainda a capacidade dessas partículas em atingir tumores sólidos com maior facilidade, principalmente porque podem ter sua superfície modificada e ainda visando uma liberação sítio-específica que ocorrem através do aumento de permeação e retenção vascular do fármaco especificamente nos tecidos tumorais sólidos (Pérez-Herrero e Fernandez-Medarde, 2015; Souza, 2013), neste trabalho, além de testar o potencial das tiazolidinonas na sua forma livre, também damos início ao estudo de uma formulação de nanocápsulas poliméricas contendo essas moléculas.

## **2. Objetivos**

### **2.1. Objetivo Geral**

O objetivo geral desse trabalho foi avaliar o potencial terapêutico de compostos derivados de tiazolidinonas para o tratamento de gliomas.

### **2.2. Objetivos específicos**

#### **Capítulo 1**

- Avaliar se uma série de 16 moléculas de tiazolidinonas afeta os parâmetros de viabilidade, proliferação e morte celular na linhagem C6 de glioblastoma multiforme.
- Verificar se as tiazolidinonas induzem citotoxicidade em culturas primárias de astrócitos;
- Avaliar, através do modelo de implante de glioma em cérebro de ratos, se as tiazolidinonas possuem atividade antitumoral *in vivo*.
- Avaliar se os níveis de óxido nítrico no soro de animais submetidos ao implante de glioma e tratados com compostos de tiazolidinonas está alterado.
- Avaliar se os compostos de tiazolidinonas apresentam hepato e nefrotoxicidade quando administrados *in vivo*.

#### **Capítulo 2**

- Desenvolver nanocápsulas contendo compostos de tiazolidinonas.
- Comparar o efeito de compostos de tiazolidinonas na forma livre e em nanocápsulas sobre a viabilidade e proliferação *in vitro* da linhagem C6 de glioblastoma multiforme.
- Verificar a citotoxicidade de nanocápsulas contendo compostos de tiazolidinonas em cultura primária de astrócitos.
- Avaliar se as nanocápsulas contendo os compostos de tiazolidinonas apresentam hepato e nefrotoxicidade e alteram parâmetros de estresse oxidativo quando administradas *in vivo*.

### **Capítulo 3**

- Sintetizar uma nova classe de moléculas de tiazolidinonas.
- Avaliar a atividade anti-inflamatória *in vivo* dos compostos de tiazolidinonas.
- Avaliar o efeito de compostos de tiazolidinonas sobre a viabilidade da linhagem C6 de glioblastoma multiforme.
- Verificar se os compostos de tiazolidinonas induzem citotoxicidade em culturas primárias de astrócitos.

Artigo publicado pela revista “Chemico-Biological Interactions”

Synthetic 2-aryl-3-((piperidin-1-yl)ethyl)thiazolidin-4-ones exhibit selective *in vitro* antitumoral activity and inhibit cancer cell growth in a preclinical model of glioblastoma multiforme.

Elita F. da Silveira<sup>1\*</sup>, Juliana H. Azambuja<sup>2</sup>, Taíse Rosa de Carvalho<sup>3</sup>, Alice Kunzler<sup>3</sup>, Daniel S. da Silva<sup>3</sup>, Fernanda C. Teixeira<sup>3</sup>, Rodrigo Rodrigues<sup>3</sup>, Fátima T. Beira<sup>4</sup>, Rita de Cássia Sant Anna Alves<sup>5</sup>, Roselia M. Spanevello<sup>3</sup>, Wilson Cunico<sup>3</sup>, Francieli M. Stefanello<sup>3</sup>, Ana P. Horn<sup>1</sup> and Elizandra Braganhol<sup>2\*</sup>.

<sup>1</sup>Programa de Pós-Graduação em Ciências Fisiológicas, Departamento de Morfologia, Instituto de Ciências Biológicas, Universidade Federal do Rio Grande, Rio Grande, RS, Brasil.

<sup>2</sup>Departamento de Ciências Básicas da Saúde, Universidade Federal de Ciências da Saúde de Porto Alegre, Porto Alegre, RS, Brasil.

<sup>3</sup>Laboratório de Química Aplicada à Bioativos, Centro de Ciências Químicas, Farmacêuticas e de Alimentos, Universidade Federal de Pelotas, Pelotas, RS, Brasil.

<sup>4</sup>Departamento de Fisiologia e Farmacologia, Instituto de Biologia, Universidade Federal de Pelotas, Pelotas, RS, Brasil.

<sup>5</sup>Departamento de Patologia e de Medicina Legal, Universidade Federal de Ciências da Saúde de Porto Alegre, Porto Alegre, RS, Brasil.

**\*Corresponding Authors**

Elita Ferreira da Silveira (elitafs24@gmail.com)

Universidade Federal de Rio Grande - FURG

Avenida Itália, Km 8, Campus Carreiros

CEP: 96.203-900, Rio Grande, RS, Brasil Phone: +55 53 3293 6987

Elizandra Braganhol (e-mail: ebraganhol@ufcspa.edu.br)

Universidade Federal de Ciências da Saúde (UFCSPA)

Rua Sarmiento Leite, 245 – Prédio Principal – sala 304

CEP: 90.050-170, Porto Alegre, RS, Brasil Phone: +55 51 3303 8762

## **Abstract**

Glioblastoma multiforme (GBM) is the worst form of primary brain tumor, which has a high rate of infiltration and resistance to radiation and chemotherapy, resulting in poor prognosis for patients. Recent studies show that thiazolidinones have a wide range of pharmacological properties including antimicrobial, anti-inflammatory, anti-oxidant and anti-tumor. Here, we investigate the effect antiglioma in vitro of a panel of sixteen synthetic 2-aryl-3-((piperidin-1-yl)ethyl)thiazolidin-4-ones where 13 of these decreased the viability of the glioma cells 30 to 65% (100 $\mu$ M ) compared with controls. The most promising compounds such as **4d**, **4l**, **4m** and **4p** promoted glioma reduction of viability greater than 50%, were further tested at lower concentrations (12.5, 25, 50 and 100  $\mu$ M). Also, the data showed that the compounds **4d**, **4l**, **4m** and **4p** induced cell death primarily through necrosis and late apoptosis mechanisms. Interestingly, none of these 2-aryl-3-((piperidin-1-yl)ethyl)thiazolidin-4-ones were cytotoxic for primary astrocytes, which were used as a non-transformed cell model, indicating selectivity. Our results also show that the treatment with sub-therapeutic doses of 2-aryl-3-((piperidin-1-yl)ethyl)thiazolidin-4-ones (**4d**, **4l** and **4p**) reduced in vivo glioma growth as well as malignant characteristics of implanted tumors such as intratumoral hemorrhage and peripheral pseudopalisading. Importantly, 2-aryl-3- ((piperidin-1-yl)ethyl) thiazolidin-4-ones treatment did not induce mortality or peripheral damage to animals. Finally, 2-aryl-3-((piperidin-1-yl)ethyl)thiazolidin-4-ones also changed the nitric oxide metabolism which may be associated with reduced growth and malignity characteristics of gliomas. These data indicates for the first time the therapeutic potential of synthetic 2-aryl-3-((piperidin-1-yl)ethyl)thiazolidin-4-ones to GBM treatment.

**Keywords:** thiazolidinones, C6 glioma, astrocytes, cell death.

## 1. Introduction

Glioblastoma multiforme (GBM) is the most common and lethal primary brain tumor, exhibiting morphological and gene expression similarities with glial cells such as astrocytes, oligodendrocytes and its precursors [1]. Additionally, the presence of an inflammatory microenvironment composed of non-malignant cells, such as immune cells and fibroblasts, is associated with increased malignancy through modulation of glioma cell proliferation and angiogenesis, which results in a poor prognosis for patients and a challenge for oncology [2-3].

The most common treatment for GBM is the surgical resection, whenever possible, [4], followed by radio and chemotherapy with temozolomide (TMZ) that is maintained as an adjuvant therapy for at least six months [5]. However, these tumors are resistant to therapeutic strategies and their high rate of proliferation and infiltrative growth patterns precludes curative neurosurgery, resulting in a low rate survival of 12 months for patients [6]. In addition, the blood-brain barrier (BBB) limits the drug delivery to central nervous system (CNS), favoring the development of chemoresistance [7]. As an alternative for the treatment, lipophilic compounds stand out because they have the ability to overcome BBB, reaching the target site of disease [7].

Recent studies have been reported the potential of biologically active five-membered thiazolidinones. Such heterocyclic class has occupied a prominent position in the medicinal chemistry field [8-9]. There are reports showing the wide range of pharmacological properties of thiazolidinones, including antimicrobial [10], anti-inflammatory [11], antioxidant [12] and anti-tumor activities [13]. These molecules are also considered peroxisome proliferator-activated (PPAR) receptors agonists showing hypoglycemic, antineoplastic and anti-inflammatory activities [14]. The mechanisms by which synthetic thiazolidinones contribute to anti-tumoral activity remain controversial. However, data from literature suggest the involvement of these compounds in the control of cell proliferation by inducing apoptosis [15-16] or by acting as inhibitors of cyclooxygenases, which seems to be important in the cancer-related inflammation by producing inflammatory mediators related to angiogenesis [17].

Considering the important biological properties of thiazolidinones and that the actions described can be important for the treatment of GBM, this study aimed to investigate *in vitro* and *in vivo* antiproliferative activity and therapeutic potential of synthetic 2-aryl-3-((piperidin-1-yl)ethyl)thiazolidin-4-ones for the treatment of gliomas.



## 2. Materials and methods

**Reagents.** Dulbecco's modified Eagle's medium (DMEM), Fungizone, penicillin/streptomycin, 0.25 % trypsin/EDTA solution and fetal bovine serum (FBS) were obtained from Gibco (Gibco BRL, Carlsbad, CA, USA). All other chemicals and solvents used were of analytical or pharmaceutical grade.

**Thiazolidinone synthesis.** The 2-aryl-3-((piperidin-1-yl)ethyl)thiazolidin-4-ones **4a-p** were synthesized by one-pot reactions from 1-(2-aminoethyl)piperidine, arenealdehydes and mercaptoacetic acid in according to a previous paper published by us [18]. Analogues thiazolidinones containing arenealdehydes groups substituted by electron-withdrawing (F, Cl, NO<sub>2</sub>) or electron-releasing groups (OH, OCH<sub>3</sub>, CH<sub>3</sub>) at 2- 3- and 4-positions were used to study the cytotoxic potential. The general structure of thiazolidinones **4a-p** is shown in Figure 1.

### **General cell culture procedures.**

**i) Glioma cultures.** Rat C6 malignant glioma cell line was obtained from American Type Culture Collection (Rockville, MD, USA). Cells were grown and maintained in low-glucose DMEM containing 0.1% fungizone and 100 U/L penicillin/streptomycin and supplemented with 5% FBS. Cells were kept at 37°C in a humidified atmosphere with 5% CO<sub>2</sub>.

**ii) Primary astrocyte cultures.** Astrocyte cultures were prepared as follow: cortex of newborn Wistar rats (1-2 days old) were removed and dissociated mechanically in a Ca<sup>+2</sup> and Mg<sup>+2</sup> free balanced salt solution (pH 7.4; 137 mM NaCl, 5.36 mM KCl, 0.27 mM Na<sub>2</sub>HPO<sub>4</sub>, 1.1 mM KH<sub>2</sub>PO<sub>4</sub>, and 6.1 mM glucose). After centrifugation at 1,000 g for 5 min, the pellet was suspended in DMEM supplemented with 10% FBS. The cells (5×10<sup>4</sup>) were seeded in poly-L-lysine-coated 96-well plates. Following 4 h of seeding, plates were gently shaken and washed with PBS and medium was changed to remove neuron and microglia contaminants. Cultures were allowed to grow to confluence by 20-25 days. Medium was replaced every 4 days [19-20]. The procedures were approved by the Ethics Committee of Federal University of Pelotas (Protocol number 9219).

**In vitro cell culture treatment.** Sixteen synthetic 2-aryl-3-((piperidin-1-yl)ethyl)thiazolidin-4-ones (**4a** to **4p**) were firstly dissolved in sterile DMSO at the concentration

of 100 mM (stock solution) and further diluted in DMEM with 5% (glioma) or 10% (astrocytes) FBS to obtain 12.5, 25, 50 and 100  $\mu\text{M}$ . The C6 glioma cell line was seeded at  $1 \times 10^3$  cells/well in DMEM/5% FBS in 96 multiwell plates in a final volume of 100  $\mu\text{L}$  and the cells were allowed to growth for 24 h. Astrocyte cultures were prepared as described above. Cell cultures were exposed to synthetic 2-aryl-3-((piperidin-1-yl)ethyl) thiazolidin-4-ones (12.5 to 100  $\mu\text{M}$ ) for 48 or 72 h. Appropriate controls containing DMEM 5%/10% FBS or 0.01% DMSO were performed.

**Cell viability assay.** Dehydrogenases-dependent 3-(4,5-dimethyl)-2,5-diphenyl tetrazolium bromide (MTT) reduction was used to estimate viability of glioma and astrocyte cell cultures. This method is based on the ability of viable cells to reduce MTT and form a blue formazan product. MTT solution (sterile stock solution of 5 mg/mL) was added to the incubation medium in the wells at a final concentration of 0.5 mg/mL. The cells were left for 60 min at 37°C in a humidified 5%  $\text{CO}_2$  atmosphere. The medium was then removed and plates were shaken with DMSO for 30 min. The optical density of each well was measured at 492 nm and results were expressed as absorbance [21].

**Propidium iodide assay.** Cell damage was assessed by fluorescent image analysis of propidium iodide (PI) uptake. At the end of the treatments, C6 glioma and astrocyte cell cultures were incubated with PI (7.5  $\mu\text{M}$ ) for 1 h. PI fluorescence was excited at 515–560 nm using an inverted microscope (Olympus IX71, Tokyo, Japan) fitted with a standard rhodamine filter. Images were captured using a digital camera connected to the microscope.

**Annexin-V binding assay.** C6 glioma cells were subcultured into 6-well plates ( $5 \times 10^4$  cells/well) and were treated with synthetic 2-aryl-3-((piperidin-1-yl)ethyl) thiazolidin-4-ones (**4d**, **4l**, **4m** and **4p**; 100  $\mu\text{M}$ ) for 72 h. Control and treated cells were trypsinized and externalized phosphatidylserine was labeled with annexin V and PI (Life Technologies; Waltham, MA, USA) following the manufacturer's instructions. Viable (annexin<sup>-</sup>/PI<sup>-</sup>), apoptotic (annexin<sup>+</sup>/PI<sup>-</sup>) and late apoptotic/necrotic (annexin<sup>+</sup>/PI<sup>+</sup>) cells were characterized as previously described [22] in an Attune FACS (Applied Biosystems, Waltham, MA, USA).

***Glioma implantation.*** C6 glioma cells were cultured to approximately 70% confluence and a total of  $1 \times 10^6$  cells in 3  $\mu$ L DMEM/ 5% FBS was injected in the right striatum at a depth of 6.0 mm (coordinates with regard to bregma: 0.5 mm posterior and 3.0 mm lateral) of male Wistar rats (250-350 g, 8 weeks old) anesthetized by intraperitoneal (*i.p.*) administration of ketamine and xilazine [23]. All procedures used in the present study followed the Principles of Laboratory Animal Care from NIH and the Brazilian laws and were approved by the Ethical Committee of the Federal University of Pelotas (Protocol number 9219).

***Treatment of animals.*** Five days after glioma implantation, the animals were randomly divided into four groups as follows: (1) Control (DMSO-treated); (2) 2-(2-chlorophenyl)-3-((piperidin-1-yl)ethyl)thiazolidin-4-one **4d** (3) 2-(2-methoxyphenyl)-3-((piperidin-1-yl)ethyl) thiazolidin-4-one **4l**; (4) 2-(2,6-chlorophenyl)-3-((piperidin-1-yl)ethyl)thiazolidin-4-one **4p** (treated with 5mg/Kg/day of thiazolidin-4-ones dissolved in DMSO). The treatment was administered *i.p.* to the animals for 15 consecutive days. After 20 days (5 days for glioma implantation+15 days for treatment), the rats were decapitated and the entire brain was removed, sectioned and fixed with 10% paraformaldehyde (pH 7.4). Blood samples were collected from all animals for posterior enzymatic assays (alanine aminotransferase, aspartate aminotransferase, creatinine urea and C-reactive protein) using commercial kits (Labtest).

***Pathological analysis and tumor volume quantification.*** The fixed tissue sections were sectioned and stained with hematoxylin–eosin (HE) and pathological analysis of at least three slides was carried out by a pathologist in a blinded manner. Glioma cell proliferation was assessed by counting the number of mitotic glioma cell nuclei in ten randomly chosen fields ( $\times 200$ ) per tumor (Olympus America Inc., Center Valley, PA, USA). Tumor size was quantified by analyzing images captured with a digital camera connected to a microscope with Image Tool Software (Department of Dental Diagnostic Science, The University of Texas Health Science Center, San Antonio, TX, USA). The total volume ( $\text{mm}^3$ ) of the tumor was computed by summing the segmented areas and by multiplication of the slice resolution [24].

**Nitrite determination.** The amount of NO formed was estimated by measuring nitrite levels in serum of glioma-implanted rats by Greiss reaction [25]. Briefly, 100  $\mu$ L of samples were mixed with 100  $\mu$ L sulfanilamide in 5% phosphoric acid, followed by a incubation of 10 min at room temperature. Then, 100  $\mu$ L n-1 l-naphthylethylenediamine (NED) 0.1% was added to the samples and incubated in the dark for 10 min to complete the reaction. The absorbance was determined in a spectrophotometer at 540 nm. The amount of nitrite in the serum was compared to a standard curve of known concentrations of sodium nitrate. Data was expressed as nmolar of NO.

**Statistical analysis.** Data were expressed as mean  $\pm$  standard deviation. The comparisons of means were analyzed by one-way analysis of variance (ANOVA) followed by Tukey *post hoc* test when the F value was significant. Differences between mean values were considered significant when  $P \leq 0.05$ . Analyses were performed using Prism GraphPad Software.

## Results

**Synthetic 2-aryl-3-((piperidin-1-yl)ethyl)thiazolidin-4-ones selectively decreases C6 glioma cell viability but not in astrocytes.** The potential antiglioma activity of synthetic 2-aryl-3-((piperidin-1-yl)ethyl)thiazolidin-4-ones **4a-p** was evaluated. First, we determined whether the 16 different 2-aryl-3-((piperidin-1-yl)ethyl)thiazolidin-4-ones may reduce the C6 glioma cell viability (Fig. 2). To answer this question, glioma cell cultures were exposed to 100  $\mu$ M of 2-aryl-3-((piperidin-1-yl)ethyl)thiazolidin-4-ones and cell viability was evaluated by MTT assay following 48 h of treatment. Cells exposed to 0.01% DMSO were considered control. As shown in Figure 2, all sixteen synthetic 2-aryl-3-((piperidin-1-yl)ethyl)thiazolidin-4-ones, except **4b**, **4f** and **4k**, were effective to decrease around 30% to 65% the glioma cell viability when compared to control, which indicates the antiglioma potential of this class of heterocycles. Four of them (**4d**, **4l**, **4m** and **4p**) reduced more than 50% the glioma viability, 55%, 54%, 65% and 62%, respectively. These compounds were selected for further tests in a time-concentration curve responses (Fig. 3). Glioma treatment with different 2-aryl-3-((piperidin-1-yl)ethyl)thiazolidin-4-ones concentrations (12.5, 25, 50 and 100  $\mu$ M) was carried out by 48 and 72 h (Fig. 3, panels A-H). Overall, the treatment of C6 glioma cell line with synthetic 2-aryl-3-((piperidin-1-yl)ethyl)thiazolidin-4-ones resulted in a

decrease of cell viability when compared to control, exhibiting concentration and time dependence profiles, particularly for **4d** and **4p** molecules. When cells were exposed to **4d**, the decrease of cell viability after 48 h and 72 h of treatment ranged from 18 to 78% (Fig. 3, panels A and B). The compounds **4l** and **4m** promoted a reduction of cell viability after 48 and 72 h only at the highest concentration (100  $\mu$ M; Fig. 3, panels C to F). The 2-(2,6-chlorophenyl)-3-((piperidin-1-yl)ethyl)thiazolidin-4-one **4p** showed the best result after 48 h of treatment, reducing 31% and 66% cell viability at 50  $\mu$ M and 100  $\mu$ M, respectively; following 72 h of treatment the reduction of cell viability ranged from 47% to 82% for 25, 50 and 100  $\mu$ M (Fig. 3; panels G and H). In parallel, primary astrocyte cultures were used as a non-transformed cell model to assess the selectivity of thiazolidinones (Fig. 3, panels I and J). Notably, only at 100  $\mu$ M the compound **4p** promoted significant astrocyte cytotoxicity after 72 h exposure. The other compounds do not cause any significant changes in cell growth of astrocytes at this concentration.

***2-aryl-3-((piperidin-1-yl)ethyl)thiazolidin-4-ones promote C6 glioma cell death via necrosis and late apoptosis-dependent pathways.*** Membrane cell permeability was evaluated by PI incorporation in glioma and astrocyte cultures following **4d**, **4l**, **4m** and **4p** (100  $\mu$ M) treatment for 72 h (Fig. 4, panels A, B and C). In addition to decrease cancer cell viability, thiazolidinones also promoted a significant reduction of glioma cell density, morphological alterations and PI incorporation when compared to control (Fig. 4A). Of note, no alterations were observed in astrocytes exposed to 2-aryl-3-((piperidin-1-yl)ethyl)thiazolidin-4-ones (Fig. 4B). These results suggest that the anti-proliferative effect of 2-aryl-3-((piperidin-1-yl)ethyl)thiazolidin-4-ones is selective to cancer cells and it may be mediated by necrosis. However, the involvement of other cell death pathways cannot be excluded.

To better evaluate the mechanisms involved in the suppression of cancer cell proliferation, C6 cells were exposed to 2-aryl-3-((piperidin-1-yl)ethyl)thiazolidin-4-ones **4d**, **4l**, **4m** and **4p** (100  $\mu$ M) for 72 h and then the externalization (flip-flop) of phosphatidylserine and/or PI staining was evaluated by flow cytometry (Fig. 4C). 2-(2-chlorophenyl)-3-((piperidin-1-yl)ethyl)thiazolidin-4-one **4d** promoted a reduction of ~25% of C6 glioma viable cells and induced mainly late apoptosis in 17% cell population (Annexin<sup>+</sup>/PI<sup>+</sup>). The compound **4l** decreased in ~79% the glioma cell

viability and elicited necrosis in majority of C6 cells, totalizing 44% cell population (Annexin<sup>-</sup>/PI<sup>+</sup>) and late apoptosis in 33% of death cells (Annexin<sup>+</sup>/PI<sup>+</sup>). 2-(3-methoxyphenyl)-3-((piperidin-1-yl)ethyl)thiazolidin-4-one **4m** reduced in ~16% the population of viable cells, inducing cell death mainly by late apoptosis in 10% of cells (Annexin<sup>+</sup>/PI<sup>+</sup>). Finally, 2-(2,6-chlorophenyl)-3-((piperidin-1-yl)ethyl)thiazolidin-4-one **4p** was cytotoxic to ~78% of glioma cells and elicited early apoptosis in 5% cell population (Annexin<sup>+</sup>/PI<sup>+</sup>), necrosis in 29% (Annexin<sup>-</sup>/PI<sup>+</sup>) and late apoptosis in 44% (Annexin<sup>+</sup>/PI<sup>+</sup>). Taken together, these results suggest that these 2-aryl-3-((piperidin-1-yl)ethyl)thiazolidin-4-ones induced C6 cell death by modulating mainly necrosis and late apoptosis cell death pathways.

***Synthetic 2-aryl-3-((piperidin-1-yl)ethyl)thiazolidin-4-ones inhibit in vivo GBM growth and do not cause mortality and metabolic toxicity in rats.*** 2-aryl-3-((piperidin-1-yl)ethyl)thiazolidin-4-ones **4d**, **4l** and **4p** exhibited promising antiglioma activity *in vitro* as evidenced by flow cytometry analysis, we further evaluated the potential of such compounds to inhibit *in vivo* GBM growth. Glioma cells were implanted by intracranial cell injection in adult Wistar rats as described in material and methods. The rat glioma model is a useful *in vivo* tool for evaluating anticarcinogenic properties of promising molecules, since the tumor is induced in immunocompetent animals, thus reproducing the inflammatory microenvironment of the GBM [26]. The animals were treated with 2-aryl-3-((piperidin-1-yl)ethyl)thiazolidin-4-ones **4d**, **4l** and **4p** exhibited promising antiglioma activity *in vitro* as evidenced by flow cytometry analysis, we further evaluated the potential of such compounds to inhibit *in vivo* GBM growth. (5 mg/kg/day) for 15 days. Control group received equivalent volume of DMSO (vehicle). Twenty days after glioma implantation rat brains were fixed and tissue blocks were processed for HE staining. 2-aryl-3-((piperidin-1-yl)ethyl)thiazolidin-4-ones **4d**, **4l** and **4p** treatment reduced in 45% ( $112.3 \pm 17.0 \text{ mm}^3$ ), 73% ( $56.8 \pm 25.0 \text{ mm}^3$ ) and 50% ( $101.8 \pm 39.0 \text{ mm}^3$ ) tumor volume, respectively, when compared to control ( $201.9 \pm 41.9 \text{ mm}^3$ ) (Fig. 5). Pathological analysis revealed that 2-aryl-3-((piperidin-1-yl)ethyl)thiazolidin-4-ones treatment also reduced pathological characteristics related to increased glioma malignancy (Fig. 5; Table 1), including intratumoral hemorrhage, peritumoral edema and peripheral pseudopalisading (Table 1). In addition, a significant decrease in the mitotic index in **4l** treated group was observed (Table 1). It has been shown that nitric oxide production conferrers chemoresistance in

gliomas, promotes neovascularization and tumor invasiveness acting adversely on patient outcome [27-28]. As shown in Figure 6, both **4d** and **4p** treatment decreased the production of NO from glioma-bearing rats when compared to control (60% and 70%, respectively) (Fig. 6). Importantly, the treatment did not cause mortality or exercised toxicity evaluated from ALT and AST activity (liver damage markers); creatinine and serum urea levels (kidney damage markers); CRP (inflammation marker) (Table 2). Taken together, these results support the idea that 2-aryl-3-((piperidin-1-yl)ethyl)thiazolidin-4-ones exhibit promising anti-glioma activity without promoting peripheral toxicity.

## Discussion

Although intense effort to develop new therapies to improve the median survival of patients diagnosed with GBM, effective strategies are still lacking and GBM remains a challenge to oncology. Furthermore the high glioma proliferation and invasion rates represent an obstacle for most antineoplastic agents [29]. In this context, the class of heterocyclic thiazolidinones exhibit valuable biological applications in medicine as antitumor, anticonvulsant, antimicrobial, and anti-tuberculosis [30]. The present work demonstrates that a serie of 2-aryl-3-((piperidin-1-yl)ethyl)thiazolidin-4-ones previously synthesized by our group exhibit *in vitro* and *in vivo* antiglioma activity. Firstly, a screening of sixteen 2-aryl-3-((piperidin-1-yl)ethyl)thiazolidin-4-ones was performed to evaluate *in vitro* glioma cell viability and revealed the **4d**, **4l**, **4m** and **4p** as the most promising ones. Further *in vitro* experiments showed that such molecules exhibited no toxicity to normal astrocytes, indicating selectivity to cancer cells. Finally, treatment with **4d**, **4l** and **4p** in a rat glioma model confirmed the antiglioma activity *in vivo* without inducing peripheral toxicity to the animals.

Studies show that the antitumor properties of 4-thiazolidinones and heterocycles related are probably due to its affinity to modulate anticancer targets as JNK pathway [31], tumor necrosis factor TNF [32], anti-apoptotic Bcl-xL-BH3 [33] and avb3 integrin receptor [34]. Here we demonstrated that among of the 16 molecules tested, four (**4d**, **4l**, **4m** and **4p**) induced more than 50% of cytotoxicity at the highest concentration tested (100  $\mu$ M) and that the antiglioma activity remains at lower concentrations (12.5, 25, and 50  $\mu$  M), indicating an efficient antitumor activity. In this study, the aryl group attached at thiazolidine ring was substituted with 2-, 3- and 4- positions by electron-withdraw or electron-release groups. Our findings shows that the type of electronic effect of

substituent on aryl did not change the activity, however, we emphasize that the most promising results were obtained for thiazolidinones containing 2-substituted aryl groups, suggesting that the ortho position on aryl ring is important to reduce the viability of the glioma cells, since this position was substituted in three of the four most active compounds (**4d**, **4l** and **4p**). Confirming our findings, addition of two groups ortho (2,6-Cl, **4p**) further enhances the reduction activity of glioma cell viability. In accordance, data from literature show that promising biological activity of derivatives of 4-thiazolidinones can be attributed to substituent groups that cause changes in the physico-chemical and structural patterns of such synthetic compounds [35].

Thiazolidinones also promote a significant decrease in the glioma cell density, leading to morphological changes and necrosis/late apoptosis induction. Normally, changes on cell survival, as well as in cell damage, are secondary characteristics after cell cycle deregulation and apoptosis [36]. In this regard, studies show that some classes of thiazolidinones can inhibit tubulin polymerization, leading to cell cycle arrest and apoptosis [37]. Taken together, these results suggest that the series of 2-aryl-3-((piperidin-1-yl)ethyl)thiazolidin-4-ones tested induces C6 glioma death by modulating cell pathways related to cell survival.

In addition, as the most promising results were obtained with molecules containing 2-substituted groups (**4d**, **4l** and **4p**), we further performed *in vivo* analysis in a preclinical model of glioma. The treatment with 2-aryl-3-((piperidin-1-yl)ethyl)thiazolidin-4-ones **4d**, **4l** and **4p** significantly reduced *in vivo* glioma growth as well as the malignancy characteristics. Of note, treatment with these 2-aryl-3-((piperidin-1-yl)ethyl)thiazolidin-4-ones did not result in mortality or induced liver/kidney damage. Although it was demonstrated that NO may modulate negatively *in vivo* tumor growth, some studies indicate that it could promote metastasis or cancer-related inflammation depending on cell microenvironment, NO levels, redox status, cell type and adaptation [38]. In our work, two compounds which exhibit 2-Cl substituent (**4d** and **4p**) were able to decrease the production of NO, and among them, **4p** which has two chloro substituents (2,6-Cl) was able to further decrease NO levels. These data suggest that chloro substituent seems to be important to inhibit the production of NO. We suggest that the reduction of NO levels may explain the anticancer activity of **4d** and **4p**. However, the 2-(2-methoxyphenyl)-3-((piperidin-1-yl)ethyl)thiazolidin-4-one **4l** which has 2-OCH<sub>3</sub> group as substituent did not alter the nitric oxide synthase activity, being its anticancer activity independent of this effect.



In conclusion, our data show at first time the antitumor potential of 2-aryl-3-((piperidin-1-yl)ethyl)thiazolidin-4-ones. In addition, our results suggest that the position of the substituent of aryl group in 2-aryl-3-((piperidin-1-yl)ethyl)thiazolidin-4-ones can be an important factor for antitumor efficiency, since three of the best 2-aryl-3-((piperidin-1-yl)ethyl)thiazolidin-4-ones have a substituent at 2-position of the phenyl ring. Finally subtherapeutic doses of 2-aryl-3-((piperidin-1-yl)ethyl)thiazolidin-4-ones were efficient to decrease the tumor growth and malignant characteristics in a pre-clinical model of gliomas, suggesting these compounds as a possible novel therapeutic modality for the treatment of brain tumors in the future.

### **Compliance with Ethical Standards**

Conflict of interest statement:

Elita F. da Silveira declares that she has no conflict of interest.

Juliana H. Azambuja declares that she has no conflict of interest.

Táise Rosa de Carvalho declares that she has no conflict of interest.

Alice Kunzler declares that she has no conflict of interest

Daniel S. da Silva declares that he has no conflict of interest

Fernanda C. Teixeira declares that she has no conflict of interest

Rodrigo Rodrigues declares that he has no conflict of interest

Fátima T. Beira declares that she has no conflict of interest

Rita de Cássia Sant Anna Alves declares that she has no conflict of interest

Roselia M. Spanevello declares that she has no conflict of interest

Wilson Cunico declares that he has no conflict of interest

Francieli M. Stefanello declares that she has no conflict of interest

Ana P. Horn declares that she has no conflict of interest

Elizandra Braganhol declares that she has no conflict of interest

### **Funding**

This work was supported by the Brazilian agencies: Conselho Nacional de Desenvolvimento Científico e Tecnológico (CNPq – Grant number 482055/2013-8), Coordenação de Aperfeiçoamento de Pessoal de Nível Superior (CAPES) and Fundação de Amparo à Pesquisa do Estado do Rio Grande do Sul (FAPERGS – Grant number 11/2068-7). E.F. da Silveira, J.H. Azambuja, A. Kunzler and D. Silva were recipients of CAPES fellowship.

## **Ethical approval**

All applicable international, national, and/or institutional guidelines for the care and use of animals were followed. All procedures used in the present study followed the Principles of Laboratory Animal Care from NIH and the Brazilian laws and were approved by the Ethical Committee of the Federal University of Pelotas (Protocol number 9219).

## **References**

1. Holland EC (2001). Progenitor cells and glioma formation. *Current Opinion in Neurology* 14(6):683-8.
2. Nieto-Sampedro, M., Valle Argos, B., Gómez-Nicola, D., Fernández-Mayoralas, A., NietoDiaz, M (2011). Inhibitors of Glioma Growth that Reveal the Tumour to the Immune System. *Clin. Med. Insights Oncol* 5: 265-314.
3. Borisov KE, Sakaeva DD (2015). The immunosuppressive microenvironment of malignant gliomas. *Arkh Patol* 77: 54–63.
4. Louis DN, Ohgaki H, Wiestler OD, Cavenee WK, Burger PC, Jouvet A, Scheithauer BW, Kleihues P (2007). The 2007 WHO classification of tumours of the central nervous system. *Acta Neuropathol.* 114(5):547.
5. Mrugala MM (2013). Advances and challenges in the treatment of glioblastoma: a clinician's perspective. *Discov Med*, v. 15, n 83, p. 221-30.
6. Stupp R, Hegi ME, Gilbert MR, Chakravarti A (2007). Chemoradiotherapy in malignant glioma: standard of care and future directions. *J Clin Oncol*; 25: 4127–36.
7. Soffietti R, Leoncini B, Ruda R (2007). New developments in the treatment of malignant gliomas. *Expert Rev Neurother*; 7: 1313–26.
8. Jain, A.K; Vaidya, A; Ravichandran, V. ; Kashaw, S.K. Agrawal, R.K (2012). Recent developments and biological activities of thiazolidinone derivatives: a review, *Bioorg. Med. Chem.* 20: 3378-3395.
9. Tripathi, A.C., Gupta, S.J., Fatima, G.N., Sonar, P.K., Verma, A., Saraf, S.K. (2014) 4-Thiazolidinones: The advances continue... *Eur. J. Med. Chem.* 72:52.
10. Patel, D. ; Kumari, P. ; Patel, N. (2012). Synthesis and biological evaluation of some thiazolidinones as antimicrobial agents, *Eur. J. Med. Chem.* 48: 354-362.

11. Deep, A. ; Jain, S. ; Sharma, P.C. Phogat, P. ; Malhotra, M (2012). Synthesis of 2-(aryl)-5-(arylidene)-4-thiazolidinone derivatives with potential analgesic and antiinflammatory activity, *Med. Chem. Res.* 21:1652-1659.
12. Saundane, A.R; Yarlakatti, M. ; Walmik, P. ; Katkarf, V. (2012). Synthesis, antioxidant and antimicrobial evaluation of thiazolidinone, azetidinone encompassing indolylthienopyrimidines. *J. Chem. Sci.* 124:469-481.
13. Wang, S. ; Zhao, Y. Zhang, G; Lv, Y. ; Zhang, N.; Gong P. (2011). Design, synthesis and biological evaluation of novel 4-thiazolidinones containing indolin-2-one moiety as potential antitumor agent, *Eur. J. Med. Chem.* 46:3509-3518.
14. Murphy, G.J. ; Holder, J.C (2000). PPAR-gamma agonists: therapeutic role in diabetes, inflammation and cancer. *Trends in Pharmacological Sciences* 46:9e474.
15. Moorkoth, S (2015). Synthesis and Anti-cancer Activity of Novel Thiazolidinone Analogs of 6-Aminoflavone. *Chem Pharm Bull.* 63(12):974-85.
16. Wan Y, Wu S, Xiao G, Liu T, Hou X, Chen C, Guan P, Yang X, Fang H (2015). Design, synthesis and preliminary bioactivity studies of 2-thioxo-4-thiazolidinone derivatives as Bcl-2 inhibitors. *Bioorg Med Chem.* 1;23(9):1994-2003.
17. Abdelazeem, AH; Gouda, AM; Omar, HA; Tolba, MF. (2014). Design, synthesis and biological evaluation of novel diphenylthiazole-based cyclooxygenase inhibitors as potential anticancer agents. *Bioorg Chem,* 57:132-41.
18. Kunzler, A ; Neuenfeldt, P D. ; Das Neves, A M. ; Pereira, Claudio M.P. ; Marques, G H. ; Nascente, P S. ; Fernandes, M H.V. ; Hubner, S O. ; Cunico, W (2013). Synthesis, antifungal and cytotoxic activities of 2-aryl-3-((piperidin-1-yl)ethyl)thiazolidinones. *European Journal of Medicinal Chemistry,* v. 64, p. 74-80.
19. Da Frota Jr ML, Braganhol E, Canedo AD, Klamt F, Apel MA, Mothes B, Lerner C, Battastini AM, Henriques AT, Moreira JC (2009). Brazilian marine sponge *Polymastia janeirensis* induces apoptotic cell death in human U138MG glioma cell line, but not in a normal cell culture. *Investig New Drugs* 27(1):13–20.
20. Silveira, E. F. ; Chassot, J.M ; Teixeira, F.C ; Azambuja, J. H. ; Debom, G. ; Rodrigues, R. S. ; Beira, F.T ; Pino, F.A.B.D ; Lourenço, A. S. ; Horn, A. P. ; Cruz, L. ; Spanevello, R. ; Braganhol, E. (2013). Ketoprofen-loaded polymeric nanocapsules selectively inhibit cancer cell growth in vitro and in preclinical model of glioblastoma multiforme. *Investigational New Drugs,* v. 31, p. 1424-1435.
21. Mosmann, T (1983). Rapid colorimetric assay for cellular growth and survival: application to proliferation and cytotoxicity assays. *J Immunol Methods* 65, 55-63.

22. Casciola-Rosen L, Rosen A, Petri M, Schliessel M (1996) Surface blebs on apoptotic cells are sites of enhanced procoagulant activity: implications for coagulation events and antigenic spread in systemic lupus erythematosus. *Proc Natl Acad Sci USA* 20 93(4):1624-1629.
23. Shrivastava A, Kuzontkoski PM, Groopman JE, Prasad A (2011). Cannabidiol induces programmed cell death in breast cancer cells by coordinating the cross-talk between apoptosis and autophagy. *Mol Cancer Ther.*10(7):1161–1172.
24. Braganhol E, Morrone FB, Bernardi A, Huppes D, Meurer L, Edelweiss MI, Lenz G, Wink MR, Robson SC, Battastini AM (2009) Selective NTPDase2 expression modulates in vivo rat glioma growth. *Cancer Sci* 100(8):1434–1442
25. Stuehr DJ, Nathan CF (1989). Nitric oxide. A macrophage product responsible for cytostasis and respiratory inhibition in tumor target cells. *J Exp Med*, v. 169, p. 1543-1555.
26. Watters JJ, Schartner JM, Badie B (2005). Microglial function in brain tumors. *J Neurosci Res* 81:447–455.
27. Yang D, Yin JH, Mishra S, Mishra R, Hsu CY (2002). NO-mediated chemoresistance in C6 glioma cells. *Ann. N.Y. Acad. Sci.* v. 962, p. 8-17.
28. Yang D, Yin J, Mishra S, Mishra R, Hsu CY (2004). Nitric oxid and BCNU chemoresistance in C6 glioma cells : role of S-nitrosoglutathione. *Free Radic. Biol. Med.* v. 36, p. 1317-1328.
29. Aktas Y, Andrieux K, Alonso MJ, Calvo P, Gürsoy RN, Couvreur P, Capan Y (2005). Preparation and in vitro evaluation of chitosan nanoparticles containing a caspase inhibitor. *Int J Pharm* 298:378–383
30. Jain, A.K; Vaidya, A; Ravichandran, V. ; Kashaw, S.K. Agrawal, R.K (2012). Recent developments and biological activities of thiazolidinone derivatives: a review, *Bioorg. Med. Chem.* 20: 3378-3395.
31. Cutshall, N.S; O'Day . C. M (2005). Prezhdo, Bioorg. Rhodanine derivatives as inhibitors of JSP-1 *Bioorganic & Medicinal Chemistry Letters* 15 3374e 3379.
32. Carter, PH; Scherle, PA; Muckelbauer, JK; Voss, ME; Liu, RQ; Thompson, LA; Tebben, AJ; Solomon, KA; Lo, YC; Li, Z; Strzemienski, P; Yang, G; Falahatpisheh, N; Xu, M; Wu, Z; Farrow, NA; Ramnarayan, K; Wang, J; Rideout, D; Yalamoori, V; Domaille, P; Underwood, DJ; Trzaskos, JM; Friedman, SM; Newton, RC; Decicco, CP. (2001). Photochemically enhanced binding of small molecules to the

tumor necrosis factor receptor-1 inhibits the binding of TNF-alpha. Proc Natl Acad Sci U S A. (21):11879-84.

33. Degterev A, Lugovskoy A, Cardone M, Mulley B, Wagner G, Mitchison T, Yuan J.(2001). Identification of small-molecule inhibitors of interaction between the BH3 domain and Bcl-xL. Nat Cell Biol. 3(2):173-82.

34. Dayam R, Aiello F, Deng J, Wu Y, Garofalo A, Chen X, Neamati N. (2006). Discovery of small molecule integrin alphavbeta3 antagonists as novel anticancer agents. J Med Chem., 49(15):4526-34.

35. Verçozza, G. L.; Feitosa, D. D.; Alves, A. J.; Aquino, T. M.; Lima, J. G.; Araújo, J. M.; Cunha, I. G. B.; Goes, A. J. S (2009). Síntese e avaliação da atividade antimicrobiana de novas 4- tiazolidinonas obtidas a partir de formilpiridina tiossemicarbazonas. Quim. Nova. v. 32, p.1405-1410.

36. Chumak VV, Fil MR, Panchuk RR, Zimenkovsky BS, Havrylyuk DY, Lesyk RB (2014). Study of antineoplastic action of novel isomeric derivatives of 4-thiazolidinone. Ukr Biochem J.;86:96-105.

37. C Zhang, S Zhai, X Li, Q Zhang, L Wu, Y Liu, C Jiang, H Zhou, F Li, S Zhang, G Su, B Zhang and B Yan (2014). Synergistic action by multi-targeting compounds produces a potent compound combination for human NSCLC both in vitro and in vivo. Cell Death and Disease, 5, 1138.

38. Hussain SP, Trivers GE, Hofseth LJ, et al. (2004). Nitric oxide, a mediator of inflammation, suppresses tumorigenesis. Cancer Res.;64:6849–53.

## Legend and Figures

Figure 1

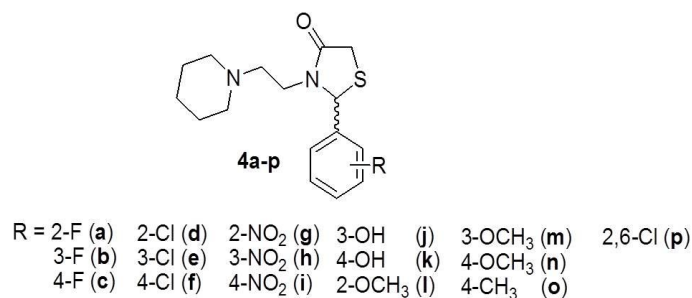


**Figure1.** General structure of 2-(aryl)-3-[(2-piperidin-1-yl)ethyl]thiazolidin-4-ones (**4a-p**).

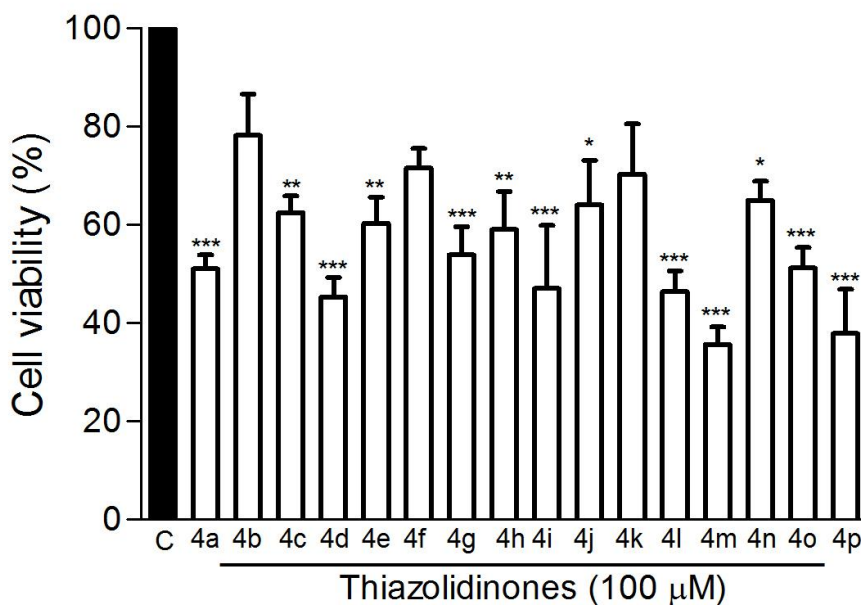


**Figure 2.** Effect of thiazolidinones in glioma cell viability. C6 glioma cell cultures were exposed to a panel of 16 synthetic thiazolidinones (**4a-4p**; 100  $\mu$ M) for 48 h, and the cell viability was assessed by MTT. Appropriate controls containing 0.01% DMSO were performed. The values represent the mean $\pm$ SD of at least three independent experiments. Data were analyzed by ANOVA followed by *post-hoc* comparisons (Tukey-Kramer test). \*, \*\*, \*\*\* Significantly different from control cells ( $P < 0.05$ ;  $P < 0.01$ ;  $P < 0.001$ , respectively).

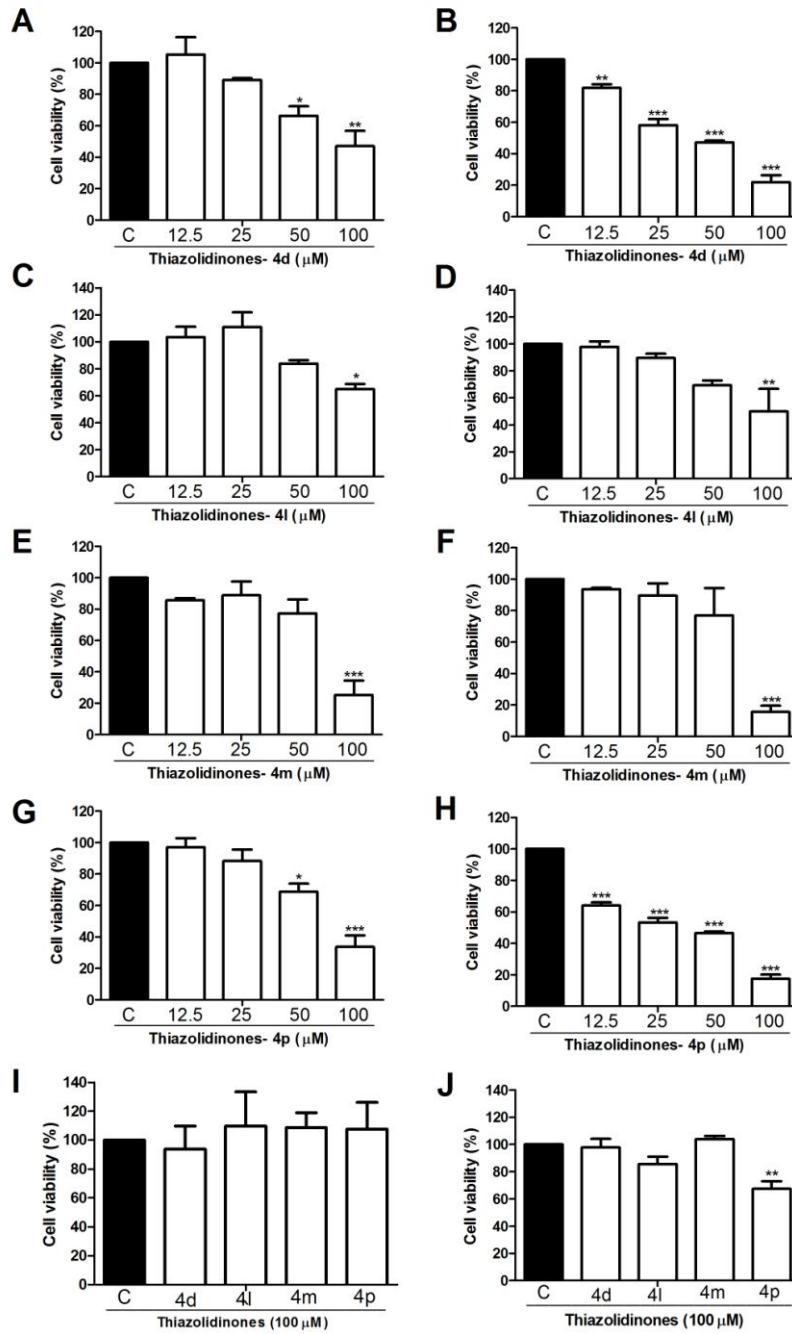


**Figure 3.** Time-course and concentration effect of different thiazolidinones on glioma and astrocyte cell viability. C6 glioma cell line (A-H) and primary astrocyte cultures (I, J) were treated for 48 h (left panel) or 72 h (right panel) with different concentrations (12.5 - 100 μM) of synthetic thiazolidinones (**4d**; **4l**; **4m**; **4p**) and MTT assay was carried out. Appropriate controls containing 0.01% DMSO were performed. The values represent the mean±SD of at least three independent experiments. Data were analyzed by ANOVA followed by *post-hoc* comparisons (Tukey-Kramer test). \*, \*\*, \*\*\* Significantly different from control cells ( $P < 0.05$ ;  $P < 0.01$ ;  $P < 0.001$ , respectively).

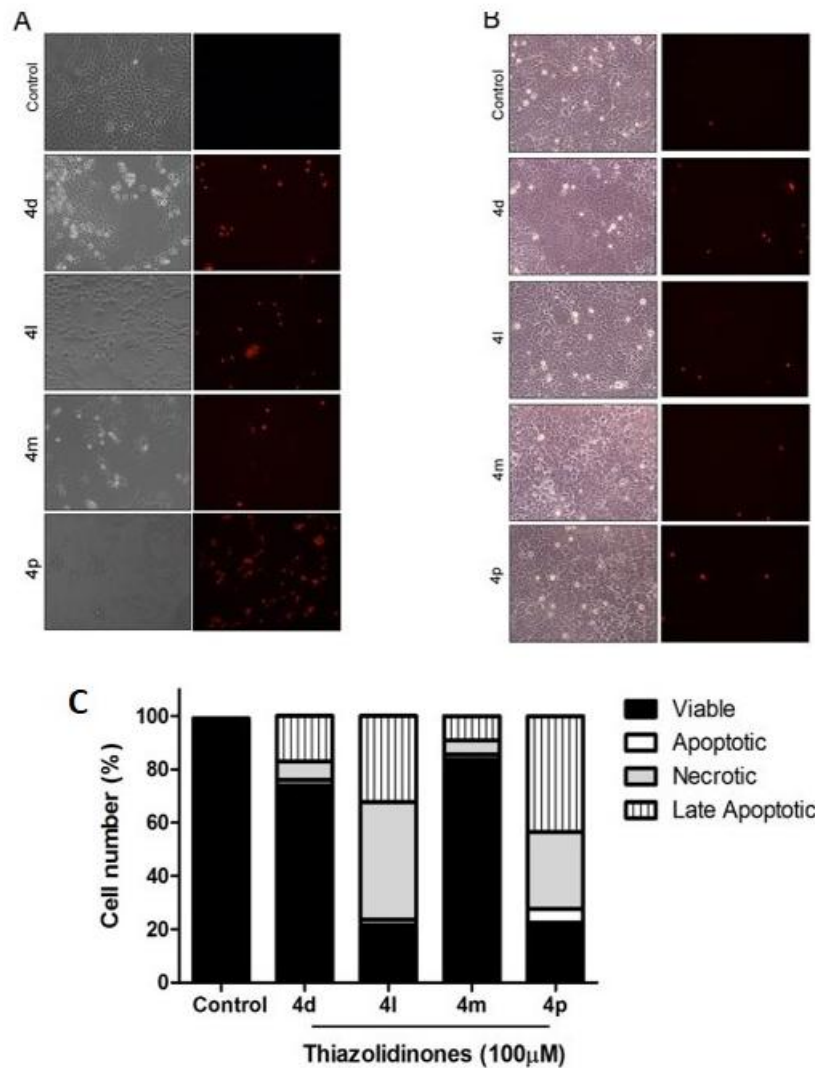


**Figure 4.** Propidium iodide (PI) incorporation in C6 glioma cells and in astrocytes following 2-aryl-3-((piperidin-1-yl)ethyl)thiazolidin-4-ones treatment and analysis of 2-aryl-3-((piperidin-1-yl)ethyl)thiazolidin-4-ones effect on glioma C6 cell death. Cell cultures were exposed to different molecules (4d, 4l, 4m and 4p; 100 mM) and after 72 h of treatment glioma cells (panel A) or primary astrocytes (panel B) were incubated with PI diluted in culture medium. Appropriate controls containing 0.01% DMSO were performed. Fluorescence (right panel) and phase contrast (left panel) microphotographs were taken using an Olympus inverted microscope (20 $\times$  magnification). (C) The C6 glioma cell death was evaluated by Annexin V-FITC bound phosphatidylserine and red fluorescence of DNA-bound PI in individual glioma cells by flow cytometry. (For interpretation of the references to colour in this figure legend, the reader is referred to the web version of this article.)



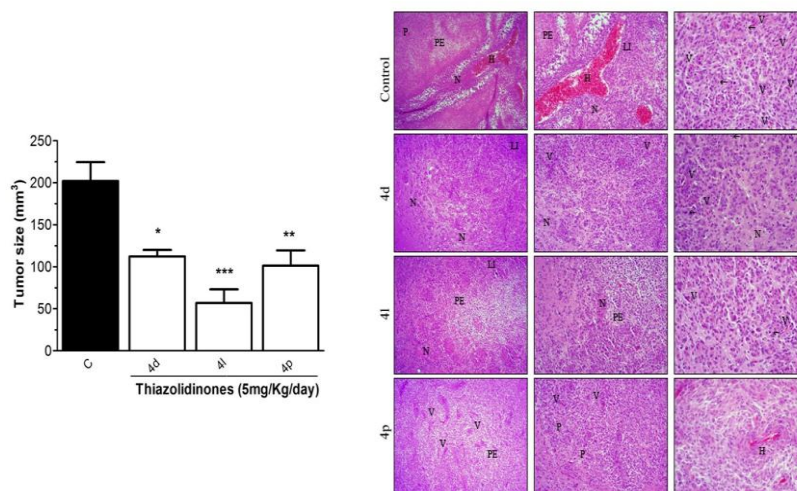


**Figure 5.** Tumor size quantification and histological characteristics of glioma-implanted rats and treated with of 2-aryl-3-((piperidin-1-yl)ethyl)thiazolidin-4-ones. Glioma-implanted rats were treated as described in materials and methods. For tumor size quantification, images were captured from HE slices of implanted glioma using a digital camera connected to a microscope and total volume (mm<sup>3</sup>) was determined using Image Tool Software™. Representative HE sections of implanted control gliomas denote histological characteristics that define glioblastoma multiforme: intratumoral hemorrhage (H); peripheric pseudopalisade (P), necrosis (N), peritumoral edema (PE), lymphocytic infiltration (LI), vascular proliferation (V) and mitotic cells (arrows). Note that thiazolidinone treatment reduces the histological characteristics related to increased glioma malignity. The complete analysis is shown in Table 1. Magnification 100x, 200x and 400x for left, central and right panels, respectively. The values represent the mean±SD of at least five animals per group. Data were analyzed by ANOVA followed by post-hoc comparisons (Tukey’s test). \*,\*\*,\*\*\* Significantly different from control cells. ( $P<0.05$ ;  $P<0.01$ ;  $P<0.001$ , respectively).

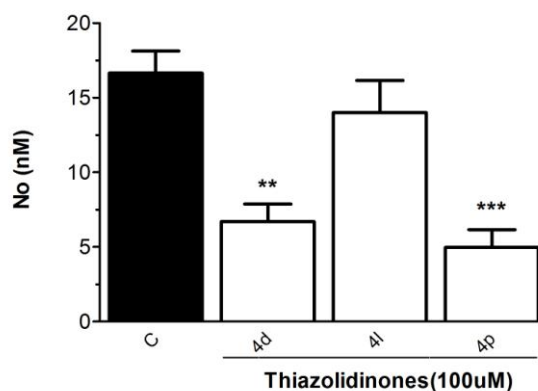


**Figure 6.** Nitrite determination in serum of glioma-implanted rats treated with thiazolidinones.. Animals were treated as described in materials and methods and NO production was determined by Greiss assay Values represent the mean ± SD of at least five animals per group. Data were analyzed by ANOVA followed by post-hoc comparisons (Tukey’s test). \*,\*\*,\*\*\* Significantly different from control cells. ( $P<0.05$ ;  $P<0.01$ ;  $P<0.001$ , respectively).

Manuscrito 1: submetido à revista “Colloids and Surfaces B: Biointerfaces

**2-(2-methoxyphenyl)-3-((piperidin-1-yl)ethyl)thiazolidin-4-one-loaded polymeric nanocapsules: *in vitro* anti-glioma activity and *in vivo* toxicity evaluation.**

<sup>1</sup>\*Elita Ferreira da Silveira, <sup>2</sup>Luana Mota Ferreira, <sup>2</sup>Mailine Gehrcke, <sup>2</sup>Letícia Cruz, <sup>3</sup>Nathália Stark Pedra, <sup>3</sup>Priscila Treptow Ramos, <sup>3</sup>Natália Pontes Bona, <sup>3</sup>Mayara Sandrielly Pereira Soares, <sup>3</sup>Rodrigo Rodrigues, <sup>3</sup>Rosélia Maria Spanevello, <sup>3</sup>Wilson Cunico, <sup>3</sup>Francieli M. Stefanello, <sup>4</sup>Juliana Hofstater Azambuja, <sup>1</sup>Ana Paula Horn, <sup>4</sup>\*Elizandra Braganhol.

<sup>1</sup>Programa de Pós-Graduação em Ciências Fisiológicas, Instituto de Ciências Biológicas, Universidade Federal do Rio Grande, Rio Grande, RS, Brazil.

<sup>2</sup>Programa de Pós-graduação em Ciências Farmacêuticas, Centro de Ciências da Saúde, Universidade Federal de Santa Maria, Santa Maria, Brazil.

<sup>3</sup>Programa de Pós-Graduação em Bioquímica e Bioprospecção, Centro de Ciências Químicas, Farmacêuticas e de Alimentos, Universidade Federal de Pelotas, Pelotas, RS, Brazil.

<sup>4</sup>Departamento de Ciências Básicas da Saúde, Universidade Federal de Ciências da Saúde de Porto Alegre, Porto Alegre, RS, Brazil.

**\*Corresponding Authors**

Elita Ferreira da Silveira (elitafs24@gmail.com)

Universidade Federal de Rio Grande - FURG

Avenida Itália, Km 8, Campus Carreiros

CEP: 96.203-900, Rio Grande, RS, Brasil Phone: +55 53 3293 6987

Elizandra Braganhol (ebraganhol@ufcspa.edu.br)

Universidade Federal de Ciências da Saúde (UFCSPA)

Rua Sarmento Leite, 245 – Prédio Principal – sala 304

CEP: 90.050-170, Porto Alegre, RS, Brasil Phone: +55 51 3303 8762

## Abstract

Among gliomas types, glioblastoma multiforme (GBM) is considered the most malignant and the worst form of primary brain tumor. It is characterized by high infiltration rate and great angiogenic capacity. The presence of an inflammatory microenvironment contributes to chemo/radioresistance, resulting in poor prognosis for patients. Recent data show that thiazolidinones have a wide range of pharmacological properties, including anti-inflammatory and antiglioma activities. Nanocapsules of biodegradable polymers become an alternative to cancer treatment since they provide targeted drug delivery and could overcome blood-brain barrier. Thus, here we investigated *in vitro* anti-glioma activity and the potential *in vivo* toxicity of 2- (2-methoxyphenyl) -3- ((piperidin-1-yl) ethyl) thiazolidin-4-one-loaded polymeric nanocapsules (**4L-N**). Nanocapsules were prepared and characterized in terms of particle size, polydispersity index, zeta potential, pH, molecule content and encapsulation efficiency. Treatment with **4L-N** selectively decreased C6 glioma cell viability and proliferation, being even more efficient than the free-form molecule (**4L**). In addition **4L-N** did not promote toxicity to primary astrocytes. We further demonstrated that the treatment with sub-therapeutic dose of **4L-N** did not alter weight or cause mortality and did not cause toxicity or peripheral damage to rats. Finally **4L** as well as **4L-N** did not alter makers of oxidative damage, such as TBARS levels and total sulfhydryl content, and did not change antioxidant enzymes SOD and CAT activity in liver and brain of rats. Taken together, these data indicate that the nanoencapsulation of **4L** has potentiated its antiglioma effect and does not cause *in vivo* toxicity.

**Keywords:** thiazolidinones, nanocapsules, C6 glioma, astrocytes, toxicity

## 1. Introduction

Glioblastoma (GBM) is the most common and lethal brain tumor, accounting for about 40% of all primary tumors and 78% of the malignant tumors of the central nervous system (CNS) [1]. GBM exhibits morphological and gene expression similarities with glial cells, such as astrocytes, oligodendrocytes and their precursors [2]. Currently, the protocol adopted for the treatment of patients diagnosed with glioblastoma is surgical resection whenever possible [3], followed by radio/chemotherapy with temozolomide (TMZ), which is considered the chemotherapy of first choice. The adjuvant therapy is maintained for at least six months [4, 5]. These tumors present significant resistance to treatment because they have a high rate of proliferation and angiogenesis and ability to infiltrate adjacent tissues making neurosurgery difficult. Thus, therapeutic strategies are limited by chemoresistance development and high recurrence rates [5-6]. Another characteristic that limits the treatment of these tumors is the difficulty of chemotherapy to cross the blood-brain barrier (BBB), being a limiting factor for an efficient treatment.

In the search for new and effective therapeutic targets, heterocyclic compounds, such as 4-thiazolidinones, stand out to have a wide range of pharmacological properties, including antimicrobial activity [7], anti-inflammatory [8], antifungal [9] antioxidants [10], anticancer, among others [11-12-13]. Recent studies have shown that these compounds may possibly control cell proliferation through induction of apoptosis [14-15] and inhibition of cyclooxygenases [16], thereby controlling cancer-related inflammation [16].

In the search for new medicines carriers, nanocapsules have been considered a promising tool to improve the passage of bioactive molecules through BBB,

contributing to increased therapeutic efficacy and reduced side effects of conventional chemotherapy. Moreover, these particles are capable of becoming invisible to the monitic phagocytic system, which favors the targeting of the formulation to the tumor microenvironment and promotes its uptake [17].

In a recent work, we have demonstrated the synthesis [18] and the *in vitro* and *in vivo* antiglioma potential of a series of thiazolidinones, wherein the 2-(2-methoxyphenyl)-3-((piperidin-1-yl)ethyl)thiazolidin-4-one **4L** considerably reduced tumor volume in an *in vivo* rat glioblastoma model [19] (Fig. 1). In an attempt to circumvent conventional clinical problems of cancer treatment, including incidence of side effects, low selectivity and inability to achieve CNS, the aim of the present work was the development of nanocapsules of 2-(2-methoxyphenyl)-3-((piperidin-1-yl)ethyl)thiazolidin-4-one (4L) in order to investigate their *in vitro* antiglioma potential and *in vivo* toxicity.

**Figure 1:** Structure of 2-(2-methoxyphenyl)-3-((piperidin-1-yl)ethyl)thiazolidin-4-one **4L** [18].

## 2. Experimental Procedures

### 2.1 Reagents.

Dulbecco's modified Eagle's medium (DMEM), Fungizone, penicillin/streptomycin, 0.25% trypsin/EDTA solution and fetal bovine serum (FBS) were obtained from Gibco (Gibco BRL, Carlsbad, CA, USA). Poly ( $\epsilon$ -caprolactone)

(PCL) (MW: 80 KDa) and Span 80<sup>®</sup> (sorbitan monooleate) were acquired from Sigma Aldrich (São Paulo, Brazil). Tween 80<sup>®</sup> (polysorbate 80) and MCT (medium chain triglycerides) were furnished by Delaware (Brazil). All other chemicals and solvents used were of analytical or pharmaceutical grade.

## ***2.2 Preparation of nanocapsule suspensions***

Nanocapsule suspensions were prepared by interfacial deposition of preformed polymer. An organic phase consisting of polymer [PCL] (0.100 g), acetone (27 mL), Span 80<sup>®</sup> (0.077 g), compound **4L** (0.01 g) and MCT (330  $\mu$ L) were maintained for 60 min under moderate magnetic stirring at 40°C. After all components were solubilized, the organic phase was injected into 53 mL of an aqueous dispersion of Tween 80<sup>®</sup> (0.077 g) and kept under magnetic stirring for 10 min. Subsequently, organic solvent and part of water were removed by evaporation under reduced pressure to achieve a final volume of 10 mL and **4L** at a concentration of 1.0 mg/mL (**4L-N**). For comparison purposes, formulations without drug were also made (**NC**). All formulations were prepared in triplicate.

## ***2.3 Characterization of nanocapsule suspensions***

Granulometric distribution was performed by laser diffraction (Mastersizer<sup>®</sup> 3000E, Malvern Instruments, UK) after diluting the samples in distilled water. A laser obscuration of 15% and refractive index of 1.59 was used to perform the measurements. Particle sizes and polydispersity indexes were determined by photon correlation spectroscopy (Zetasizer Nanoseries, Malvern Instruments, UK) after dilution of samples with ultrapure water (1:500). The zeta potentials were measured using the same instrument after the dilution of the samples in 10 mM NaCl (1:500) by

microeletrophoresis. The pH of the nanocapsule suspensions was verified by direct immersion of electrode from a calibrated potentiometer (Model PH 21, Hanna Instruments, São Paulo, Brazil) in the formulations. Measurements were taken at room temperature ( $25 \pm 2^\circ\text{C}$ ).

The total **4L** content in nanocapsule suspensions was determined by the HPLC method. For this, 150  $\mu\text{L}$  of the nanocapsule suspension were diluted in 10 mL of methanol, sonicated for 30 min, filtered through a 0.45  $\mu\text{m}$  membrane and injected into HPLC system. The **4L** quantification was performed on a LC-10A HPLC system (Shimadzu, Japan) equipped with a LC-20AT pump, an UV-VIS SPD-M20A detector, a CBM-20A system controller and a SIL-20A HT valve sample automatic injector. Separation was achieved at room temperature using a Gemini  $\text{C}_{18}$  Phenomenex column (150 mm x 4.60 mm, 5  $\mu\text{m}$ ; 110  $\text{Å}$ ) coupled to a  $\text{C}_{18}$  guard column. The isocratic mobile phase consisted of methanol and water (90:10, v/v) at 1 mL/min of flow rate. The **4L** was detected at 279 nm. The method was linear ( $r=0.995$ ) in the concentration range of 5.0 - 25.0  $\mu\text{g/mL}$ .

For the encapsulation efficiency determination, an aliquot of formulation was placed in a 10,000 MW centrifugal device (Amicon<sup>®</sup> Ultra, Millipore) and free molecules were separated from the nanocapsules by the ultrafiltration/centrifugation technique for 10 min at 2,200 g. The ultrafiltrate was analyzed by HPLC. The difference between **4L** total and free concentrations, and the ultrafiltrate, was respectively calculated as encapsulation efficiency (EE%) of the NCs following equation:  $\text{EE} = [(\text{total content} - \text{free content})/\text{total content}] \times 100$ .



## **2.4 Photostability study**

For the purposes of photostability study, 700  $\mu\text{L}$  of **4L** methanolic solution (1 mg/mL) and **4L-N** (1 mg/mL) were placed individually in cuvettes with lids arranged at a fixed distance and subsequently exposed to ultraviolet radiation (Phillips TUV Long Life Lamp-UVC, 30 W) for 120 min in a mirrored chamber (1 m  $\times$  25 cm  $\times$  25 cm). At time intervals (0, 15, 45, 60, 90 and 120 min), aliquots of 150  $\mu\text{L}$  were withdrawn and diluted in methanol to determine the concentration of thiazolidinone in each sample by HPLC. To discard the influence of other factors, the cuvettes containing the samples, wrapped in aluminum foil (dark controls), were also evaluated.

## **2.5 *In vitro* Thiazolidinone release study**

The thiazolidinone *in vitro* release from nanocapsules was evaluated by the dialysis bag diffusion technique. For this, 1.0 mL of **4L** methanolic solution or nanocapsules (**4L-N**) were placed in the dialysis bag (MWCO 10,000, Spectra Por 7) and immersed in 150 mL of phosphate buffer (pH 7.4): ethanol (70:30, v/v), maintained at 37°C and under continuous magnetic stirring at 50 rpm. At predetermined times, 1 mL aliquots were withdrawn and replaced with the same volume of fresh medium to maintain *sink* conditions. The amount of released thiazolidinone **4L** was quantified by HPLC as previously described.

## **2.6 General Cell Culture Procedures**

### **2.6.1 C6 rat glioblastoma cell line**

Cells were purchased from American Type Culture Collection (Rockville, MD, USA) and were cultured in DMEM containing 0.1% Fungizone and 100 U/L

penicillin/streptomycin and supplemented with 5% (v/v) fetal bovine serum (FBS, Gibco). Cells were maintained at 37°C in a humidified atmosphere with 5% CO<sub>2</sub>.

### *2.6.2 Rat cortical astrocyte primary cultures*

Astrocyte primary culture was prepared as previously described [19]. Briefly, the cerebral cortex of newborn (1-2 day old) Wistar rats (CEEA license number 9219) was removed and mechanically dissociated in Ca<sup>+2</sup>/Mg<sup>+2</sup>-free buffer (pH 7.4). After centrifugation at 1000 g for 10 min, pellet was suspended in DMEM supplemented with 10% FBS and cells (3 x 10<sup>4</sup>) were seeded in 96-well plates previously coated with poly-L-lysine for better adherence of cells. Following 4h of cell seed, culture medium was changed. Cultures were allowed to grow to confluence, around 20-25 days. Culture medium was replaced every 4 days.

### *2.7 In vitro treatment*

Synthetic 4L was first dissolved in sterile 0.01% DMSO at 100 mM concentration (stock solution) and further diluted in 5% DMEM (glioma) or 10% (astrocytes) FBS to obtain the desired concentrations and 4L-N was Prepared as described above. C6 glioma cells or astrocyte cultures were exposed for 48 or 72 h to 4L or 4L-N at the following concentrations 6.25, 12.5, 25, and 50 µM. Control cells were treated with equivalent volume of vehicle (DMSO) or unloaded drug-nanocapsule (NC).

### *2.8 Cell viability assay*

Cell mitochondrial viability was assessed by MTT assay. This experiment is based on the ability of cells, which remain viable, in reducing MTT and forming a blue formazan product. Following treatment, medium was withdrawn and cells were exposed to MTT solution (0.5 mg/mL) prepared in DMEM/5% or 10% FBS for 90 min at 37°C

in a 5% CO<sub>2</sub> humidified atmosphere. The solution was then removed and the plates were shaken with DMSO for 30 min. The optical density of each well was measured at 492 nm. The results were expressed as absorbance.

### ***2.9 Determination of cell proliferation by Sulforodamine B assay.***

Following 48 or 72 h treatment, cells were gently washed and 50% trichloroacetic acid was added for 45 min for cell attachment. After this period, acid was removed and five washes were performed with distilled water until the reagent was completely removed, followed by 30 min incubation with 0.4% sulfarodamine. The solution was then removed and 5 washes were made with 1% acetic acid for the complete removal of non-complexed dye with proteins. Finally, SRB was eluded with 10 mM Tris solution. The optical density of each well was measured at 530 nm in a spectrophotometer.

### ***2.10 Propidium iodide assay***

Cell damage was assessed by fluorescent imaging of propidium iodide (PI) uptake. At the end of the treatments, C6 glioma cells were incubated with PI (7.5 µM) for 1 h. PI fluorescence was excited at 515-560 nm using an inverted microscope (Olympus IX71, Tokyo, Japan) equipped with a standard rhodamine filter. The images were captured using a digital camera connected to microscope.

### ***2.11 In vivo treatment***

#### ***2.11.1 Animals***

Male Wistar rats (60 days old), were obtained from Central Animal House of Federal University of Pelotas (Pelotas, RS, Brazil). Animals were maintained under

conventional conditions on a 12/12 h light/dark cycle at an air-conditioned constant temperature ( $22 \pm 1^\circ\text{C}$ ) colony room. Rats had free access to 20% (w/w) protein commercial chow and water. Animal care followed the official governmental guidelines in compliance with Federation of Brazilian Societies for Experimental Biology and was approved by the Committee of Ethics and Animal Experimentation of the Federal University of Pelotas, under license number: CEEA 9219.

### 2.11.2 Treatment protocol

Animals were randomly divided into five groups as follows: (1) Control (rats water treated); (2) Control canola oil; (3) **4L** (rats treated with 5 mg/Kg/day of thiazolidin-4-ones dissolved in oil) (4) **4L-N** (rats treated with 5 mg/Kg/day of thiazolidin-4-ones-loaded nanocapsules) (5) Blank nanocapsules (rats treated with drug-unloaded nanocapsules) (**NC**). Animals received the treatments by gavage for 5 consecutive days. During the treatment period, animals were weighed daily. After treatment time, animals were anesthetized and euthanized. Immediately blood, brain and liver were removed for further analysis.

### **2.12 Serum preparation and biochemical analysis**

Blood was collected without anticoagulant and immediately centrifuged at 2,500 g for 15 min at RT. The clot was removed and the resulting serum was stored at  $-80^\circ\text{C}$  for further biochemical determination. Hepatic and renal functions were evaluated using the enzymatic assays alanine aminotransferase (ALT), aspartate aminotransferase (AST), creatinine and urea. These analyses were performed using a commercial kit (LABTEST, Diagnostica S.A., Minas Gerais, Brazil).

### ***2.13 Tissue preparation***

For oxidative stress parameter determination, tissues from brains and livers were homogenized in 10 volumes (1:10 w/v) of 20 mM sodium phosphate buffer, pH 7.4 containing 140 mM KCl. Homogenates were centrifuged at 2,500 g for 10 min at 4°C. Pellet was discarded and supernatant was separated and used for biochemical determination.

### ***2.14 Oxidative stress parameters in liver and kidney***

#### ***2.14.1 Thiobarbituric acid reactive substances (TBARS) quantification***

TBARS levels were determined as previously described by Esterbauer and Cheeseman (1990) [20]. For the assay, the already homogenized tissues were mixed with trichloroacetic acid (10%) and thiobarbituric acid (0.67%) and incubated in a dry block at 100°C for 30 min. TBARS levels were determined by absorbance at 535 nm. Results were reported as nmol of TBARS per mg of protein.

#### ***2.14.2 Total quantification of sulfhydryl (SH) content***

Total sulfhydryl content was quantified as previously described by Aksenov and Markesbery (2001) [21], which is based on the reduction of DTNB by thiols, which in turn becomes oxidized (disulfide) generating a yellow derivative (TNB) whose absorption is measured at 412 nm in a spectrophotometer. First, homogenates were added to a PBS buffer at pH 7.4 containing EDTA. Reaction was started by the addition of 5,5'-dithio-bis (2-nitrobenzoic acid) (DTNB). Results were reported as nmol TNB per mg protein.

#### ***2.14.3 Superoxide dismutase (SOD) activity***

Total SOD activity was measured according to described by Misra and Fridovich (1972) [22]. This assay is based on inhibition of self-oxidation of superoxide dependent

adrenaline to adenocarbon in a spectrophotometer set at 480 nm. The intermediate in this reaction is superoxide, which is eliminated by SOD. A unit of SOD was defined as the amount of enzyme to cause 50% inhibition of adrenaline self-oxidation. The specific activity of SOD was reported as units per mg protein.

#### 2.14.4 Catalase (CAT) activity

CAT activity was assayed by the method of Aebi (1984) [23]. The decomposition of 30 mM H<sub>2</sub>O<sub>2</sub> in 50 mM potassium phosphate buffer (pH 7.0) was continuously monitored with a spectrophotometer at 240 nm for 180 s in a thermostat (37°C). One unit of the enzyme is defined as the number of hydrogen peroxide consumed per minute and the specific activity reported for units per mg protein.

#### 2.14.5 Protein determination

Protein was determined by the method of Lowry et al. (1951) [24] using bovine serum albumin as standard.

### **2.15 Statistical analysis**

Data sets were analyzed using one-way or two-way ANOVA followed by a Tukey test for multiple comparisons. Significance was considered when  $p < 0.05$  in all analyses. Data are expressed as mean  $\pm$  SD or mean  $\pm$  SEM when indicated

## **3. Results**

### ***Preparation and characterization of thiazolidinone 4L nanocapsules***

After preparation, 4L, 4L-N and NC, respectively, exhibited homogeneous appearance without visible precipitates. Table 1 shows physicochemical characterization of formulations. In order to discard the presence of particles in the micrometer size range, laser diffraction analysis was performed. Any microparticle

population was observed for both formulations. Besides that, 50% of particle presented size around 554 nm and the *Span* was less than 2.0, indicating a narrow distribution. By photon correlation spectroscopy particles with size between 276–243 nm and polydispersity index around 0.2 were observed. Zeta potential values were negative and pH was in the neutral range. The thiazolidinone did not significantly alter the physicochemical parameters. The molecule content was close to the theoretical value (1 mg/mL) and the encapsulation efficiency was higher than 98%.

**Table 1.** Physicochemical characterization of **4L-N** and **NC**

	<b>4L-N</b>	<b>NC</b>
<b>Mean diameter (nm)</b>	243 ± 3	276 ± 2
<b>PDI</b>	0.215 ± 0.010	0.234 ± 0.012
<b>Zeta Potential (mV)</b>	-9.0 ± 0.4	-7.9 ± 0.2
<b>pH</b>	6.7 ± 0.2	8.0 ± 0.1
<b>Drug content (%)</b>	97.74 ± 4.71	-
<b>EE (%)</b>	98.85	-
<b>Granulometric distribution</b>		
<b>D<sub>4,3</sub> (µm)</b>	0.671	0.597
<b>D<sub>0,9</sub> (µm)</b>	0.986	0.688
<b>D<sub>0,5</sub> (µm)</b>	0.554	0.450
<b>D<sub>0,1</sub> (µm)</b>	0.367	0.306
<b>Span</b>	1.120	0.844

Physicochemical characterization of formulations: PDI: polydispersity index; EE%: encapsulation efficiency.

### ***In vitro photostability study***

In order to evaluate the nanostructures ability to protect **4L** thiazolidinone against photodegradation, **4L-N** and **4L** methanolic solution (**4L**-free molecule) samples were exposed to UVC radiation (Fig. 2). After 120 min of exposure, approximately 78% of thiazolidinone **4L-N** associated to nanocapsules kept unchanged. On the other hand, only 44% of free molecule **4L** was remained under the same

conditions. Statistical analysis shows that the degradation of thiazolidinone methanolic solution starts in 45 min of exposure. For dark control, **4L** concentration was close to 100%, which discards the influence of chamber temperature on drug degradation (*data not shown*).

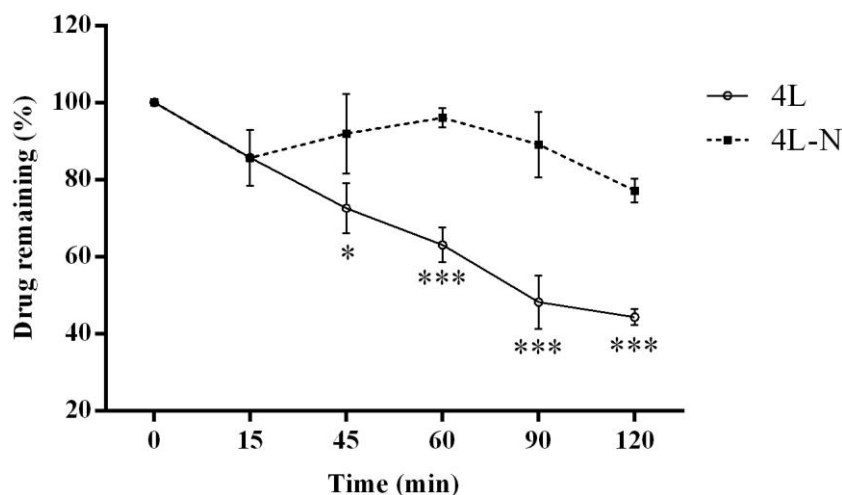


**Figure 2.** Photostability of 4L and 4L-N. Evaluation of the ability of nanostructures to protect 4L thiazolidinone against photodegradation. Values represent mean  $\pm$  SD of at least three independent experiments. Data were analyzed by ANOVA two-way followed by post-hoc comparisons (Tukey-Kramer test). \*, \*\*, \*\*\* Significantly different from control ( $P < 0.05$ ;  $P < 0.01$ ;  $P < 0.001$ , respectively).

### *In vitro* thiazolidinone release study

Concerning *in vitro* drug release experiments, Figure 3 shows that **4L-N** could control thiazolidinone release in comparison to **4L**. In a 6 h period, almost 95% of free **4L** was released while 67% of thiazolidinone **4L** was released from **4L-N** in the same period, showing that the nanocarrier was able to prolong thiazolidinone release. Two-way ANOVA analyzes shows that nanocapsules began to prolong the release from 4h incubation.



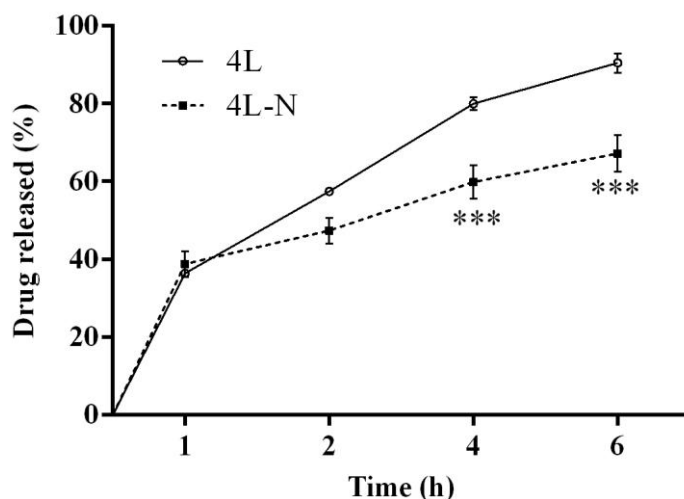


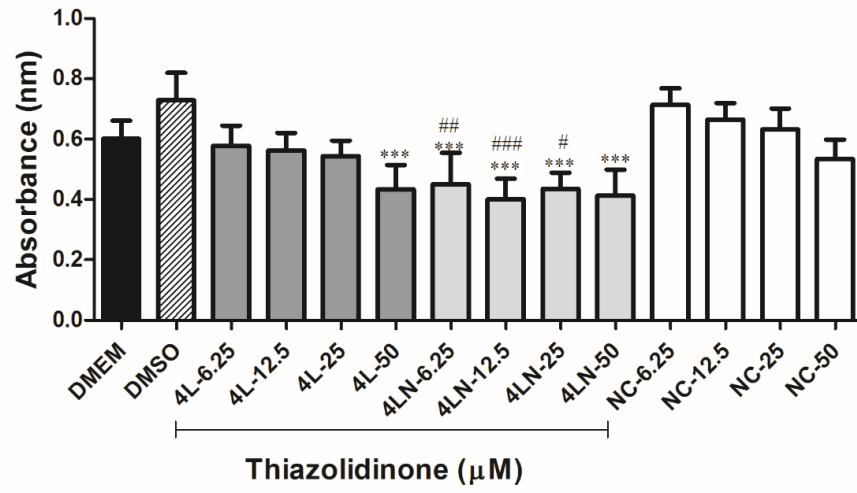
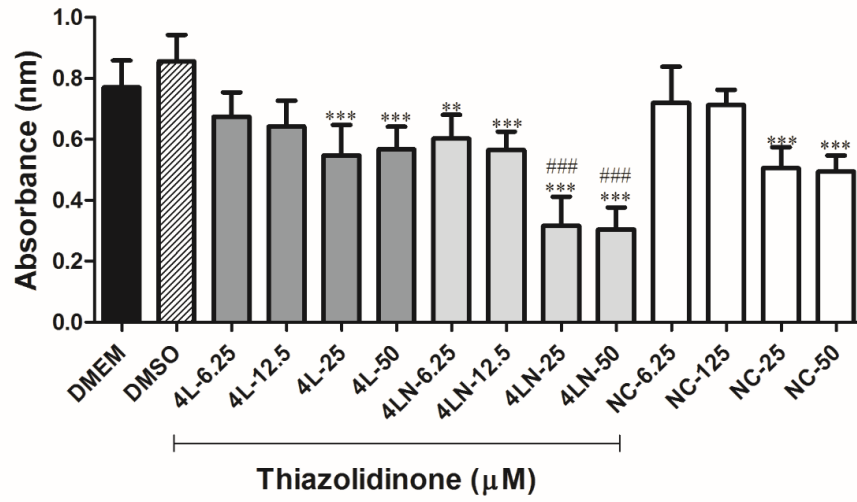
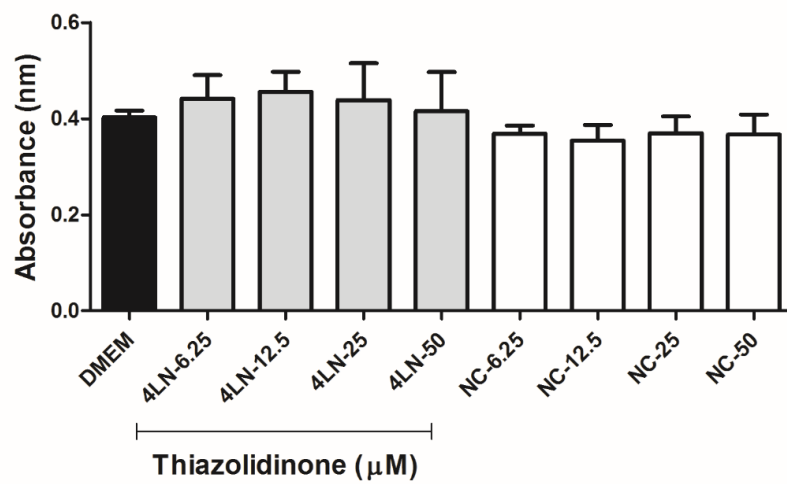
**Figure 3.** Thiazolidinone release. The values represent the mean  $\pm$  SD of at least three independent experiments. Data were analyzed by ANOVA two-way followed by post-hoc comparisons (Tukey-Kramer test). \*, \*\*, \*\*\* Significantly different from control ( $P < 0.05$ ;  $P < 0.01$ ;  $P < 0.001$ , respectively).

***Synthetic 2-(2-methoxyphenyl)-3-((piperidin-1-yl)ethyl)thiazolidin-4-one selectively decreases C6 glioma cell viability***

As shown previously, the class of 2-aryl-3-((piperidin-1-yl)ethyl)thiazolidin-4-ones shows a promising antiglioma activity and compound 2-(2-methoxyphenyl)-3-((piperidin-1-yl)ethyl)thiazolidine-4-one (**4L**) showed the best antiglioma potential *in vitro* and did not present cytotoxicity to astrocytes. Also, this compound showed 73% reduction of *in vivo* rat glioma growth [19]. Here, we nanoencapsulated **4L** compound in order to potentiate its activity. Firstly, we evaluated if **4L** and **4L-N** differentially reduce C6 glioma cell viability (Fig. 4). For this, glioma cells were exposed to 6.25, 12.5, 25 and 50  $\mu$ M of **4L** or **4L-N** and cell viability was assessed by MTT after 48 and 72 h of treatment. Cells exposed to DMEM/5% FBS, DMSO (0.01%), or NC were considered controls.

As shown in Figure 4, **4L** was able to reduce 27% of cell viability at 50  $\mu$ M following 48 h of treatment when compared to control, which reproduces data already

published by our group [19]. In the same way, **4L-N** reduced cell viability by 32.44%, 27.62%, 33.44% and 25.12% at 6.25, 12.5, 25 and 50  $\mu\text{M}$ , respectively, after 48 h of treatment. When the same experiment was carried out for 72 h, **4L** reduced cell viability in  $\sim 30\%$  at 25 and 50  $\mu\text{M}$ , while **4L-N** induces viability reduction at all concentrations, starting from 21.81% at 6.25  $\mu\text{M}$  until 60.51% at the highest concentration tested (50  $\mu\text{M}$ ). We also notice that the nanoencapsulated molecule showed an increase of 34.15% of cell toxicity in relation to 4L-free molecule at highest concentration tested (50  $\mu\text{M}$ ), showing the efficiency of nanoencapsulation to improve antiglioma activity. In general, treatment with **4L** or **4L-N** decreased cell viability when compared to controls, exhibiting concentration and time dependence. Of note, NB (drug- unloaded nanocapsule) caused significant decrease in glioma cell viability only in at longest time (72 h) and in the highest concentrations tested. We suggest that this effect can be related to interpolation of polymer and Tween 80<sup>®</sup> present in the composition of the nanocapsule and, furthermore, by the prolonged cell incubation time. In parallel, primary astrocyte cultures were used as an untransformed cell to evaluate **4L-N** cytotoxicity selectivity (Fig. 4, panel C). Notably, neither **4L** free molecule [19] nor **4L-N** promoted significant cytotoxicity in astrocytes after 72 h of exposure.

**A****B****C**

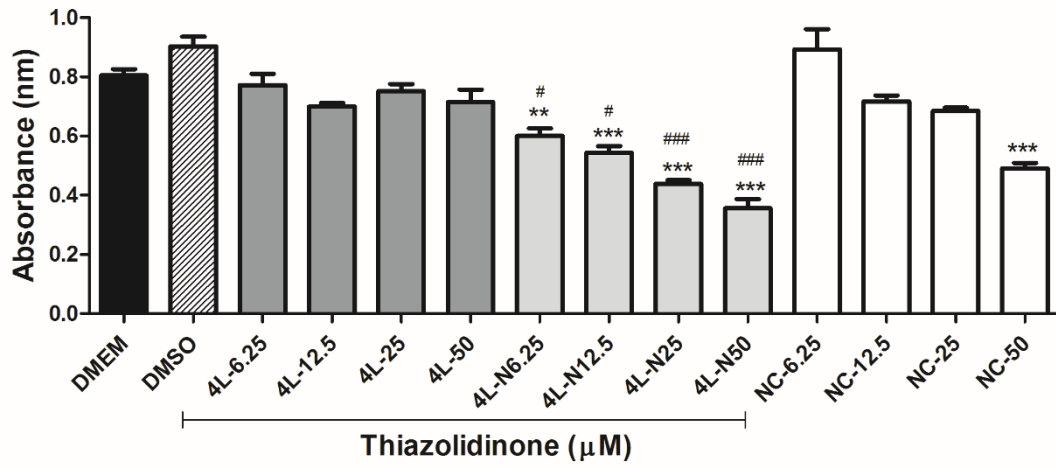
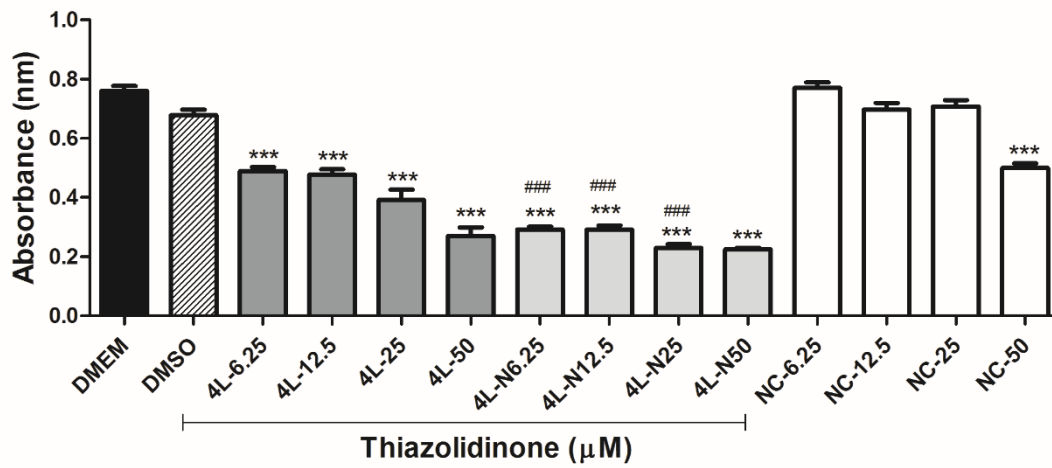
**Figure 4.** Time-concentration effect of 4L thiazolidinone on C6 glioma and primary astrocyte viability. C6 glioma cell line (A and B) and primary astrocyte cultures (C) were treated for 48 h (panel A) or 72 h (panel B and C) with increasing concentrations of 4L or 4L-N as indicated and MTT assay was performed. Appropriate controls were performed for each group. Values represent the mean  $\pm$  SD of at least three independent experiments. Data were analyzed by ANOVA followed by post-hoc comparisons (Tukey-Kramer test). \*, \*\*, \*\*\* Significantly different from the respective control, #, ##, ### Significant difference between free (4L) or nanocapsuled molecule (4L-N) ( $p < 0.05$ ;  $p < 0.01$ ;  $p < 0.001$ , respectively).

### ***Synthetic 2-(2-methoxyphenyl)-3-((piperidin-1-yl)ethyl)thiazolidin-4-on decreases C6 glioma cell proliferation***

Through the sulfarodamine B assay, we evaluated whether 4L and 4L-N were able to reduce C6 glioma cell proliferation (Fig. 5). Glioma cells were exposed to 4L or 4L-N and after 48 or 72 h of treatment, proliferation was evaluated. Controls containing 0.01% DMSO, DMEM/5% FBS or blank nanocapsule (NC) were used. As shown in Figure 5, 4L decreased glioma cell proliferation by 35 to 65% following treatment with increasing concentrations of thiazolidinones (6.25-50  $\mu$ M) for 72 h, while after 48 h of treatment no changes were observed. On the other hand, 4L-N reduced C6 cell proliferation in all times (48 or 72 h) and concentrations tested (6.25-50  $\mu$ M). Indeed, the decrease of cell proliferation ranged from 25-56% and 60-70% following 48 or 72 h of exposure, respectively. We note that while in its free form the 4L thiazolidinone did not prove to be efficient in decreasing glioma cell proliferation at 48 hours, the 4L-N nanoencapsulated molecule was efficient in all tested concentrations, including in the smaller ones.

Experiments with molecule-unloaded nanocapsules (NC) have also been performed and the result is close to that shown in MTT, where NC alone is able to reduce glioma viability at higher concentrations. In general, both 4L or 4L-N treatments

decreased C6 glioma cell proliferation compared to controls, and we conclude that 4L nanoencapsulation may further enhance its promising antiglioma effect. Notably, results show that even at lowest concentration tested, **4L-N** is 25% more effective than **4L** in reducing glioma proliferation.

**A****B**

**Figure 5.** Effect of **4L** or **4L-N** on C6 glioma cell proliferation. C6 glioma cell line was treated for 48 h (panel A) or 72 h (panel B) at different concentrations (6.25-50 $\mu$ M) of **4L** synthetic thiazolidinone (free or in nanocapsules). The sulfarodamine B assay was performed. Appropriate controls were performed for each group. Values represent mean  $\pm$  SD of at least three independent experiments. Data were analyzed by ANOVA followed by post-hoc comparisons (Tukey-Kramer test). \*, \*\*, \*\*\*Significantly different from control cells, #, ##, ### Significant difference between free or nanocapsule molecule ) (p < 0.05; p < 0.01; p < 0.001, respectively).

***2- (2-methoxyphenyl)-3-((piperidin-1-yl)ethyl)thiazolidin-4-one promotes C6 glioma cell death***

Permeability of cell membrane was assessed by incorporation of propidium iodide (PI). Concentrations of 12.5, 25, or 50  $\mu$ M were chosen and treatment with **4L** or **4L-N** were performed for 48 h (Fig. 6). Cells exposed to DMEM/5% FBS, DMSO (0.01%) or drug-unloaded nanocapsules were used as controls. **4L** in its free form was able to decrease viability of cancer cells, whereas **4L-N** promoted cell morphological alterations and PI incorporation when compared to controls. These results suggest that the antiproliferative effect of **4L** is potentiated when the molecule is nanoencapsulated and its effect can be mediated by necrosis. However, the involvement of other cell death pathways could not be excluded.

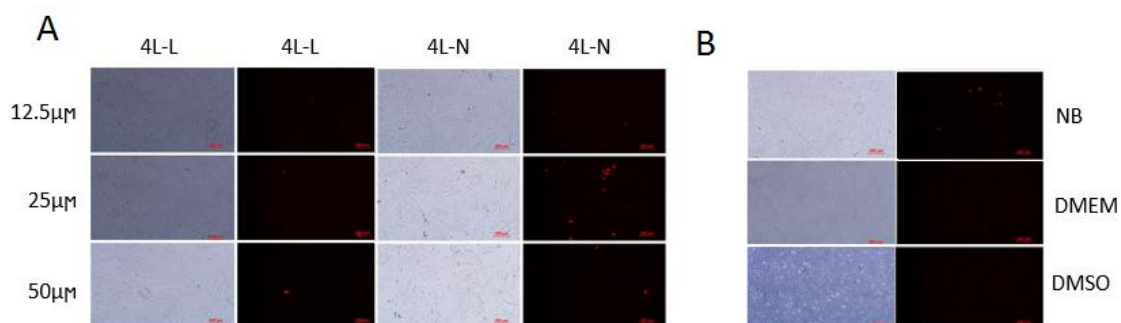


**Figure 6.** Incorporation of propidium iodide (PI) into C6 glioma cells after treatment with 4L or 4L-N. Cells were exposed to increasing concentrations of 4L or 4L-N and after 48 h of treatment the glioma cells (panel A) were incubated with diluted PI in culture medium. Appropriate controls (panel B) containing DMEM, 0.01% DMSO or blank nanocapsules were performed. Fluorescence (right panel) and phase contrast (left panel) micrographs were performed using an Olympus inverted microscope.

***4L or 4L-N does not cause weight loss, metabolic toxicity and mortality in rats.***

We also evaluated the toxicity of 4L and 4L-N *in vivo*. Animals (60 days old Wistar rats) were orally treated with 4L or 4L-N (5 mg/kg/day) for 5 days. Control groups received an equivalent volume of canola oil (vehicle) or drug-unloaded nanocapsule (NC). Treatment with both 4L and 4L-N did not cause weight loss or mortality (Fig. 7). Cellular toxicity was assessed by ALT and AST activity (liver damage markers) and creatinine and serum urea levels (markers of kidney damage), and no alterations were observed in these parameters (Table 2). Taken together, these results support the idea that both 4L and 4L-N did not promote peripheral toxicity.

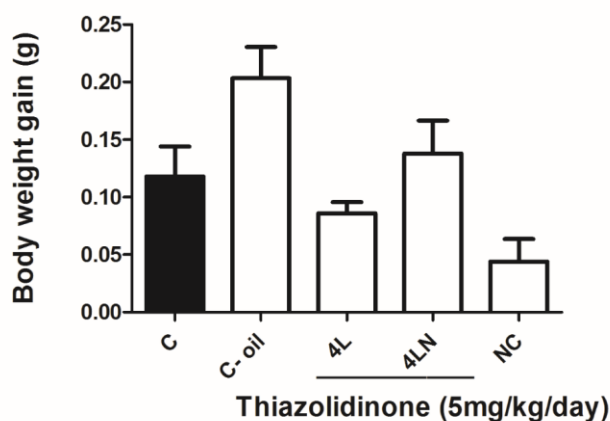


**Figure 7:** Analysis of weight gain in controlled or treated rats (n=8). Animals were treated with free 4L thiazolidinone (5 mg/kg/day) or in nanocapsules (4L-N) or controls (canola oil or molecule-free nanocapsule). The values represent the mean  $\pm$  SD. Data were analyzed by ANOVA.



**Table 2.** Serum markers of tissue damage in control, 4L or 4L-N-treated rats (n=8). Animals were treated via gavage with 4L or 4L-N (5 mg/kg/day) for 5 days. Control rats were treated with equivalent volume of canola oil (vehicle) or NC. Values represent mean±SD. Data were analyzed by ANOVA.

	Control	C-oil	4L	4LN	NC
AST (U/L)	96.60±33.31	152.80±20.14	157.40±45.19	144.00±23.70	141.60±36.71
ALT (U/L)	42.00±3.93	45.00±6.20	47.60±5.94	44.80±6.30	48.20±3.42
Urea (mg/dL)	43.20±3.19	45.80±5.11	43.20±3.03	47.00±3.53	43.20±3.19
Creatinine (mg/dL)	0.46±0.07	0.53±0.08	0.55±0.04	0.52±0.02	0.50±0.05

Serum markers of tissue damage: AST: Aspartate aminotransferase; ALT: Alanine aminotransferase.

#### *Evaluation of oxidative stress parameters in brain and liver of rats*

First, no changes were observed in both brain and liver of the 4L or 4L-N group compared to the control group. Regarding the profile of oxidative stress parameters in the brain, that can be seen in Figure 8, there was no change in the levels of TBARS ( $F_{(4-13)}=0.37$ ,  $P > 0.05$ ) and total sulfhydryl content ( $F_{(4-18)}=0.64$ ,  $P > 0.05$ ) as well as in the activity of the antioxidant enzymes SOD ( $F_{(4-17)}=1.15$ ,  $P > 0.05$ ) and CAT ( $F_{(4-18)}=1.57$ ,  $P > 0.05$ ) in the 4L, 4L-N and NC groups when compared to the control group.

Similar results were found in the liver as shown in figure 9. No change was observed in TBARS ( $F_{(4-18)}=3.12$ ,  $P > 0.05$ ) levels, total sulfhydryl content ( $F_{(4-17)}=3.87$ ,  $P > 0.05$ ) and activity of antioxidant enzymes SOD ( $F_{(4-18)}=1.91$ ,  $P > 0.05$ ) and CAT ( $F_{(4-20)}=0.62$ ,  $P > 0.05$ ) liver of rats treated with 4L, 4LN as well as NC.

### Brain

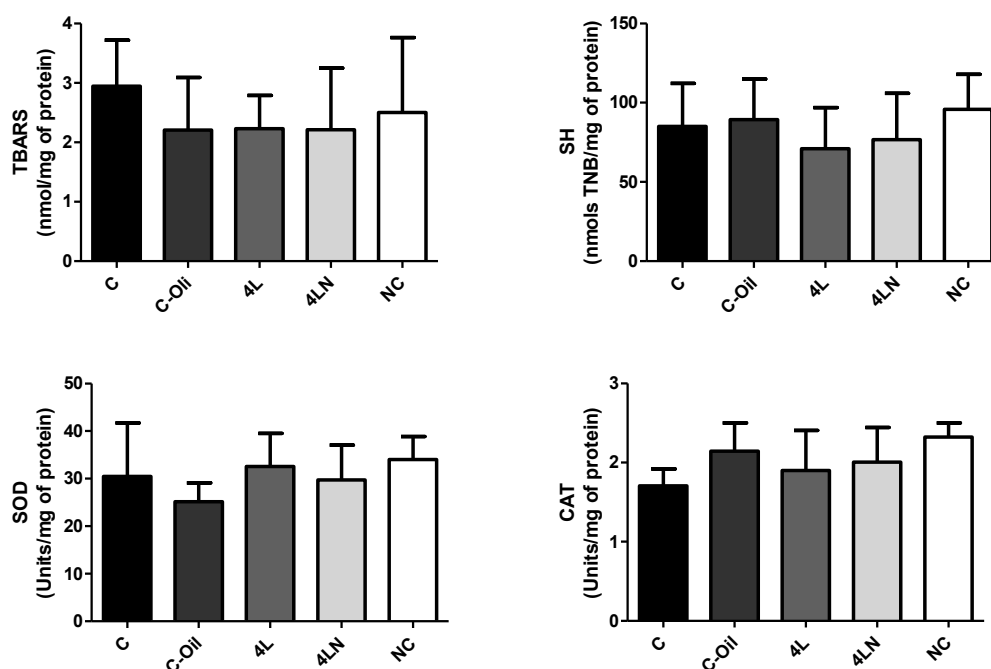
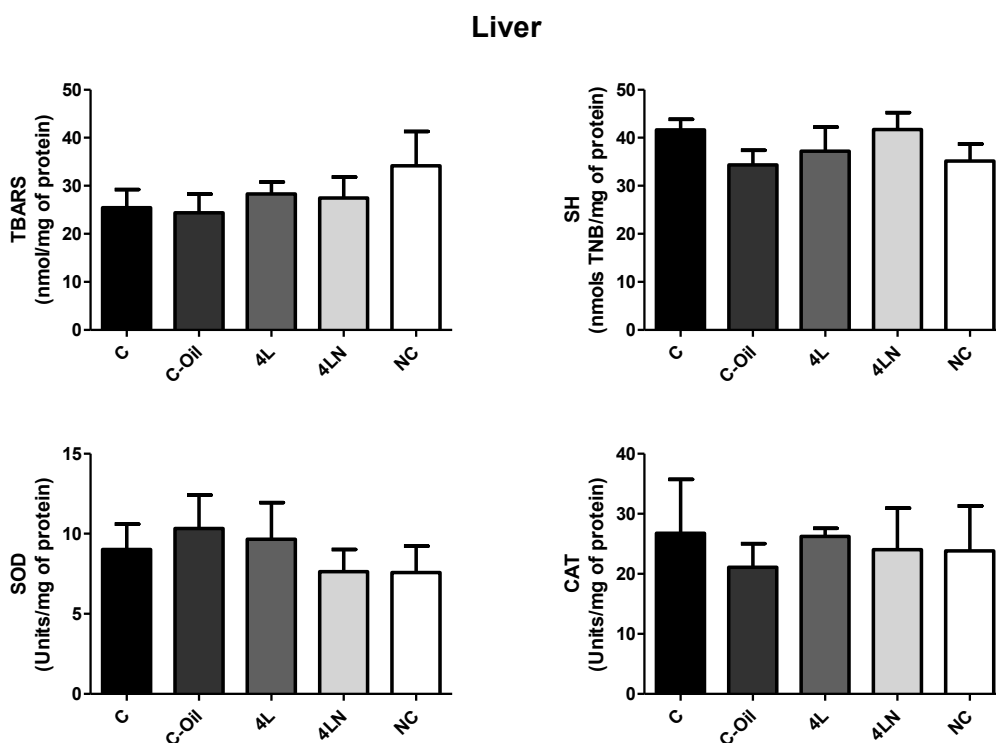


Figure 8: Analysis of oxidative stress parameters TBARS (A), total sulfhydryl content (B) and activities of antioxidant enzymes superoxide dismutase (SOD) (C) and catalase (CAT) (D) in brain of rats 5 days after treatment with 4L, 4LN and NC compounds. Values are expressed as mean  $\pm$  SD ( $n = 4-5$ ). TBARS levels were reported as nmol TBARS per mg protein, total sulfhydryl content as nmol TNB per mg protein and SOD and CAT are express as unit per mg pf protein. Data were analyzed by ANOVA followed by Tukey–Kramer test.



**Figure 9:** Analysis of oxidative stress parameters TBARS (A), total sulphydryl content (B) and activities of antioxidant enzymes superoxide dismutase (SOD) (C) and catalase (CAT) (D) in liver of rats 5 days after treatment with 4L, 4L-N and NC compounds. Values are expressed as mean  $\pm$  SD ( $n = 4-6$ ). TBARS levels were reported as nmol TBARS per mg protein, total sulphydryl content as nmol TNB per mg protein and SOD and CAT are express as unit per mg pf protein. Data were analyzed by ANOVA followed by Tukey–Kramer test.

#### 4. Discussion

Glioblastoma multiforme is an extremely aggressive, uncured tumor with a high rate of proliferation and infiltration, as well as a large angiogenic capacity [25]. Despite intense efforts to develop new therapies for patients diagnosed with this type of tumor, GBM eradication is still not available making it a challenge for most antineoplastic agents [26]. Thiazolidinones have a large number of different biological applications [11]. In a previous study published by our group, some 2-aryl-3-((piperidin-1-yl)ethyl)thiazolidin-4-ones demonstrated *in vitro* and *in vivo* antiglioma activities [19]. Among all compounds tested, the best result was found for 2-(2-methoxyphenyl)-3-

((piperidin-1-yl)ethyl)thiazolidin-4-one **4L**. In this work, that compound was nanoencapsulated with the aim of further improving its antitumor ability. Nanocapsules are promising alternatives in therapeutics and are able to become invisible to the monitic phagocytic system, which favors the targeting of the formulation to the microenvironment of the tumor and facilitate the passage of bioactive molecules through BBB, there by increasing therapeutic efficacy and reducing side effects [17]. Are also capable of which increase the stability of substances protecting against photo or chemical degradation, increasing molecule stability and reducing drug toxicity [27, 28, 29, 30]. Features like these are usually found in to nanocapsules prepared by the interfacial deposition of preformed polymer employing PCL as polymer and MCT as oil core [31, 32, 33]. The zeta potential values were negative which is probably due to the PCL, which is a polyester [34] and to polysorbate 80 that confers a steric stabilization and presents a negative charge surface density [33]. The pH values are in the neutral range and also are in accordance to the nanocapsules prepared by the method employed in this study and are suitable for parenteral administration.

Aiming to determine **4L** photostability and nanocapsules ability to protect the molecule against degradation, the formulations were exposed to UVC radiation. As a first point, we can suggest that **4L** is a photolabile molecule, since after 120 min of exposure the content decrease significantly. On the other hand, when this molecule is nanoencapsulated, **4L** content kept unchanged. This result can be explained by PCL presence in nanocapsule vesicular structure because it is a semi-crystalline polymer and is able to reflect and/or scatter ultraviolet light [35, 36]. Additionally, nanometric size of polymeric nanocapsules can contribute to photostability improvement and scattering radiation.

Concerning *in vitro* drug release study, it is possible to observe a molecule controlled release in comparison to **4L** methanolic solution. After 6h of experiment, 100% of free **4L** had been released, while around 70% were released from nanocapsules. Controlled release is one advantage attributed to nanostructured systems and the presence of the polymer can be the main barrier to drug delivery. The drug release can be dependent on the polymer erosion and/or drug diffusion to the dissolution medium and the lipophilic molecules have high affinity to oil core and consequently present a slow drug delivery [33, 34].

We analyzed the effect of **4L** and **4L-N** on *in vitro* viability and proliferation of glioma cells. Treatment with (**4L**) selectively decreased cell viability and proliferation of C6 glioma line, while the molecule **4L-N** at both treatment times (48 and 72 h) a greater potential for efficiency of 61% and the proliferation of 71% in the highest concentrations tested. In addition, we verified that **4L-N** promoted a decrease in viability and cell density, caused morphological changes and incorporation of PI when compared to control. These results suggest that the antiproliferative effect of compound is enhanced by nanoencapsulation and its effect can be mediated by necrosis. However, the involvement of other cell death pathways can not be excluded since changes in cell viability and survival, as well as the occurrence of cell damage, is secondary to cell cycle dysregulation and development of apoptotic cell characteristics [37]. Recent studies show that the class of 5-ene-4-thiazolidinones have anticancer effects through reversible blockade of the cell cycle progression at the G2/M phase boundary leading to the induction of apoptosis [38]. In addition, thiazolidinones groups still act as inhibitors of anti-apoptotic protein-protein interactions - occurring between Bcl-2 and Bax family [39], as selective inhibitors of extracellular signal-regulated kinases-1 and 2 (ERK1/2) [40] and still as inhibitors of CDK1 [41, 42] and CDK1/cyclin B [42]. Thiazolidinones

have affinity for different molecular targets, however, apoptosis induced by 4-thiazolidinones and their derivatives has been demonstrated in different types of cancer cells [43, 44, 45].

The search for new molecules with important antitumor activity and low toxicity for normal cells is strongly prioritized [46]. In previous studies we have already shown that the thiazolidinone **4L** was not toxic to primary astrocytes [19]. Here we demonstrate that this thiazolidinone in its nanoencapsulated form (**4L-N**) also shows no toxicity to normal cells, being selective to tumoral astrocytes. Current chemotherapy presents many options with little specificity and high toxicity and this represents a limitation to cancer treatment [47]. Thus, considering the therapeutic potential of the **4L** or **4L-N** thiazolidinone demonstrated in *in vitro* tests, investigation of the potential toxicity of these molecules becomes relevant. It is important to emphasize that in this study **4L-N** did not promote either mortality or systemic toxicity to the animals, with normal, Alt, Ast, creatinine and urea levels. In addition, animals treated with **4L-N** did not exhibit weight loss throughout the treatment. Similar data to these have already shown that these polymer nanostructures did not promote systemic toxicity [34].

Oxidative stress reflects an imbalance between pro-oxidants and antioxidant compounds that can cause irreversible damage to biomolecules that lead to cell dysfunction [48, 49]. However, oxidative stress can be defined as homeostatic, non-specific defensive response of the organism to the challenges, in addition to contributing to pathogenesis of various diseases. Therefore, this is an important point to be investigated in the search for new therapeutic potentials. Recent studies with molecules derived from 4-thiazolidinones did not alter the level of ROS, whereas doxorubicin elevated the indices significantly; in addition, doxorubicin decreased the activity of antioxidant enzymes such as, SOD, GPO and Cat in rats blood, whereas thiazolidinones

had less prominent results. These data show that 4-thiazolidinone derivatives have a greater safety regarding alterations in the antioxidant defense system when compared to doxorubicin, a chemotherapeutic already used in the clinic [50]. Our results indicated that the thiazolidinone **4L** as well as **4L-N** do not alter the parameters of oxidative stress in liver and brain. As shown above, they did not alter markers of oxidative damage, such as TBARS levels, a marker for lipid peroxidation and total sulfhydryl content. In addition, no change in the activity of antioxidant enzymes such as SOD and CAT was observed in the liver and brain of rats. Taken together, these data suggest that exposure to the **4L** or **4L-N** thiazolidinone did not induce oxidative stress in rats.

### **Conclusion**

In conclusion, our data show for the first time **4L** thiazolidinone-loaded nanocapsules as an alternative for the treatment of glioma. In addition, nanocapsule formulation (**4L-N**) have *in vitro* antitumor activity even more efficient than molecule in its free form (**4L**), does not induce toxicity to normal astrocytes in culture or to rats, as indicated in *in vivo* experiments, which suggests a possible the safety of formulations. Data shown here support additional studies to test 2-(2-methoxyphenyl)-3-((piperidin-1-yl)ethyl)thiazolidin-4-one-loaded polymeric nanocapsules in a preclinical glioma model as a novel therapeutic modality for the treatment of brain tumors in the future.

### **Acknowledgments**

The authors thank to FAPERGS (11/2068-7; 16/2551-0000265-7) for financial support. CNPq (307330/2012-5; 310846/2014-5) is also acknowledged.

## References

1. G. P. Dunn; I. F. Dunn; W. T. Curry. *Cancer Immunity*, 7, 2007, 12-28.
2. E. C. Holland. *Current Opinion in Neurology*, 14, 6, 2001, 683-8.
3. D. N. Louis, H. Ohgaki, O. D. Wiestler, W. K. Cavenee, P. C. Burger, A. Jouvett, B. W. Scheithauer, P. Kleihues. *Acta Neuropathol*, 114, 5, 2007, 547.
4. M. M. Mrugala. *Discov Med*, 15, 83, 2013, 221-30.
5. R. Stupp, M.E. Hegi, M.R. Gilbert, A. Chakravarti. *J. Clin. Oncol*, 25, 26, 2007, 4127-4136.
6. R. Soffietti, B. Leoncini, R. Ruda. *Expert Rev. Neurother.* 7, 2007, 1313-1326.
7. D. Patel, P. Kumari, N. Patel. *Eur. J. Med. Chem.* 48, 2012, 354-362.
8. A. Deep, S. Jain, P.C. Sharma, P. Phogat, M. Malhotra. *Med. Chem. Res.* 21, 2012, 1652-1659.
9. R. B. Lesyk, B. S. Zimenkovsky. *Curr. Org. Chem*, 8, 2004, 1547- 1577.
10. A. R. Saundane, M. Yarlakatti, P. Walmik, V. Katkarf. *J. Chem. Sci.* 124, 2012, 469 e 481.
11. A. C. Tripathi, S. J. Gupta, G. N. Fatima, P. K. Sonar, A. Verma, S. K. Saraf. *Eur. J. Med. Chem.* 72, 2014, 52-77.
12. D. Havrylyuk, B. Zimenkovsky, O. Vasylenko, L. Zaprutko, A. Gzella, R. Lesyk. *Eur. J. Med. Chem.* 44, 4, 2009, 1396–1404.
13. D. Kaminsky, B. Zimenkovsky, R. Lesyk. *Eur. J. Med. Chem.* 44, 9, 2009, 3627–3636.
14. S. Moorkoth. *Chem. Pharm. Bull.* 63, 12, 2015, 974-985.
15. Y. Wan, S. Wu, G. Xiao, T. Liu, X. Hou, C. Chen, P. Guan, X. Yang, H. Fang. *Bioorg. Med. Chem.* 23, 9, 2015, 1994-2003.



16. A.H. Abdelazeem, A.M. Gouda, H.A. Omar, M.F. Tolba. *Bioorg. Chem.* 57, 2014, 132-141
17. B. Obermeier, R. Daneman, R. M. Ransohoff. *Nat. Med.* 19, 2013, 1584-1596.
18. A. Kunzler, P.D. Neuenfeldt, A. M. Das Neves, M. P. Pereira, M.P. Claudio, G. H. Marques, P. S. Nascente, M.H.V. Fernandes, S. O. Hubner, W. Cunico. *European Journal of Medicinal Chemistry.* 64, 2013, 74-80.
19. E. F. da Silveira, J. H. Azambuja, T. R. de Carvalho, A. Kunzler, D. S. da Silva, F. C. Teixeira, R. Rodrigues, F. T. Beira, S. S. R. Alves, R.M. Spanevello, W. Cunico, F.M. Stefanello, A. P. Horn, E. Braganhol. *Chemico-Biological Interactions*, 266, 2017, 1-9.
20. H. Esterbauer, K. H. Cheeseman. *Methods Enzymol* 186, 1990, 407–421.
21. M. Y. Aksenov, W. R. Markesbery. *Neurosci Lett* 302, 2001, 141–145.
22. H. P. Misra, I. Fridovich. *J Biol Chem* 247, 1972, 3170–3175.
23. H. Aebi. *Methods Enzymol* 105, 1984, 121–126.
24. O. H. Lowry, N. J. Rosebrough, A. L. Farr, R. J. Randall *J Biol Chem* 193, 1951, 265–275.
25. K.E. Borisov, D.D. Sakaeva. *Arkh Patol.* 77, 2015, 54-63.
26. V. V. Chumak, M. R. Fil, R. R. Panchuk, B. S. Zimenkovsky, D. Y. Havrylyuk, R. B. Lesyk, et al. *Ukr Biochem J.* 2014, 86, 96-105.
27. S.S. Santos, A. Lorenzoni, N.S. Pegoraro, L.B. Denardi, S.H. Alves, S.R. Schaffazick, et al. *Colloids Surf B*, 116, 2014, 270–276.
28. J.M. Chassot, D. Ribas, E.F. Silveira, L.D. Grünspan, C.C. Pires, P.V. Farago, et al. *J. Nanosci. Nanotechnol.* 15, 2015, 855–864.

29. A. Zanotto-Filho, K. Coradini, E. Braganhol, et al. *Eur J Pharm Biopharm.* 2013;83, 2, 2013, 156-167.
30. M. C. Fontana, A. Beckenkamp, A. Buffon, R. C. R. Beck. *Int J Nanomedicine.* 9, 2014, 2979-2991.
31. A. F. Ourique, A. R. Pohlmann, S. S. Guterres, et al. *Int J Pharm.* 352, 2008, 1- 4.
32. R. B. Friedrich, M. C. Fontana, R. C. R. Beck, et al. *Quim Nova.* 31, 2008, 1131-1136.
33. M. C. Fontana, K. Coradini, S. S. Guterres, et al. *J Biomed Nanotechnol.* 3, 2009, 254-263).
34. J.M. Chassot, D. Ribas, E.F. Silveira, L.D. Grünspan, C.C. Pires, P.V. Farago, et al. *J. Nanosci. Nanotechnol.* 15, 2015, 855–864.
35. A. R. Pohlmann, F. N. Fonseca, K. Paese, et al. *Expert Opin Drug Deliv.* 10, 5, 2013, 623-38.
36. J. S. Almeida, F. Lima, S. D. Ros, et al. *Nanoscale Res Lett.* 10, 2010, 1603-10.
37. A. Degterev, A. Lugovskoy, M. Cardone, B. Mulley, G. Wagner, T. Mitchison, J. Yuan. *Nat. Cell Biol.* 3, 2001, 173–182.
38. J. Senkiv, N. Finiuk, D. Kaminsky, D. Havrylyuk, M. Wojtyra, I. Kril, R. Lesyk. *European journal of medicinal chemistry*, 2016, 117, 33-46.
39. A. A. Lugovskoy, A. I. Degterev, A. F. Fahmy, P. Zhou, J. D. Gross, J. Yuan, G. Wagner. *J. Am. Chem. Soc.* 124, 7, 2002, 1234–1240.
40. K.Y. Jung, R. Samadani, J. Chauhan, K. Nevels, J.L. Yap, J. Zhang, S. Worlikar, M.E. Lanning, L. Chen, M. Ensey, S. Shukla, R. Salmo, G. Heinzl, C. Gordon, T. Dukes, A.D. MacKerell, Jr.P. Shapiro, S. Fletcher. *Org. Biomol. Chem.* 11, 2013, 3706–3732.
41. L. T. Vassilev, C. Tovar, S. Chen, D. Knezevic, X. Zhao, H. Sun, D. C. Heimbrosk, L. Chen. *PNAS*, 103, 2006, 10660–10665.

42. S. Chen, L. Chen, N. T. Le, C. Zhao, A. Sidduri, J. P. Lou, C. Michoud, L. Portland, N. Jackson, J.J. Liu, F. Konzelmann, F. Chi, C. Tovar, Q. Xiang, Y. Chen, Y. Wen, L. T. Bioorg. Med. Chem. Lett. 17, 2007, 2134–2138.
43. S. Chandrappa, C.V. Kavitha, M.S. Shahabuddin, K. Vinaya, C.A. Kumar, S.R. Ranganatha, S.C. Raghavan, K.S. Rangappa. Bioorg. Med. Chem. 17, 2009, 2576–2584.
44. F. E. Onen-Bayram, I. Durmaz, D. Scherman, J. Herscovici, R. Cetin-Atalay. Bioorg. Med. Chem. 20, 2012, 5094–5102.
45. W. Li, Z. Wang, V. Gududuru, B. Zbytek, A.T. Slominski, J.T. Dalton, D.D. Miller. Anticancer Res. 27, 2007, 883–888.
46. V. V. Chumak, M. R. Fil, R. R. Panchuk, B. S. Zimenkovsky, D. Y. Havrylyuk, R. B. Lesyk, & R. S. Stoika. The Ukrainian biochemical journal, 86, 2014, 96-105.
47. R. V. Chari. Accounts of chemical research, 41, 2007, 98-107.
48. R. E. Gonsette, R. E. Journal of the neurological sciences, 274, 2008, 48-53.
49. S. Ljubisavljevic. Molecular neurobiology, 53, 2016, 744-758.
50. L. I. Kobylinska, N. M. Boiko, R. R. Panchuk, I. I. Grytsyna, L. P. Biletska, R. B. Lesyk, ... & R. S. Stoika. Croatian medical journal, 57, 2016, 151-16.

Manuscrito 2: submetido à revista “European Journal of Medicinal Chemistry”

**The anti-inflammatory, antitumor and cytotoxic activities of synthetic thiazolidinones from 3-morpholinopropylamine.**

Elita F. Silveira,<sup>1\*</sup> Daniela P. Gouvêa,<sup>2</sup> Flávia A. Vasconcellos,<sup>2</sup> Gabriele A. Berwaldt,<sup>2</sup> Juliana H. Azambuja,<sup>3</sup> Adriana M. Neves,<sup>2</sup> Renata P. Sakata,<sup>4</sup> Wanda P. Almeida,<sup>4</sup> Ana P. Horn,<sup>1</sup> Elizandra Braganhol,<sup>3</sup> Wilson Cunico.<sup>2\*</sup>

<sup>1</sup> Programa de Pós-Graduação em Ciências Fisiológicas, Instituto de Ciências Biológicas, Universidade Federal do Rio Grande, Rio Grande, RS, Brazil.

<sup>2</sup> Centro de Ciências Químicas, Farmacêuticas e de Alimentos, Universidade Federal de Pelotas, Pelotas, RS, Brazil.

<sup>3</sup> Departamento de Ciências Básicas da Saúde, Universidade Federal de Ciências da Saúde de Porto Alegre, Porto Alegre, RS, Brazil.

<sup>4</sup> Instituto de Química e Faculdade de Ciências Farmacêuticas, Universidade Estadual de Campinas, Campinas, SP, Brazil.

**\*Corresponding Authors**

Elita Ferreira da Silveira (elitafs24@gmail.com)

Universidade Federal de Rio Grande - FURG

Avenida Itália, Km 8, Campus Carreiros

CEP: 96.203-900, Rio Grande, RS, Brasil Phone: +55 53 3293 6987-81113646

Wilson Cunico (wjcunico@yahoo.com.br)

Universidade Federal de Pelotas (UFPel)

## Abstract

Heterocyclic compounds such as thiazolidinones stand out because their important pharmacological properties. The aim of this work was to synthesize 2-aryl-3-(3-morpholinopropyl)thiazolidin-4-ones and to verify their potential anti-inflammatory and antiglioma activities. Sixteen 2-aryl-3-(3-morpholinopropyl)thiazolidin-4-ones were easily synthesized by one-pot reactions from 3-morpholinopropylamine, arenealdehydes and mercaptoacetic acid in moderate to excellent yields (31-98%) and were identified and characterized by  $^1\text{H}$  and  $^{13}\text{C}$  NMR, mass and HRMS techniques. By means of a croton oil-induced ear edema model in mice, nine compounds (**4a**, **4b**, **4d**, **4f**, **4g**, **4h**, **4j**, **4m** and **4p**) showed inflammation inhibition values between 50 to 71% at 166 mg/kg. The antiglioma study was performed in C6 cells exposed to different concentrations of these nine thiazolidinones and the cell viabilities were measured by MTT assay. Thiazolidinones **4a**, **4d**, **4f** and **4h**, which have electron withdrawing groups as substituents, were able to reduce the viability of C6 cells (greater than 50% at 100  $\mu\text{M}$ ). In addition, all thiazolidinones showed no toxicity in the primary astrocytes. These preliminary data indicate the therapeutic potential of compounds bearing both important heterocyclic thiazolidinone and morpholine as anti-inflammatory and for GBM treatment.

**Keywords:** thiazolidinones, morpholine, anti-inflammatory, antiglioma.

## 1. Introduction

Literature shows a wide range of pharmacological properties for compounds with a thiazolidinone ring that have shown at least sixteen different therapeutic targets, including anti-inflammatory, antitumor and antiglioma activities [1, 2, 3].

Inflammation is a physiological process that comprises the organism's biological response prior to infection or tissue injury involving a coordinated action between the immune system and the tissue in which the injury occurred [4]. The inflammatory response, mediated by cells, may be important for both tumor progression and elimination [5]. Studies show that the relationship between cancer and inflammation establishes that the immune network may be involved in regulating the development and growth of glioma [6]. Glioblastoma multiform (GBM) is the most common and lethal primary brain tumor presenting morphological and gene expression similarities with glial cells, such as astrocytes, oligodendrocytes and their precursors [7]. The presence of an inflammatory microenvironment is associated with increased malignancy of the glioma through the modulation of cellular proliferation and angiogenesis, which results in poor prognosis for patients [8]. Malignant gliomas generate several immunomodulatory mechanisms that result in evasion and suppression of the immune system. The constitutive activity of NF- $\kappa$ B in cancer cells was related to the expression of apoptosis resistance genes (bcl-xL and survivin) and inflammation genes (IL1- $\beta$ , IL-6 and COX-2) [9]. Cyclooxygenase (COX) is a well-known enzyme that catalyzes the conversion of arachidonic acid to prostaglandins (PGs) in cells. Although COX is widely studied as an anti-inflammatory target, COX-2 is also important in the pathogenesis of cancer [10]. In addition, the inflammatory microenvironment



constituted mainly by macrophages contributes to invasion, progression and positive correlation with malignancy and consequent low prognosis for patients with glioma [11]. Thus, the discovery of polypharmacological drugs with affinity for different targets, such as inflammation and cancer may be considered an advantage, especially for the treatment of lethal brain tumor. For this reason, it is necessary the development of new biological compounds with subsequent optimization to obtain a broad spectrum of biological activities.

In recent works, we investigated anti-inflammatory and antitumor activities of different compounds derived from thiazolidinones [12, 13, 14]. In these previous works, we used 1-(2-aminoethyl)piperidine [14] and 4-(2-aminoethyl)morpholine [12] as primary amine precursors. In this work, our objective was to synthesize a new series of thiazolidinones from an analogue amine precursor, the 4-(3-aminopropyl)morpholine (Figure 1). In addition, knowing that changes in the structure of the compound lead to changes in its properties and even in its therapeutic potential, we also studied the anti-inflammatory, antiglioma and cytotoxicity activities of 2-aryl-3-(3-morpholinopropyl)thiazolidin-4-ones.

## **2. Results e Discussion**

### *2.1. Chemistry*

Desired 2-aryl-3-(3-morpholinopropyl)thiazolidin-4-ones **4** were synthesized from one-pot reactions using similar condition reported in recent paper published by us due to similarity of both amines, 4-(3-aminopropyl)morpholine **2** and 4-(2-aminoethyl)morpholine [12]. The progresses of reactions were monitored by TLC

(hexane/ethyl acetate, 3:1 proportion) and/or GC analysis. First, the reaction of 3-morpholinopropylamine **2** and arenealdehydes **1a-r** in reflux of toluene for 3 h led to formation of intermediate imine. After, the mercaptoacetic acid **3** was added and the mixture was continuing refluxed for more 16 hours to intramolecular cyclization (**Scheme 1**). Thiazolidinones **4a-p** were obtained in moderated to excellent yields after purification by washing with hot hexane (31-98%). The lowest yields were found for thiazolidinones bearing hydroxyl group (**4m** and **4n**) and a possible explanation is the water solubility of product in the extraction step. Arenealdehyde precursors were chosen to afford analogues containing fluoro, chloro, methoxy, nitro, methyl and hydroxyl groups at 2, 3 or 4-position of phenyl ring.

All compounds are novel, except thiazolidinone **4b** (CAS 485399-10-8 [15]). Compounds **4l** (CAS 920537-81-1) and **4p** (CAS 920537-87-7) were also previously characterized, however as hydrochloride salts [16]. The thiazolidinones **4a-p** were identified and characterized by  $^1\text{H}$  and  $^{13}\text{C}$  NMR, with the assistance 2D spectra (HSQC and HMBC), GC-MS and HRMS (supplementary information). All data are in agreement with proposal structures. As expected, H2 appears as doublet coupling spatially with H5a (syn coupling with  $^4J$ ) and diastereotopic methylene groups (H5, H6, H7 and H8) appears as two set of signals. As we already observed in previous works [12, 13], it was confirmed by HSQC the inversion of H6/C6 and H8/C8 relationship; while H6 is more deshielded than H8, C6 is less deshielded than C8. It is also interesting to note the HRMS spectra: two peaks were observed in all cases; one is the molecular ion ( $\text{M}^+ + \text{H}$ ); and other is a fragment generate by the cleavage of molecular ion with morpholine group ( $\text{M}^+ - 87$ ).

## 2.2. Anti-inflammatory activity

The 12-o-tetradecanoylforor-13-acetate (TPA) ester present in croton oil (*Croton tiglium* L.) was used to investigate anti-inflammatory activity because of its potent edema induction ability.

Firstly, the topical application of croton / TPA oil is realized, which, after 3 hours, promotes the formation of edema and acute inflammation. Thus we performed the treatments with the respective compounds and after 18 hours the thickness of the ear was measured using an external electronic micrometer [12, 17]. A single investigator performed the measurements for each experiment to minimize variations of the technique [18,19]. Table 1 shows the results of *in vivo* anti-inflammatory activities of the seventeth thiazolidin-4-ones. Among them, nine had more than 50% of anti-inflammatory activity, a promising result. These findings show that the increase of carbon link between thiazolidine and morpholine rigs is well tolerated since no lack of activity was observed. The exception was compound **4o** (R=4-OH) and a possible explanation is the low lipophilicity of this compound. In general, thiazolidinones with propylenic chain showed better results than previous thiazolidinones studied by us with an ethylenic chain [12]. Compounds **4a**, **4b**, **4d**, **4f**, **4g**, **4h**, **4j**, **4m** and **4p** had inhibition values between 50 to 71% at the test concentration used (166 mg/Kg). It is important to note that the position of substituent at phenyl ring is more important than the electronic nature of such groups. All thiazolidinones bearing a 2-substituted phenyl ring showed more than 50% anti-inflammatory action, independent of the substituent.

### 2.3. Antitumoral activity

Considering that the inflammatory micro-environment contributes to the progression of gliomas and that the control of the environment could reduce tumor malignancy, the nine compounds with improved effects in inflammatory activity (up to 50%) were tested via comparative cytotoxicity against C6 glioma cell line and primary astrocytes.

The high rates of proliferation and invasion represent an obstacle to treatment of affected patients with gliomas. The development of effective medicines for GBM therapy is still a challenge in this particular context thiazolidinones exhibit valuable biological applications in medicine as antineoplastic agents [20], anti-microbial [21], anti-inflammatory [22] and antioxidant activity [23]. It is known that there is evidence indicating that chronic inflammation provides conditions which favor the progression of cancer [24, 25]. According to this and with the results of anti-inflammatory study, the C6 antiglioma potential of thiazolidinones **4a**, **4b**, **4d**, **4f**, **4g**, **4h**, **4j**, **4m** and **4p** was evaluated. For this experiment, glioma cell cultures were exposed to different concentrations of thiazolidinones (6.25, 12.5, 25, 50, 100, 250 and 500  $\mu$ M) and cell viabilities were measured by MTT assay after 72 h treatment (**Figure 2**). The cell proliferation analysis showed that the treatment with thiazolidinones reduced the viability of C6 glioma selectively, while no toxicity was observed in astrocytes, a non-transformed cell model (**Figure 3**). Control cells were kept for the same time without such treatment or were treated with a concentration of DMSO as described in Materials and Methods.

All nine compounds were capable to reduce glioma viability. Thiazolidinone **4a** was able to reduce cell viability above 50% at concentrations of 100  $\mu\text{M}$ , 250  $\mu\text{M}$  and 500  $\mu\text{M}$  (50%, 60% and 80%, respectively). Compound **4b** decreased cell viability by 50% at the concentration of 250  $\mu\text{M}$ . Compound **4d** only has statistic difference at 50  $\mu\text{M}$  and it was able to induce a reduction of over 50% of glioma cell viability above 100  $\mu\text{M}$  concentrations. The **4f** shows the antineoplastic potential in all concentrations tested with reduction over 70% of the glioma cell viability at 100  $\mu\text{M}$  and 85% when treated at 500  $\mu\text{M}$ . Compound **4g** has antineoplastic activity starting at 12.5  $\mu\text{M}$  and shows a reduction of cell viability over 50% at 250  $\mu\text{M}$  and 80% at 500  $\mu\text{M}$ . Thiazolidinone **4h** showed concentration-dependent effect with a reduction of about 50% in viability of the glioma cells at concentration of 100  $\mu\text{M}$ . Compound **4j** has antineoplastic potential at all concentrations tested reducing 15% of glioma feasibility at 6.25  $\mu\text{M}$  and above 50% at the highest concentration (500  $\mu\text{M}$ ), while **4p** presented viability reduction above 50% only from the concentration of 250  $\mu\text{M}$ , reaching 70% reduction in the highest concentration. Finally, thiazolidinone **4m** only reduced the viability of the glioma cells about 40% at 500  $\mu\text{M}$ .

These results highlight thiazolidinones **4a**, **4d**, **4f** and **4h** that decreased more than 50% of cell viability at 100  $\mu\text{M}$  and about 80% at the highest concentration tested. It is interesting to note that these four compounds have an electron-withdraw group as substituent in phenyl ring (fluoro, chloro and nitro), suggesting that this electronic effect could be important to activity. These results are in accordance to recent findings by our research group studying C6 glioma cells. Thiazolidinones from 4-(methylthio)benzaldehyde induced reduction of C6 viability in a range of 61.0 to 81.7%

at 100  $\mu\text{M}$  [13]. Already, some piperidine-thiazolidinones also induced 50-85% C6 viability at the same concentrations [14].

Other important finding is the low cytotoxicity of all thiazolidinones in astrocytes. Even in the highest concentrations tested, only compound **4d** showed toxicity, reducing about 40% the cell viability at 500  $\mu\text{M}$ . These results suggest that our compounds showed good selectivity for C6 tumor cells. In comparasion with others thiazolidinones published by us, these compounds seems to be more safe, once it was found toxic effect in one compound at 100  $\mu\text{M}$  [14] and in four compounds at 250  $\mu\text{M}$  [13].

Studies have shown that the antitumor properties of thiazolidin-4ones and related heterocycles are probably due to their affinity to modulate the JNK pathway [26], tumor necrosis factor TNF [27] and anti-apoptotic Bcl-XL biocomplex BH3 [28]. However, the mechanism that correlates cancer and inflammation are not well understood. The presence of an inflammatory microenvironment by nonmalignant cells, such as lymphocytes, microglia and macrophages is associated with increased cell proliferation, modulating angiogenesis, and thus a most malignant glioma [8]. In addition, studies suggest that interactions between leukocytes, platelets and cancer cells also promote angiogenesis and subsequent tumor invasion [29, 30].

It is known that there is a positive correlation between COX-2 expression and poor prognostic survival of GBM patients [31, 32, 33], suggesting that COX-inhibiting anti-inflammatory drugs could also be considered for GBM treatment. Thus, we suggest that thiazolidinones with anti-inflammatory potential may also have a greater antitumor potential.

In conclusion, sixteen compounds containing both thiazolidinone and morpholine heterocycles bound by a propionic link were synthesized and fully characterized. In addition, the biological properties of such compounds have been reported. Anti-inflammatory activity was determined and nine compounds showed reduction in inflammation between 50 to 71%. In addition, we obtained four compounds (**4a**, **4d**, **4f** and **4h**) with improved antiglioma activity in vitro, which reduced more than 50% of cell viability of glioma at 100  $\mu$ M. It is also important to emphasize that these morpholine-thiazolidinones do not promote changes in the growth of astrocyte cells, a model of untransformed cells, so our results suggest that these thiazolidinones are selective target for cancer. These results allow us to continue studying this class of compounds and mechanisms.

### **3. Experimental**

#### *4.1. Chemistry*

The chemical materials were purchased from Sigma Aldrich and were utilized without complementary purification. The progress of reactions were monitored by thin layer chromatography (TLC, using silica gel 60F253 aluminum sheets; visualization by ultraviolet light 254 nm; eluent hexane/ethyl acetate 3:1) and by Shimadzu Gas Chromatograph GC-2010, Column L.D., 0,25mm; Column length, 30m. Column Head Pressure, 14 psi, program: T<sub>0</sub> = 50 °C; t<sub>0</sub> = 2.0 min; rate 16.0 °C/min; T<sub>f</sub> = 250 °C; t<sub>f</sub> = 10.0 min; Inj. = 250 °C; Det. = 270 °C. Melting points were determined in open capillaries using a Fisatom model 430 apparatus and are uncorrected. GC–MS analyses

were performed on a GC 2010-plus GC-MS-QP2010SE System AOC-20i – auto injector.  $^1\text{H}$  and  $^{13}\text{C}$  NMR spectra were recorded using a Bruker DRX 400 spectrometer ( $^1\text{H}$  at 400.14 MHz and  $^{13}\text{C}$  at 100.61 MHz) or a Bruker Avance 500 spectrometer ( $^1\text{H}$  at 500.13 MHz and  $^{13}\text{C}$  at 125.75 MHz) in  $\text{CDCl}_3$  containing TMS as in internal standard. The high-resolution mass spectrometry analyses were performed in a LTQ-XL Orbitrap Discovery apparatus from Thermo Scientific, with electron spray ionization (ESI).

#### 4.1.1. General synthesis of 2-aryl-3-(3-morpholinopropyl)thiazolidin-4-ones **4a-p**

The 4-(3-aminopropyl)morpholine **2** (1 mmol) and corresponding arenaldehyde **1a-p** (1 mmol) in toluene (70 mL) were refluxed in a Dean-Stark trap for 3 hours. After, the mercaptoacetic acid **3** (2 mmol) was added and the mixture was refluxed for more 16 hours. The organic layer was washed with a saturated solution of  $\text{NaHCO}_3$  (3 x 30 mL), dried with  $\text{MgSO}_4$  and concentrated to give the products. When necessary, the compounds were washed with a hot hexane solution to furnish the pure products.

##### 4.1.1.1. 2-(2-fluorophenyl)-3-(3-morpholinopropyl)thiazolidin-4-one **4a**

Yield 69%, white solid m.p. 78-80 °C,  $^1\text{H}$  NMR  $\delta$  (500 MHz, ppm,  $J_{\text{H-H}}=\text{Hz}$ ,  $\text{CDCl}_3$ ): 7.28 (ddd, 1H, Ar,  $^3J=7.3$ ,  $^3J=7.2$ ,  $^4J=1.7$ ); 7.20 (ddd, 1H, Ar,  $^3J=7.6$ ,  $^3J=7.5$ ,  $^4J=1.7$ ); 7.11 (dd, 1H, Ar,  $^3J=8.1$ ;  $^3J=7.6$ ); 7.02 (dd, 1H, Ar,  $^3J=8.6$ ,  $^3J=8.4$ ); 5.95 (d, 1H, H2,  $^4J=1.8$ ); 3.76 (dd, 1H, H5a,  $^2J=15.4$ ,  $^4J=1.7$ ); 3.68-3.57 (m, 6H, H5b, H6a and H10); 2.72 (ddd, 1H, H6b,  $^2J=14.0$ ,  $^3J=7.7$ ,  $^3J=7.7$ ); 2.31-2.20 (m, 6H, H8a, H8b and H9); 1.69 (ddd, 1H, H7a,  $^2J=13.8$  Hz,  $^3J=7.8$  Hz); 1.57 (ddd, 1H, H7b,  $^2J=14.0$  Hz,  $^3J=7.1$  Hz).  $^{13}\text{C}$  NMR  $\delta$  (125 MHz, ppm,  $J_{\text{C-F}}=\text{Hz}$ ,  $\text{CDCl}_3$ ): 171.4 (C4); 160.4 (d,  $^1J=248.8$ ),



130.6 (d,  $^3J=8.4$ ), 127.9 (d,  $^4J=2.9$ ), 127.1 (d,  $^2J=11.6$ ), 124.9 (d,  $^3J=3.6$ ), 116.1 (d,  $^2J=21.3$ ) (Ar); 66.8 (2C, C10); 57.1 (d,  $^3J=4.4$ , C2); 55.8 (C8); 53.4 (2C, C9); 41.4 (C6); 32.7 (C5); 23.6 (C7). HRMS-[ESI] for  $C_{15}H_{19}FN_2O_2S$  (M + H)<sup>+</sup>: 325.1381; found 325.1387. GC-MS *m/z* (%): 324 (M<sup>+</sup>, 7); 281 (1); 236 (1); 153 (2); 129 (12); 100 (100); 56 (10).

#### 4.1.1.2. 3-(fluorophenyl)-3-(2-morpholin-4-propyl)thiazolidin-4-one **4b** [15]

#### 4.1.1.3. 2-(4-fluorophenyl)-3-(3-morpholinopropyl)thiazolidin-4-one **4c**

Yield 75%, yellow oil,  $^1H$  RMN  $\delta$  (500 MHz, ppm,  $J_{H-H}$ =Hz, DMSO- $d_6$ ): 7.48 (dd, 2H, Ar,  $^3J=8.7$ ;  $^3J=8.6$ ); 7.24 (dd, 2H, Ar,  $^3J=8.8$ ,  $^3J=8.8$ ); 5.89 (d, 1H, H2,  $^4J=1.6$ ); 3.86 (dd, 1H, H5a,  $^2J=15.5$ ,  $^4J=1.7$ ); 3.68 (d, 1H, H5b,  $^2J=15.5$ ); 3.49-3.39 (m, 5H, H6a and H10); 2.67 (ddd, H6b;  $^2J=14.0$ ;  $^3J=8.6$ ,  $^3J=8.4$ ); 2.23-2.13 (m, 6H, H8a, H8b and H9); 1.64-1.56 (m, 1H, H7a); 1.45-1.39 (m, 1H, H7b).  $^{13}C$  NMR  $\delta$  (125 MHz, ppm,  $J_{C-F}$ =Hz, DMSO- $d_6$ ): 170.4 (C4); 162.1 (d,  $^1J=245.4$ ), 136.6 (d,  $^4J=2.8$ ), 129.3 (2C, d,  $^3J=8.6$ ), 115.6 (2C, d,  $^2J=21.2$ ) (Ar); 66.0 (2C, C10); 61.4 (C2); 55.1 (C8); 52.9 (2C, C9); 40.6 (C6); 31.9 (C5); 22.9 (C7). HRMS-[ESI] for  $C_{15}H_{19}FN_2O_2S$  (M + H)<sup>+</sup>: 325.1381; found 325.1389. GC-MS *m/z* (%): 324 (M<sup>+</sup>, 4); 281 (2); 207 (6); 153 (2); 129 (14); 100 (100); 56 (10).

#### 4.1.1.4. 2-(2-chlorophenyl)-3-(3-morpholinopropyl)thiazolidin-4-one **4d**

Yield 52%, colorless oil,  $^1H$  RMN  $\delta$  (400 MHz, ppm,  $J_{H-H}$ =Hz,  $CDCl_3$ ): 7.44-7.39 (m, 1H, Ar); 7.33-7.27 (m, 2H, Ar); 7.21-7.17 (m, 1H, Ar); 6.19 (d, 1H, H2,  $^4J=1.6$ ); 3.87 (dt, 1H, H6a,  $^2J=14.1$ ,  $^3J=7.2$ ); 3.83 (dd, 1H, H5a,  $^2J=14.6$ ,  $^4J=1.2$ ); 3.75-3.65 (m, 5H, H5b and H10); 2.76 (ddd, 1H, H6b,  $^2J=14.0$ ,  $^3J=7.3$ ,  $^3J=7.2$ ); 2.43-2.26 (m, 6H, H8a, H8b and H9); 1.88-1.63 (m, 2H, H7a and H7b).  $^{13}C$  NMR  $\delta$  (100 MHz, ppm,  $CDCl_3$ );

171.8 (C4); 137.3, 132.8, 130.2, 129.7, 127.8, 126.9 (Ar); 66.9 (2C, C10); 60.3 (C2); 55.8 (C8); 53.5 (2C, C9); 41.7 (C6); 32.7 (C5); 23.7 (C7). HRMS-[ESI] for  $C_{15}H_{19}ClN_2O_2S$  (M + H)<sup>+</sup>: 341.1085; found 341.1088.

#### 4.1.1.5. 2-(3-chlorophenyl)-3-(3-morpholinopropyl)thiazolidin-4-one **4e**

Yield 86%, yellow oil, <sup>1</sup>H RMN δ (400 MHz, ppm,  $J_{H-H}$ =Hz, CDCl<sub>3</sub>): 7.26 (m, 2H, Ar); 7.23 (br, 1H, Ar); 7.13-7.11 (m, 1H, Ar); 5.55 (d, 1H, H2, <sup>4</sup> $J$ =1.8); 3.75 (dd, 1H, H5a, <sup>2</sup> $J$ =15.5, <sup>4</sup> $J$ =1.9); 3.65-3.58 (m, 6H, H5b, H6a and H10); 2.70 (ddd, 1H, H6b, <sup>2</sup> $J$ =14.1, <sup>3</sup> $J$ =8.2, <sup>3</sup> $J$ =8.1); 2.29-2.24 (m, 4H, H9); 2.22-2.15 (m, 2H, H8a, H8b); 1.69-1.60 (m, 1H, H7a); 1.56-1.47 (m, 1H, H7b). <sup>13</sup>C NMR δ (50 MHz, ppm, CDCl<sub>3</sub>): 171.1 (C4); 135.1; 132.8, 130.4, 129.4, 127.1; 125.0 (Ar); 66.9 (2C, C10); 63.2 (C2); 55.8 (C8); 53.8 (2C, C9); 41.4 (C6); 32.8 (C5); 23.7 (C7). GC-MS  $m/z$  (%): 340 (M<sup>+</sup>, 1); 281 (2); 207 (4); 129 (3); 100 (100); 56 (6).

#### 4.1.1.6. 2-(4-chlorophenyl)-3-(3-morpholinopropyl)thiazolidin-4-one **4f**

Yield 60%, yellow oil, <sup>1</sup>H RMN δ (500 MHz, ppm,  $J_{H-H}$ =Hz, CDCl<sub>3</sub>): 7.29 (d, 2H, Ar, <sup>3</sup> $J$ =8.5); 7.18 (d, 2H, Ar, <sup>3</sup> $J$ =8.5); 5.58 (d, 1H, H2, <sup>4</sup> $J$ =1.7); 3.72 (dd, 1H, H5a, <sup>2</sup> $J$ =15.5, <sup>4</sup> $J$ =1.8); 3.64-3.55 (m, 6H, H5b, H6a and H10); 2.69 (ddd, 1H, H6b, <sup>2</sup> $J$ =14.0, <sup>3</sup> $J$ =8.3, <sup>3</sup> $J$ =8.2); 2.30-2.15 (m, 6H, H8a, H8b and H9); 1.68-1.58 (m, 1H, H7a); 1.57-1.46 (m, 1H, H7b). <sup>13</sup>C NMR δ (125 MHz, ppm, CDCl<sub>3</sub>): 171.1 (C4); 138.7, 137.6, 129.8 (2C), 127.6 (2C) (Ar); 66.6 (2C, C10); 60.7 (C2); 55.6 (C8); 53.4 (2C, C9); 41.4 (C6); 32.5 (C5); 23.5 (C7). HRMS-[ESI] for  $C_{15}H_{19}ClN_2O_2S$  (M + H)<sup>+</sup>: 341.1085; found 341.1092. GC-MS  $m/z$  (%): 340 (M<sup>+</sup>, 2); 254 (2); 129 (10); 100 (100); 56 (10).

#### 4.1.1.7. 3-(3-morpholinopropyl)-2-(2-nitrophenyl)thiazolidin-4-one **4g**

Yield 66%, yellow oil,  $^1\text{H}$  RMN  $\delta$  (250 MHz, ppm,  $J_{\text{H-H}}=\text{Hz}$ ,  $\text{CDCl}_3$ ): 8.06 (d, 1H, Ar,  $^3J=8.1$ ); 7.69 (dd, 1H, Ar,  $^3J=7.5$ ,  $^3J=7.4$ ); 7.45 (dd, 1H, Ar,  $^3J=7.9$ ,  $^3J=7.6$ ); 7.23 (d, 1H Ar,  $^3J=7.8$ ); 6.3 (s, 1H, H2); 3.81 (ddd, 1H, H6a,  $^2J=13.6$ ,  $^3J=6.9$ ,  $^3J=6.7$ ); 3.66-3.60 (m, 5H, H5a and H10); 3.51 (d, 1H, H5b,  $^2J=15.8$ ); 2.63 (ddd, 1H, H6b,  $^2J=13.9$ ,  $^3J=7.1$ ,  $^3J=6.9$ ); 2.35-2.20 (m, 6H, H8a, H8b and H9); 1.82-1.60 (m, 2H, H7a and H7b).  $^{13}\text{C}$  NMR  $\delta$  (75 MHz, ppm,  $\text{CDCl}_3$ ): 171.0 (C4); 148.6, 142.3, 132.8, 130.3, 124.1, 121.9 (Ar); 68.7 (2C, C10); 62.7 (C2); 55.6 (C8); 53.5 (2C, C9); 41.4 (C6); 32.7 (C5); 25.5 (C7). HRMS-[ESI] for  $\text{C}_{15}\text{H}_{19}\text{N}_3\text{O}_4\text{S}$  ( $\text{M} + \text{H}$ ) $^+$ : 352.1326; found 352.1332. GC-MS  $m/z$  (%): 355 ( $\text{M}^+$ , 2); 281 (12); 207 (35); 100 (100); 56 (12). GC-MS  $m/z$  (%): 355 ( $\text{M}^+$ , 2); 281 (5); 207 (10); 100 (100); 56 (12).

#### 4.1.1.8. 3-(3-morpholinopropyl)-2-(3-nitrophenyl)thiazolidin-4-one **4h**

Yield 47%, brown oil,  $^1\text{H}$  RMN  $\delta$  (400 MHz, ppm,  $J_{\text{H-H}}=\text{Hz}$ ,  $\text{CDCl}_3$ ): 8.21 (ddd, 1H, Ar,  $^3J=8.0$ ,  $^4J=1.1$ ,  $^4J=0.9$ ); 8.15 (dd, 1H, Ar,  $^4J=1.9$ ,  $^4J=1.8$ ); 7.64 (ddd, 1H, Ar,  $^3J=7.7$ ,  $^4J=1.3$ ,  $^4J=1.2$ ); 7.59 (dd, 1H, Ar,  $^3J=7.9$ ,  $^3J=7.8$ ); 5.76 (d, 1H, H2,  $^4J=1.8$ ); 3.84 (dd, 1H, H5a,  $^2J=15.6$ ,  $^4J=1.9$ ); 3.75-3.65 (m, 6H, H5b, H6a and H10); 2.71 (ddd, 1H, H6b,  $^2J=14.0$ ,  $^3J=8.0$ ,  $^3J=7.9$ ); 2.37-2.24 (m, 6H, H8a, H8b and H9); 1.76-1.68 (m, 1H, H7a); 1.66-1.58 (m, 1H, H7b).  $^{13}\text{C}$  NMR  $\delta$  (100 MHz, ppm,  $\text{CDCl}_3$ ): 171.1 (C4); 146.7, 142.5, 132.8, 130.1, 124.2, 122.1 (Ar); 66.8 (2C, C10); 63.2 (C2); 55.7 (C8); 53.5 (2C, C9); 41.4 (C6); 32.7 (C5); 21.6 (C7). HRMS-[ESI] for  $\text{C}_{15}\text{H}_{19}\text{N}_3\text{O}_4\text{S}$  ( $\text{M} + \text{H}$ ) $^+$ : 352.1326; found 352.1327. GC-MS  $m/z$  (%): 355 ( $\text{M}^+$ , 2); 281 (4); 220 (4); 207 (8); 100 (100); 56 (15).

#### 4.1.1.9. 3-(3-morpholinopropyl)-2-(4-nitrophenyl)thiazolidin-4-one **4i**

Yield 87%, brown oil,  $^1\text{H}$  RMN  $\delta$  (500 MHz, ppm,  $J_{\text{H-H}}=\text{Hz}$ ,  $\text{CDCl}_3$ ): 8.32 (d, 2H, Ar,  $^3J=8.8$ ); 7.73 (d, 2H, Ar,  $^3J=8.8$ ); 6.10 (d, 1H, H2,  $^4J=1.6$ ); 3.96 (dd, 1H, H5a,  $^2J=15.5$ ,  $^4J=1.7$ ); 3.76 (d, 1H, H5b,  $^2J=15.6$ ); 3.61-3.56 (m, 5H, H6a and H10); 2.68 (ddd, 1H, H6b,  $^2J=13.9$ ,  $^3J=8.4$ ,  $^3J=8.3$ ); 2.31-2.27 (m, 6H, H8a, H8b and H9); 1.68-1.65 (m, 1H, H7a); 1.63-1.51 (m, 1H, H7b).  $^{13}\text{C}$  NMR  $\delta$  (125 MHz, ppm,  $\text{DMSO-d}_6$ ): 171.1 (C4); 148.2, 147.2, 127.6 (2C), 124.5 (2C) (Ar); 66.8 (2C, C10); 63.1 (C2); 56.8 (C8); 53.5 (2C, C9); 41.3 (C6); 32.8 (C5); 23.6 (C7). HRMS-[ESI] for  $\text{C}_{15}\text{H}_{19}\text{N}_3\text{O}_4\text{S}$  ( $\text{M} + \text{H}$ ) $^+$ : 352.1326; found 352.1330. GC-MS  $m/z$  (%): 355 ( $\text{M}^+$ , 2); 281 (5); 207 (15); 100 (100); 56 (10).

#### 4.1.1.10. 2-(2-methoxyphenyl)-3-(3-morpholinopropyl)thiazolidin-4-one **4j**

Yield 96%, yellow oil,  $^1\text{H}$  RMN  $\delta$  (200 MHz, ppm,  $J_{\text{H-H}}=\text{Hz}$ ,  $\text{CDCl}_3$ ): 7.32 (t, 1H, Ar,  $^3J=8.2$ ); 7.1 (d, 1H, Ar,  $^3J=7.4$ ); 6.95 (m, 2H, Ar); 6.07 (s, 1H, H2); 3.92-3.54 (m, 10H, H5a, H5b, H6a, H10 and  $\text{OCH}_3$ ); 2.79 (ddd, 1H, H6b,  $^2J=13.9$ ,  $^3J=7.4$ ,  $^3J=7.2$ ); 2.43-2.26 (m, 6H, H8a, H8b and H9); 1.78-1.64 (m, 2H, H7a and H7b).  $^{13}\text{C}$  NMR  $\delta$  (50 MHz, ppm,  $\text{CDCl}_3$ ): 171.9 (C4); 156.8, 129.8, 127.8, 126.5, 120.8, 110.9 (Ar); 66.1 (2C, C10); 58.1 (C2); 55.8 ( $\text{OCH}_3$ ); 55.6 (C8); 53.5 (2C, C9); 41.5 (C6); 32.6 (C5); 23.8 (C7). HRMS-[ESI] for  $\text{C}_{17}\text{H}_{24}\text{N}_2\text{O}_3\text{S}$  ( $\text{M} + \text{H}$ ) $^+$ : 337.1580; found 337.1581.

#### 4.1.1.11. 2-(3-methoxyphenyl)-3-(3-morpholinopropyl)thiazolidin-4-one **4k**

Yield 98%, yellow oil,  $^1\text{H}$  RMN  $\delta$  (600 MHz, ppm,  $J_{\text{H-H}}=\text{Hz}$ ,  $\text{CDCl}_3$ ): 7.23 (dd, 1H, Ar,  $^3J=7.9$ ,  $^3J=7.8$ ); 6.82-6.80 (m, 2H, Ar); 6.75 (dd, 1H, Ar,  $^4J=2.07$ ,  $^4J=2.05$ ); 5.56 (d, 1H, H2,  $^4J=1.9$ ); 3.75-3.72 (m, 4H, H5a and  $\text{OCH}_3$ ); 3.62-6.57 (m, 6H, H5b, H6a and H10); 2.73 (ddd, 1H, H6b,  $^2J=14.1$ ,  $^3J=8.4$ ;  $^3J=8.3$ ); 2.27-2.14 (m, 6H, H8a, H8b and H9);

1.66-1.59 (m, 1H, H7a); 1.56-1.49 (m, 1H, H7b).  $^{13}\text{C}$  NMR  $\delta$  (150 MHz, ppm,  $\text{CDCl}_3$ ); 171.2 (C4); 160.1, 141.1, 130.1, 119.4, 114.3, 112.3 (Ar); 66.8 (2C, C9); 63.7 (C2); 55.8 ( $\text{OCH}_3$ ); 55.7 (C8); 53.4 (2C, C10); 41.3 (C6); 32.8 (C5); 23.6 (C7). HRMS-[ESI] for  $\text{C}_{17}\text{H}_{24}\text{N}_2\text{O}_3\text{S}$  ( $\text{M} + \text{H}$ ) $^+$ : 337.1580; found 337.1582. GC-MS  $m/z$  (%): 336 ( $\text{M}^+$ , 3); 281 (2); 207 (6); 129 (13); 100 (100); 56 (12).

#### 4.1.1.12. 2-(4-methoxyphenyl)-3-(3-morpholinopropyl)thiazolidin-4-one **4l**

Yield 80%, yellow oil,  $^1\text{H}$  RMN  $\delta$  (500 MHz, ppm,  $J_{\text{H-H}}=\text{Hz}$ ,  $\text{DMSO-D}_6$ ): 7.32 (d, 2H, Ar,  $^3J=8.7$ ); 6.95 (d, 2H, Ar,  $^3J=8.7$ ); 5.78 (d, 1H, H2,  $^4J=1.5$ ); 3.81 (dd, 1H, H5a,  $^2J=15.4$ ,  $^4J=1.7$ ); 3.78 (s, 3H,  $\text{OCH}_3$ ); 3.64 (d, 1H, H5b,  $^2J=15.4$ ); 3.48 (t, 4H, H10,  $^3J=4.4$ ); 3.44-3.38 (m, 1H, H6a); 2.64 (ddd, 1H, H6b,  $^2J=14.0$ ,  $^3J=8.7$ ,  $^3J=8.5$ ); 2.20-2.11 (m, 6H, H8a, H8b and H9); 1.63-1.55 (m, 1H, H7a); 1.44-1.36 (m, 1H, H7b).  $^{13}\text{C}$  NMR  $\delta$  (125 MHz, ppm,  $\text{DMSO-d}_6$ ); 170.3 (C4); 159.5, 131.7, 128.6 (2C), 114.1 (2C) (Ar); 66.0 (2C, C10); 62.0 (C2); 55.2 ( $\text{OCH}_3$ ); 55.1 (C8); 52.9 (2C, C9); 40.5 (C6); 32.1 (C5); 23.0 (C7). GC-MS  $m/z$  (%): 336 ( $\text{M}^+$ , 3); 281 (2); 207 (7); 129 (12); 100 (100); 56 (7).

#### 4.1.1.13. 2-(2-hydroxyphenyl)-3-(3-morpholinopropyl)thiazolidin-4-one **4m**

Yield 31%, brown oil,  $^1\text{H}$  RMN  $\delta$  (200 MHz, ppm,  $J_{\text{H-H}}=\text{Hz}$ ,  $\text{CDCl}_3$ ): 7.21 (td, 2H, Ar,  $^3J=7.3$ ,  $^4J=1.5$ ); 6.89 (dt, 2H, Ar,  $^2J=14.9$ ,  $^3J=7.6$ ); 5.99 (s, 1H, H2); 3.86-3.64 (m, 7H, H5a, H5b, H6a and H10); 2.87-2.75 (m, 1H, H6b); 2.39-2.23 (m, 6H, H8a, H8b and H9); 1.80-1.61 (m, 2H, H7a and H7b).  $^{13}\text{C}$  NMR  $\delta$  (50 MHz, ppm,  $\text{CDCl}_3$ ); 171.9 (C4); 156.8, 129.8, 127.8, 126.5, 120.9, 111.0 (Ar); 66.9 (2C, C10); 58.1 (C2); 55.9 (C8); 53.5 (2C, C9); 41.5 (C6); 32.6 (C5); 23.8 (C7). HRMS-[ESI] for  $\text{C}_{16}\text{H}_{22}\text{N}_2\text{O}_3\text{S}$  ( $\text{M} +$

H)<sup>+</sup>: 323.1424; found 323.1429. GC-MS *m/z* (%): 322 (M<sup>+</sup>, 6); 236 (2); 129 (5); 114 (4); 100 (100); 56 (7).

#### 4.1.1.14. 2-(3-hydroxyphenyl)-3-(3-morpholinopropyl)thiazolidin-4-one **4n**

Yield 31%, yellow oil, <sup>1</sup>H NMR δ (200 MHz, ppm, *J*<sub>H-H</sub>=Hz, CDCl<sub>3</sub>); 7.25-7.14 (m, 1H, Ar); 6.82-6.70 (m, 3H, Ar); 5.60 (s, 1H, H2); 3.86-3.54 (m, 7H, H5a, H5b, H6a and H10); 2.78-2.89 (m, 1H, H6b); 2.38-2.30 (m, 6H, H8a, H8b and H9); 1.71-1.57 (m, 2H, H7a and H7b). <sup>13</sup>C NMR δ (50 MHz, ppm, CDCl<sub>3</sub>); 171.8 (C4); 157.4, 140.8; 130.4, 118.6, 116.8; 113.9 (Ar); 66.8 (2C, C10); 63.5 (C2); 55.8 (C8); 53.5 (2C, C9); 41.4 (C6); 32.9 (C5); 23.6 (C7). HRMS-[ESI] for C<sub>16</sub>H<sub>22</sub>N<sub>2</sub>O<sub>3</sub>S (M + H)<sup>+</sup>: 323.1424; found 323.1426.

#### 3.1.1.15. 2-(4-hydroxyphenyl)-3-(3-morpholinopropyl)thiazolidin-4-one **4o**

Yield 55%, yellow solid m.p. 76-79 °C, <sup>1</sup>H NMR δ (200 MHz, ppm, *J*<sub>H-H</sub>=Hz, CDCl<sub>3</sub>); 7.15 (d, 2H, Ar, <sup>3</sup>*J*=8.0); 6.80 (d, 2H, Ar, <sup>3</sup>*J*=8.0); 5.60 (s, 1H, H2); 3.84-3.56 (m, 7H, H5a, H5b, H6a and H10); 2.80-2.74 (m, 1H, H6b); 2.49-2.23 (m, 6H, H8a, H8b and H9); 1.77-1.46 (m, 2H, H7a and H7b). HRMS-[ESI] for C<sub>16</sub>H<sub>22</sub>N<sub>2</sub>O<sub>3</sub>S (M + H)<sup>+</sup>: 323.1424; found 323.1426. GC-MS *m/z* (%): 322 (M<sup>+</sup>, 4); 236 (2); 129 (10); 100 (100); 56 (5).

#### 4.1.1.16. 3-(3-morpholinopropyl)-2-(*p*-tolyl)thiazolidin-4-one **4q**

Yield 45%, white solid, m.p. 93-96 °C, <sup>1</sup>H NMR δ (400 MHz, ppm, *J*<sub>H-H</sub>=Hz, CDCl<sub>3</sub>); 7.26 (d, 2H, Ar, <sup>3</sup>*J*=8.0); 7.20 (d, 2H, Ar, <sup>3</sup>*J*=8.0); 5.78 (d, 1H, H2, <sup>4</sup>*J*=1.3); 3.81 (dd, 1H, H5a, <sup>2</sup>*J*=15.5, <sup>4</sup>*J*=1.6); 3.64 (d, 1H, H5b, <sup>2</sup>*J*=15.5); 3.49-3.40 (m, 5H, H6a and H10); 2.62 (ddd, 1H, H6b, <sup>2</sup>*J*=14.0, <sup>3</sup>*J*=8.6, <sup>3</sup>*J*=8.4); 2.20-2.09 (m, 6H, H8a, H8b and H9); 1.63-1.57 (m, 1H, H7a); 1.44-1.38 (m, 1H, H7b). <sup>13</sup>C NMR δ (100 MHz, ppm,

DMSO-d<sub>6</sub>); 175.5 (C4); 139.2, 136.4, 129.8 (2C), 126.9 (2C) (Ar); 66.0 (C2, C10); 62.2 (C2); 55.2 (C8); 53.0 (2C, C9); 40.7 (C6); 32.1 (C5); 23.0 (C7); 20.7 (CH<sub>3</sub>). HRMS-[ESI] for C<sub>17</sub>H<sub>24</sub>N<sub>2</sub>O<sub>2</sub>S (M + H)<sup>+</sup>: 321,1631; found 321,1633.

#### 4.2. Determination of anti-inflammatory effect in ear edema

Experiments were performed using male BALB/c mice. The animals were controlled at room temperature (22 ± 3 °C), with access to water and food *ad libitum*. The animals were acclimatized to the laboratory 1 h before starting the experiments. All procedures used in this study were approved in accordance with the guidelines of the Ethical Committee in Animal Experimentation of the Federal University of Pelotas (CEEA licence number 1021). BALB/c mice weighing 30 g, in mean, were divided into three animals in each group. Edema was induced for 3 hours with croton oil at a concentration of 2 mg/ear, dissolved in acetone. The compounds, 5 mg (166 mg/kg) and indomethacin, 1 mg (33 mg/kg) were dissolved in acetone. All suspensions were administered by topical application in a constant volume of 20 µl per ear mouse and prepared in the vehicle acetone (20%). The anti-inflammatory potency of thiazolidin-4-ones was compared with standard drug indomethacin [34].

Edema was quantified by the increase in ear thickness of mice upon inflammatory challenge. Ear thickness was measured after induction of the inflammatory response using a Digimess Electronic Outside Micrometer (Great, MT-045B). The micrometer was applied near the tip of the ear just distal to the cartilaginous ridges, and the thickness was recorded in micrometers [18,19].

#### *4.3. Inhibition of inflammation analysis*

The percentage protection of edema (inhibition of inflammation) measure was obtained at 18 h after application of compounds and was calculated according to the formula: percentage of anti-inflammatory activity =  $100 (1 - V_t/V_c)$ , where  $V_t$  and  $V_c$  are the volume of edema in test compounds and control groups edema, respectively [12, 35].

#### *4.4. General cell culture procedures*

The rat (C6) GBM cell lines were obtained from American Type Culture Collection (Rockville, MD, USA). Cells were grown and maintained in DMEM containing 0.1% (Fungizone®) and 100 U/L penicillin/streptomycin and supplemented with 10% (v/v) fetal bovine serum (FBS; Gibco). Cells were kept at 37 °C in a humidified atmosphere with 5% CO<sub>2</sub>.

Primary astrocyte cultures were prepared as previously described. Briefly, cortex of newborn Wistar rats (1–2 days old) (CEEA licence number 9219) were removed and dissociated mechanically in a Ca<sup>+2</sup> and Mg<sup>+2</sup> free balanced salt solution, pH 7.4. After centrifugation at 1,000 rpm for 10 min, the pellet was resuspended in DMEM supplemented with 10% FBS. The cells ( $3 \times 10^4$ ) were plated in poly-L-lysine-coated 96-well plates. After 4h plating, plates were gently shaken and medium was changed. Cultures were allowed to grow to confluence by 20–25 days. Medium was replaced every 4 days.



#### *4.5. In vitro treatment*

Synthetic thiazolidinones were dissolved in DMSO. The glioma cells and astrocyte cultures were exposed for 72 h to formulations of thiazolidinones at the following concentrations 6.25, 12.5, 25, 50, 100, 250 and 500  $\mu$ M. Control cells were treated with vehicle (DMSO).

#### *4.6. Cell viability assay*

Following treatments, cell viability was assessed by MTT assay. This method is based on the ability of viable cells to reduce MTT and form a blue formazan product. MTT solution (sterile stock solution of 5 mg/mL) was added to the incubation medium in the wells at a final concentration of 0.5 mg/mL. The cells were left for 90 min at 37 °C in a humidified 5% CO<sub>2</sub> atmosphere. The medium was then removed and plates were shaken with DMSO for 30 min. The optical density of each well was measured at 492 nm. Results were expressed as absorbance.

#### *4.7. Statistical analysis*

Data sets were analyzed using one-way ANOVA followed by a Tukey test for multiple comparisons. Significance was considered at  $p < 0.05$  in all analyses. Data are expressed as mean  $\pm$  SD.

## **Acknowledgments**

The authors thank to UFPel, FAPERGS (11/2068-7) and CAPES (23038.007284/2012-02) for financial support. CNPq (307330/2012-5) is also acknowledged.

## **Ethical approval**

All applicable international, national, and/or institutional guidelines for the care and use of animals were followed. All procedures used in the present study followed the Principles of Laboratory Animal Care from NIH and the Brazilian laws and were approved by the Ethical Committee of the Federal University of Pelotas (Protocols number 1021 and 9219).

## **Compliance with Ethical Standards**

Conflict of interest statement:

Elita F. da Silveira declares that she has no conflict of interest.

Daniela Pires Golvêa declares that she has no conflict of interest.

Flávia A. Vasconcellos declares that she has no conflict of interest

Gabriele A. Berwaldt declares that he has no conflict of interest

Juliana H. Azambuja declares that she has no conflict of interest.

Adriana M. Neves declares that she has no conflict of interest

Renata P. Sakata that he has no conflict of interest

Wanda P. Almeida declares that she has no conflict of interest

Ana P. Horn declares that she has no conflict of interest

Elizandra Braganhol declares that she has no conflict of interest

Wilson Cunico declares that he has no conflict of interest

## References

1. Tripathi, A. C., Gupta, S. J., Fatima, G. N., Sonar, P. K., Verma, A., Saraf, S. K. 4-Thiazolidinones: The advances continue. *Eur. J. Med. Chem.* 72 (2014), 52-77.
2. Jain, A.K.; Vaidya, A.; Ravichandran, V.; Kashaw, S.K.; Agrawal, R.K. Recent developments and biological activities of thiazolidinone derivatives: A review. *Bioorganic & Medicinal Chemistry*, (2012), v. 20 p 3378–3395.
3. Kobylinska, L. I., Boiko, N. M., Panchuk, R. R., Grytsyna, I. I., Biletska, L. P., Lesyk, R. B., ... & Stoika, R. S. (2016). Putative anticancer potential of novel 4-thiazolidinone derivatives: cytotoxicity toward rat C6 glioma in vitro and correlation of general toxicity with the balance of free radical oxidation in rats. *Croatian medical journal*, 57(2), 151-163.
4. Ruslan, M. Origin and physiological roles of inflammation. *Nature* (2008);454:428-35.
5. Grivennikov, S. I.; Greten, F. R., and Karin, M. Immunity, Inflammation, and Cancer. *Cell* (2010), V.140, p883–899.
6. Zou W, Restifo NP. T(H)17 cells in tumour immunity and immunotherapy. *Nat Rev Immunol*, v. 10, n. 4, (2010) p. 248-256.
7. Holland EC. Progenitor cells and glioma formation. *Curr Opin Neurol*.14(6); (2001) 683-8.

8. Nieto-Sampedro, M et al. Inhibitors of Glioma Growth that Reveal the Tumour to the Immune System. *Clin. Med. Insights Oncol.* (2011) 5: 265-314.
9. Nogueira L et al. The NF $\kappa$ B pathway: a therapeutic target in glioblastoma. *Oncotarget* (2011); 2(8);646–653.
10. Zhang L et al. Expression patterns of 5-lipoxygenase in human brain with traumatic injury and astrocytoma. *Neuropathology* (2006) 2:99–106.
11. Braganhol E et al. Selective NTPDase2 expression modulates in vivo rat glioma growth. *Cancer Science*, v.100, (2009) n.8, p.1434-1442.
12. Gouvêa DPF et al. 2-Aryl-3-(2-morpholinoethyl)thiazolidin-4-ones: Synthesis, antiinflammatory in vivo, cytotoxicity in vitro and molecular docking studies, *Eur. J. Med. Chem.* 118 (2016) 259-265.
13. Silva, D. S. da, et al. Thiazolidin-4-ones from 4-(methylthio)benzaldehyde and 4-(methylsulfonyl)benzaldehyde: Synthesis, antiglioma activity and cytotoxicity. *Eur. J. Med. Chem.* 2016, 124, 574-582.
14. Silveira, E. F. da, et al. Synthetic 2-aryl-3-((piperidin-1-yl)ethyl)thiazolidin-4-ones exhibit selective in vitro antitumoral activity and inhibit cancer cell growth in a preclinical model of glioblastoma multiforme *Chem.-Bio Int.* 2017, 266, 1-9.
15. Justus SEA et al. Thiazolidinone compounds useful as chemokine inhibitors 2003. US 6506751 (B1).
16. Ozadali K et al. Synthesis and Biological Activities of Some Thiazolidin-4-ones, *Arzneim.-Forsch./Drug Res.* 56, (2006) 678–681.
17. Geronikaki AA et al. Computer-aided Discovery of anti-inflammatory thiazolidinones with dual cyclooxygenase/lipoxygenase inhibition, *J. Med. Chem.* 51 (2008) 1601-1609.

18. Cabrini DA et al. Analysis of the potential topical anti-inflammatory activity of *Averrhoa carambola* L. in mice, *Evid. Based Complement. Altern. Med.* 2011 (2011) 1e7.
19. Otuki, M. Fetal. Calixto, Topical anti-inflammatory effects of the ether extract from *Protium kleini* and *amyri* pentacyclic triterpene, *Europ. J. Pharm* 507 (2005) 253–259.
20. Wang S et al. Design, synthesis and biological evaluation of novel 4-thiazolidinones containing indolin-2-one moiety as potential antitumor agent. *European Journal of Medicinal Chemistry* 46 (2011) 3509 – 3518.
21. a) Patel, D.; Kumari, P.; Patel, N. Synthesis and biological evaluation of some thiazolidinones as antimicrobial agents. *Eur. J. Med. Chem.* v. 48 (2012) p. 354-362.
22. Deep, A et al. Synthesis of 2-(aryl)-5-(arylidene)-4-thiazolidinone derivatives with potential analgesic and anti-inflammatory activity. *Med. Chem. Res.*, v. 21 (2012) p. 1652–1659.
23. Saundane, AR et al. Synthesis, antioxidant and antimicrobial evaluation of thiazolidinone, azetidinone encompassing indolylthienopyrimidines. *J. Chem. Sci.*, v.124 (2012) p. 469–481.
24. Lin WW, Karin M. A cytokine-mediated link between innate immunity, inflammation, and cancer. *J Clin Invest* 117(5) (2007) 1175–1183
25. Watters JJ, Schartner JM, Badie B. Microglial function in brain tumors. *J Neurosci Res* (2005) 81:447–455.
26. Cutshall, NS; O'Day CM. Prezhdo, Bioorg. Rhodanine derivatives as inhibitors of JSP-1 *Bioorganic & Medicinal Chemistry Letters* (2005) 15; 3374 e 3379.
27. Carter, PH et al. Photochemically enhanced binding of small molecules to the tumor necrosis factor receptor-1 inhibits the binding of TNF-alpha. *Proc Natl Acad Sci U S A.* (2001). (21):11879-84.

28. Degterev A, et al. Identification of small-molecule inhibitors of interaction between the BH3 domain and Bcl-xL. *Nat Cell Biol.* (2001) 3(2):173-82.
29. Chen M, Geng JG. P-selectin mediates adhesion of leukocytes, platelets, and cancer cells in inflammation, thrombosis, and cancer growth and metastasis. *Arch Immunol Ther Exp (Warsz)* (2006) 54:75–84.
30. Sprague DL et al. The role of platelet CD154 in the modulation in adaptive immunity. *Immunol (2007) Res* 39:185–193
31. Shono T et al. Cyclooxygenase2 expression in human gliomas: prognostic significance and molecular correlations. *Cancer Res* (2011) 61(11):4375–4381
32. Schönthal AH. Exploiting cyclooxygenase-(in)dependent properties of COX-2 inhibitors for malignant gliomatherapy. *Anticancer Agents Med Chem* (2010) 10(6):450–461.
33. Dovizio M et al. Mode of action of aspirin as a chemopreventive agent. *Recent Results Cancer Res* (2013) 191:39–65.
34. Rajahamsa AKL et al. Potbhare, Multi-model confirmatory evaluation of anti-inflammatory, analgesic and antioxidant activities of Puranjivar oxburghii wall, *Int. J. Biomed. Adv. Res.* (2013) 12, 921-932.
35. Kumar, V et al. Synthesis of some novel 2,5-disubstituted thiazolidinones from a long chain fatty acid as possible anti-inflammatory, analgesic and hydrogen peroxide scavenging agents, *J. Enzyme Inhib. Med. Chem.* (2011) 26 198-203.
36. Trott O, Olson A. AutoDock Vina: improving the speed and accuracy of docking with a new scoring function, efficient optimization, and multi-threading, *J. Comput. Chem.* 31 (2010) 455-461.

<b>Table 1.</b> The <i>in vivo</i> anti-inflammatory activity of thiazolidinones <b>4a-p</b>			
Comp.	R	M.W. <sup>a</sup>	Edema ear <sup>b</sup> anti-inflammatory activity (%) <sup>c</sup>
<b>4a</b>	2-F	324.41	61.90
<b>4b</b>	3-F	324.41	69.00
<b>4c</b>	4-F	324.41	47.47
<b>4d</b>	2-Cl	340.87	65.80
<b>4e</b>	3-Cl	340.87	nd
<b>4f</b>	4-Cl	340.87	52.08
<b>4g</b>	2-NO <sub>2</sub>	351.42	71.40
<b>4h</b>	3-NO <sub>2</sub>	351.42	50.98
<b>4i</b>	4-NO <sub>2</sub>	351.42	44.10
<b>4j</b>	2-OCH <sub>3</sub>	336.45	51.20
<b>4k</b>	3-OCH <sub>3</sub>	336.45	47.25
<b>4l</b>	4-OCH <sub>3</sub>	336.45	45.49
<b>4m</b>	2-OH	322.42	71.42
<b>4n</b>	3-OH	322.42	36.20
<b>4o</b>	4-OH	322.42	15.80
<b>4p</b>	4-CH <sub>3</sub>	320.45	58.50
Indometacin		357.77	62.36

**Table 1.** The anti-inflammatory activity of 4a-p thiazolidinones by *in vivo* experiment of mouse edema induced by chroot oil in mice. <sup>a</sup> g/mol molecular weight; <sup>b</sup> 166 mg/Kg; <sup>c</sup> % measured at 18h; nd – not determinate

## Legend, Figures and Schemes

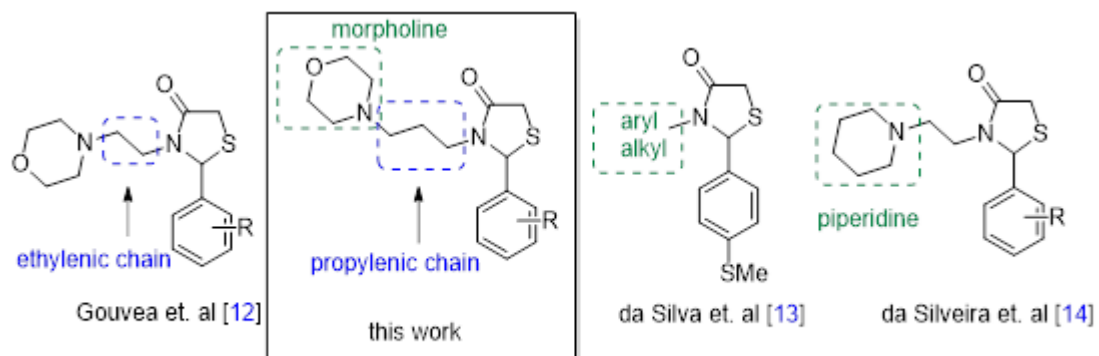


**Figure 1:** Designed for proposed thiazolidin-4-ones



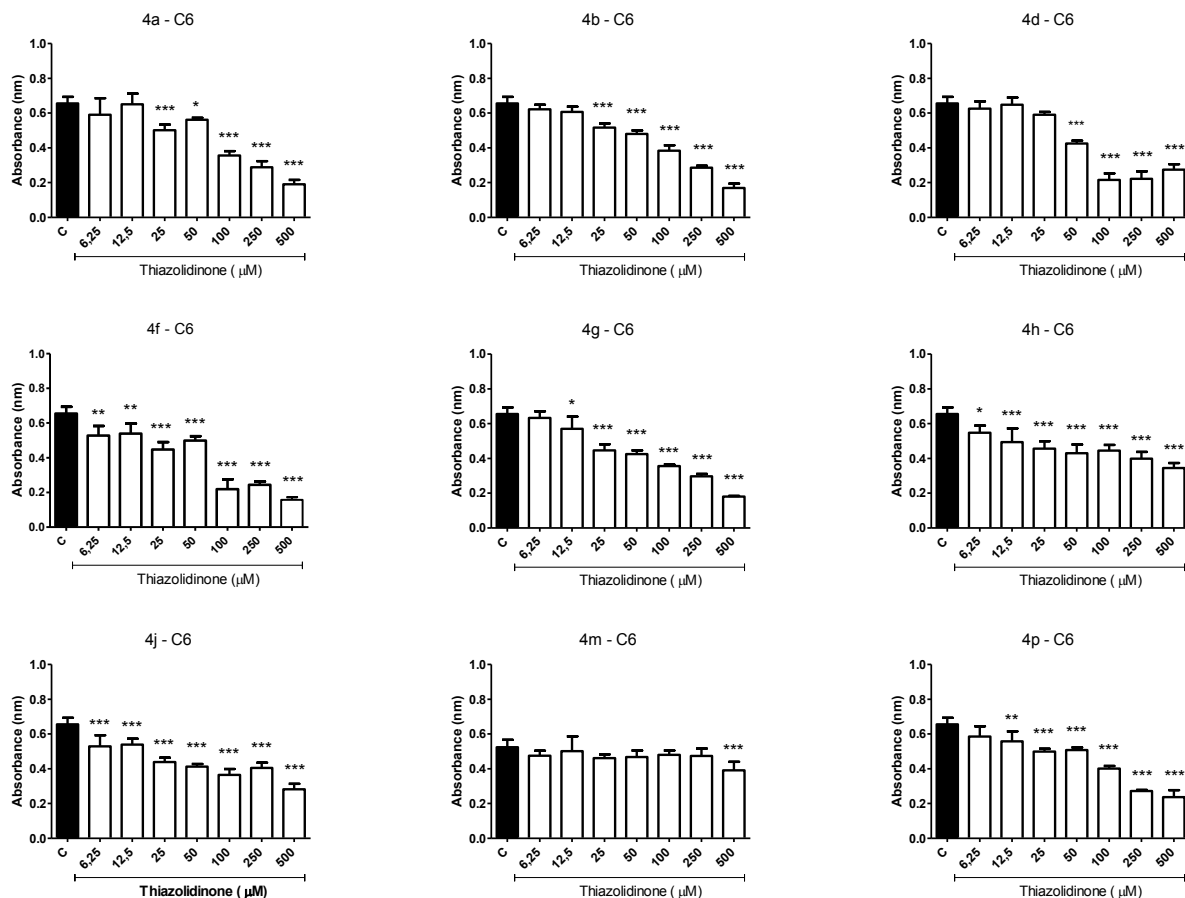


**Figure 2.** Antitumoral effect of thiazolidinones against glioma cell lines. The values represent the mean  $\pm$  SD of at least three independent experiments carried out in triplicate. Data were analyzed by ANOVA followed by post-hoc comparisons (Tukey-Kramer test). \* Significantly different from Control treated cells ( $p < 0.05$ ).

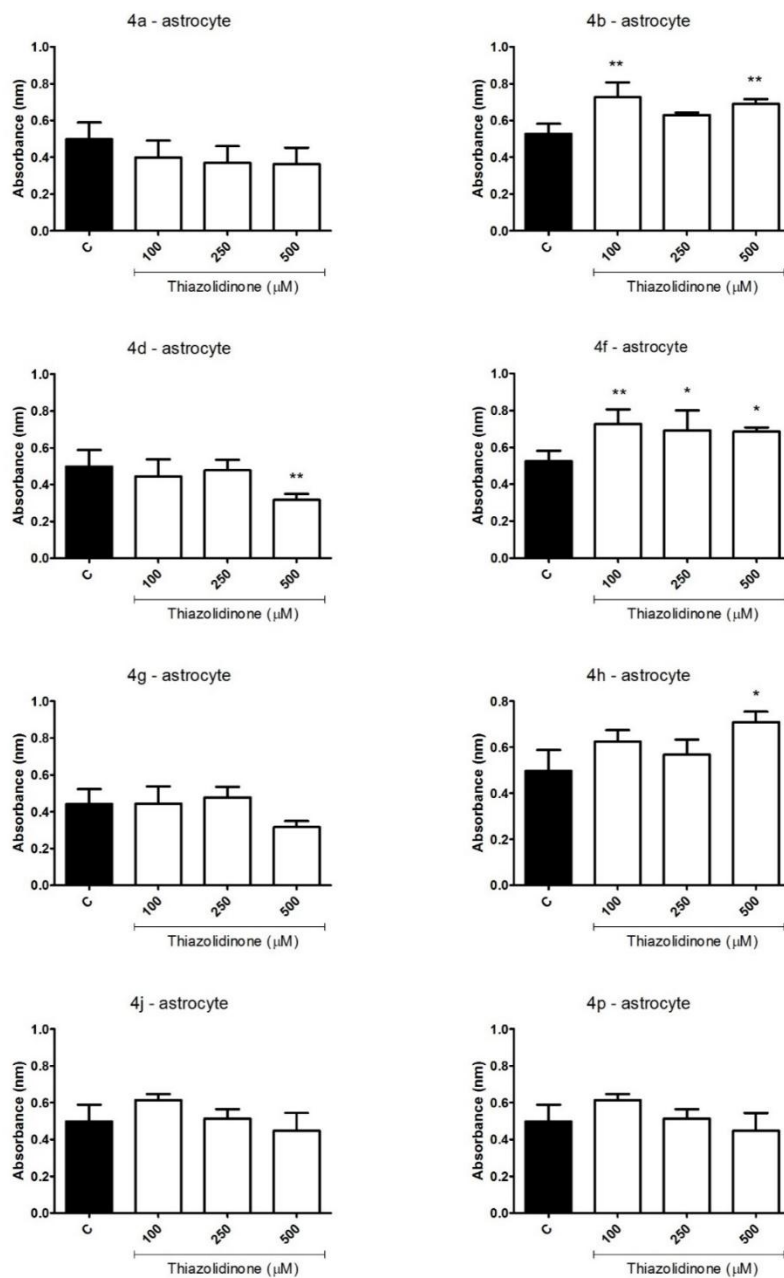
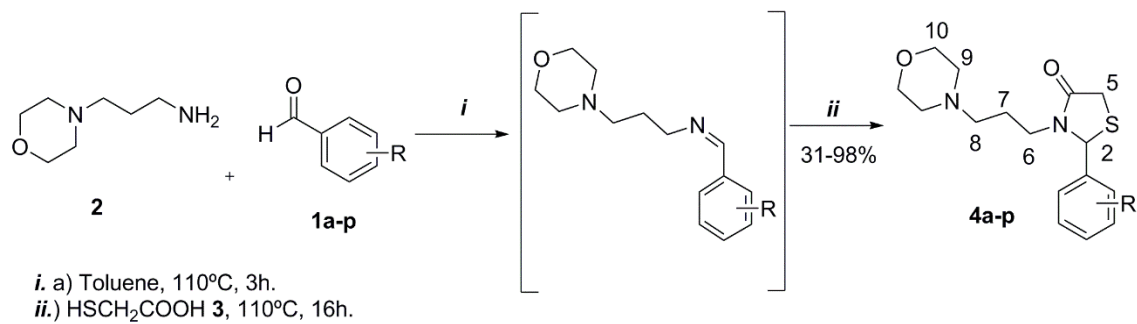


**Figure 3.** Comparative cytotoxicity of thiazolidinone against primary astrocytes. The values represent the mean  $\pm$  SD of at least three independent experiments carried out in triplicate. Data were analyzed by ANOVA followed by post-hoc comparisons (Tukey-Kramer test). \*Significantly different from Control or treated cells ( $p < 0.05$ ).



**Scheme 1.** Synthesis 2-aryl-3-(3-morpholinopropyl)thiazolidin-4-ones **4a-p**.

#### 4. Discussão geral

O câncer, em geral, é definido como a proliferação desordenada de células, que invadem tecidos e órgãos formando tumores malignos (Pérez-Herrero e Fernández-Medarde, 2015). Sabe-se que o microambiente tumoral leva a uma série de mudanças, como angiogênese, presença de processos inflamatórios, presença de espécies reativas provocando estresse oxidativo, dano ao DNA das células, entre outros fatores (Mattheolabkis, Rigas e Constantinides, 2012; Pérez-Herrero e Fernández-Medarde, 2015). Todos esses fatores fazem com que o câncer seja uma doença multifatorial, ou seja, que desencadeia uma série de sintomas e outras desordens, acarretando num alto índice de mortalidade e morbidade (American Cancer Society, 2015). Atualmente, as terapias disponíveis no mercado para o tratamento do câncer desencadeiam uma série de efeitos adversos, o que leva a uma baixa eficácia na terapia. Muitas vezes, as medicações empregadas no tratamento acabam por atingir também as células saudáveis, deixando o paciente ainda mais debilitado (Mei et al, 2013). Para os gliomas, além dos problemas já relatados, existem ainda mais obstáculos no tratamento, como a presença da barreira hematoencefálica (Behin et al, 2003; Jain, 2012; Da Silveira et al, 2013; Bernardi et al, 2013) e a resistência desenvolvida por estes tumores, que acarreta em necessidade de altas doses dos quimioterápicos e efeitos colaterais graves (Altieri et al., 2014, Bae et al., 2014). Diante disso, a busca por alternativas mais eficazes e menos tóxicas continua sendo muito relevante e, embora exista um intenso esforço para desenvolver novas terapias para melhorar a baixa sobrevivência de pacientes com diagnóstico, principalmente de GBM, estratégias efetivas ainda não estão disponíveis. Assim, o GBM continua a ser um desafio para a oncologia e um obstáculo para a maioria dos agentes antineoplásicos (Chumak et al, 2014).

Nesse contexto, a classe de moléculas derivadas de tiazolidinonas se destaca por apresentar atividade antiinflamatória e antitumoral promissora (Wang, 2011; Tripathi et al, 2014; Jain et al, 2012), inclusive em gliomas (Kobylinska et al, 2016; Silva et al, 2016; Avdieiev et al, 2014). Neste trabalho, demonstramos que alguns compostos de uma série de 2-iril-3-((piperidin-1-il)etil)tiazolidin-4-onas, previamente sintetizadas pelo nosso grupo de pesquisa (Kunzler et al, 2013), exibem atividade antitumoral *in vitro* e *in vivo*. Inicialmente, realizamos testes com dezesseis moléculas (**4a-p**), que

variavam o substituinte (F, Cl, NO<sub>2</sub>, OH, OCH<sub>3</sub>) e sua respectiva posição no anel aromático (2, 3, 4). Através da avaliação da viabilidade celular, selecionamos as 4 moléculas com efeitos mais promissores (**4d**, **4l**, **4m** e **4p**). As mesmas foram testadas contra astrócitos primários e não apresentaram toxicidade, indicando seletividade para células cancerígenas. As tiazolidinonas também promoveram uma diminuição significativa na densidade celular do glioma, levando a alterações morfológicas e indução de necrose e apoptose tardia. Normalmente, mudanças na sobrevivência celular são características secundárias após desregulação do ciclo celular e apoptose (Chumak et al, 2014). Diversos trabalhos já mostram que derivados de tiazolidinonas possuem atividade antitumoral devido a indução de apoptose (Zhang et al, 2014; Onen-Bayram et al, 2012; Chumak et al, 2014; Senkiv et al, 2016), indução essa que pode ocorrer de diferentes maneiras, sendo por meio da inibição de vias de sinalização como a PARP, MAPK, JNK, Bcl-2-, CDK1/ciclina B ou por vias dependentes da ativação de cascatas de caspases (Asati et al, 2014). Salientamos que os resultados mais promissores foram obtidos para tiazolidinonas contendo grupos substituídos na posição 2 do anel aromático, uma vez que esta posição foi substituída em três dos quatro compostos mais ativos (**4d**, **4l** e **4p**), sugerindo que essa posição orto é importante para reduzir a viabilidade das células de glioma. Confirmando nossas descobertas, notamos que a adição de dois grupos orto (2,6-Cl, **4p**) aumenta ainda mais a atividade de redução da viabilidade celular do glioma em cultura. Esses resultados deram suporte para realizarmos experimentos *in vivo* através do modelo pré-clínico de implante de glioma, que foi realizado com as moléculas com melhores resultados *in vitro* (**4d**, **4l** e **4p**). O tratamento nos animais reduziu significativamente o crescimento dos gliomas *in vivo* (**4d**, **4l** e **4p** reduziram respectivamente 45%, 73% e 50% do volume do tumor quando comparados ao controle), bem como suas características de malignidade. O mesmo não resultou em mortalidade e não causou hepato ou nefrotoxicidade nos animais, demonstrando a segurança dos compostos. Salientamos que esse é um trabalho inédito quanto a testes com derivados de tiazolidinonas em modelo pré-clínico de GBM. Por fim, descobrimos que o substituinte Cl parece ser importante para inibir a produção de óxido nítrico (NO) e sugerimos que a redução dos níveis de NO pode explicar a atividade antitumoral dos compostos **4d** e **4p**. Outros compostos derivados de

tiazolidinonas como o benzilideno-4-tiazolidinonas também apresentarem capacidade de redução de NO (Crascì et al, 2015). No entanto, a 2-(2-metoxifenil)-3-((piperidin-1-il)etil)tiazolidin-4-ona **4I** não altera a atividade da óxido nítrico sintase, sendo sua atividade antitumoral independente desse efeito. Em conclusão, os dados do nosso primeiro capítulo mostram pela primeira vez o potencial antitumoral da classe de 2-aril-3-((piperidin-1-il)etil)tiazolidin-4-onas, e dentre todos os compostos testados, o melhor resultado foi encontrado para 2-(2-metoxifenil)-3-((piperidin-1-il)etil)tiazolidin-4-ona, a molécula **4I**.

Existem várias peculiaridades que se tornam obstáculos para uma terapia efetiva de gliomas, como alterações nos mecanismos bioquímicos, alterações nas vias de sinalização de processos de apoptose e proliferação celular, o sistema ativo de efluxo da glicoproteína P que é responsável pela resistência a múltiplas drogas (MDR) (Carrett-dias, et al, 2016) e a dificuldade que muitos fármacos encontram em transpor a BHE. Assim, a partir do conjunto de dados que obtivemos e frente aos bons resultados que estão sendo encontrados na área da nanomedicina, objetivamos nanoencapsular a molécula **4I**, tentando assim desvendar se o seu nanoencapsulamento potencializaria seu efeito antiglioma.

Os nanosistemas têm sido utilizados para o tratamento de uma série de doenças e, segundo alguns autores, seus principais alvos são o câncer, doenças inflamatórias e doenças neurológicas (Dimer et al, 2013; Mei et al, 2013). Os nanocarreadores possuem a característica de entrega direcionada de fármacos, aumentam o acúmulo de drogas anticancerígenas no local do tumor e minimizam os efeitos colaterais prejudiciais associados aos efeitos fora do alvo da terapia (Taghdisi et al, 2016). As nanocápsulas são alternativas promissoras na terapêutica, que aumentam a estabilidade das moléculas, porque protegem contra foto ou degradação química, aumenta a estabilidade da molécula e ainda são capazes de reduzir a toxicidade do fármaco (Santos et al, 2014; Chassot et al, 2015).

No nosso segundo capítulo, realizamos o desenvolvimento de nanocápsulas poliméricas contendo tiazolidinonas (**4L-N**) que foram caracterizadas em termos de distribuição granulométrica, tamanho de partícula e índices de polidispersão, potencial zeta, pH, conteúdo de moléculas e eficiência de encapsulamento onde todos os testes se

mantiveram dentro ou próximo ao padrão esperado. Determinamos também a fotoestabilidade de **4L** e **4L-N** e a capacidade das nanocápsulas em protegerem a molécula contra a degradação. As formulações foram expostas à radiação UVC e podemos sugerir que **4L** é uma molécula fotolábil, uma vez que após 120 minutos de exposição o conteúdo diminuiu significativamente. Por outro lado, quando esta molécula foi nanoencapsulada, seu conteúdo manteve-se inalterado. Este resultado encontrado pode ser devido à presença de PCL na estrutura vesicular das nanocápsulas, por ser um polímero semicristalino e capaz de refletir e / ou espalhar luz ultravioleta (Almeida et al, 2010; Pohlmann et al, 2013).

No estudo de liberação de fármaco in vitro, foi possível observar uma liberação controlada em **4L-N** em comparação com a solução metanólica **4L**. A liberação controlada é uma vantagem atribuída a sistemas nanoestruturados e a presença do polímero pode ser a maior barreira à entrega de fármacos (Santos et al, 2014; Chassot et al, 2015). A liberação do fármaco pode ser dependente da erosão do polímero e / ou da difusão do fármaco para o meio de dissolução e as moléculas lipofílicas têm alta afinidade com o núcleo oleoso e conseqüentemente apresentam uma liberação mais lenta de fármaco (Chassot et al, 2015). Esses dados mostram que obtivemos sucesso no processo de nanoencapsulamento da molécula 2- (2-metoxifenil)-3-((piperidin-1-il)etil)tiazolidin-4-ona, com posterior otimização da molécula quanto a sua estabilidade e fotodegradação.

Os experimentos de atividade antitumoral foram realizados comparativamente, tentando sempre analisar se o nanoencapsulamento da molécula foi capaz de otimizar sua atividade. Analisamos a viabilidade e a proliferação de células de glioma tratadas com **4L** e **4L-N**. Em ambos os testes, a molécula **4L-N** foi mais eficiente, atingindo 60,51% de redução na viabilidade e 70,39% de redução na proliferação de células de glioma C6 nos tempos e concentrações mais altas testadas. Além disso, observamos que a **4L-N** promoveu uma diminuição da viabilidade e da densidade celular, causou alterações morfológicas e aumentou a incorporação de PI quando comparado ao controle. Em conjunto, estes resultados sugerem que o efeito antiproliferativo do composto 2- (2-metoxifenil) -3 - ((piperidin-1-il) etil) tiazolidin-4-ona é otimizado quando nanoencapsulado. Sugerimos também que seu efeito pode ser mediado por

necrose. No entanto, o envolvimento de outras vias de morte celular não pode ser excluído, uma vez que as mudanças na vitalidade e sobrevivência celular, bem como a ocorrência de dano celular, são secundárias à desregulação do ciclo celular e ao desenvolvimento de características de células apoptóticas (Chandrappa et al, 2009). Dados da literatura mostram diferentes classes de derivados de tiazolidinonas com efeito através de indução de apoptose, como a classe de 5-eno-4-tiazolidinonas (Chen et al, 2007). Grupos de tiazolidinonas ainda atuam como inibidores das interações proteína-proteína anti-apoptóticas na família Bcl-2 e Bax (Onen-Bayram et al, 2012) e como inibidores seletivos de (ERK1/2) (Zimenkovsky et al, 2004). Sabemos ainda que as tiazolidinonas possivelmente têm afinidade por diferentes alvos moleculares, sendo a apoptose induzida por 4-tiazolidinonas e seus derivados demonstrada em diferentes tipos de células cancerígenas (Gonsette et al, 2008; Ljubisavljevic et al, 2016).

Como dito anteriormente, a quimioterapia atual para gliomas apresenta pouca especificidade e alta toxicidade, com graves efeitos colaterais e esses fatores representam uma limitação ao tratamento. Dessa forma, existe a necessidade de encontrar moléculas que possuam importante atividade antitumoral, porém com baixa toxicidade para células normais. Como em nosso primeiro capítulo, já demonstramos que a tiazolidinona **4L** não foi tóxica para astrócitos primários (Silveira et al, 2017). Aqui demonstramos que **4L-N** também não mostra toxicidade para células astrocíticas normais, sendo seletiva às células tumorais.

Considerando o potencial terapêutico demonstrado por **4L-N** em testes *in vitro*, investigamos a toxicidade dessas moléculas *in vivo* e observamos que **4L-N** não promoveu mortalidade ou toxicidade sistêmica. Além disso, os animais tratados com **4L-N** não apresentaram perda de peso ao longo do tratamento. Os dados também refletem a segurança biológica do PCL, um polímero sintético presente na composição da nanocápsula, biodegradável e biocompatível, o que corrobora com resultados já demonstrados na literatura (Fontana et al., 2010, Bitencourt et al, 2016) e especificamente em gliomas (Zanotto-filho et al, 2013), onde em estudos anteriores do grupo também não causou toxicidade *in vivo* (Silveira et al, 2013).



Analizamos também parâmetros de estresse oxidativo que poderiam estar alterados caso as moléculas fossem potencialmente tóxicas, e os resultados indicaram que a tiazolidinona **4L**, bem como **4L-N**, não alteram marcadores de dano oxidativo, como os níveis de TBARS, um marcador para a peroxidação lipídica e o teor total de sulfidrilas, um marcador de dano as proteínas. Além disso, nenhuma alteração na atividade de enzimas antioxidantes, como SOD e CAT, foi observada no fígado e no cérebro de ratos, demonstrando que a exposição à **4L** ou **4L-N** não induziu estresse oxidativo em ratos. Kobylinska e colaboradores (2016) mostraram que moléculas derivadas de 4-tiazolidinonas não alteraram o nível de ROS, enquanto doxorubicina elevou os índices significativamente, além de diminuir a atividade de enzimas do sistema antioxidante como, SOD, GPO e CAT em sangue de ratos. Esses dados mostram que derivados de 4-tiazolidinonas possuem uma maior segurança quanto a alterações no sistema de defesa antioxidante quando comparados a doxorubicina, um quimioterápico já usado na clínica.

Os dados do nosso segundo capítulo apresentam a primeira nanocápsula carregada com tiazolidinona como alternativa para o tratamento do glioma. Podemos observar que **4L-N** tem uma atividade antitumoral *in vitro* ainda mais eficiente do que a molécula na sua forma livre, não apresentando toxicidade para células normais, e em estudos *in vivo*, as doses sub-terapêuticas não foram tóxicas para animais. Os dados aqui mostrados suportam estudos adicionais para testar nanocápsulas poliméricas carregadas com 2-(2-metoxifenil)-3-((piperidin-1-il) etil)tiazolidin-4-ona em um modelo pré-clínico como uma nova modalidade terapêutica para o tratamento de gliomas. Abre-se assim uma perspectiva futura para a utilização dessas moléculas.

Analisando os dados dos nossos capítulos 1 e 2, verificamos o grande potencial antitumoral da série de 2-aril-3-((piperidin-1-il)etil)tiazolidin-4-onas, no entanto, sabemos que modificações estruturais na molécula acarretam em mudanças nas propriedades físico-químicas, sendo possível até mesmo um aumento do seu potencial terapêutico. Assim, uma nova série de derivados de tiazolidinonas foi sintetizada com modificações que acreditávamos que poderiam potencializar seu efeito. Enquanto a série de 2-aril-3-((piperidin-1-il)etil)tiazolidin-4-onas é proveniente da (1-aminoetil)piperidina, que contém em sua estrutura o heterociclo piperidina e uma cadeia

etilênica, a nova classe de tiazolidinonas sintetizadas, 2-aryl-3-(3-morfolinopropil)tiazolidin-4-onas, é derivada da 4-(3-aminopropil)morfolina, que contém em sua estrutura o heterociclo morfolina e uma cadeia propilênica, como mostramos na figura 8 que segue abaixo.

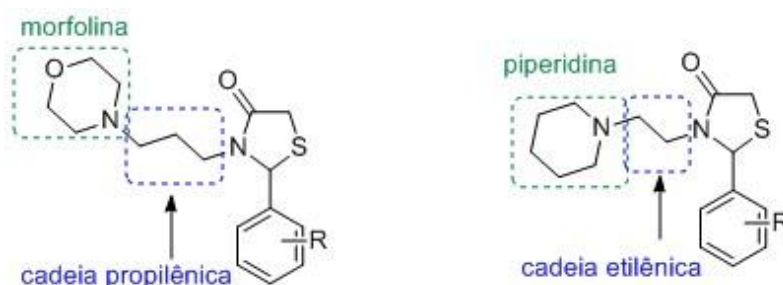


Figura 8. Comparação entre a série de moléculas 2-aryl-3-((piperidin-1-yl)etil)tiazolidin-4-onas e 2-aryl-3-(3-morfolinopropil)tiazolidin-4-onas.

Sabendo que existe uma perspectiva positiva para compostos com atividade polifarmacológica, a descoberta de compostos bioativos que possuam afinidade com diferentes alvos pode ser considerada uma vantagem. O objetivo principal desse trabalho foi a descoberta de uma molécula com potencial atividade antitumoral. Conforme descrito na literatura, o microambiente inflamatório contribui para invasão e progressão dos gliomas (Zhai, Heppner e Tsirka, 2011; Charles et al, 2011) e um infiltrado inflamatório constituído principalmente por macrófagos está positivamente correlacionado com malignidade e consequente pior prognóstico para pacientes com GBM (Sakaeva, 2015; Azambuja et al, 2017). Assim, o controle desse ambiente poderia reduzir a malignidade tumoral. Dessa forma, neste capítulo 3, após realizarmos a síntese de uma nova classe de moléculas, propusemos dois testes biológicos, um anti-inflamatório e um antitumoral, para testar nossas novas moléculas. Primeiramente testamos a atividade anti-inflamatória das 16 moléculas sintetizadas por meio de um modelo de edema de orelha induzido por óleo de cróton em camundongos e nove dos compostos (**4a**, **4b**, **4d**, **4f**, **4g**, **4h**, **4j**, **4m** e **4p**) apresentaram valores de inibição da inflamação entre 50 e 71%. Cabe ressaltar que dados já publicados por nosso grupo de pesquisa mostram a atividade anti-inflamatória da série de 2-aryl-3-(2-

morfolinoetil)tiazolidin-4-onas, que contém o anel morfolina e uma cadeia etilênica. Esses dados mostram que as melhores moléculas apresentaram inibição da inflamação entre 48 e 54% (Gouvêa et al, 2016). Assim, concluímos que os nossos novos compostos apresentaram melhores resultados para atividade anti-inflamatória do que as tiazolidinonas anteriormente estudadas.

Os nove compostos com efeitos melhorados na atividade anti-inflamatória foram testados contra linhagens celulares de glioma C6 e astrócitos primários. Primeiramente, cabe ressaltar que apenas um composto apresentou toxicidade em astrócitos e somente na sua maior concentração (**4d**-500  $\mu$ M). Os outros compostos não apresentaram toxicidade nesse modelo de célula não-tumoral. Em comparação com as outras tiazolidinonas já estudadas por nós anteriormente, esses compostos parecem ser mais seguros, uma vez que nas anteriores foi encontrado efeito tóxico em quatro compostos já na concentração de 250  $\mu$ M (Silva et al, 2016).

Consideramos como melhores resultados de atividade antiglioma *in vitro* as tiazolidinonas **4a**, **4d**, **4f** e **4h**, que foram capazes de reduzir a viabilidade das células em 50% na concentração de 100 $\mu$ M e em cerca de 80% na maior concentração testada (500  $\mu$ M). A análise antitumoral *in vitro* mostrou que o tratamento com 2-aril-3-(3-morfolinopropil)tiazolidin-4-onas reduziu significativamente a viabilidade do glioma, sendo seletiva para as células tumorais. Nos dados do nosso primeiro capítulo, obtivemos como melhores resultados uma redução na viabilidade celular entre 50 e 84% em uma concentração de (100  $\mu$ M), o que nos indica que a classe de 2-aril-3-((piperidin-1-il)etil)tiazolidin-4-onas apresenta uma maior atividade antiglioma que a nova classe sintetizada de 2-aril-3-(3-morfolinopropil)tiazolidin-4-onas, que obteve essa mesma redução, porém somente em concentrações maiores. Concluímos que essa nova classe de moléculas que foram sintetizadas apresentou um importante aumento no seu potencial em relação a atividade anti-inflamatória. No entanto, para a atividade antitumoral *in vitro*, permanece sendo mais potente a classe de moléculas apresentada em nosso primeiro capítulo. Esses são dados *in vitro* preliminares, com perspectiva de serem complementados com experimentos de proliferação, análise de ciclo e morte celular e posterior análise no modelo pré-clínico de glioma.

## 5. Conclusão e perspectivas

Nossos dados mostraram pela primeira vez o potencial antitumoral da classe de 2-aryl-3-((piperidin-1-il)etil)thiazolidin-4-onas. Concluimos que a posição do substituinte pode ser um fator importante para a eficiência antitumoral, uma vez que as três moléculas que apresentaram os melhores resultados tem um substituinte na posição 2 do anel aromático. Salientamos também a presença do substituinte Cl em duas dessas moléculas. Além disso, doses subterapêuticas de 2-(2-metoxifenil)-3-((piperidin-1-il)etil)thiazolidin-4-ona (**4L**) diminuíram em 70% o crescimento tumoral e as características malignas em um modelo pré-clínico de gliomas. Essa molécula com melhor resultado *in vivo*, quando nanoencapsulada, tem uma atividade antitumoral *in vitro* ainda mais eficiente do que a molécula na sua forma livre, não induzindo citotoxicidade a astrócitos primários, e não acarretando em mortalidade ou toxicidade sistêmica em ratos, como indicado em experimentos *in vivo*, o que sugere uma possível segurança das formulações. Nossos resultados suportam estudos adicionais para testar nanocápsulas poliméricas carregadas com 2-(2-metoxifenil)-3-((piperidin-1-il)etil)thiazolidin-4-ona em um modelo pré-clínico de glioma.

Nesse trabalho, uma nova série 2-aryl-3-(3-morpholinopropyl)thiazolidine-4-onas foi sintetizada, com modificações que acreditávamos que poderiam potencializar o efeito antiglioma. Salientamos que as moléculas com melhores resultados também apresentavam o substituinte Cl em sua estrutura. No entanto essa nova classe necessita de concentrações mais altas para obter o mesmo efeito da classe de 2-aryl-3-((piperidin-1-il)etil)thiazolidin-4-onas (ilustrado no resumo comparativo – Figura 8).

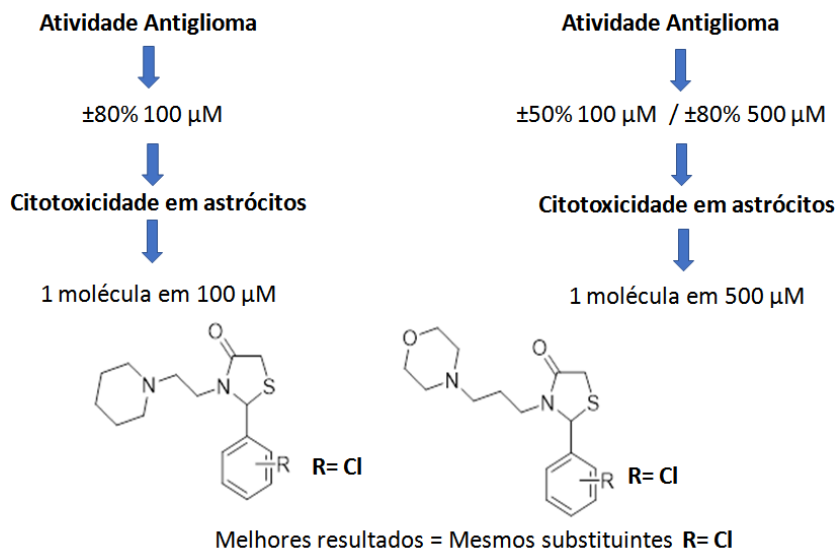
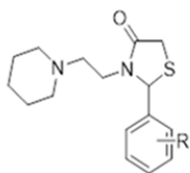


**Figura 8.** Resumo comparativo entre as classes de tiazolidinonas

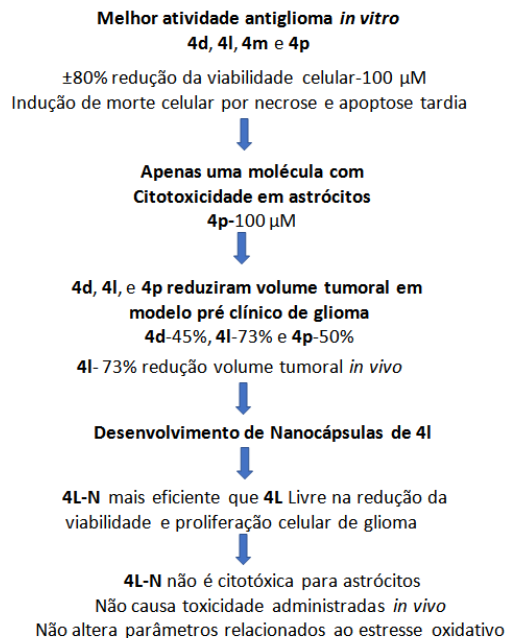
Sendo assim, existe a necessidade de mais estudos como de proliferação, tipo de morte, ciclo celular e experimentos *in vivo* para uma melhor análise do efeito antiglioma das 2-aryl-3-(3-morfolinopropil)thiazolidine-4-onas.

Por fim, através dos resultados obtidos nessa tese de Doutorado (sumarizados na Figura-9), concluímos que derivados de tiazolidinonas sintéticas possuem excelente potencial para uma futura modalidade terapêutica para gliomas.

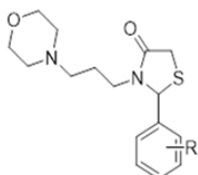
## 2-aril-3-((piperidin-1-il)etil)tiiazolidin-4-onas



Compostos	R
4a	2-F
4b	3-F
4c	4-F
4d	2-Cl
4e	3-Cl
4f	4-Cl
4g	2-NO <sub>2</sub>
4h	3-NO <sub>2</sub>
4i	4-NO <sub>2</sub>
4j	3-OH
4k	4-OH
4l	2-OCH <sub>3</sub>
4m	3-OCH <sub>3</sub>
4n	4-OCH <sub>3</sub>
4o	4-CH <sub>3</sub>
4p	2,6-Cl



## 2-aril-3-(3-morfolinopropil)tiiazolidin-4-onas



Compostos	R
4a	2-F
4b	3-F
4c	4-F
4d	2-Cl
4e	3-Cl
4f	4-Cl
4g	2-NO <sub>2</sub>
4h	3-NO <sub>2</sub>
4i	4-NO <sub>2</sub>
4j	2-OH
4k	3-OH
4l	4-OH
4m	2-OCH <sub>3</sub>
4n	3-OCH <sub>3</sub>
4o	4-OCH <sub>3</sub>
4p	4-CH <sub>3</sub>

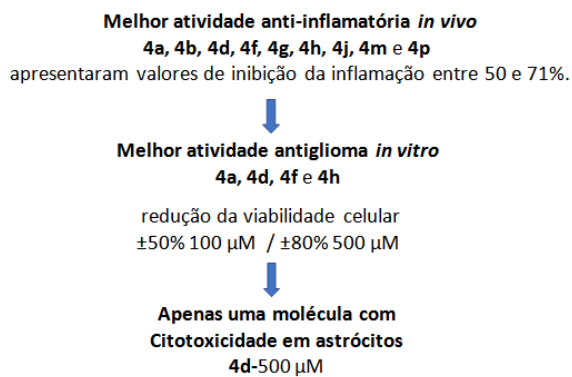


Figura 9. Resumo dos resultados obtidos nesta tese de Doutorado.

## 6. Bibliografia geral

- Ahmed, R., Oborski, M. J., Hwang, M., Lieberman, F. S., & Mountz, J. M. (2014). Malignant gliomas: current perspectives in diagnosis, treatment, and early response assessment using advanced quantitative imaging methods. *Cancer management and research*, 6, 149.
- Almeida, J. S., Lima, F., Da Ros, S., Bulhões, L. O., de Carvalho, L. M., & Beck, R. C. (2010). Nanostructured systems containing rutin: in vitro antioxidant activity and photostability studies. *Nanoscale research letters*, 5 (10), 1603.
- Altieri, R., Agnoletti, A., Quattrucci, F., Garbossa, D., Specchia, F. C., Bozzaro, M., & Ducati, A. (2014). Molecular biology of gliomas: present and future challenges. *Translational medicine@ UniSa*, 10, 29.
- Arshad, A., Yang, B., Bienemann, A. S., Barua, N. U., Wyatt, M. J., Woolley, M. & Gill, S. S. (2015). Convection-enhanced delivery of carboplatin PLGA nanoparticles for the treatment of glioblastoma. *PloS one*, 10, (7), e0132266.
- Asati, V; Mahapatra, D.K; Bharti, S.K. (2014). Thiazolidine-2,4-diones as multi-targeted scaffold in medicinal chemistry: potential anticancer agents, *Eur. J. Med. Chem.* 87, 814–833.
- Armstrong, G. T., Conklin, H. M., Huang, S., Srivastava, D., Sanford, R., Ellison, D. W. & Gajjar, A. (2010). Survival and long-term health and cognitive outcomes after low-grade glioma. *Neuro-oncology*, 13, (2), 223-234.
- Avdieiev, S., Gera, L., Havrylyuk, D., Hodges, R. S., Lesyk, R., Ribrag, V., & Kavsan, V. (2014). Bradykinin antagonists and thiazolidinone derivatives as new potential anti-cancer compounds. *Bioorganic & medicinal chemistry*, 22, (15), 3815-3823.
- Bitencourt, P. E., Ferreira, L. M., Cargnelutti, L. O., Denardi, L., Boligon, A., Fleck, M., ... & Alves, S. H. (2016). A new biodegradable polymeric nanoparticle formulation containing *Syzygium cumini*: Phytochemical profile, antioxidant and antifungal activity and in vivo toxicity. *Industrial Crops and Products*, 83, 400-407.
- Behin A, Hoang-Xuan K, Carpentier AF, Delattre JY. (2003). Primary brain tumours in adults. *Lancet*, 361, 323-331.
- Bernardi, A., Zilberstein, A. C. C. V., Jäger, E., Campos, M. M., Morrone, F. B., Calixto, J. B., ... & Battastini, A. M. O. (2009). Effects of indomethacin-loaded nanocapsules in experimental models of inflammation in rats. *British journal of pharmacology*, 158, (4), 1104-1111.

Bernardi, A., Frozza, R. L., Hoppe, J. B., Salbego, C., Pohlmann, A. R., Battastini, A. M. O., & Guterres, S. S. (2013). The antiproliferative effect of indomethacin-loaded lipid-core nanocapsules in glioma cells is mediated by cell cycle regulation, differentiation, and the inhibition of survival pathways. *International journal of nanomedicine*, 8, 711.

Blattman, J. N., & Greenberg, P. D. (2004). Cancer immunotherapy: a treatment for the masses. *Science*, 305(5681), 200-205.

Brat, D. J., Scheithauer, B. W., Fuller, G. N., & Tihan, T. (2007). Newly codified glial neoplasms of the 2007 WHO Classification of Tumours of the Central Nervous System: angiocentric glioma, pilomyxoid astrocytoma and pituicytoma. *Brain pathology*, 17, (3), 319-324.

Bromberg, J. E., & Van Den Bent, M. J. (2009). Oligodendrogliomas: molecular biology and treatment. *The Oncologist*, 14, (2), 155-163.

Cairncross, J. G., Ueki, K., Zlatescu, M. C., Lisle, D. K., Finkelstein, D. M., Hammond, R. R., ... & Ramsay, D. A. (1998). Specific genetic predictors of chemotherapeutic response and survival in patients with anaplastic oligodendrogliomas. *JNCI: Journal of the National Cancer Institute*, 90, (19), 1473-1479.

Carrett-Dias, M., de Souza Votto, A. P., Filgueira, D. D. M. V. B., Almeida, D. V., Vallochi, A. L., D'Oca, M. G. M., ... & Trindade, G. S. (2011). Anti-MDR and antitumoral action of acetylsalicylic acid on leukaemic cells. *Bioscience reports*, 31(5), 391-398.

Carrett-Dias, M., Almeida, L. K., Pereira, J. L., Almeida, D. V., Filgueira, D. M. V. B., Marins, L. F., ... & Trindade, G. S. (2016). Cell differentiation and the multiple drug resistance phenotype in human erythroleukemic cells. *Leukemia research*, 42, 13-20.

Cebola, I., & Peinado, M. A. (2012). Epigenetic deregulation of the COX pathway in cancer. *Progress in lipid research*, 51, (4), 301-313.

Cerquetti, L., Sampaoli, C., Amendola, D., Bucci, B., Masuelli, L., Marchese, R., ... & Stigliano, A. (2011). Rosiglitazone induces autophagy in H295R and cell cycle deregulation in SW13 adrenocortical cancer cells. *Experimental cell research*, 317(10), 1397-1410.

Chabner, B. A., & Longo, D. L. (2015). *Manual de Oncologia de Harrison*. AMGH Editora.

Chandrappa, S., Kavitha, C. V., Shahabuddin, M. S., Vinaya, K., Kumar, C. A., Ranganatha, S. R., & Rangappa, K. S. (2009). Synthesis of 2-(5-((5-(4-chlorophenyl) furan-2-yl)methylene)-4-oxo-2-thioxothiazolidin-3-yl) acetic acid derivatives and



evaluation of their cytotoxicity and induction of apoptosis in human leukemia cells. *Bioorganic & medicinal chemistry*, 17(6), 2576-2584.

Charles, N. A., Holland, E. C., Gilbertson, R., Glass, R., & Kettenmann, H. (2011). The brain tumor microenvironment. *Glia*, 59(8), 1169-1180.

Chassot, J. M., Ribas, D., Silveira, E. F., Grünspan, L. D., Pires, C. C., Farago, P. V., ... & Cruz, L. (2015). Beclomethasone dipropionate-loaded polymeric nanocapsules: development, in vitro cytotoxicity, and in vivo evaluation of acute lung injury. *Journal of nanoscience and nanotechnology*, 15(1), 855-864.

Chen, S., Chen, L., Le, N. T., Zhao, C., Sidduri, A., Lou, J. P., ... & Konzelmann, F. (2007). Synthesis and activity of quinolinyl-methylene-thiazolinones as potent and selective cyclin-dependent kinase 1 inhibitors. *Bioorganic & medicinal chemistry letters*, 17(8), 2134-2138.

Chintala, S. K., Tonn, J. C., & Rao, J. S. (1999). Matrix metalloproteinases and their biological function in human gliomas. *International journal of developmental neuroscience*, 17(5), 495-502.

Chumak, V. V., Fil, M. R., Panchuk, R. R., Zimenkovsky, B. S., Havrylyuk, D. Y., Lesyk, R. B., & Stoika, R. S. (2014). Study of antineoplastic action of novel isomeric derivatives of 4-thiazolidinone. *The Ukrainian biochemical journal*, (86, № 6), 96-105.

Cotran, R. S., Kumar, V., Collins, T. *Patologia Estrutural e Funcional*. 6<sup>a</sup> ed. Rio de Janeiro: Editora Guanabara Koogan, 2000.

Crascì, L. P. Vicini, M. Incerti, V. Cardile, S. Avondo, A. Panico. (2015). 2-Benzisothiazolylimino-5-benzylidene-4-thiazolidinones as protective agents against cartilage destruction, *Bioorg. Med. Chem.* 23(7), 1551–1556.

Cunico, W., Gomes, C. R., Vellasco, J., & Walcimar, T. (2008). Chemistry and biological activities of 1, 3-thiazolidin-4-ones. *Mini-Reviews in Organic Chemistry*, 5(4), 336-344.

Dai C, Holland EC (2001). Glioma models. *Biochim. Biophys. Acta* 1551:M19-M27, 1999.

Dang, L., White, D. W., Gross, S., Bennett, B. D., Bittinger, M. A., Driggers, E. M., ... & Marks, K. M. (2009). Cancer-associated IDH1 mutations produce 2-hydroxyglutarate. *Nature*, 462(7274), 739.

Da Fonseca, C. O., Linden, R., Futuro, D., Gattass, C. R., & Quirico-Santos, T. (2008). Ras pathway activation in gliomas: a strategic target for intranasal administration of perillyl alcohol. *Archivum immunologiae et therapiae experimentalis*, 56(4), 267-276.

Da Silva, D. S., da Silva, C. E. H., Soares, M. S. P., Azambuja, J. H., de Carvalho, T. R., Zimmer, G. C., ... & Cunico, W. (2016). Thiazolidin-4-ones from 4-(methylthio) benzaldehyde and 4-(methylsulfonyl) benzaldehyde: Synthesis, antiglioma activity and cytotoxicity. *European journal of medicinal chemistry*, 124, 574-582.

Demuth, T., & Berens, M. E. (2004). Molecular mechanisms of glioma cell migration and invasion. *Journal of neuro-oncology*, 70(2), 217-228.

Dovizio, M., Bruno, A., Tacconelli, S., & Patrignani, P. (2013). Mode of action of aspirin as a chemopreventive agent. In *Prospects for chemoprevention of colorectal neoplasia* (pp. 39-65).

Fang, C. B., Gomes, C. M. C. D. N., Formiga, F. B., Fonseca, V. A., Carvalho, M. P., & Klug, W. A. (2013). Is the delayed surgery after neoadjuvant chemoradiation beneficial for locally advanced rectal cancer?. *ABCD. Arquivos Brasileiros de Cirurgia Digestiva*, 26(1), 31-35.

Fontana, M.C., Coradini, K., Pohlmann, A.R., et al., (2010). Nanocapsules prepared from amorphous polyesters: effect on the physicochemical characteristics, drug release, and photostability. *J. Nanosci. Nanotechnol.* 10, 3091–3099.

Friedrich, R. B.; Coradini, K.; Fonseca, F.; Guterres, S.S.; Beck, R.C.R.; Pohlmann, A.R (2016). Lipid-Core Nanocapsules Improved Antiedematogenic Activity of Tacrolimus in Adjuvant-Induced Arthritis Model. *Journal of Nanoscience and Nanotechnology*, v. 16, p.1265–1274.

Furnari, F. B., Fenton, T., Bachoo, R. M., Mukasa, A., Stommel, J. M., Stegh, A., ... & Chin, L. (2007). Malignant astrocytic glioma: genetics, biology, and paths to treatment. *Genes & development*, 21(21), 2683-2710.

Gonsette, R. E. (2008). Neurodegeneration in multiple sclerosis: the role of oxidative stress and excitotoxicity. *Journal of the neurological sciences*, 274(1), 48-53.

Gouvea, D. P., Vasconcellos, F. A., dos Anjos Berwaldt, G., Neto, A. C. P. S., Fischer, G., Sakata, R. P., ... & Cunico, W. (2016). 2-Aryl-3-(2-morpholinoethyl) thiazolidin-4-ones: Synthesis, anti-inflammatory in vivo, cytotoxicity in vitro and molecular docking studies. *European journal of medicinal chemistry*, 118, 259-265.

Granada, A., Nemen, D., Dora, C. L., Neckel, G. L., & Lemos-Senna, E. (2009). O emprego de sistemas de liberação como estratégia para melhorar as propriedades terapêuticas de fármacos de origem natural: o exemplo da camptotecina e seus derivados. *Revista de Ciências Farmacêuticas Básica e Aplicada*, 28(2), 129-139.

Gupta, S., Balasubramanian, B. A., Fu, T., Genta, R. M., Rockey, D. C., & Lash, R. (2012). Polyps with advanced neoplasia are smaller in the right than in the left colon:

implications for colorectal cancer screening. *Clinical Gastroenterology and Hepatology*, 10(12), 1395-1401.

Guterres, S. S., Alves, M. P., & Pohlmann, A. R. (2007). Polymeric nanoparticles, nanospheres and nanocapsules, for cutaneous applications. *Drug target insights*, 2, 147.

Havrylyuk, D., Zimenkovsky, B., Vasylenko, O., Zaprutko, L., Gzella, A., & Lesyk, R. (2009). Synthesis of novel thiazolone-based compounds containing pyrazoline moiety and evaluation of their anticancer activity. *European Journal of Medicinal Chemistry*, 44(4), 1396-1404.

Howe, L. R., Subbaramaiah, K., Brown, A. M., & Dannenberg, A. J. (2001). Cyclooxygenase-2: a target for the prevention and treatment of breast cancer. *Endocrine-related cancer*, 8(2), 97-114.

Herrera-Perez, M., Voytik-Harbin, S. L., & Rickus, J. L. (2015). Extracellular matrix properties regulate the migratory response of glioblastoma stem cells in three-dimensional culture. *Tissue Engineering Part A*, 21(19-20), 2572-2582.

Higashi, Y., Kanekura, T., & Kanzaki, T. (2000). Enhanced expression of cyclooxygenase (COX)-2 in human skin epidermal cancer cells: Evidence for growth suppression by inhibiting COX-2 expression. *International journal of cancer*, 86(5), 667-671.

Hussain, S. F., Yang, D., Suki, D., Aldape, K., Grimm, E., & Heimberger, A. B. (2006). The role of human glioma-infiltrating microglia/macrophages in mediating antitumor immune responses. *Neuro-oncology*, 8(3), 261-279.

Huse, J. T., & Holland, E. C. (2010). Targeting brain cancer: advances in the molecular pathology of malignant glioma and medulloblastoma. *Nature reviews. Cancer*, 10(5), 319.

Jain, A. K., Vaidya, A., Ravichandran, V., Kashaw, S. K., & Agrawal, R. K. (2012). Recent developments and biological activities of thiazolidinone derivatives: A review. *Bioorganic & medicinal chemistry*, 20(11), 3378-3395.

Johnson, D. R., Ma, D. J., Buckner, J. C., & Hammack, J. E. (2012). Conditional probability of long-term survival in glioblastoma. *Cancer*, 118(22), 5608-5613.

Jovčevska, I., Kočevar, N., & Komel, R. (2013). Glioma and glioblastoma-how much do we (not) know?. *Molecular and clinical oncology*, 1(6), 935-941.

Jung, K. Y., Samadani, R., Chauhan, J., Nevels, K., Yap, J. L., Zhang, J., ... & Shukla, S. (2013). Structural modifications of (Z)-3-(2-aminoethyl)-5-(4-ethoxybenzylidene)thiazolidine-2, 4-dione that improve selectivity for inhibiting the proliferation of

melanoma cells containing active ERK signaling. *Organic & biomolecular chemistry*, 11(22), 3706-3732.

Kanu, O. O., Mehta, A., Di, C., Lin, N., Bortoff, K., Bigner, D. D., ... & Adamson, D. C. (2009). Glioblastoma multiforme: a review of therapeutic targets. *Expert opinion on therapeutic targets*, 13(6), 701-718.

Kaloshi, G., Psimaras, D., Mokhtari, K., Dehais, C., Houillier, C., Marie, Y., ... & Sanson, M. (2009). Supratentorial low-grade gliomas in older patients. *Neurology*, 73(24), 2093-2098.

Karin M, Greten FR (2005). NF- $\kappa$ B: linking inflammation and immunity to cancer development and progression. *Nature Reviews Immunology*, v.5, p. 749–759.

Kobylinska, L. I., Boiko, N. M., Panchuk, R. R., Grytsyna, I. I., Biletska, L. P., Lesyk, R. B., ... & Stoika, R. S. (2016). Putative anticancer potential of novel 4-thiazolidinone derivatives: cytotoxicity toward rat C6 glioma in vitro and correlation of general toxicity with the balance of free radical oxidation in rats. *Croatian medical journal*, 57(2), 151-163.

Koul, H. K., Pal, M., & Koul, S. (2013). Role of p38 MAP kinase signal transduction in solid tumors. *Genes & cancer*, 4(9-10), 342-359.

Kulhari, H., Pooja, D., Shrivastava, S., Reddy, T. S., Barui, A. K., Patra, C. R., ... & Sistla, R. (2015). Cyclic-RGDfK-Directed Docetaxel Loaded Nanomicelles for Angiogenic Tumor Targeting.

Kunzler, A., Neuenfeldt, P. D., das Neves, A. M., Pereira, C. M., Marques, G. H., Nascente, P. S., ... & Cunico, W. (2013). Synthesis, antifungal and cytotoxic activities of 2-aryl-3-((piperidin-1-yl) ethyl) thiazolidinones. *European journal of medicinal chemistry*, 64, 74-80.

Ljubisavljevic, S. (2016). Oxidative stress and neurobiology of demyelination. *Molecular neurobiology*, 53(1), 744-758.

Leibovich-Rivkin, T., Liubomirski, Y., Meshel, T., Abashidze, A., Brisker, D., Solomon, H., ... & Ben-Baruch, A. (2014). The inflammatory cytokine TNF $\alpha$  cooperates with Ras in elevating metastasis and turns WT-Ras to a tumor-promoting entity in MCF-7 cells. *BMC cancer*, 14(1), 158.

Lin, W. W., & Karin, M. (2007). A cytokine-mediated link between innate immunity, inflammation, and cancer. *Journal of Clinical Investigation*, 117(5), 1175.

Louis, D. N., Ohgaki, H., Wiestler, O. D., Cavenee, W. K., Burger, P. C., Jouvet, A., ... & Kleihues, P. (2007). The 2007 WHO classification of tumours of the central nervous system. *Acta neuropathologica*, 114(2), 97-109.

Louis, D. N., Perry, A., Reifenberger, G., Von Deimling, A., Figarella-Branger, D., Cavenee, W. K., ... & Ellison, D. W. (2016). The 2016 World Health Organization classification of tumors of the central nervous system: a summary. *Acta neuropathologica*, 131(6), 803-820.

Maehama, T., & Dixon, J. E. (1999). PTEN: a tumour suppressor that functions as a phospholipid phosphatase. *Trends in cell biology*, 9(4), 125-128.

Maher, E. A., Brennan, C., Wen, P. Y., Durso, L., Ligon, K. L., Richardson, A., ... & Quackenbush, J. (2006). Marked genomic differences characterize primary and secondary glioblastoma subtypes and identify two distinct molecular and clinical secondary glioblastoma entities. *Cancer research*, 66(23), 11502-11513.

Mainardes, R. M. Desenvolvimento de nanopartículas de PLA e PLA-PEG para administração intranasal de zidovudina. 2007 Tese (Doutorado em Ciências Farmacêuticas) – Faculdade de Ciências Farmacêutica, Universidade Estadual Paulista.

Maniati, E., Soper, R., & Hagemann, T. (2010). Up for Mischief? IL-17/Th17 in the tumour microenvironment. *Oncogene*, 29(42), 5653.

Marcato, P. D., & Durán, N. (2008). New aspects of nanopharmaceutical delivery systems. *Journal of nanoscience and nanotechnology*, 8(5), 2216-2229.

Masters, S. B., & Trevor, A. J. (2016). *Basic & clinical pharmacology*. B. G. Katzung (Ed.). McGraw-Hill Medical.

Mattheolabakis, G., Rigas, B., & Constantinides, P. P. (2012). Nanodelivery strategies in cancer chemotherapy: biological rationale and pharmaceutical perspectives. *Nanomedicine*, 7(10), 1577-1590.

Medzhitov, R. (2008). Origin and physiological roles of inflammation. *Nature*, 454(7203), 428.

Mirantes, C., Espinosa, I., Ferrer, I., Dolcet, X., Prat, J., & Matias-Guiu, X. (2013). Epithelial-to-mesenchymal transition and stem cells in endometrial cancer. *Human pathology*, 44(10), 1973-1981.

Mora-Huertas, C. E., Fessi, H., & Elaissari, A. (2010). Polymer-based nanocapsules for drug delivery. *International journal of pharmaceutics*, 385(1), 113-142.

Mrugala, M. M. (2013). Advances and challenges in the treatment of glioblastoma: a clinician's perspective. *Discovery medicine*, 15(83), 221-230.

Nakamura, K., Ito, Y., Kawano, Y., Kurozumi, K., Kobune, M., Tsuda, H., ... & Hamada, H. (2004). Antitumor effect of genetically engineered mesenchymal stem cells in a rat glioma model. *Gene therapy*, 11(14), 1155.

- Nakazato, Y. (2008). Revised WHO classification of brain tumours. *Brain and nerve Shinkei kenkyu no shinpo*, 60(1), 59-77.
- Nanegrungsunk, D., Onchan, W., Chattipakorn, N., & Chattipakorn, S. C. (2015). Current evidence of temozolomide and bevacizumab in treatment of gliomas. *Neurological research*, 37(2), 167-183.
- Onen-Bayram, F. E., Durmaz, I., Scherman, D., Herscovici, J., & Cetin-Atalay, R. (2012). A novel thiazolidine compound induces caspase-9 dependent apoptosis in cancer cells. *Bioorganic & medicinal chemistry*, 20(17), 5094-5102.
- Park, S., & Ruoff, R. S. (2009). Chemical methods for the production of graphenes. *Nature nanotechnology*, 4(4), 217-224.
- Patel, D., Kumari, P., & Patel, N. (2012). Synthesis and biological evaluation of some thiazolidinones as antimicrobial agents. *European journal of medicinal chemistry*, 48, 354-362.
- Pérez-Herrero, E., & Fernández-Medarde, A. (2015). Advanced targeted therapies in cancer: drug nanocarriers, the future of chemotherapy. *European journal of pharmaceuticals and biopharmaceutics*, 93, 52-79.
- Perez-Ortiz, J. M., Tranque, P., Burgos, M., Vaquero, C. F., & Llopis, J. (2007). Glitazones induce astrogloma cell death by releasing reactive oxygen species from mitochondria: modulation of cytotoxicity by nitric oxide. *Molecular pharmacology*, 72(2), 407-417.
- Piccirillo, S. G. M., Combi, R., Cajola, L., Patrizi, A., Redaelli, S., Bentivegna, A., ... & DiMeco, F. (2009). Distinct pools of cancer stem-like cells coexist within human glioblastomas and display different tumorigenicity and independent genomic evolution. *Oncogene*, 28(15), 1807.
- Pohlmann, A. R., Fonseca, F. N., Paese, K., Detoni, C. B., Coradini, K., Beck, R. C., & Guterres, S. S. (2013). Poly ( $\epsilon$ -caprolactone) microcapsules and nanocapsules in drug delivery. *Expert opinion on drug delivery*, 10(5), 623-638.
- Poillet-Perez, L., Despouy, G., Delage-Mourroux, R., & Boyer-Guittaut, M. (2015). Interplay between ROS and autophagy in cancer cells, from tumor initiation to cancer therapy. *Redox biology*, 4, 184-192.
- Preusser, M., Haberler, C., & Hainfellner, J. A. (2006). Malignant glioma: neuropathology and neurobiology. *Wiener Medizinische Wochenschrift*, 156(11-12), 332-337.

Ramakrishna, R., Hebb, A., Barber, J., Rostomily, R., & Silbergeld, D. (2015). Outcomes in reoperated low-grade gliomas. *Neurosurgery*, 77(2), 175-184.

Rawat, M., Singh, D., Saraf, S., & Saraf, S. (2006). Nanocarriers: promising vehicle for bioactive drugs. *Biological and Pharmaceutical Bulletin*, 29(9), 1790-1798.

Rousseau, A., Mokhtari, K., & Duyckaerts, C. (2008). The 2007 WHO classification of tumors of the central nervous system—what has changed?. *Current opinion in neurology*, 21(6), 720-727.

Sakaeva, D.D. (2015). The immunosuppressive microenvironment of malignant gliomas, *Arkh. Patol.* 77, 54–63.

Santos, S. S., Lorenzoni, A., Pegoraro, N. S., Denardi, L. B., Alves, S. H., Schaffazick, S. R., & Cruz, L. (2014). Formulation and in vitro evaluation of coconut oil-core cationic nanocapsules intended for vaginal delivery of clotrimazole. *Colloids and Surfaces B: Biointerfaces*, 116, 270-276.

Saundane, A., Yarlakatti, M., Walmik, P., & KATKARf, V. I. J. A. Y. K. U. M. A. R. (2012). Synthesis, antioxidant and antimicrobial evaluation of thiazolidinone, azetidione encompassing indolylthienopyrimidines. *Journal of Chemical Sciences*, 124(2).

Senkiv, J., Finiuk, N., Kaminsky, D., Havrylyuk, D., Wojtyra, M., Kril, I., ... & Lesyk, R. (2016). 5-Ene-4-thiazolidinones induce apoptosis in mammalian leukemia cells. *European journal of medicinal chemistry*, 117, 33-46.

Silva, D. S., da Silva, C. E. H., Soares, M. S. P., Azambuja, J. H., de Carvalho, T. R., Zimmer, G. C., ... & Cunico, W. (2016). Thiazolidin-4-ones from 4-(methylthio) benzaldehyde and 4-(methylsulfonyl) benzaldehyde: Synthesis, antiglioma activity and cytotoxicity. *European journal of medicinal chemistry*, 124, 574-582.

Silveira, E. F., Azambuja, J. H., de Carvalho, T. R., Kunzler, A., da Silva, D. S., Teixeira, F. C., ... & Cunico, W. (2017). Synthetic 2-aryl-3-((piperidin-1-yl) ethyl) thiazolidin-4-ones exhibit selective in vitro antitumoral activity and inhibit cancer cell growth in a preclinical model of glioblastoma multiforme. *Chemico-Biological Interactions*, 266, 1-9.

Shono, T., Tofilon, P. J., Bruner, J. M., Owolabi, O., & Lang, F. F. (2001). Cyclooxygenase-2 expression in human gliomas. *Cancer research*, 61(11), 4375-4381.

Souza, M. C. Micelas de longo tempo de circulação como sistema nanocarreador para otimização da terapia do câncer de mama. 2013, 124f. Tese (Doutorado). Faculdade de Ciências Farmacêuticas de Ribeirão Preto – Universidade de São Paulo, Ribeirão Preto, 2013.

Stewart, B. W. K. P., & Wild, C. P. (2017). World cancer report 2014. Health.

Stupp R, et al. (2005). Radiotherapy plus concomitant and adjuvant temozolomide for glioblastoma. *The New England journal of medicine*, v.352, n.10, p.987-996.

Stupp, R; Hegi, M.E, Gilbert M.R., Chakravarti, A. (2007). Chemoradiotherapy in malignant glioma: standard of care and future directions, *J. Clin. Oncol.* 25, 4127-4136.

Suvà, M. L., Rheinbay, E., Gillespie, S. M., Patel, A. P., Wakimoto, H., Rabkin, S. D., ... & Curry, W. T. (2014). Reconstructing and reprogramming the tumor-propagating potential of glioblastoma stem-like cells. *Cell*, 157(3), 580-594.

Talibi, S. S., Talibi, S. S., Aweid, B., & Aweid, O. (2014). Prospective therapies for high-grade glial tumours: a literature review. *Annals of Medicine and Surgery*, 3(3), 55-59.

Tang, H., Liu, X., Wang, Z., She, X., Zeng, X., Deng, M., ... & Zeng, F. (2011). Interaction of hsa-miR-381 and glioma suppressor LRRC4 is involved in glioma growth. *Brain research*, 1390, 21-32.

Tripathi, A. C., Gupta, S. J., Fatima, G. N., Sonar, P. K., Verma, A., Saraf, S. K. (2014) 4-Thiazolidinones: The advances continue. *Eur. J. Med. Chem.* 72, 52-77.

Wang S et al. (2011). Design, synthesis and biological evaluation of novel 4-thiazolidinones containing indolin-2-one moiety as potential antitumor agent. *European Journal of Medicinal Chemistry* 46, 3509 – 3518.

Wen, P. Y., Macdonald, D. R., Reardon, D. A., Cloughesy, T. F., Sorensen, A. G., Galanis, E., ... & Tsien, C. (2010). Updated response assessment criteria for high-grade gliomas: response assessment in neuro-oncology working group. *Journal of Clinical Oncology*, 28(11), 1963-1972.

Yeung, Y. T., Bryce, N. S., Adams, S., Braidy, N., Konayagi, M., McDonald, K. L., ... & Munoz, L. (2012). p38 MAPK inhibitors attenuate pro-inflammatory cytokine production and the invasiveness of human U251 glioblastoma cells. *Journal of neuro-oncology*, 109(1), 35-44.

Yin, D., Ong, J. M., Hu, J., Desmond, J. C., Kawamata, N., Konda, B. M., ... & Koeffler, H. P. (2007). Suberoylanilide hydroxamic acid, a histone deacetylase inhibitor: effects on gene expression and growth of glioma cells in vitro and in vivo. *Clinical Cancer Research*, 13(3), 1045-1052.

Van Meir, E. G., Hadjipanayis, C. G., Norden, A. D., Shu, H. K., Wen, P. Y., & Olson, J. J. (2010). Exciting new advances in neuro-oncology: The avenue to a cure for malignant glioma. *CA: a cancer journal for clinicians*, 60(3), 166-193.



Vassilev L.T. et al (2006). Selective small-molecule inhibitor reveals critical mitotic functions of human CDK1, PNAS, 103(28), 10660–10665.

Verçoza, G. L., Feitoza, D. D., Alves, A. J., de Aquino, T. M., Gildo, J., Araújo, J. M., ... & da Silva Góes, A. J. (2009). Síntese e avaliação da atividade antimicrobiana de novas 4-tiazolidinonas obtidas a partir de formilpiridina tiossemicarbazonas. *Quim. Nova*, 32(6), 1405-1410.

Vredenburgh, J. J., Desjardins, A., Reardon, D. A., & Friedman, H. S. (2009). Experience with irinotecan for the treatment of malignant glioma. *Neuro-oncology*, 11(1), 80-91.

Zanotto-Filho, A., Coradini, K., Braganhol, E., Schröder, R., De Oliveira, C. M., Simões-Pires, A., ... & Beck, R. C. R. (2013). Curcumin-loaded lipid-core nanocapsules as a strategy to improve pharmacological efficacy of curcumin in glioma treatment. *European Journal of Pharmaceutics and Biopharmaceutics*, 83(2), 156-167.

Zhai, H. Heppner, F.L Tsirka, S.E. (2011). Microglia/macrophages promote glioma progression, *Glia* 59, 472–485.

Zhang, Y. et al. (2012). Efferth, Dryofragin, a phloroglucinol derivative, induces apoptosis in human breast cancer MCF-7 cells through ROS-mediated mitochondrial pathway, *Chem. Biol. Interact.* 199(2), 129–136.

## 7. Anexos

### Pareceres de aprovação do comitê de ética em experimentação animal da Universidade Federal de Pelotas.



Pelotas, 10 de fevereiro de 2014

**De:** Prof. Dr. Éverton Fagonde da Silva

*Presidente da Comissão de Ética em Experimentação Animal (CEEA)*

**Para:** Professora Elizandra Braganhol

*Centro de Ciências Químicas, Farmacêuticas e de Alimentos*

Senhora Professora:

A CEEA analisou o projeto intitulado: **“Investigação do potencial terapêutico de tiazolidinonas sintéticas para o tratamento de gliomas”**, processo nº23110.009219/2013-55, sendo de parecer **FAVORÁVEL** a sua execução, considerando ser o assunto pertinente e a metodologia compatível com os princípios éticos em experimentação animal e com os objetivos propostos.

**Solicitamos, após tomar ciência do parecer, reenviar o processo à CEEA.**

Salientamos também a necessidade deste projeto ser cadastrado junto ao Departamento de Pesquisa e Iniciação Científica para posterior registro no COCEPE (código para cadastro nº CEEA 9219).

Sendo o que tínhamos para o momento, subscrevemo-nos.

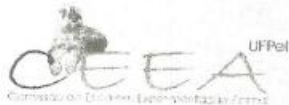
Atenciosamente,

**Prof. Dr. Éverton Fagonde da Silva**

*Presidente da CEEA*

Ciente em: 02 / 04 / 2014

Assinatura da Professora Responsável:



Pelotas, 05 de setembro de 2012

**De:** Prof. Dr. Éverton Fagonde da Silva  
*Presidente da Comissão de Ética em Experimentação Animal (CEEA)*

**Para:** Dra. Flávia Aleixo Vasconcellos  
*Centro de Ciências Químicas, Farmacêuticas e de Alimentos*

Senhora Pesquisadora:

A CEEA analisou o projeto intitulado: "Estudo da síntese, caracterização e avaliação farmacológica de Tiazolidínonas e Tiazinanonas derivadas da 3-aminopropilmorfolina", processo nº23110.007068/2012-10, sendo de parecer FAVORÁVEL a sua execução, considerando ser o assunto pertinente e a metodologia compatível com os princípios éticos em experimentação animal e com os objetivos propostos.

Solicitamos, após tomar ciência do parecer, reenviar o processo à CEEA.

Salientamos também a necessidade deste projeto ser cadastrado junto ao Departamento de Pesquisa e Iniciação Científica para posterior registro no COCEPE (código para cadastro nº CEEA 7068).

Sendo o que tínhamos para o momento, subscrevemo-nos.

Atenciosamente,

**Prof. Dr. Éverton Fagonde da Silva**  
*Presidente da CEEA*

Ciente em: 06/09 /2012

Assinatura da Pesquisadora Responsável:

### Material Suplementar Manuscrito 3.

#### The anti-inflammatory, antitumor and cytotoxicity activities of synthetic thiazolidinones from 3-morpholinopropylamine.

Elita F. da Silveira, Daniela P. Gouvêa, Flávia A. Vasconcellos, Gabriele A. Berwaldt, Juliana H. Azambuja, Adriana M. das Neves, Renata P. Sakata, Wanda P. Almeida, Ana P. Horn, Elizandra Braganhol, Wilson Cunico.

#### Supplementary Information

Table of Contents	Figure	Table	Page
<sup>1</sup> H- and <sup>13</sup> C- NMR spectra	S1-31		2-17
NMR 2D	S32-S33		18
HRMS spectra	S34-45		19-24
Mass spectra	S46-55		25-34

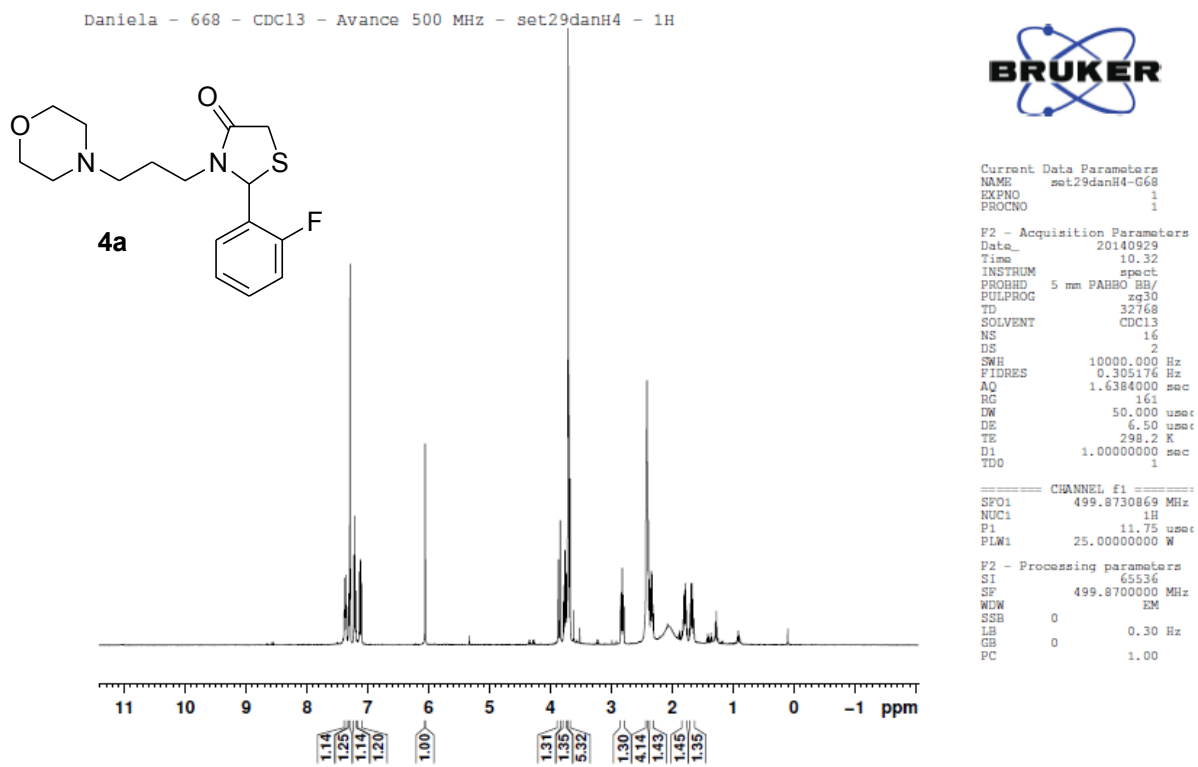


**Figure S1.** <sup>1</sup>H NMR spectrum (500 MHz, CDCl<sub>3</sub>) of compound **4a**.

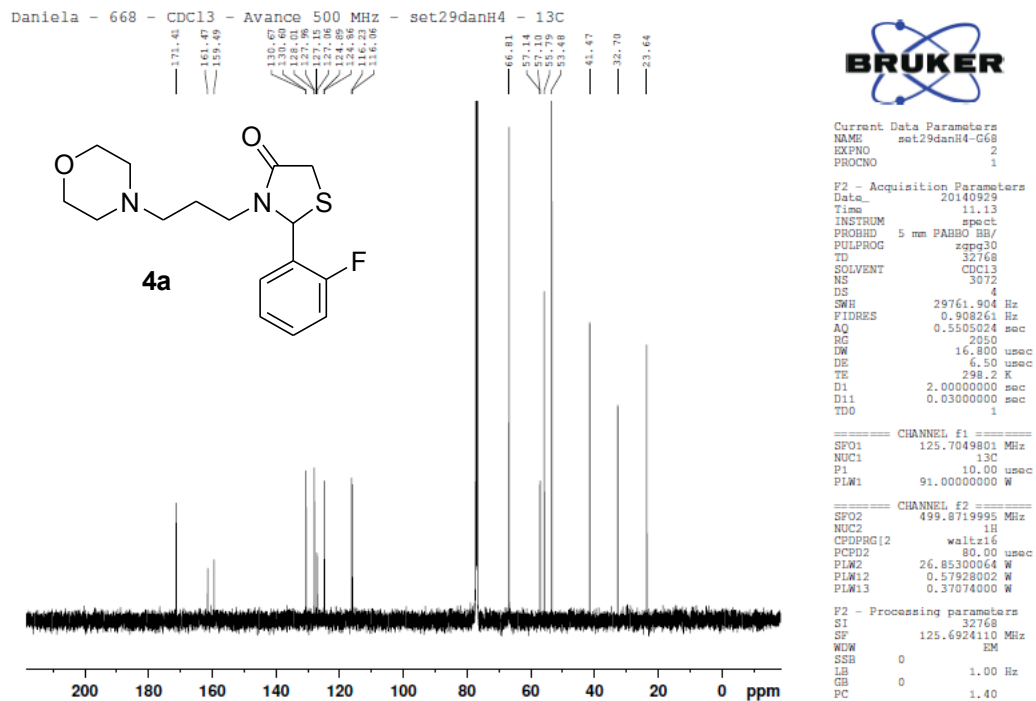
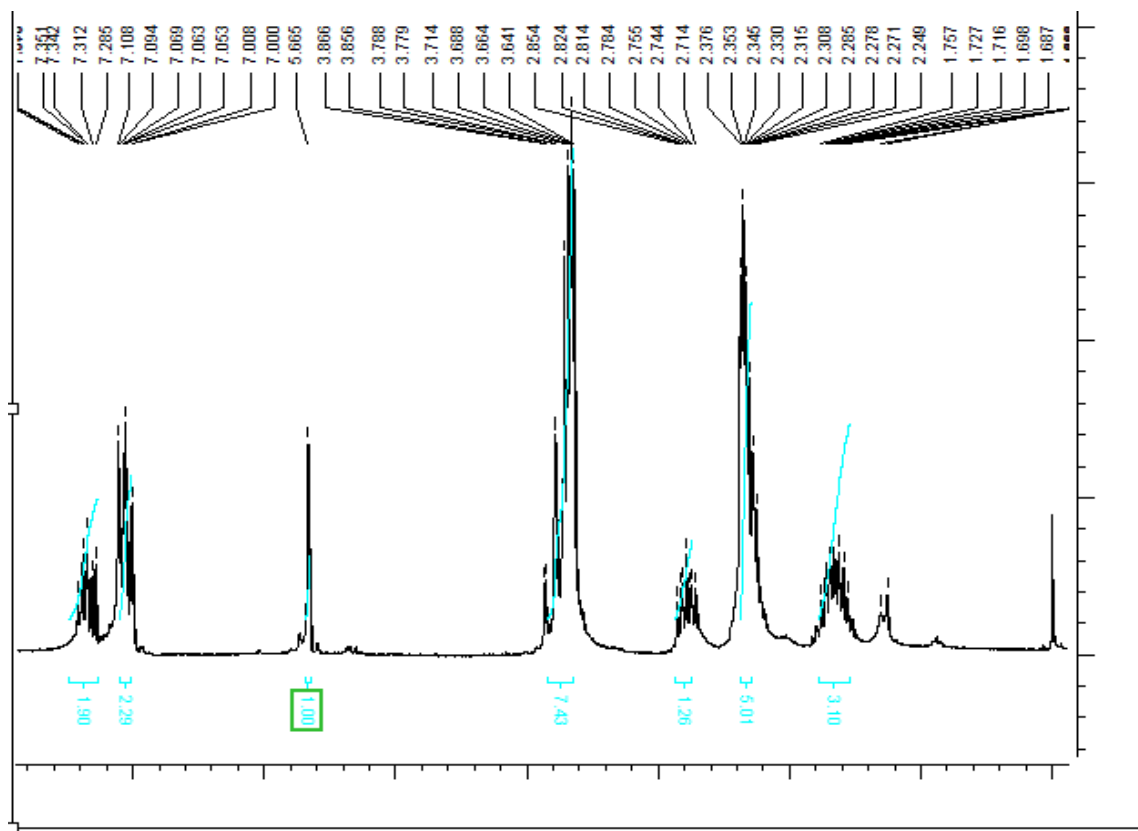
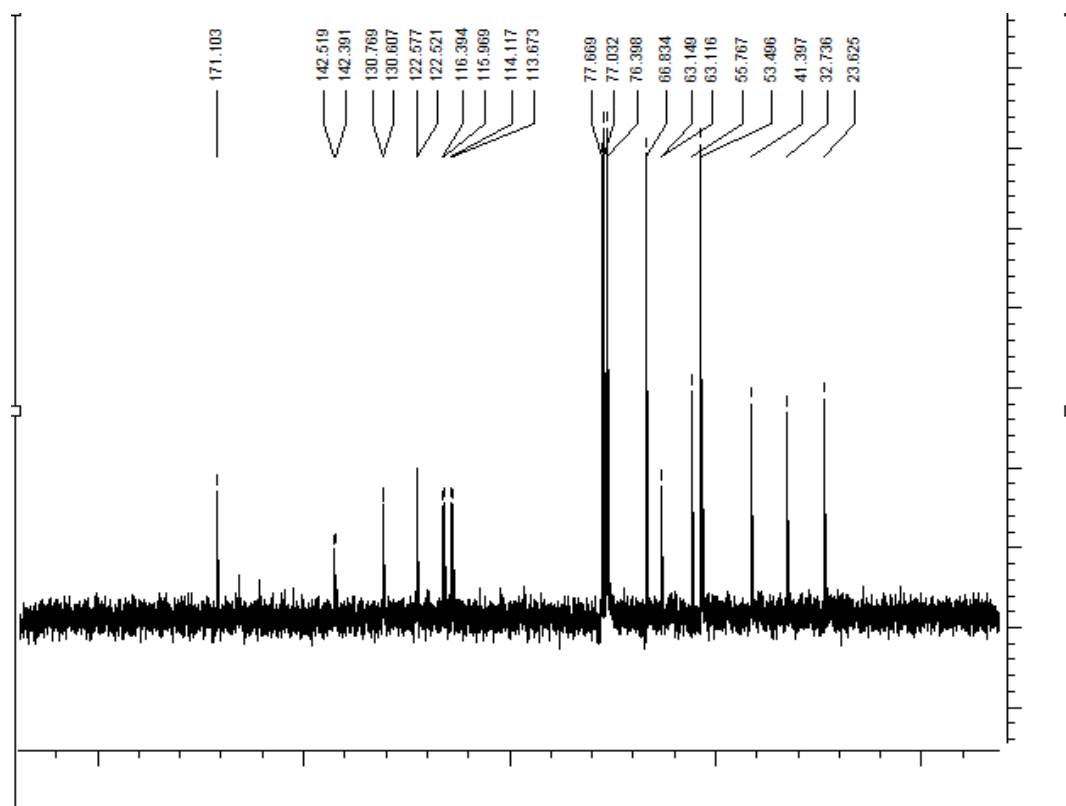


Figure S2.  $^{13}\text{C}$  NMR spectrum (125 MHz,  $\text{CDCl}_3$ ) of compound **4a**.



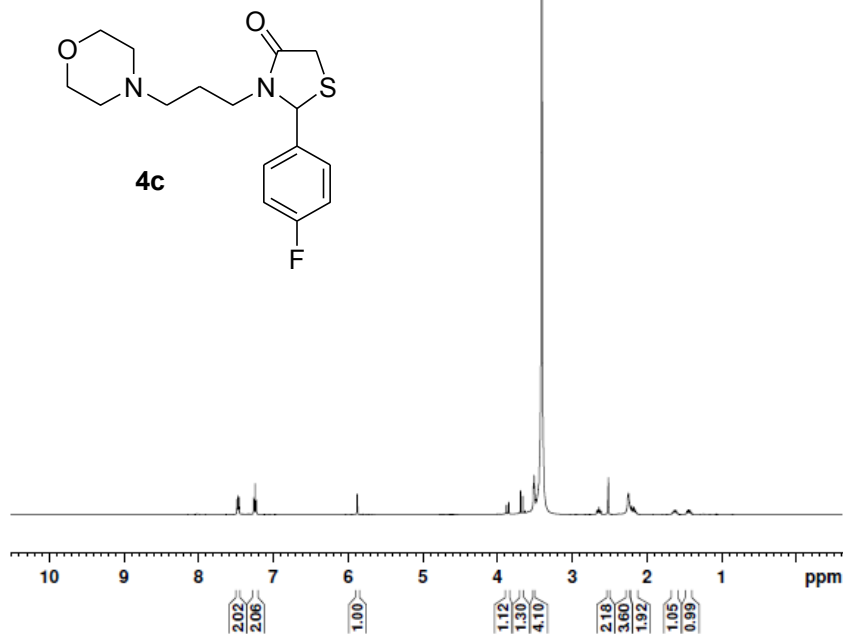
**Figure S3.** <sup>1</sup>H NMR spectrum (200 MHz, CDCl<sub>3</sub>) of compound **4b**.



**Figure S4.**  $^{13}\text{C}$  NMR spectrum (50 MHz,  $\text{CDCl}_3$ ) of compound **4b**.



Daniela - G61 - DMSO - Avance 500 MHz - nov24danH1 - 1H



Current Data Parameters  
NAME nov24danH1-g61  
EXPNO 1  
PROCNO 1

F2 - Acquisition Parameters  
Date\_ 20141124  
Time 10.15  
INSTRUM spect  
PROBHD 5 mm PABBO BB/  
PULPROG zg30  
TD 32768  
SOLVENT DMSO  
NS 16  
DS 2  
SWH 10000.000 Hz  
FIDRES 0.305176 Hz  
AQ 1.6384000 sec  
RG 80.6  
RW 50.000 usec  
DE 6.50 usec  
TE 298.1 K  
D1 1.00000000 sec  
TDO 1

==== CHANNEL f1 =====  
SFO1 499.8730869 MHz  
NUC1 1H  
P1 11.75 usec  
PLW1 25.00000000 W

F2 - Processing parameters  
SI 65536  
SF 499.8700000 MHz  
WDW EM  
SSB 0  
LB 0.30 Hz  
GB 0  
PC 1.00

Figure S5. <sup>1</sup>H NMR spectrum (500 MHz, DMSO-d<sub>6</sub>) of compound 4c.

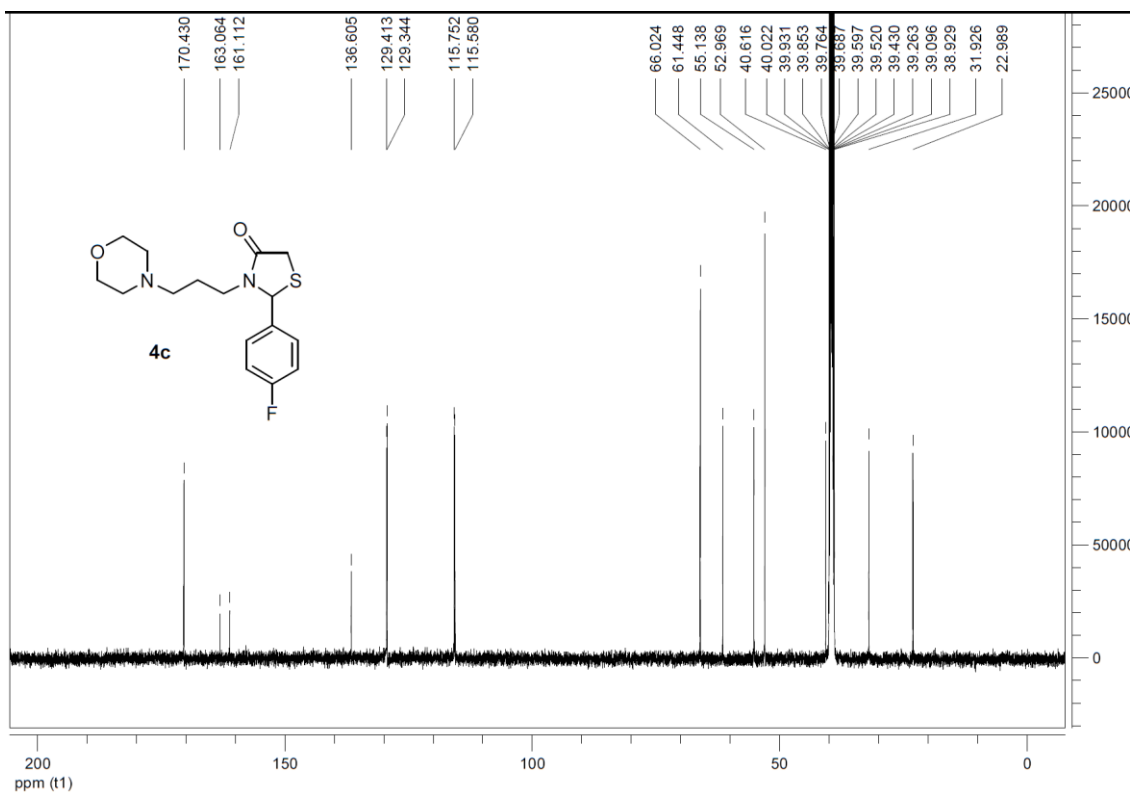


**Figure S6.**  $^{13}\text{C}$  NMR spectrum (125 MHz,  $\text{DMSO-d}_6$ ) of compound **4c**.

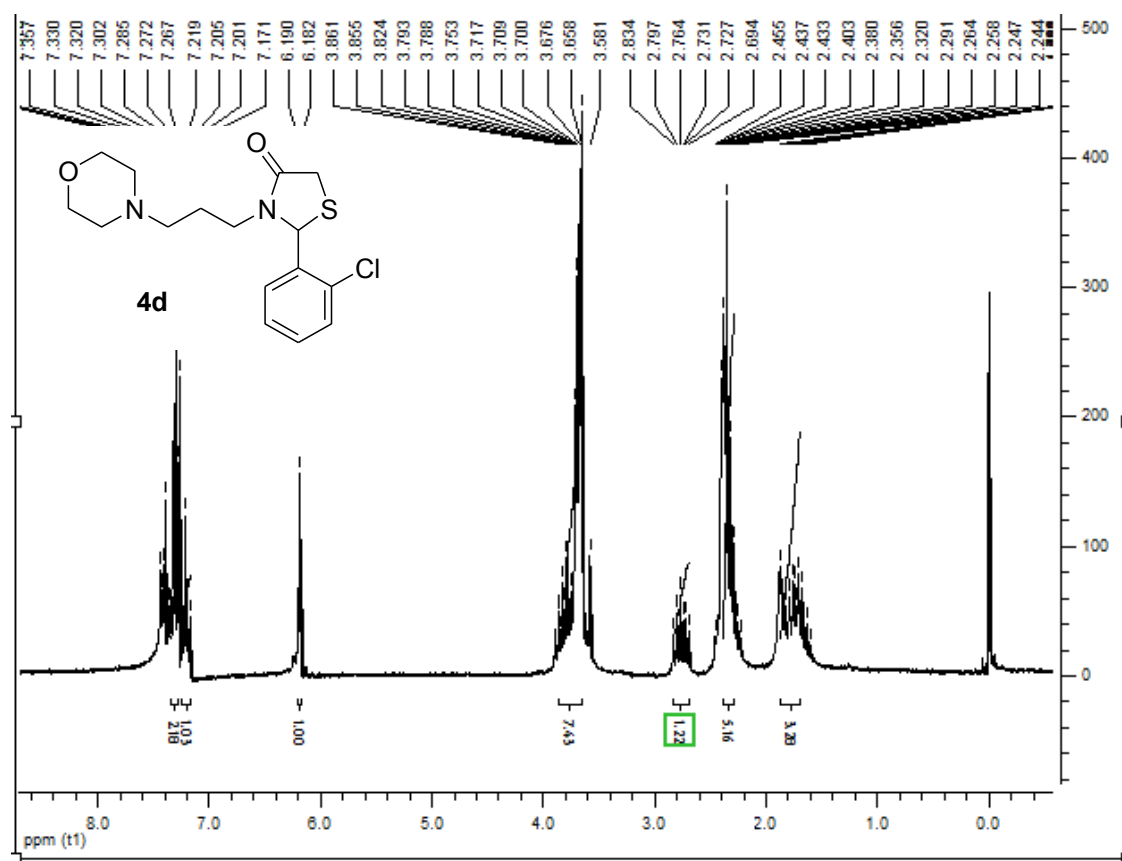


**Figure S7.**  $^1\text{H}$  NMR spectrum (500 MHz,  $\text{CDCl}_3$ ) of compound **4d**.

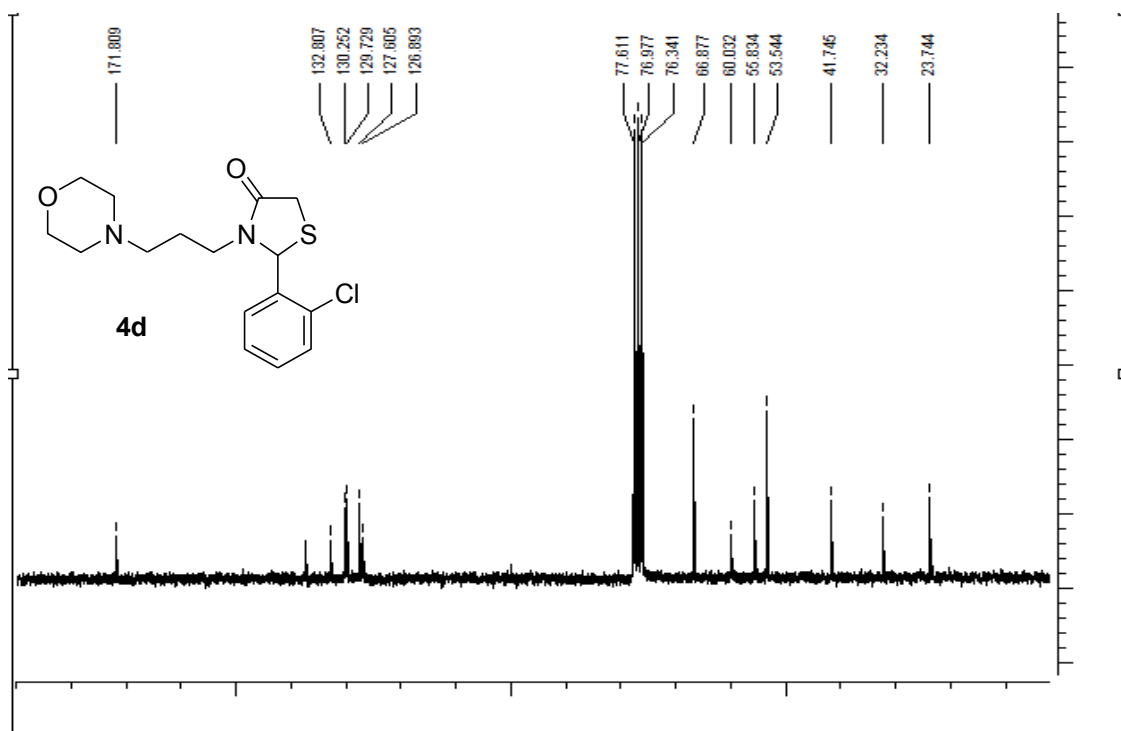


**Figure S8.**  $^{13}\text{C}$  NMR spectrum (125 MHz,  $\text{CDCl}_3$ ) of compound **4d**.

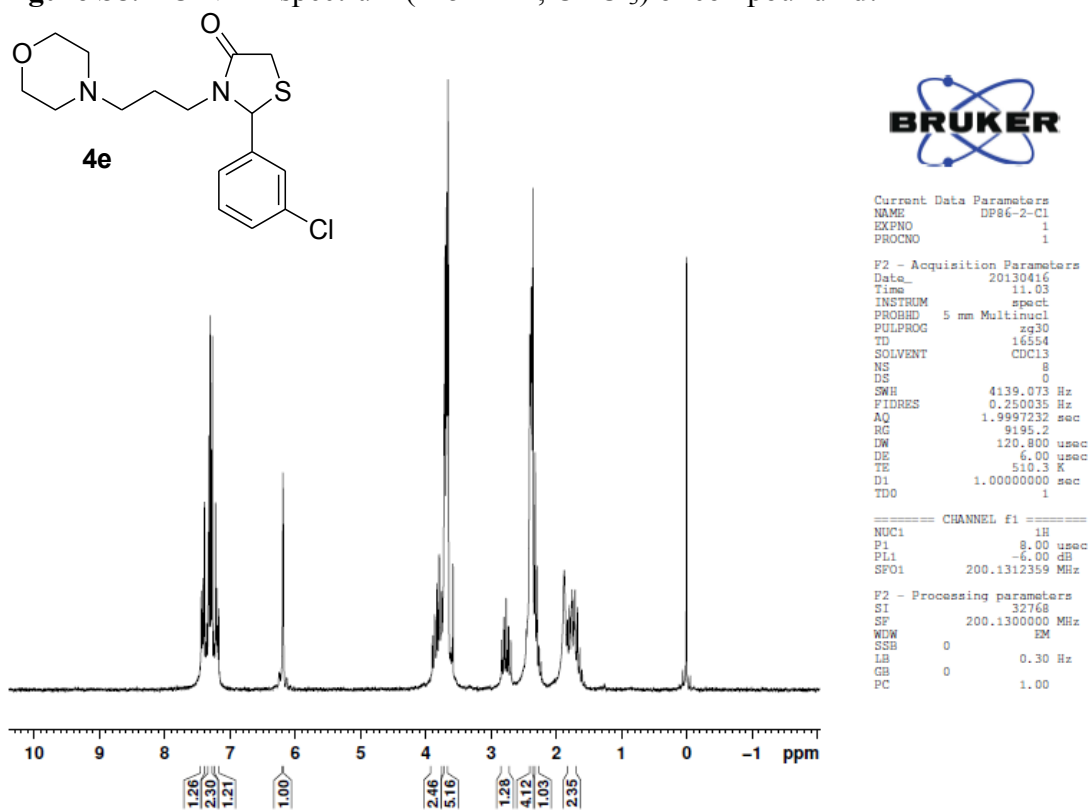


**Figure S9.**  $^1\text{H}$  NMR spectrum (500 MHz,  $\text{CDCl}_3$ ) of compound **4e**.

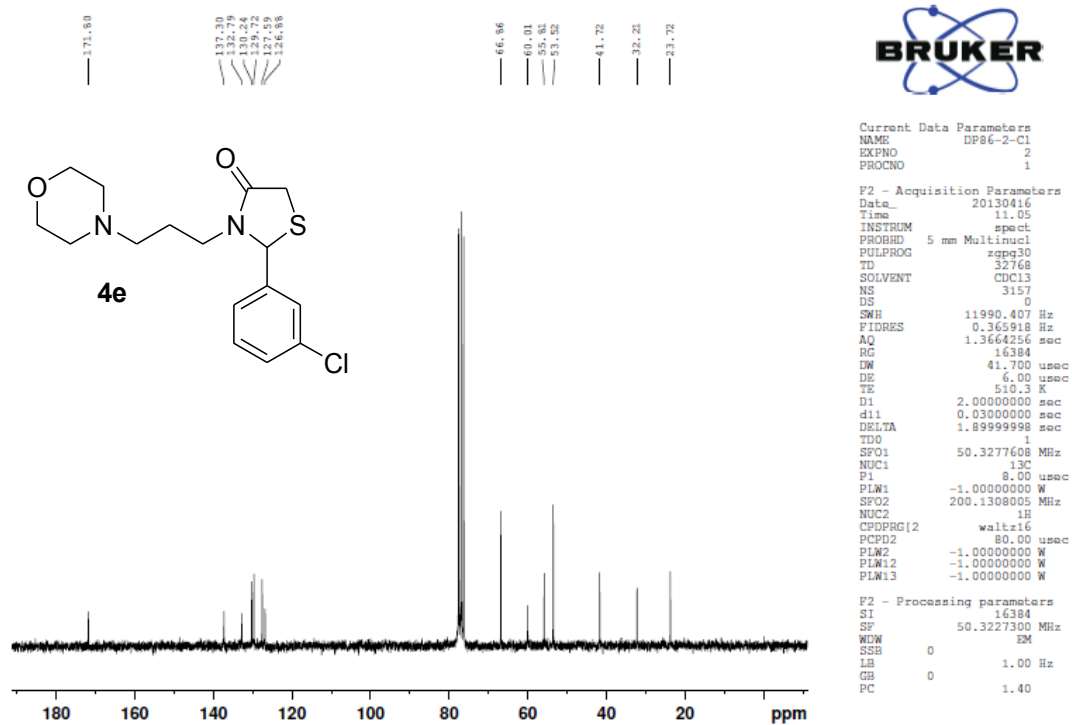


**Figure S10.**  $^{13}\text{C}$  NMR spectrum (125 MHz,  $\text{CDCl}_3$ ) of compound **4e**.

Daniela - DD22 - DMSO - Avance 500 MHz - nov24danH4- 1H

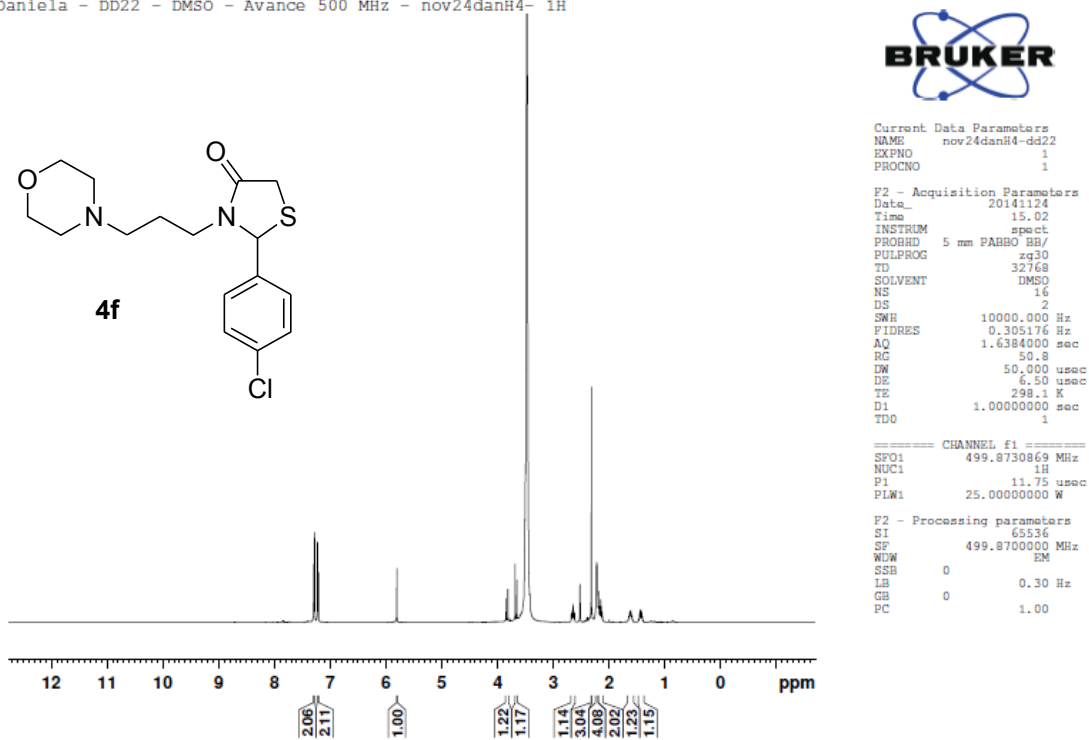


**Figure S11.**  $^1\text{H}$  NMR spectrum (500 MHz, DMSO- $d_6$ ) of compound **4f**.

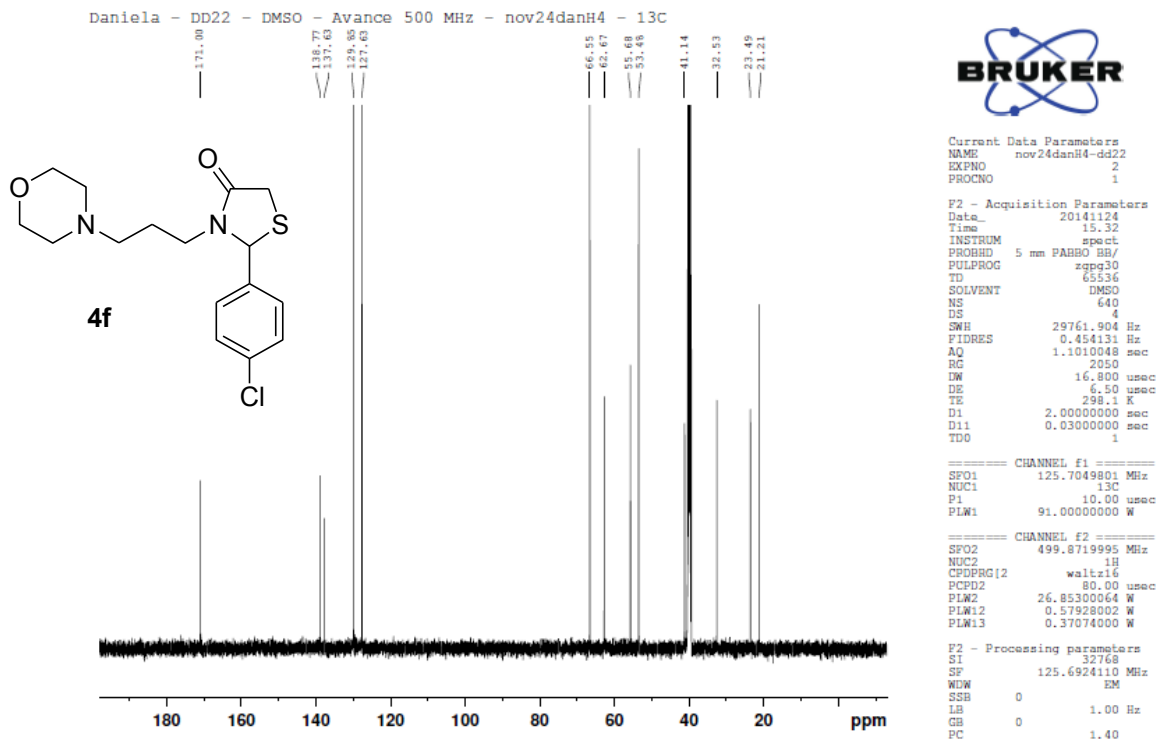
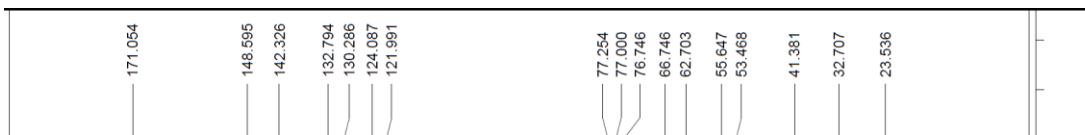
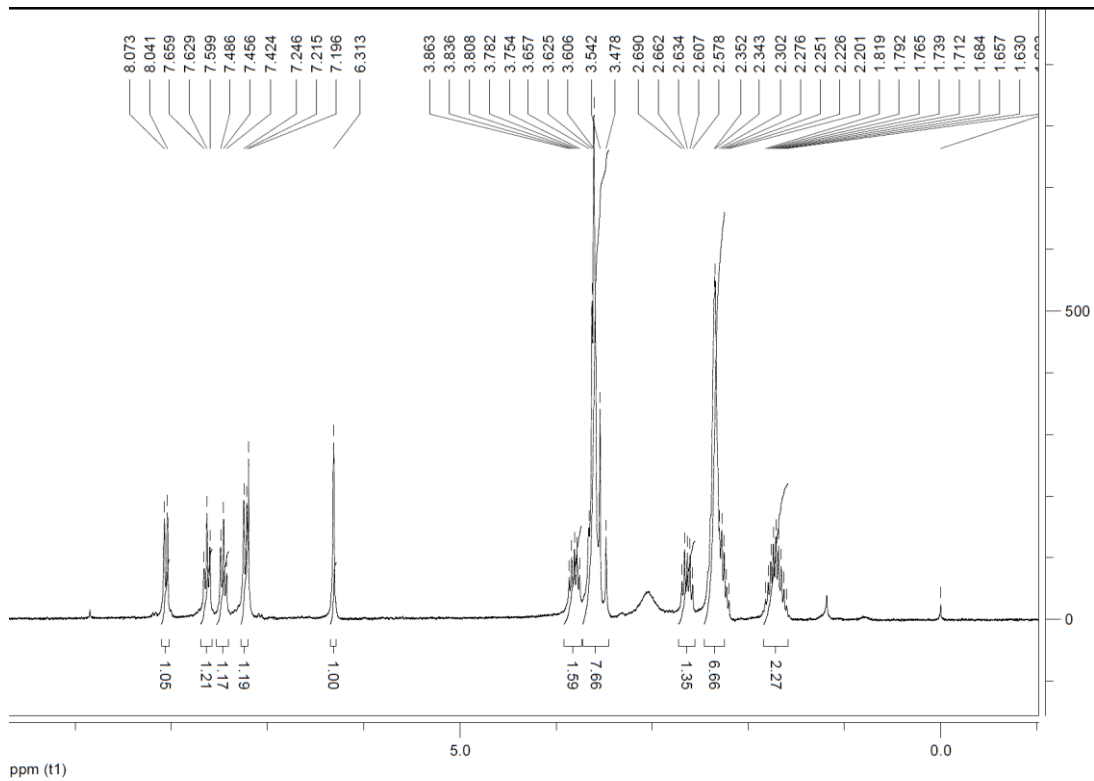


Figure S12.  $^{13}\text{C}$  NMR spectrum (125 MHz,  $\text{DMSO-d}_6$ ) of compound 4f.



**Figure S13.**  $^1\text{H}$  NMR spectrum (250 MHz,  $\text{CDCl}_3$ ) of compound **4g**.

**Figure S14.**  $^{13}\text{C}$  NMR spectrum (125 MHz,  $\text{CDCl}_3$ ) of compound **4g**.

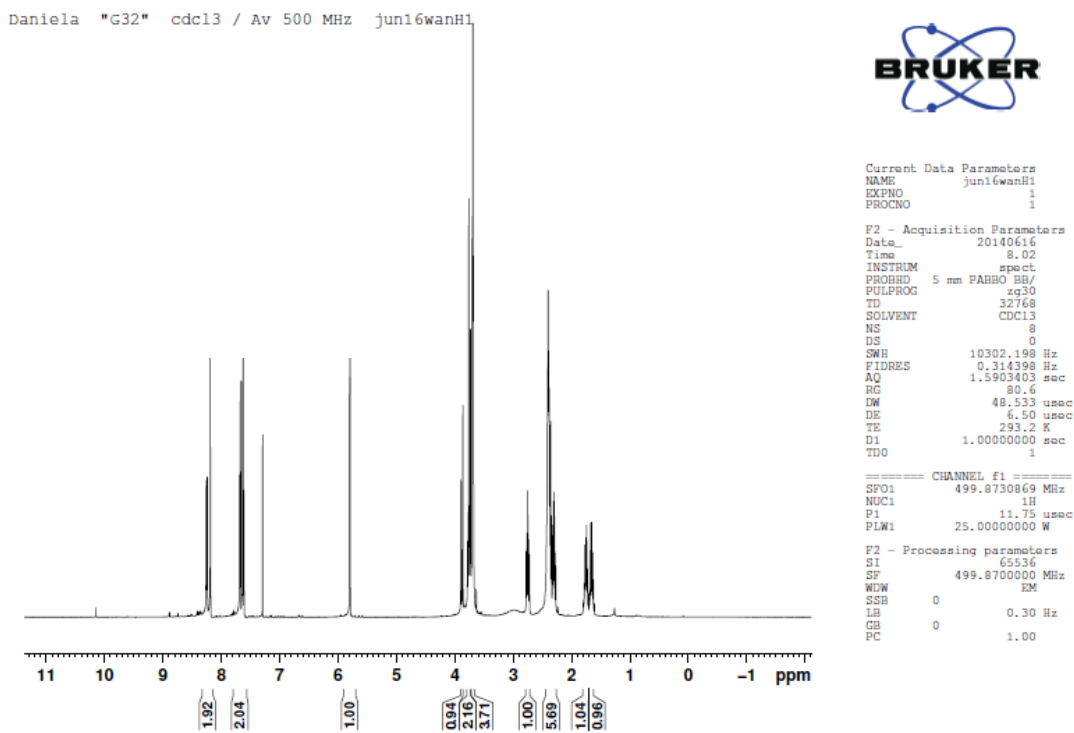


Figure S15.  $^1\text{H}$  NMR spectrum (500 MHz,  $\text{CDCl}_3$ ) of compound **4h**.

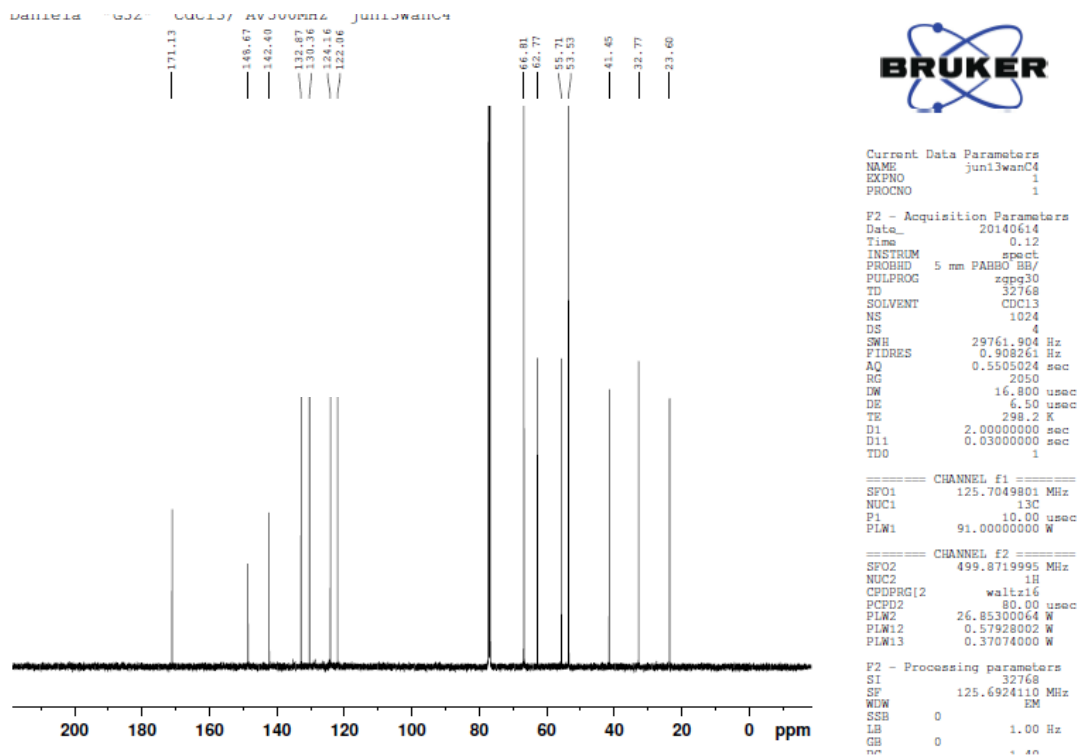
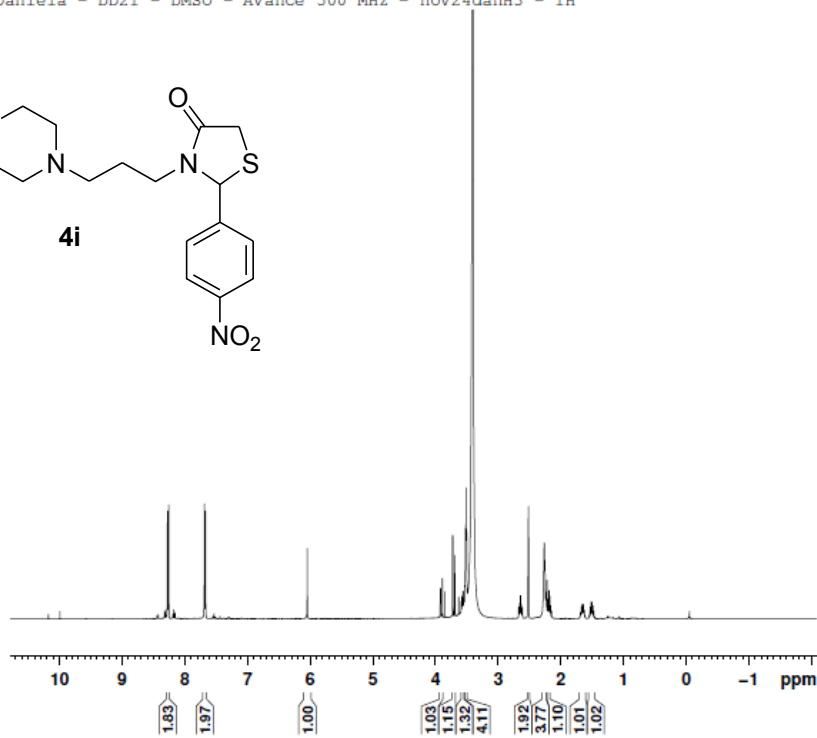
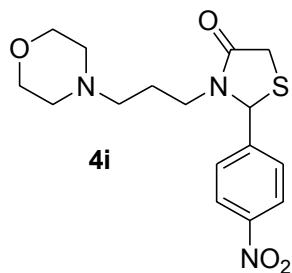


Figure S16.  $^{13}\text{C}$  NMR spectrum (125 MHz,  $\text{CDCl}_3$ ) of compound **4h**.



Daniela - DD21 - DMSO - Avance 500 MHz - nov24danH3 - 1H



```
Current Data Parameters
NAME      nov24danH3-dd21
EXPNO     1
PROCNO    1

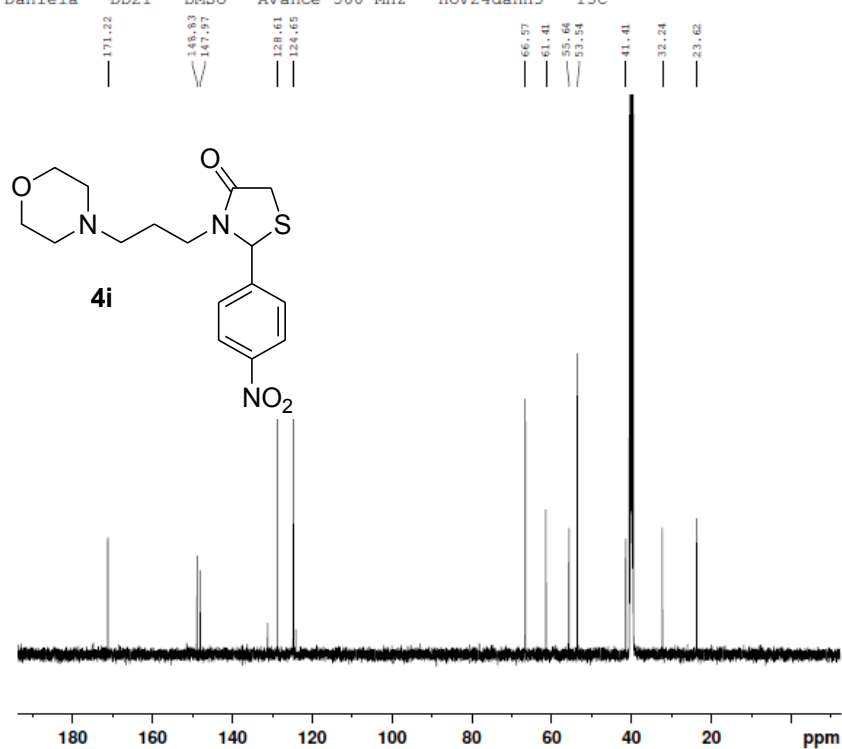
F2 - Acquisition Parameters
Date_     20141124
Time      14.03
INSTRUM   spect
PROBHD    5 mm PABBO BB/
PULPROG   zg30
TD         32768
SOLVENT   DMSO
NS         16
DS         2
SWH        10000.000 Hz
FIDRES     0.305176 Hz
AQ         1.6384000 sec
RG         90.5
DW         50.000 usec
DE         6.50 usec
TE         298.1 K
D1         1.0000000 sec
TDO        1

===== CHANNEL f1 =====
SFO1      499.873069 MHz
NUC1       1H
P1         11.75 usec
PLW1       25.0000000 W

F2 - Processing parameters
SI         65536
SF         499.8700000 MHz
WDW        EM
SSB        0
LB         0.30 Hz
GB         0
PC         1.00
```

Figure S17. <sup>1</sup>H NMR spectrum (500 MHz, DMSO-d<sub>6</sub>) of compound **4i**.

Daniela - DD21 - DMSO - Avance 500 MHz - nov24danH3 - 13C



Current Data Parameters  
NAME nov24danH3-dd21  
EXPNO 2  
PROCNO 1

F2 - Acquisition Parameters:  
Date\_ 20141124  
Time 14.09  
INSTRUM spect  
PROBHD 5 mm PABBO BB/  
PULPROG zgpg30  
TD 65536  
SOLVENT DMSO  
NS 1024  
DS 4  
SWH 29761.904 Hz  
FIDRES 0.454131 Hz  
AQ 1.1010048 sec  
RG 2050  
DW 16.800 usec  
DE 6.50 usec  
TE 298.1 K  
D1 2.0000000 sec  
D11 0.0300000 sec  
TDO 1

==== CHANNEL f1 =====  
SFO1 125.7049801 MH:  
NUC1 13C  
P1 10.00 usec  
PLW1 91.0000000 W

==== CHANNEL f2 =====  
SFO2 499.8719995 MH:  
NUC2 1H  
CPDPRG[2] waltz16  
PCPD2 80.00 usec  
PLW2 26.85300064 W  
PLW12 0.57928002 W  
PLW13 0.37074000 W

F2 - Processing parameters  
SI 32768  
SF 125.6924110 MH:  
WDW EM  
SSB 0  
LB 1.00 Hz  
GB 0  
PC 1.40

Figure S18.  $^{13}\text{C}$  NMR spectrum (125 MHz, DMSO- $d_6$ ) of compound 4i.

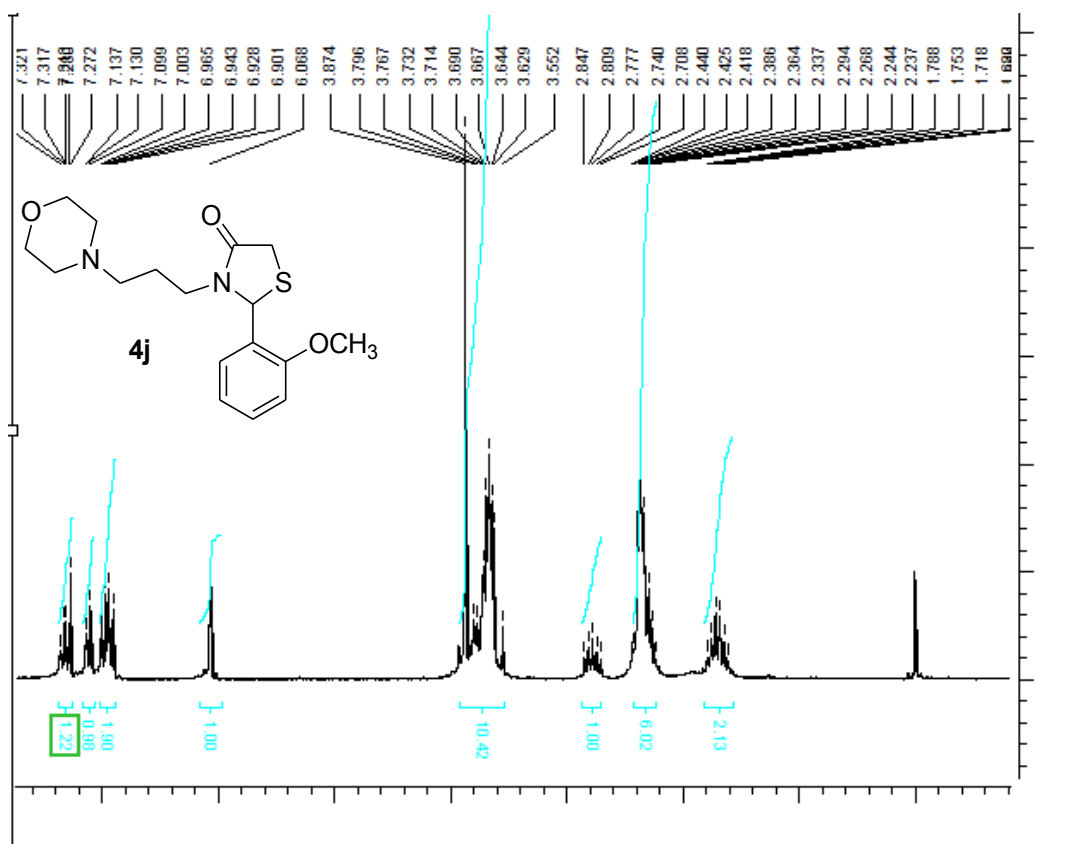


**Figure S19.** <sup>1</sup>H NMR spectrum (500 MHz, CDCl<sub>3</sub>) of compound **4j**.

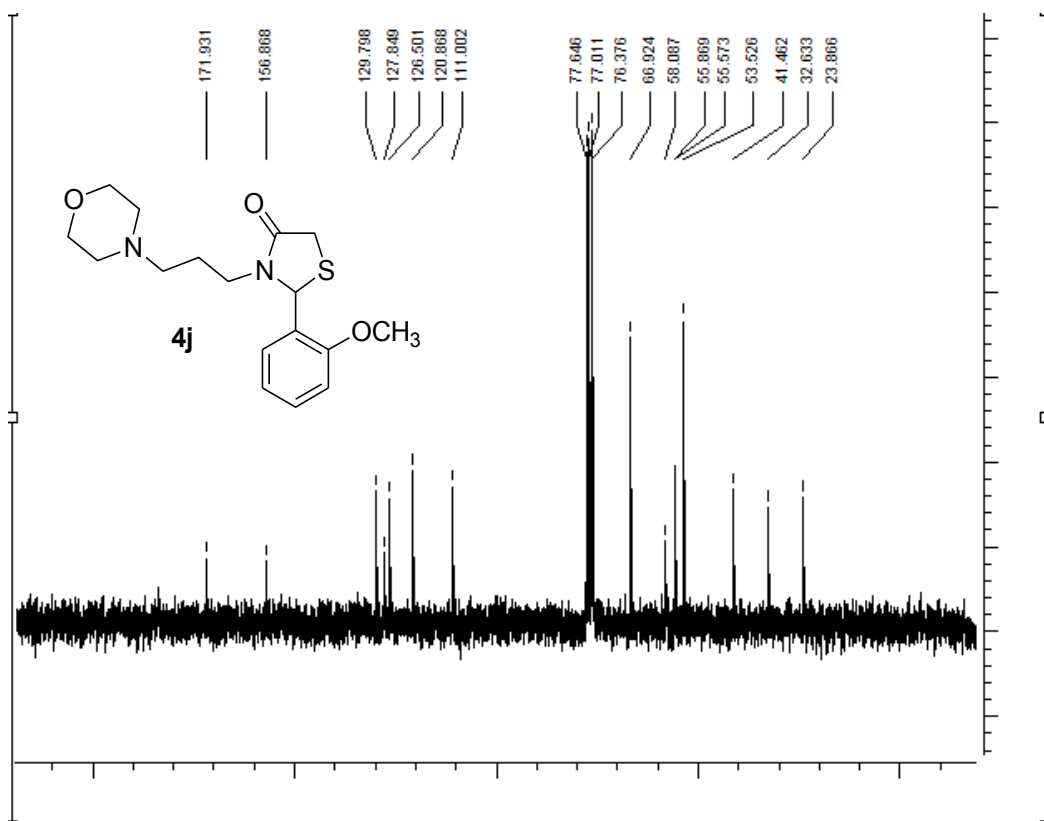


**Figure S20.**  $^{13}\text{C}$  NMR spectrum (125 MHz,  $\text{CDCl}_3$ ) of compound **4j**.

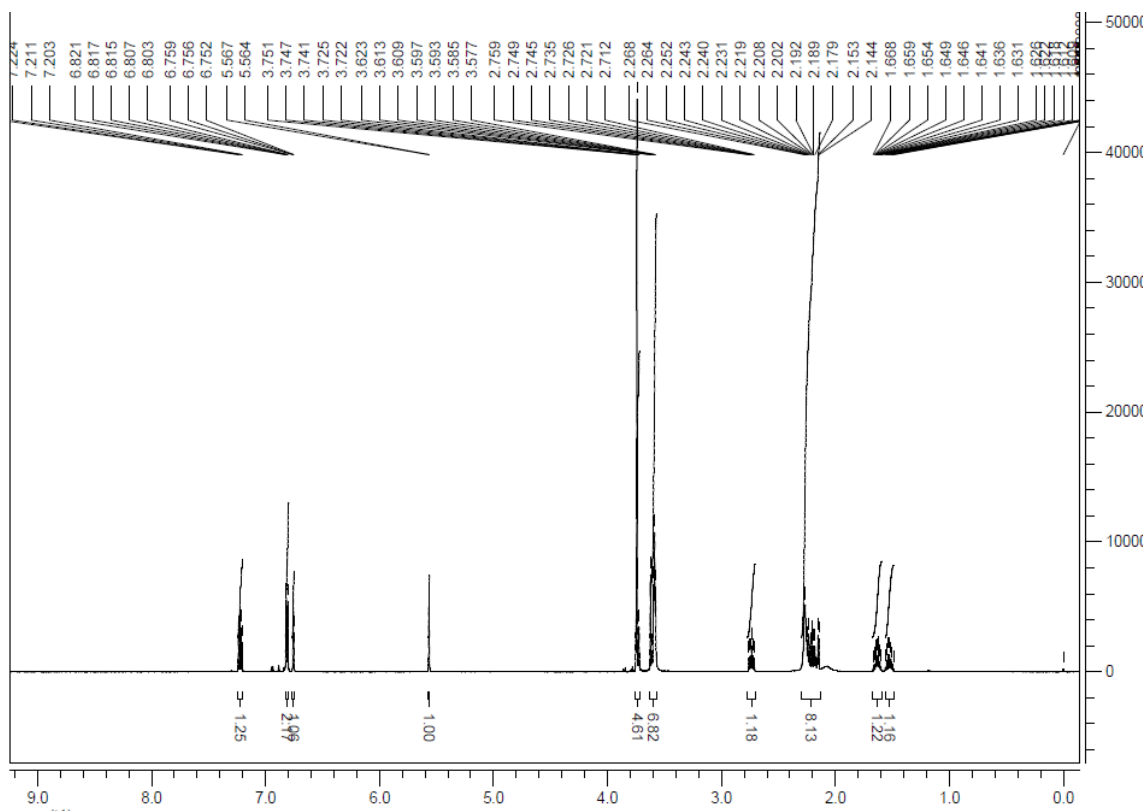


**Figure S21.**  $^1\text{H}$  NMR spectrum (600 MHz,  $\text{CDCl}_3$ ) of compound **4k**.

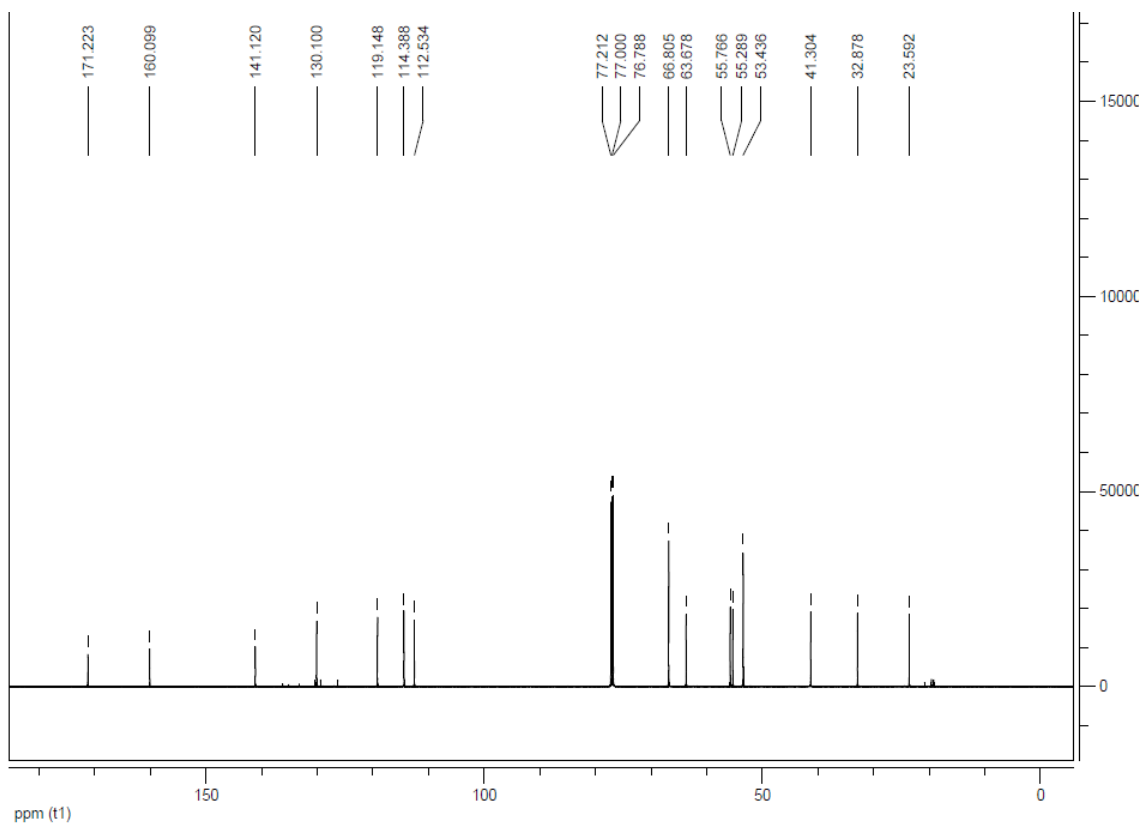


**Figure S22.**  $^{13}\text{C}$  NMR spectrum (150 MHz,  $\text{CDCl}_3$ ) of compound **4k**.

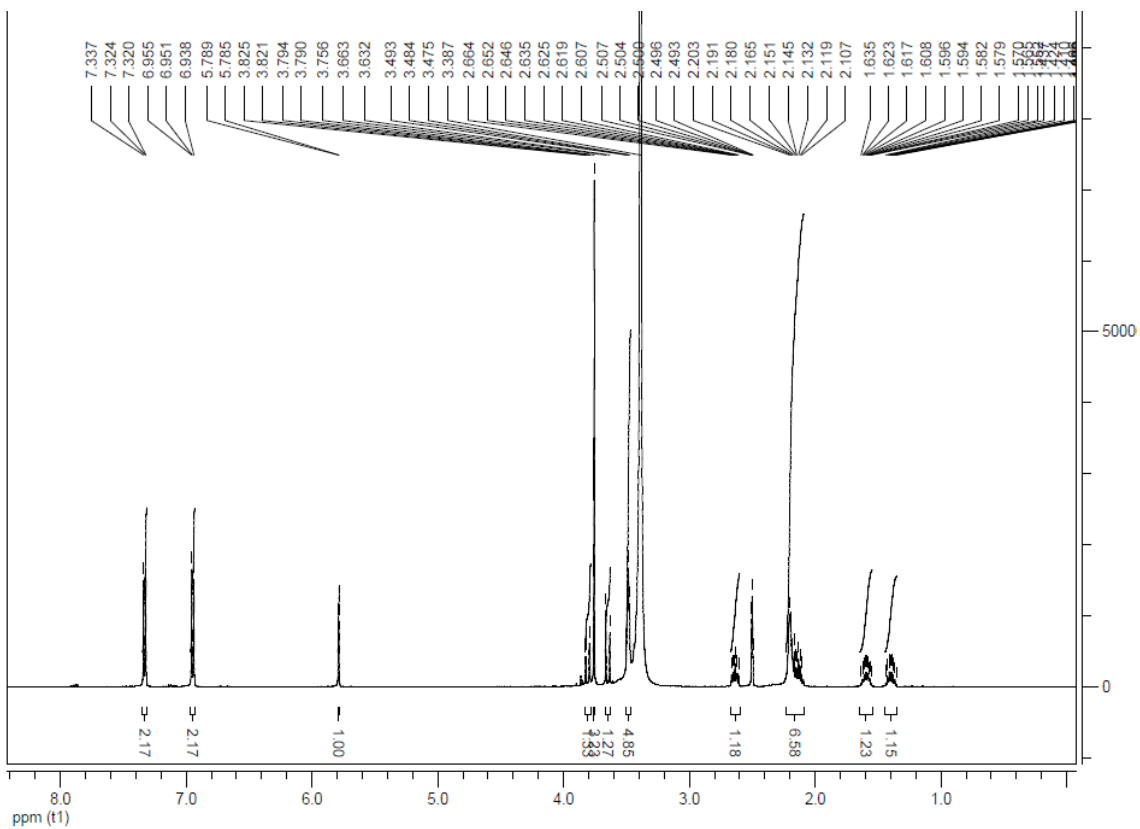


**Figure S23.**  $^1\text{H}$  NMR spectrum (500 MHz,  $\text{DMSO-d}_6$ ) of compound **4I**.

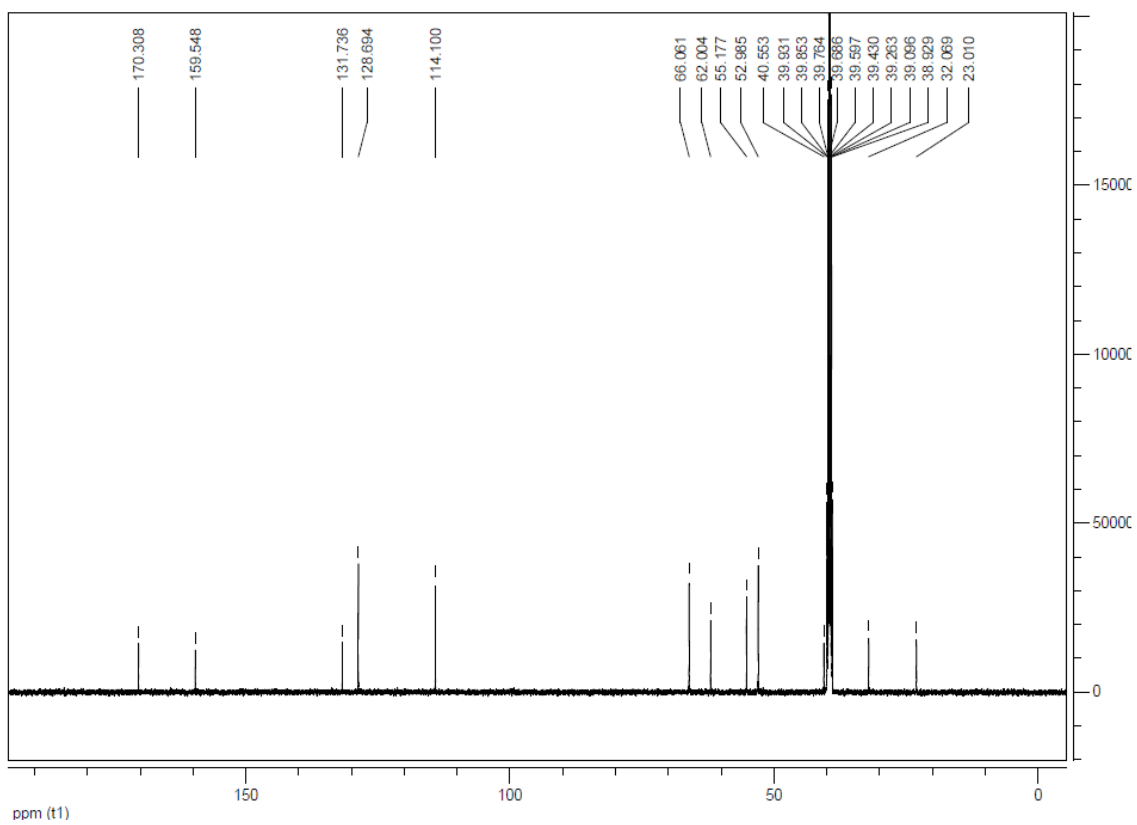


**Figure S24.**  $^{13}\text{C}$  NMR spectrum (125 MHz,  $\text{CDCl}_3$ ) of compound **4l**.



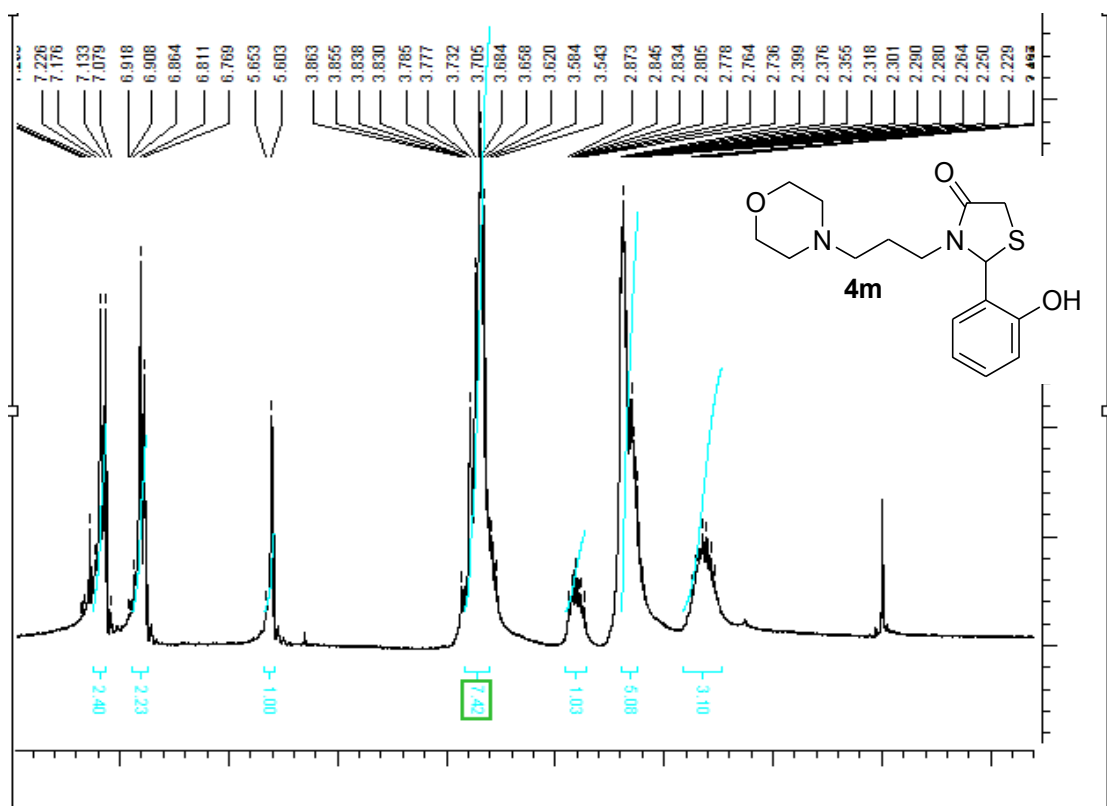


**Figure S25.** <sup>1</sup>H NMR spectrum (200 MHz, CDCl<sub>3</sub>) of compound **4m**.

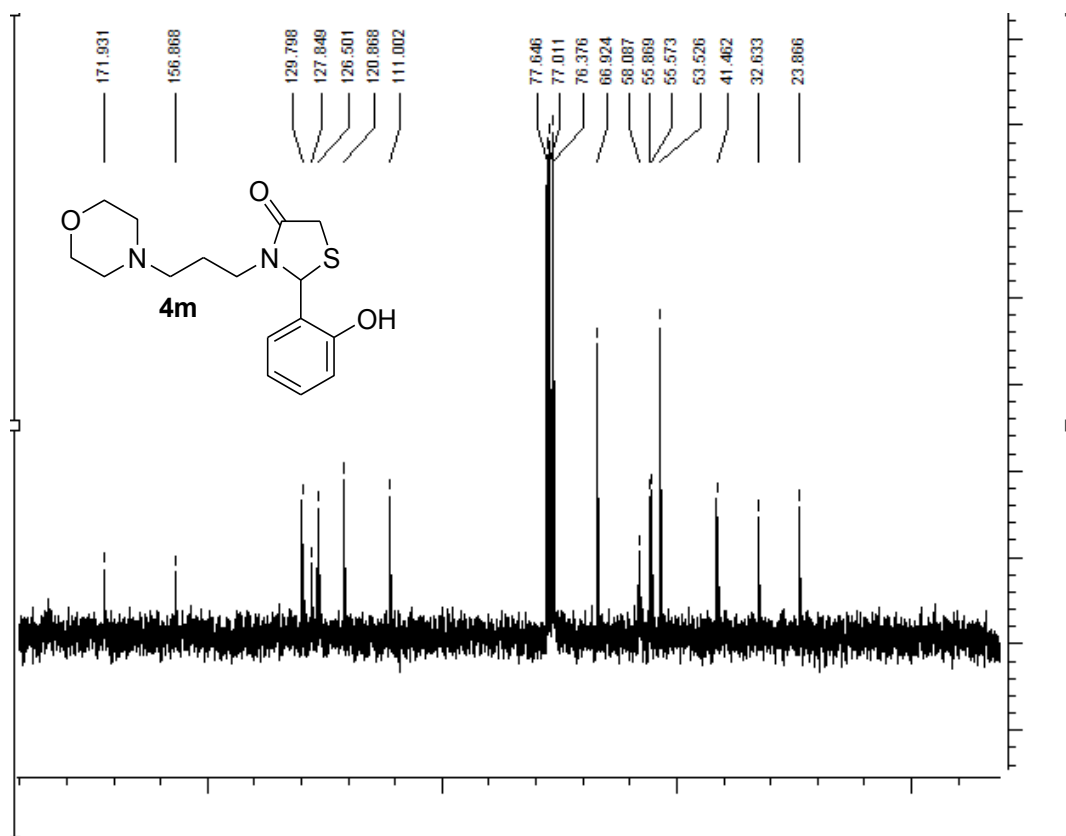


**Figure S26.** <sup>13</sup>C NMR spectrum (50 MHz, CDCl<sub>3</sub>) of compound **4m**.

jul24danH2, g47, h, cdc13

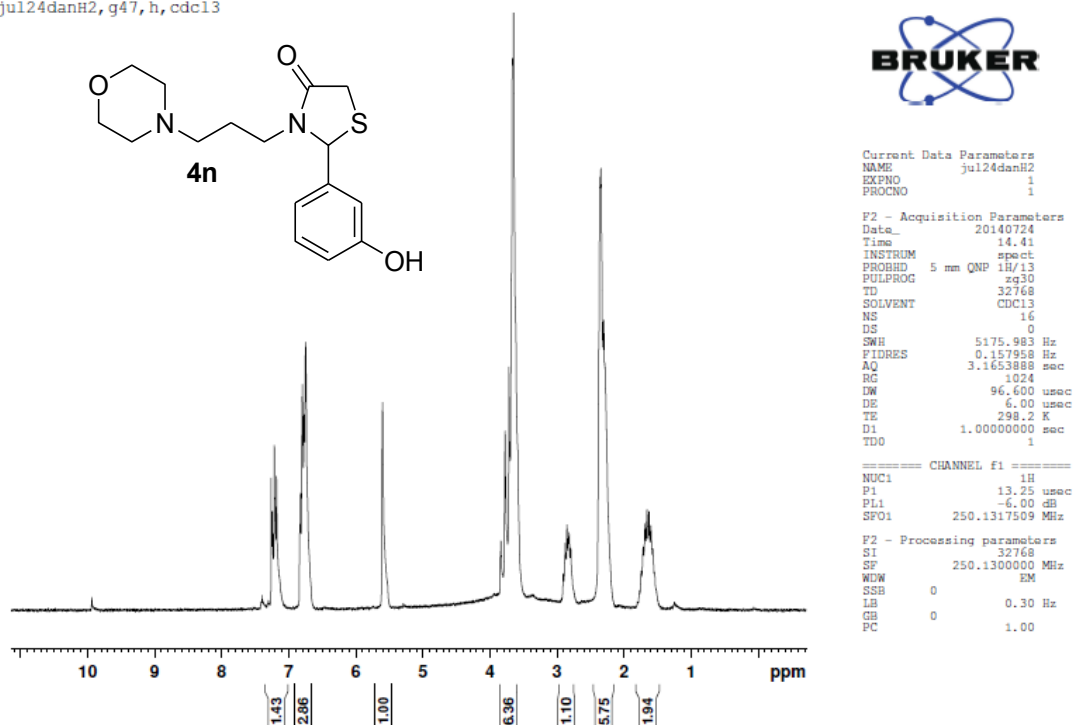
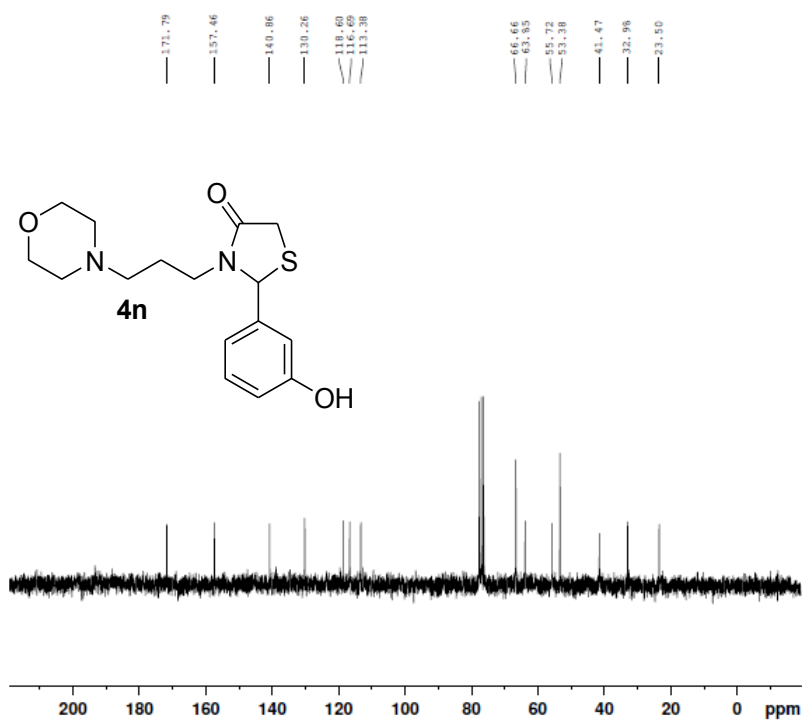


**Figure S27.**  $^1\text{H}$  NMR spectrum (250 MHz,  $\text{CDCl}_3$ ) of compound **4n**.



```

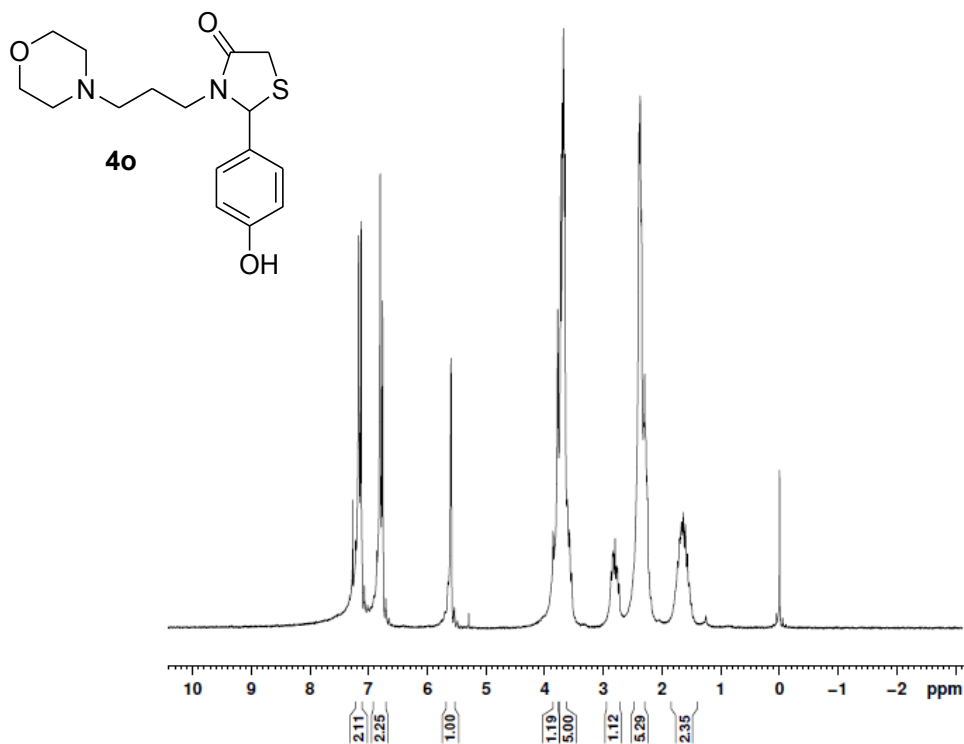
Current Data Parameters
NAME          G47-3-0H
EXPNO         2
PROCNO        1

F2 - Acquisition Parameters
Data_         20131212
Time          10.37
INSTRUM       spect
PROBHD        5 mm Multinucl
PULPROG       zgpg30
TD            32768
SOLVENT       CDCl3
NS            174
DS            0
SWH           11990.407 Hz
FIDRES        0.365918 Hz
AQ            1.3664256 sec
RG            16384
IM           41.700 usec
DE            6.00 usec
TE            300.3 K
D1            2.0000000 sec
d11           0.0300000 sec
DELTA         1.8999999 sec
TDO           1
SFO1          50.3277608 MHz
NUC1          13C
P1            8.00 usec
PLW1          -1.0000000 W
SFO2          200.1308005 MHz
NUC2          1H
CPOPRG[2]    waltz16
PCPD2         80.00 usec
PLW2          -1.0000000 W
PLW12         -1.0000000 W
PLW13         -1.0000000 W

F2 - Processing parameters
SI            16384
SF            50.3277300 MHz
WDW           EM
SSB           0
LB            1.00 Hz
GB            0
PC            1.40

```

**Figure S28.** <sup>13</sup>C NMR spectrum (50 MHz, CDCl<sub>3</sub>) of compound **4n**.



```

Current Data Parameters
NAME          G48-40H
EXPNO        1
PROCNO       1

F2 - Acquisition Parameters
Date_        20130926
Time         14.25
INSTRUM      spect
PROBHD       5 mm Multinucl
PULPROG      zg30
TD           16554
SOLVENT      CDCl3
NS           8
DS           0
SWH          4139.073 Hz
FIDRES       0.250035 Hz
AQ           1.9997232 sec
RG           2580.3
DW           120.800 usec
DE           6.00 usec
TE           510.3 K
D1           1.00000000 sec
TDO          1

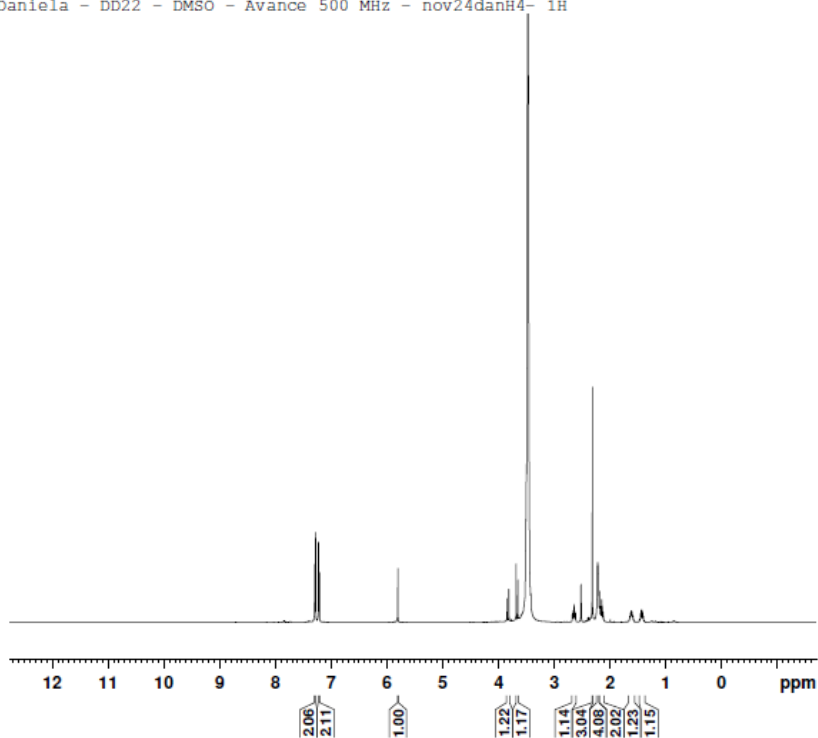
===== CHANNEL f1 =====
NUC1         1H
P1           8.00 usec
PL1          -6.00 dB
SFO1        200.1312359 MHz

F2 - Processing parameters
SI           32768
SF           200.1300000 MHz
WDW          EM
SSB          0
LB           0.30 Hz
GB           0
PC           1.00

```

**Figure S29.** <sup>1</sup>H NMR spectrum (200 MHz, CDCl<sub>3</sub>) of compound **4o**.

Daniela - DD22 - DMSO - Avance 500 MHz - nov24danH4- 1H



```
Current Data Parameters
NAME nov24danH4-dd22
EXPNO 1
PROCNO 1

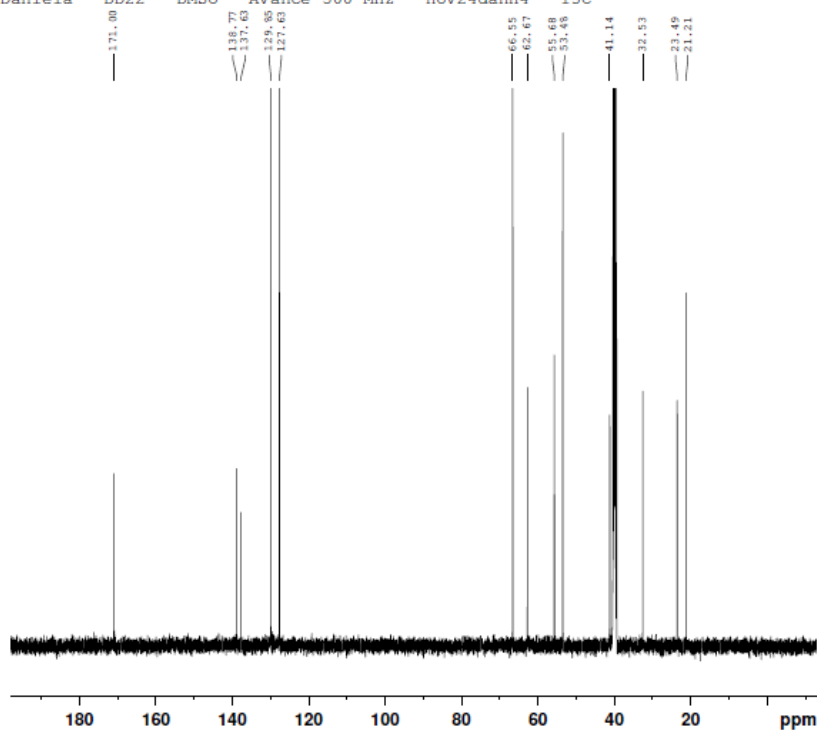
F2 - Acquisition Parameters
Date_ 20141124
Time 15.02
INSTRUM spect
PROBHD 5 mm PABBO BB/
PULPROG zg30
TD 32768
SOLVENT DMSO
NS 16
DS 2
SWH 10000.000 Hz
FIDRES 0.305176 Hz
AQ 1.6384000 sec
RG 50.8
DW 50.000 usec
DE 6.50 usec
TE 298.1 K
D1 1.00000000 sec
TDO 1

===== CHANNEL f1 =====
SFO1 499.8730869 MHz
NUC1 1H
P1 11.75 usec
PLW1 25.00000000 W

F2 - Processing parameters
SI 65536
SF 499.8700000 MHz
WDW EM
SSB 0
LB 0.30 Hz
GB 0
PC 1.00
```

Figure S30.  $^1\text{H}$  NMR spectrum (500 MHz,  $\text{CDCl}_3$ ) of compound **4q**.

Daniela - DD22 - DMSO - Avance 500 MHz - nov24danH4 - 13C



```
Current Data Parameters
NAME nov24danH4-dd22
EXPNO 2
PROCNO 1

F2 - Acquisition Parameters
Date_ 20141124
Time 15.32
INSTRUM spect
PROBHD 5 mm PABBO BB/
PULPROG zgpg30
TD 65536
SOLVENT DMSO
NS 640
DS 4
SWH 29761.904 Hz
FIDRES 0.454131 Hz
AQ 1.1010048 sec
RG 2050
DW 16.800 usec
DE 6.50 usec
TE 298.1 K
D1 2.00000000 sec
D11 0.03000000 sec
TDO 1

===== CHANNEL f1 =====
SFO1 125.7049801 MHz
NUC1 13C
P1 10.00 usec
PLW1 91.00000000 W

===== CHANNEL f2 =====
SFO2 499.8719995 MHz
NUC2 1H
CPDPRG2 waltz16
PCPD2 80.00 usec
PLW2 26.85300064 W
PLW12 0.57928002 W
PLW13 0.37074000 W

F2 - Processing parameters
SI 32768
SF 125.6924110 MHz
WDW EM
SSB 0
LB 1.00 Hz
GB 0
PC 1.40
```

**Figure S31.**  $^{13}\text{C}$  NMR spectrum (125 MHz,  $\text{CDCl}_3$ ) of compound **4q**.

Daniela "G32" cdcl3 / Av 500 MHz jun16wanH1 HSQC

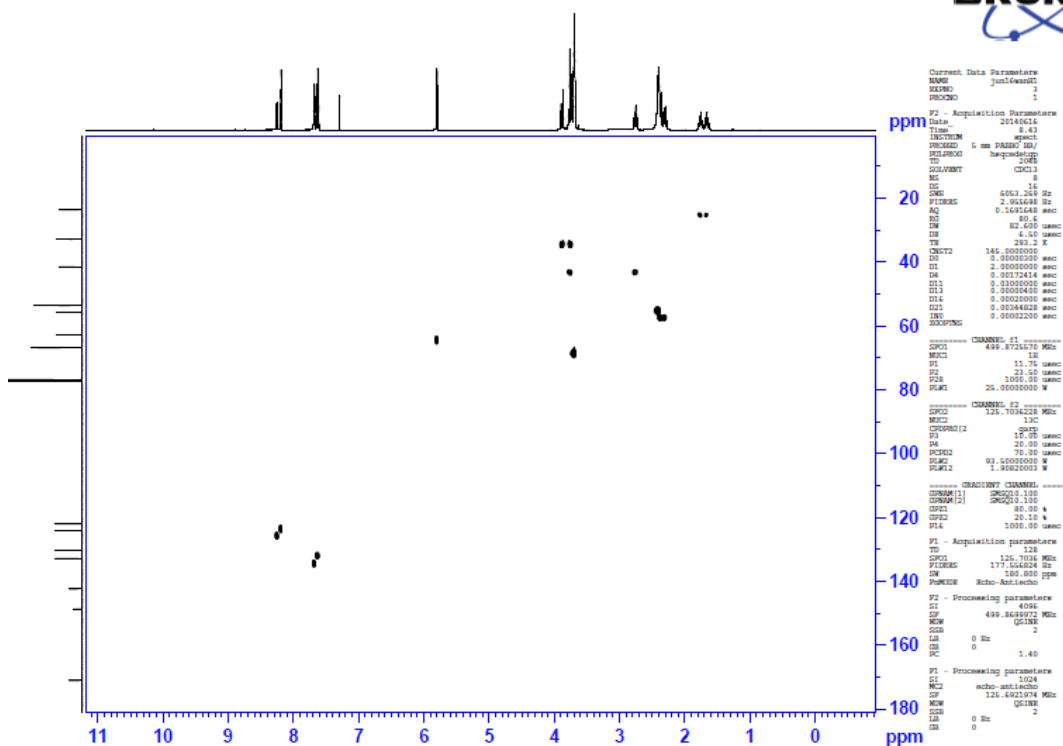


**Figure S32.** HSQC spectrum of compound **4g**.

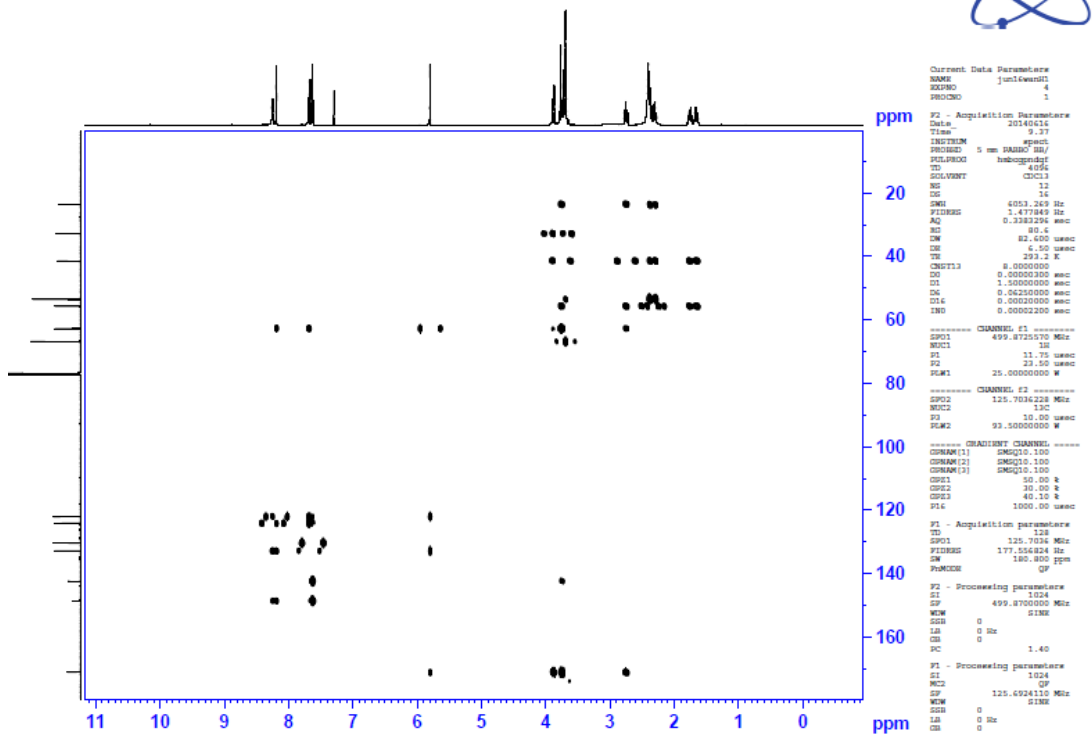
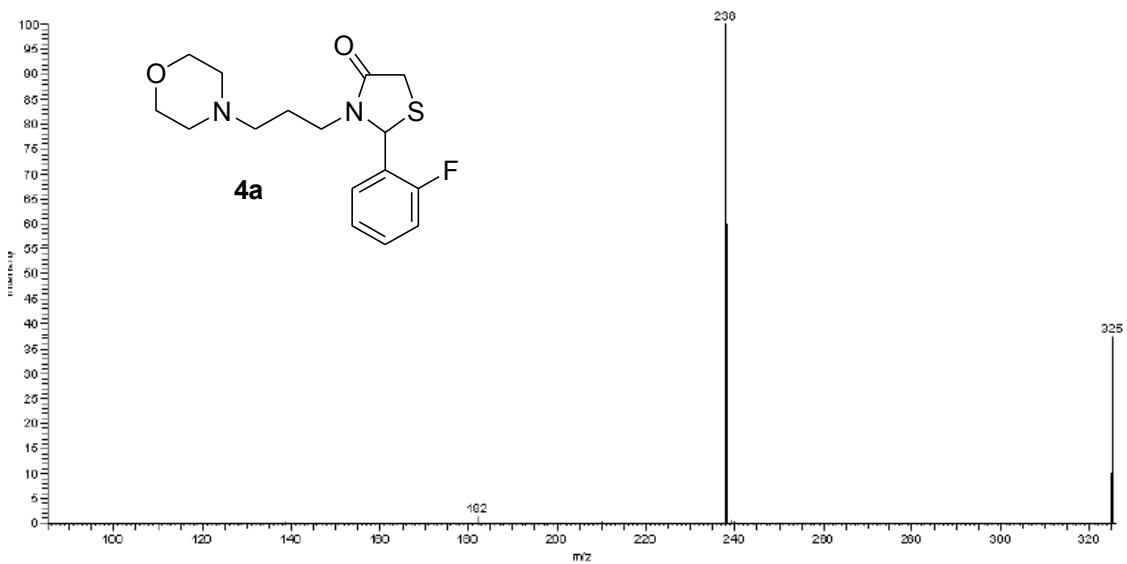


Figure S33. HMBC spectrum of compound 4g.

G68





**Figure S34.** HRMS of compound **4a**.

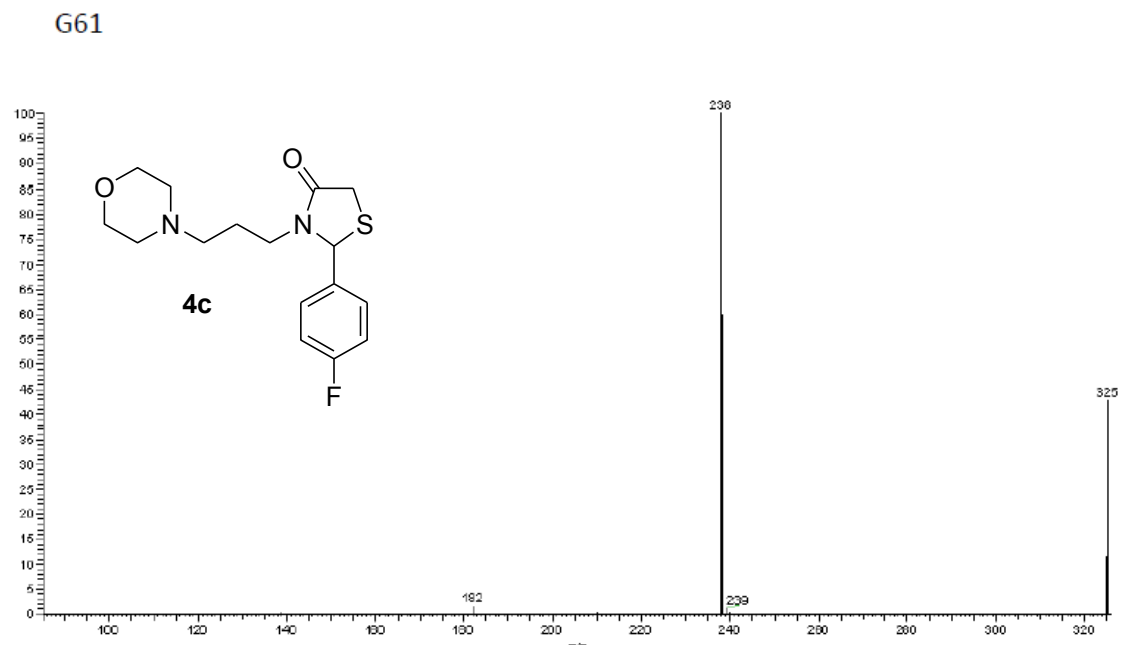


**Figure S35.** HRMS of compound **4c**.

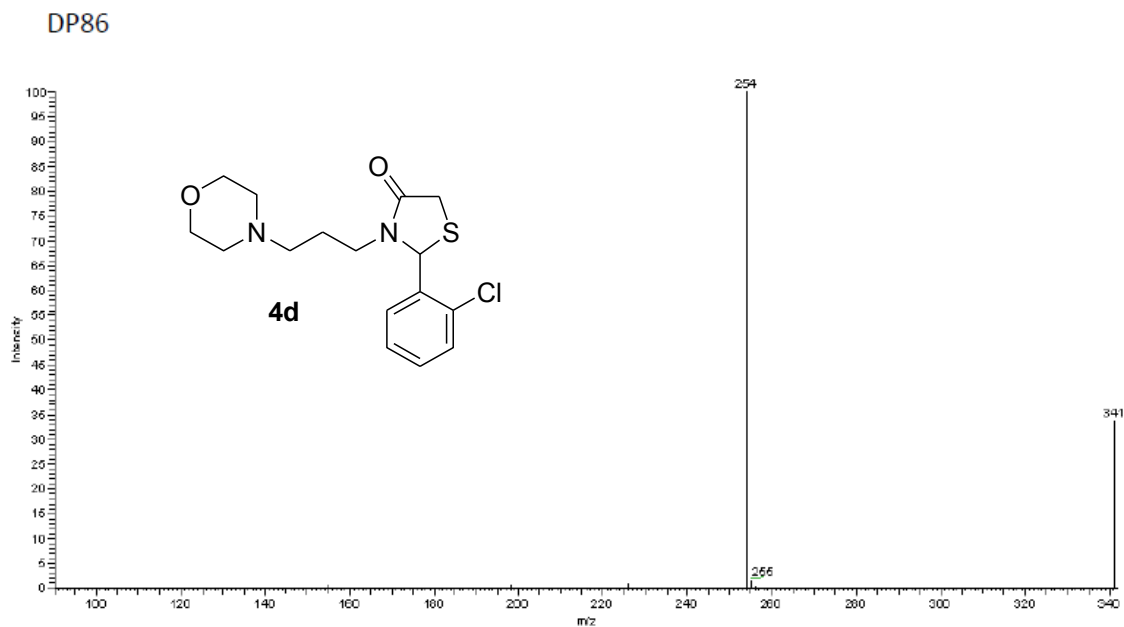


**Figure S36.** HRMS of compound **4d**.

G62

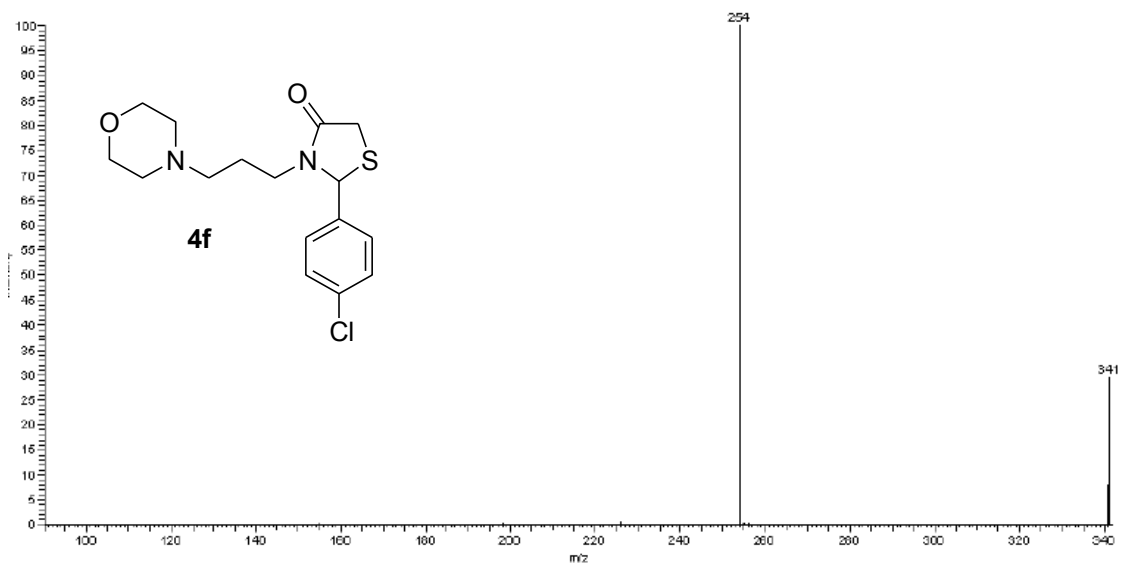


Figure S37. HRMS of compound **4f**.

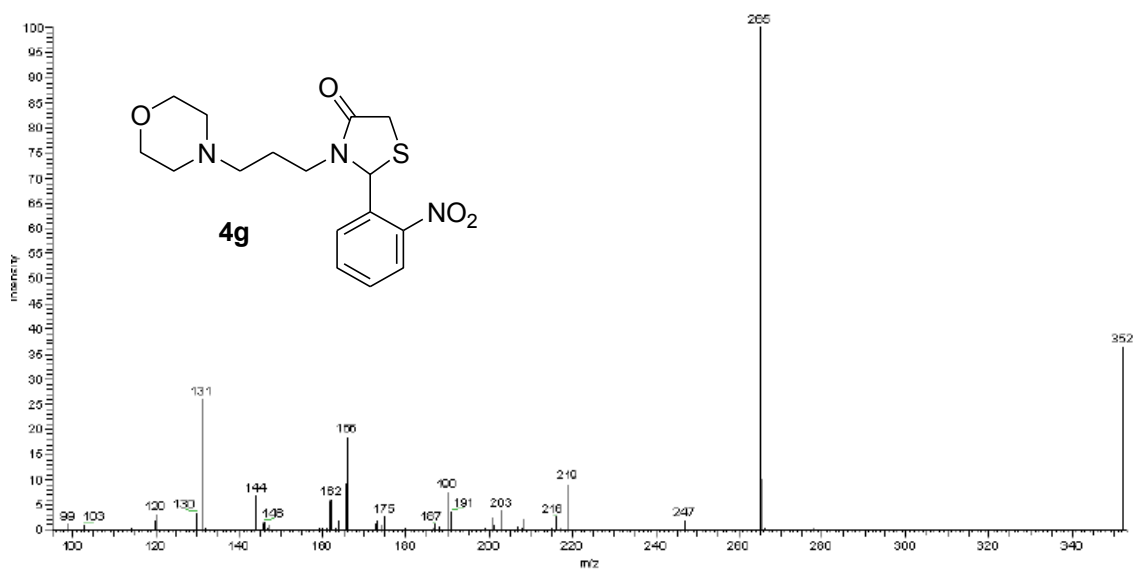


Figure S38. HRMS of compound **4g**.

G32

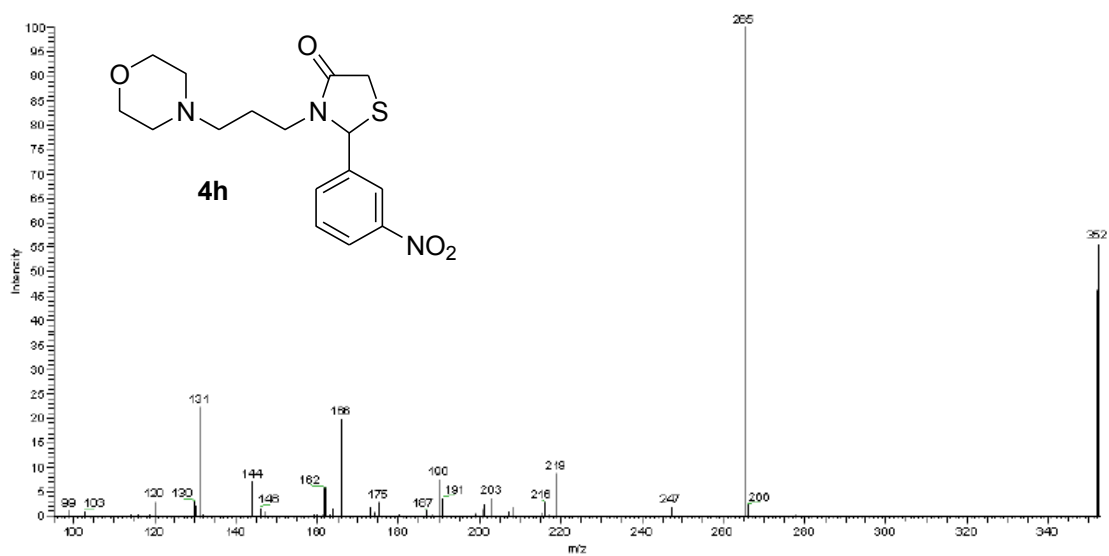


Figure S39. HRMS of compound **4h**.

DD31

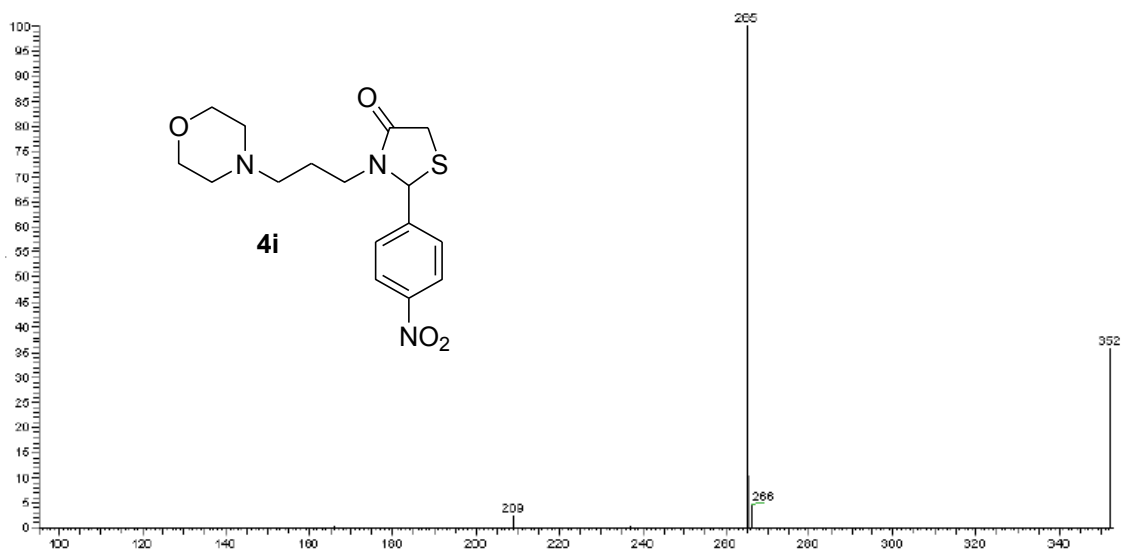


Figure S40. HRMS of compound **4i**.

G49

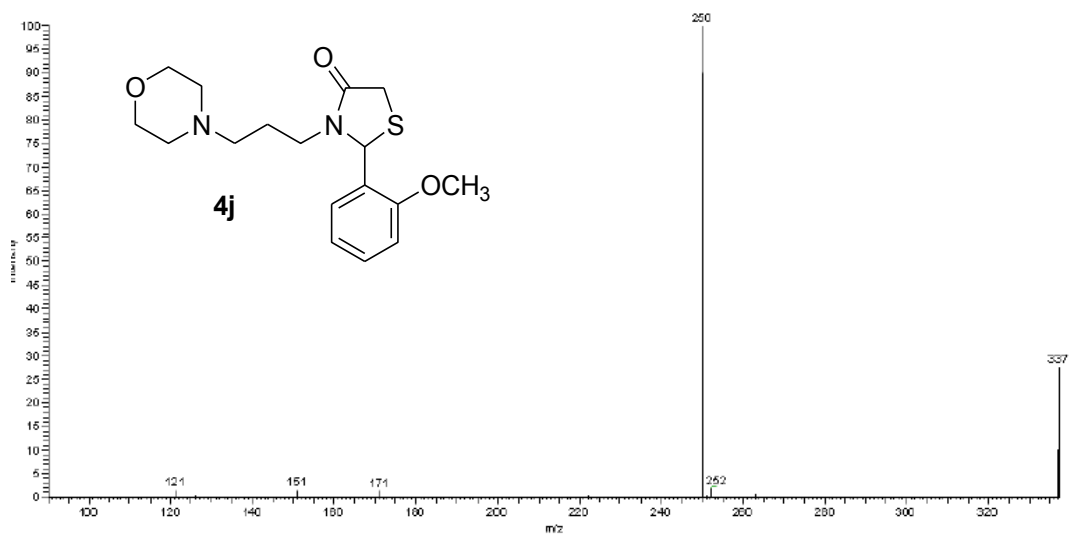


Figure S41. HRMS of compound **4j**.

G51

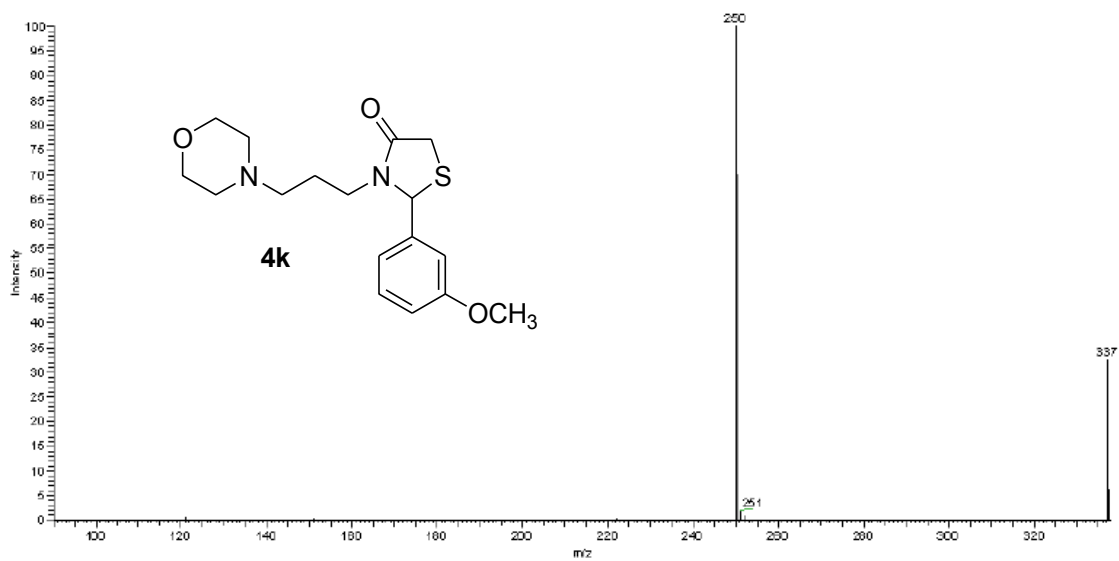


Figure S42. HRMS of compound **4k**.

G52

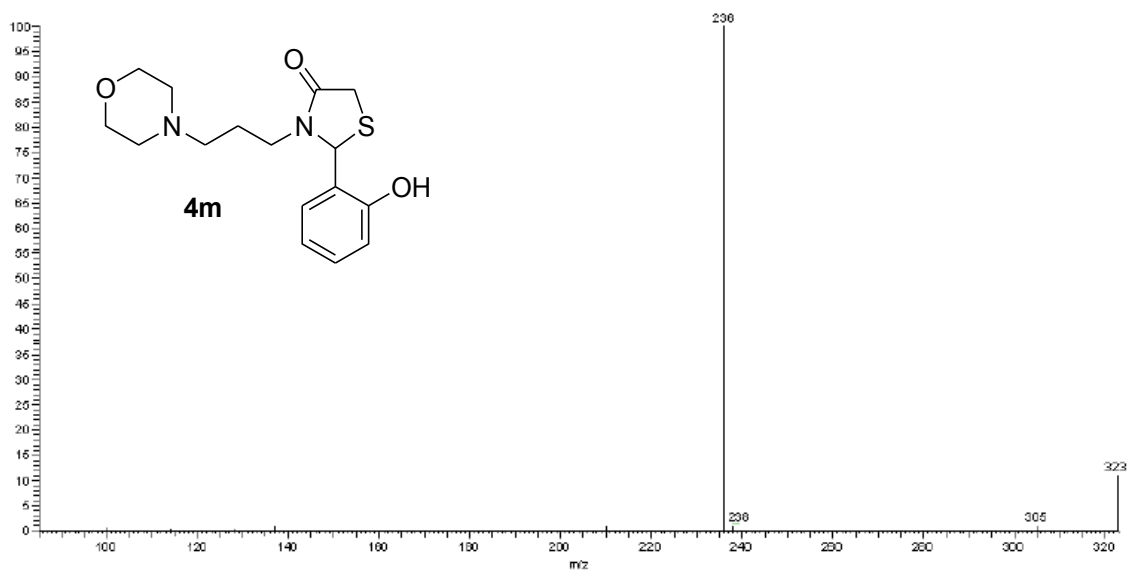


Figure S43. HRMS of compound **4m**.

G47

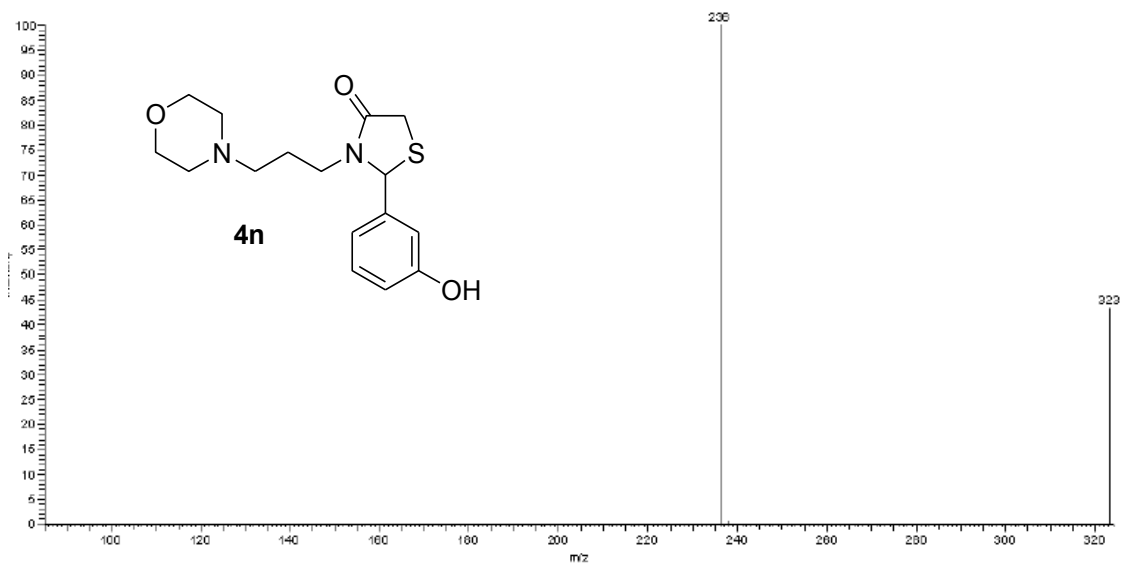
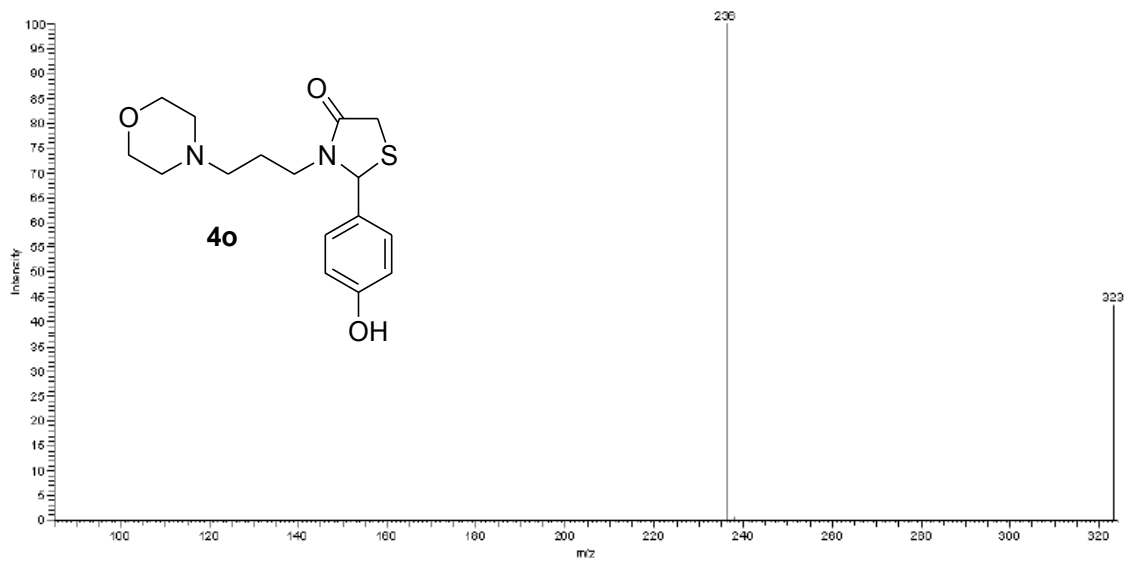
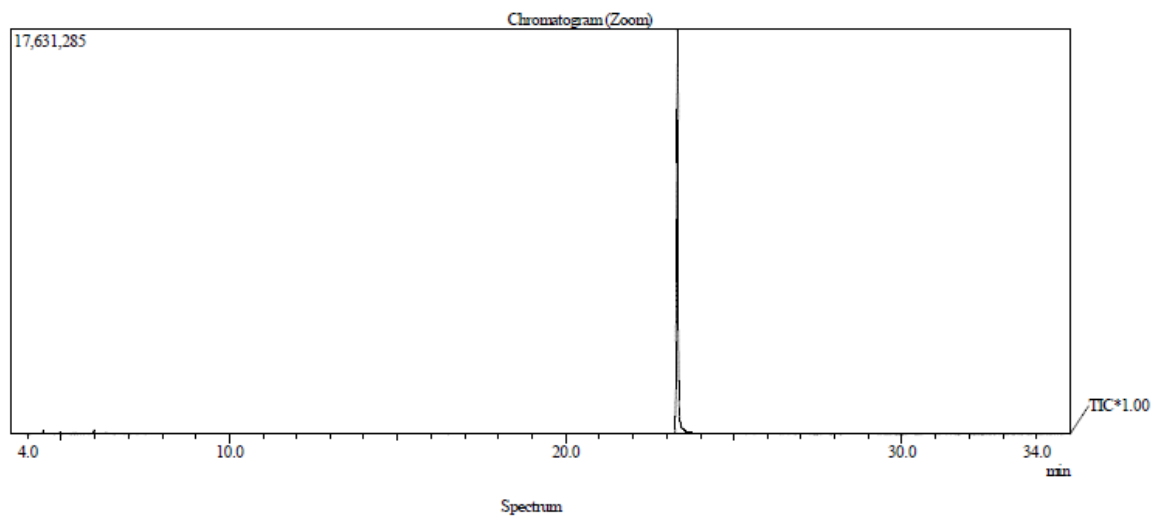


Figure S44. HRMS of compound **4n**.



**Figure S45.** HRMS of compound **4o**.



Line#: 1 R.Time: 23.333 (Scan#: 2381)  
MassPeaks: 76  
RunMode: Averaged 22.542-24.467 (2286-2517) BasePeak: 100.10 (184142)  
BG Mode: None Group 1 - Event 1

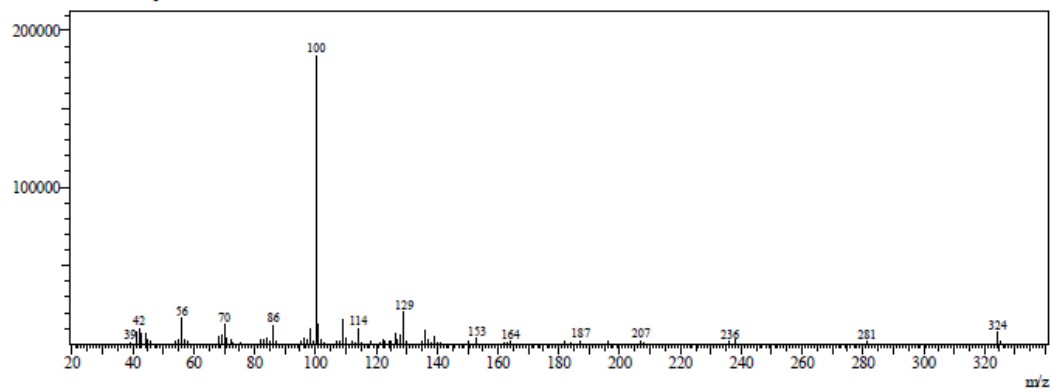
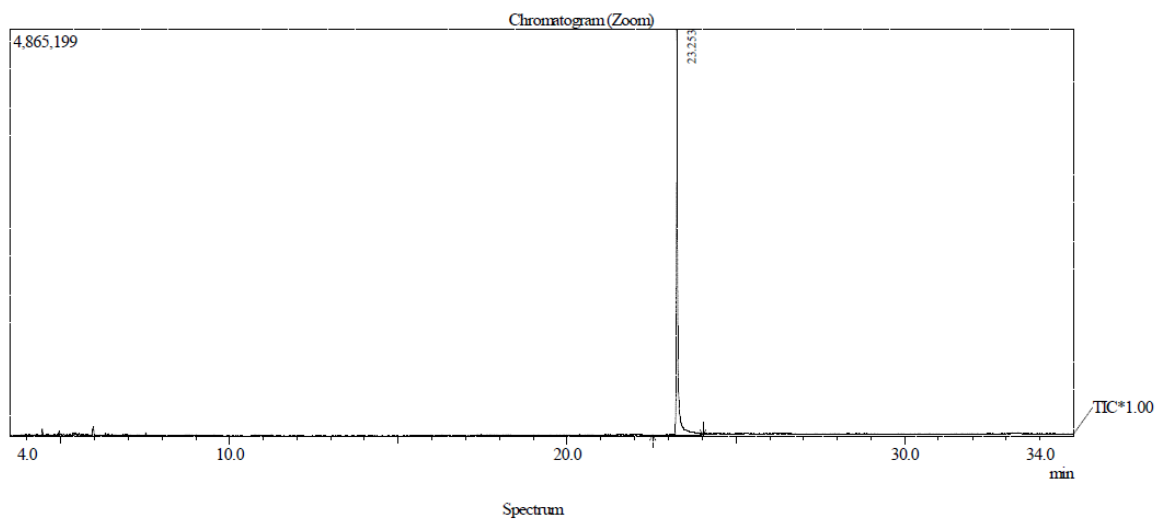


**Figure S46.** GC-MS of thiazolidinone **4a**.



Line#:1 R. Time:23.250(Scan#:2371)  
MassPeaks:85  
RawMode:Averaged 22.508-24.242(2282-2490) BasePeak:100.10(46652)  
BG Mode:None Group 1 - Event 1

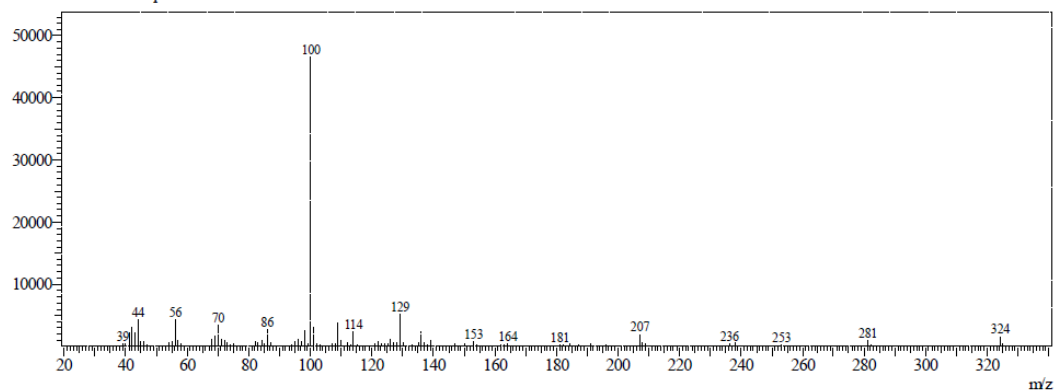
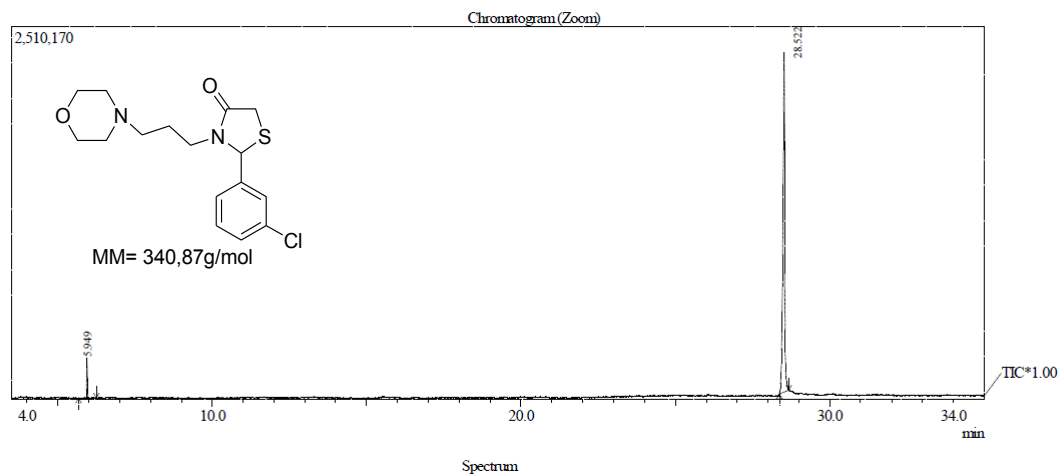


**Figure S47.** GC-MS of thiazolidinone **4c**.





Line#:1 R. Time:28.525(Scan#:3004)  
MassPeaks:87  
RawMode:Averaged 28.092-29.350(2952-3103) BasePeak:100.10(51840)  
BG Mode:None Group 1 - Event 1

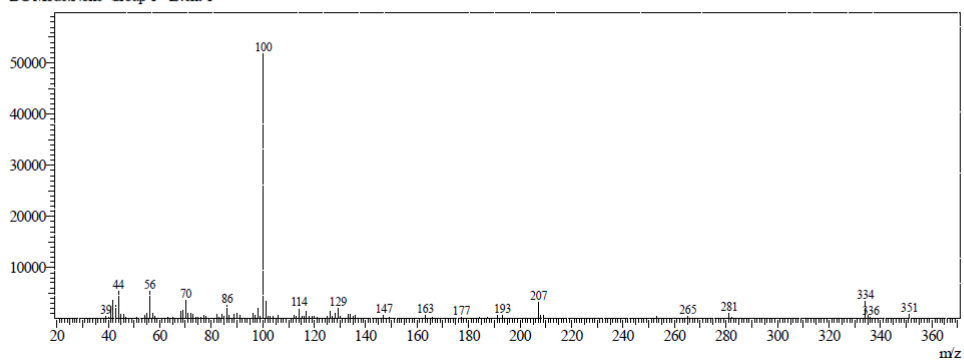
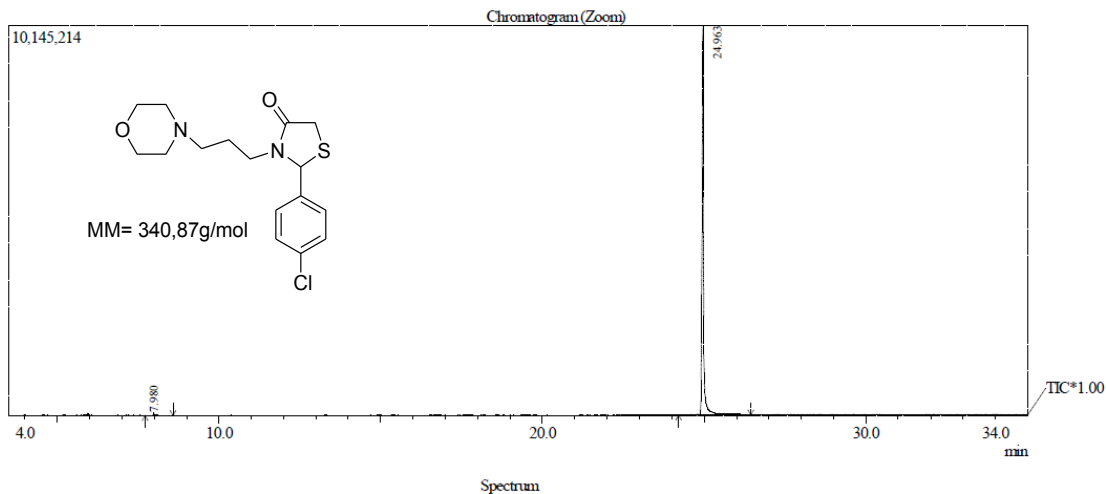


**Figura S48.** GC-MS of thiazolidinone **4e**.



Spectrum

Line#:1 R.Time:24.967(Scan#:2577)  
MassPeaks:63  
RawMode:Averaged 24.433-25.725(2513-2668) BasePeak:100.10(169179)  
BG Mode:Averaged 28.025-29.633(2944-3137) Group 1 - Event 1

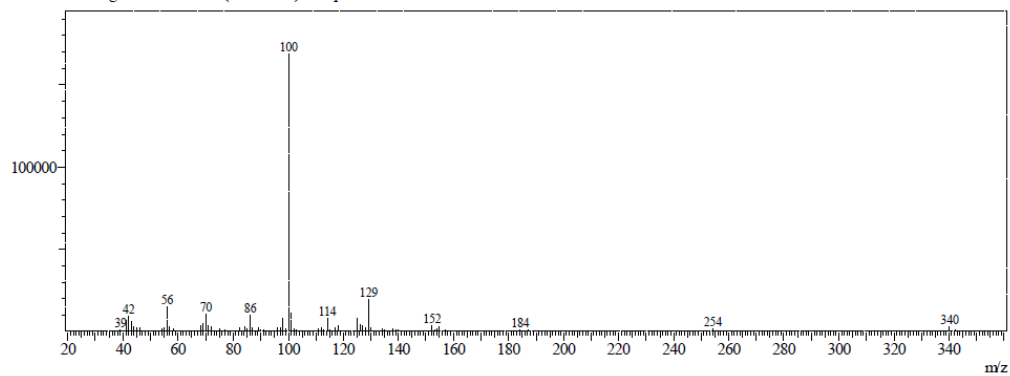
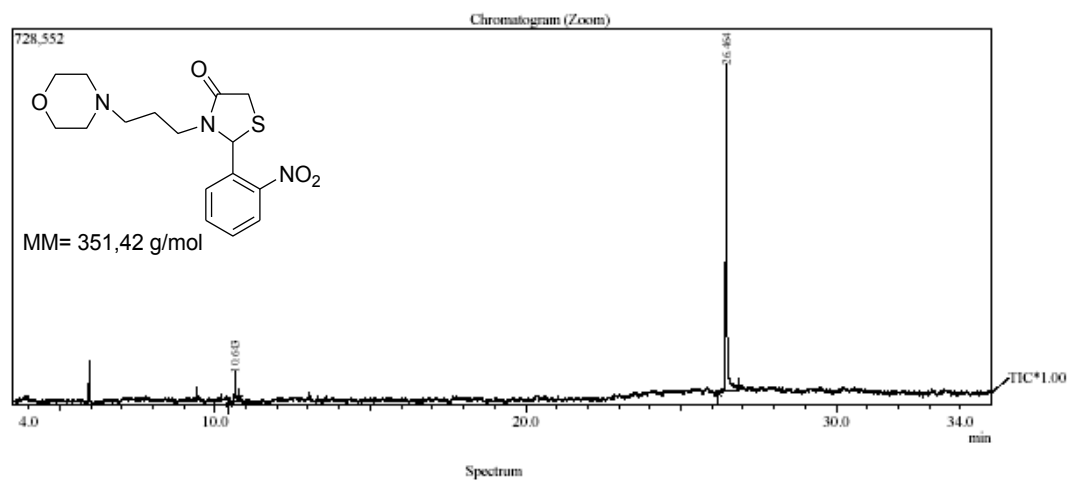


**Figure S49.**GC-MS of thiazolidinone **4f**.



Line#:1 R.Time:26.467(Scan#:2757)  
 MassPeaks:265  
 RawMode:Averaged 26.083-27.283(2711-2855) BasePeak:100.10(7135)  
 BG Mode:None Group 1 - Event 1

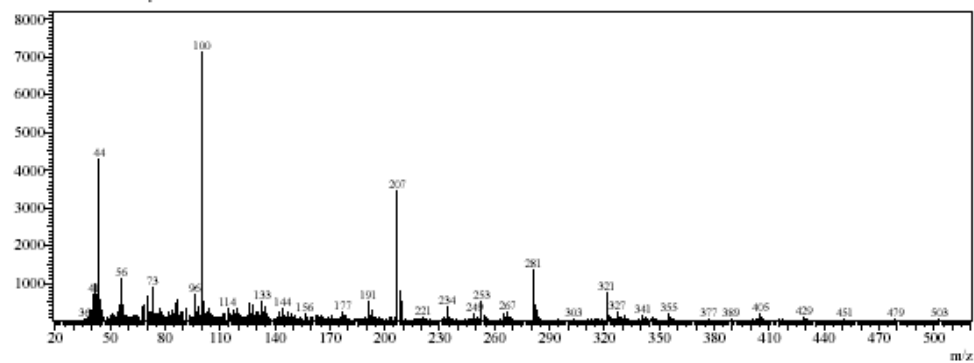
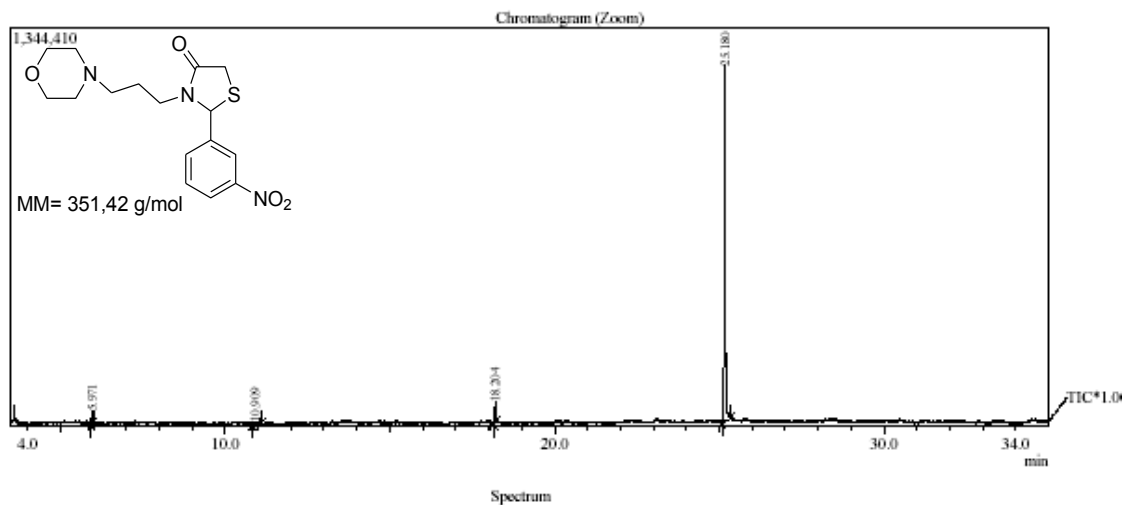


**Figure S50.** GC-MS of thiazolidinone **4g**.



Line#:1 R.Time:25.183(Scan#:2603)  
 MassPeaks:139  
 RawMode:Averaged 24.233-27.008(2489-2822) BasePeak:100.10(8405)  
 BG Mode:None Group 1 - Event 1

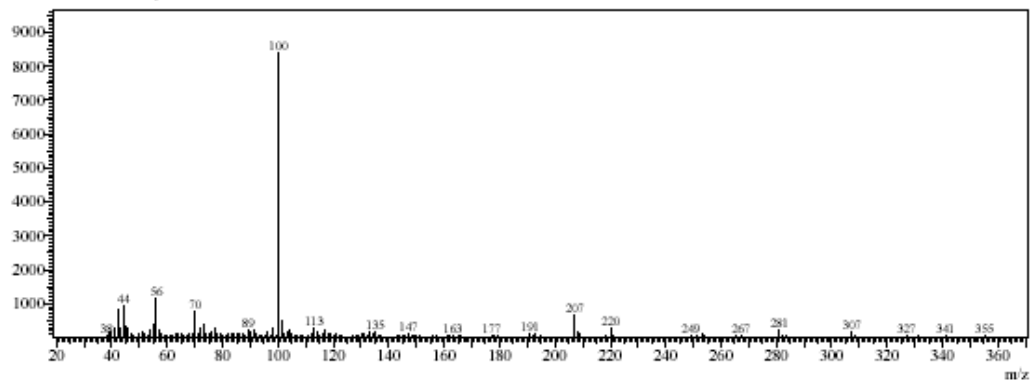
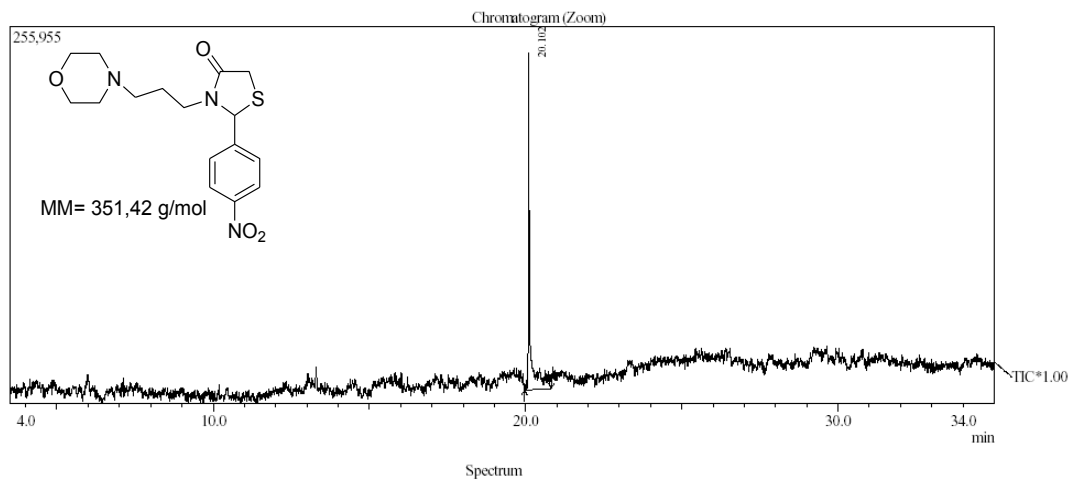
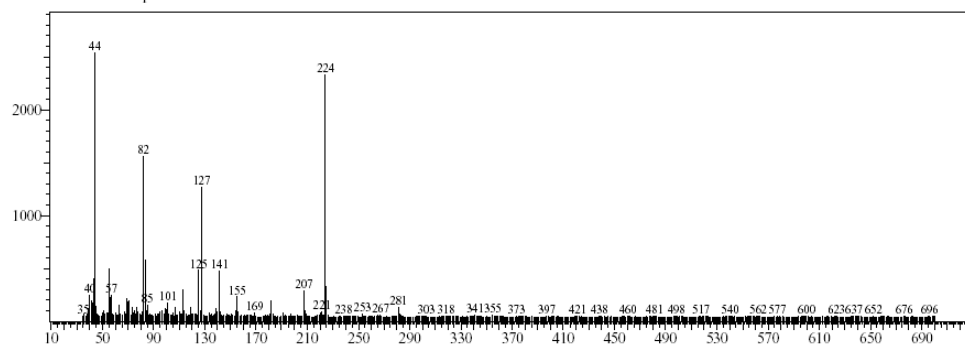


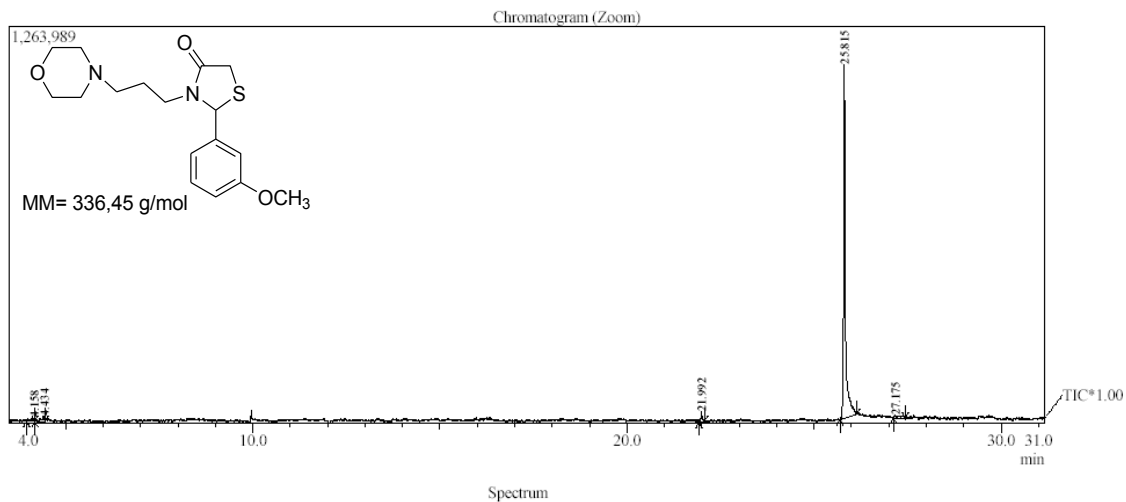
Figure S51. GC-MS of thiazolidinone 4h.



Line#:1 R.Time:20.100(Scan#:1993)  
 MassPeaks:666  
 RawMode:Averaged 19.608-20.492(1934-2040) BasePeak:44.00(2542)  
 BG Mode:None Group 1 - Event 1



**Figure S52. GC-MS of thiazolidinone 4i.**



Line#1 R.Time:25.817(Scan#:2679)  
 MassPeaks:98  
 RawMode:Averaged 25.250-26.217(2611-2727) BasePeak:100.10(20258)  
 BG Mode:Averaged 15.442-16.675(1434-1582) Group 1 - Event 1

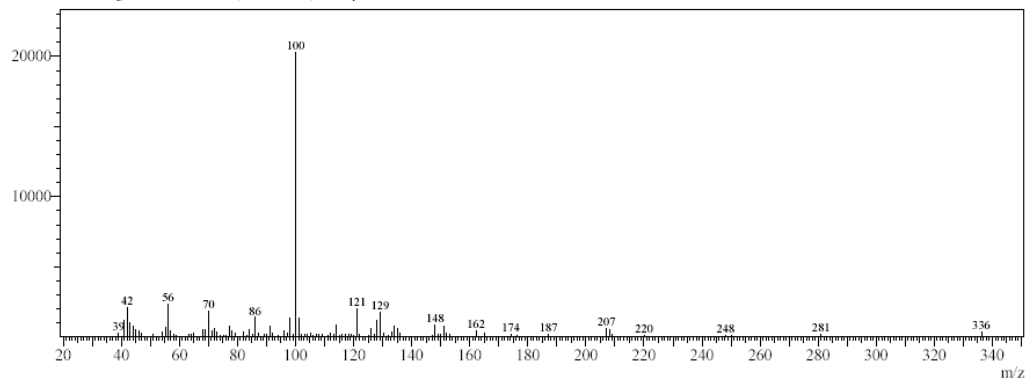
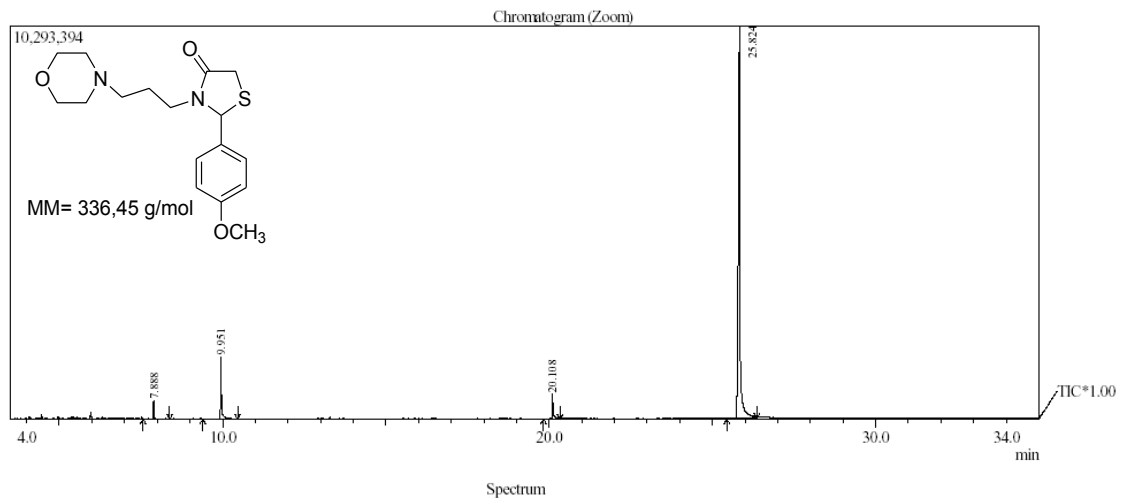


**Figure S53.** GC-MS of thiazolidinone **4k**.



Line#:1 R.Time:25.825(Scan#:2680)  
MassPeaks:78  
RawMode:Averaged 25.375-26.325(2626-2740) BasePeak:100.10(243420)  
BG Mode:Averaged 28.025-29.508(2944-3122) Group 1 - Event 1

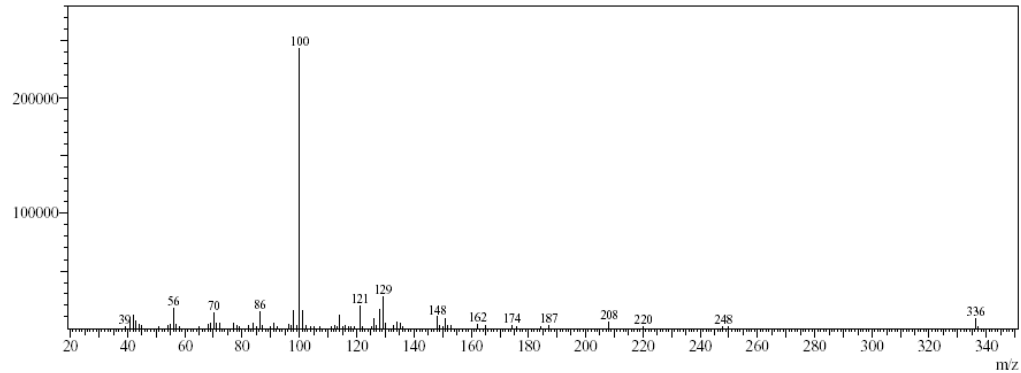
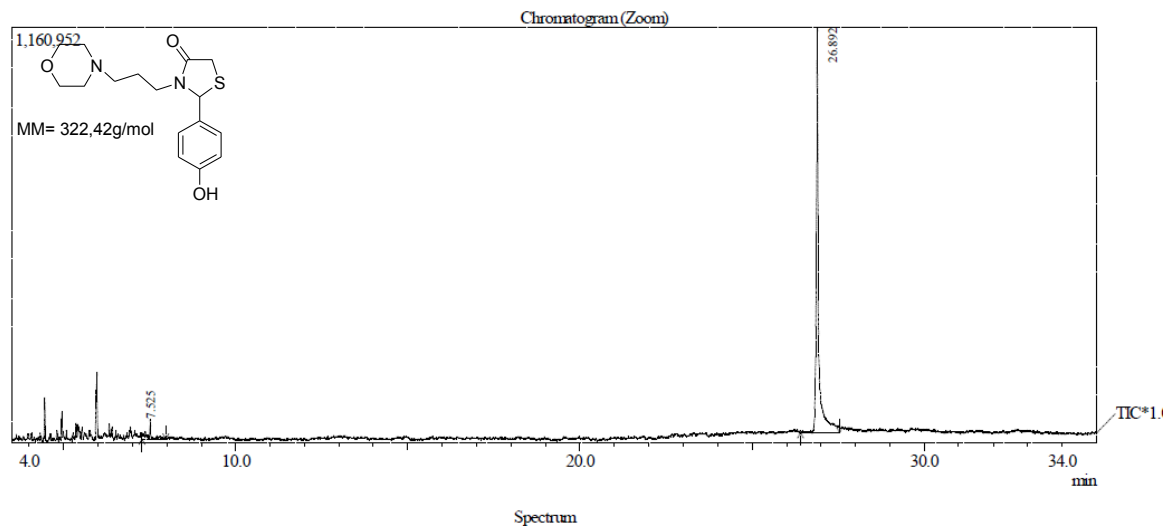


**Figure S54.** GC-MS of thiazolidinone **4l**.



Line#:1 R Time:26.892(Scan#:2808)  
MassPeaks:74  
RawMode:Averaged 25.658-27.900(2660-2929) BasePeak:100.10(13029)  
BG Mode:Averaged 28.592-29.508(3012-3122) Group 1 - Event 1

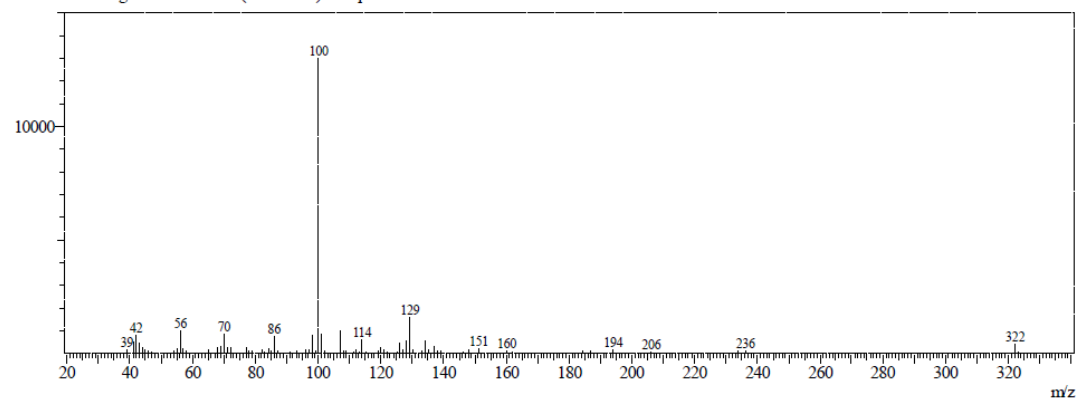


**Figure S55.** GC-MS of thiazolidinone



